

MARCH 2021
ENERGINET ELTRANSMISSION A/S

THOR OFFSHORE WIND FARM

INTEGRATED GEOLOGICAL MODEL

REPORT



FEBRUARY 2021
ENERGINET ELTRANSMISSION A/S

THOR OFFSHORE WIND FARM

INTEGRATED GEOLOGICAL MODEL

REPORT

PROJECT NO.

A205839

DOCUMENT NO.

004

VERSION

2.0

DATE OF ISSUE

March 1st 2021

DESCRIPTION

Report

PREPARED

CONN, MUOE,
MALA, KAWE,
OFN, MLRN, SPSO

CHECKED

KAPN

APPROVED

LOKL

CONTENTS

1	Executive Summary	7
2	Introduction	9
2.1	Area of Investigation	9
2.2	Scope of Work	10
3	Basis	12
3.1	Geotechnical basis	13
3.2	Geophysical and hydrographical basis	15
4	Geotechnical interpretation	18
4.1	Geotechnical soil unit overview	18
4.2	Stratigraphic interpretation based on borehole log	20
4.3	Stratigraphic interpretation based on CPT	20
4.4	Classification of soils using CPT	23
5	Geotechnical properties and variance	28
5.1	Presentation of CPT properties	29
5.2	Presentation of state properties	33
5.3	Presentation of strength and stiffness properties	35
5.4	Range of soil parameters per soil unit	39
6	Geological Setting	43
6.1	Pre-Quaternary Geology	43
6.2	Quaternary Geology	44
7	Integrated Geological Model	46
7.1	Datum, coordinate system and software	46
7.2	Assessment of existing geophysical model	46
7.3	Interpolation and adjustment of surfaces	47

7.4	Uncertainty in the grid	47
7.5	Depth conversion	48
7.6	Potential geohazards from shallow gas and organic-rich deposits	48
7.7	Stratigraphy	48
8	Conceptual Geological Model	62
8.1	Presentation of Conceptual Geological Model	62
8.2	Presentation of Soil Provinces	64
9	Leg penetration risk assessment	67
9.1	Selection of vessels	67
9.2	Geotechnical risks during jack-up	68
9.3	Risk categories across the site	74
10	List of deliverables	77
11	Conclusions	81
12	References	82

1 Executive Summary

This report describes the work and outcome of the integrated 3D model for Thor Offshore Wind Farm based on 2020 geotechnical and 2019 geophysical site investigations. The established 3D model comprises compacted and un-compacted deposits from the Holocene, Pleistocene and Miocene time periods.

Energinet is developing the Thor Offshore Wind Farm area to be tendered out during 2021-2022 and targeting complete commissioning by end 2027. The area of investigation is found approximately 20 km offshore Thorsminde on the Danish west coast and covers around 440 km². The final footprint of the OWF layout is expected to be around 220 km².

The 3D geological model is established using 2D Multi-channel Ultra High Resolution Seismic data with 240 m between north-south lines and 1000 m between east-west lines. Interpretation integrates geotechnical investigations at 67 locations including cone penetration testing and boreholes. Major soil units are assessed and described for the combined data set. Factual report and laboratory testing from the geotechnical investigation is used to establish geotechnical properties for the soil units.

The integrated geological model has 16 layers for which geological descriptions are provided. The descriptions include stratigraphic, lithological and geotechnical characteristics and distinction is made between the non-glaciated relative low strength deposits of Holocene and later Pleistocene age and the more consolidated glacial deposit from earlier in Pleistocene and from Miocene.

A soil zonation encircles the geological model and structures evaluated to have a potentially significant impact on the foundation design: low strength layers, non-glaciated layers and lateral changes or steep layer boundaries near the seabed. The soil zonation is simplified into one single map dividing the entire site into five different soil provinces.

A high-level leg penetration risk assessment has been performed in order to provide an overview of potential jack-up risks during the next project phases. This assessment has been performed for two selected vessel configurations, i.e. for a generic installation vessel and a generic O&M vessel.

Enclosures provided with the digital model present the new layers with respect to depth below seabed, thickness and lateral extent. The enclosures also visualize cumulated thickness of Holocene deposits, non-glaciated layers and glacial deposits. Furthermore 16 cross-sections distributed over the entire area show the layering in the model together with borehole information.

All enclosures are provided digitally as shapefiles. The integrated geological model is delivered as a digital 3D model in a Kingdom suite project.

2 Introduction

Energinet and the Danish Energy Agency are investigating the Thor Offshore Wind Farm (OWF) area in order to identify a developer for the project by early 2022, targeting complete commissioning by end 2027.

To enable evaluation of subsurface soil conditions and related constraints, Energinet has procured a geophysical 2D Multi-channel Ultra High Resolution Seismic (M-UHRS) survey (MMT, 2019) and preliminary geotechnical investigations (GEO, 2020). These surveys have provided the basis for an integrated geological model of the OWF area.

This report presents the results of the integrated geological modelling of the Thor OWF area of investigation as carried out by COWI July 2020 - January 2021.

2.1 Area of Investigation

The Area Of Investigation (AOI) is situated ~20 km offshore Thorsminde on the Danish west coast and covers ~440 km² (Figure 2-1, Table 1). The final footprint of the OWF layout is expected to be ~220 km².

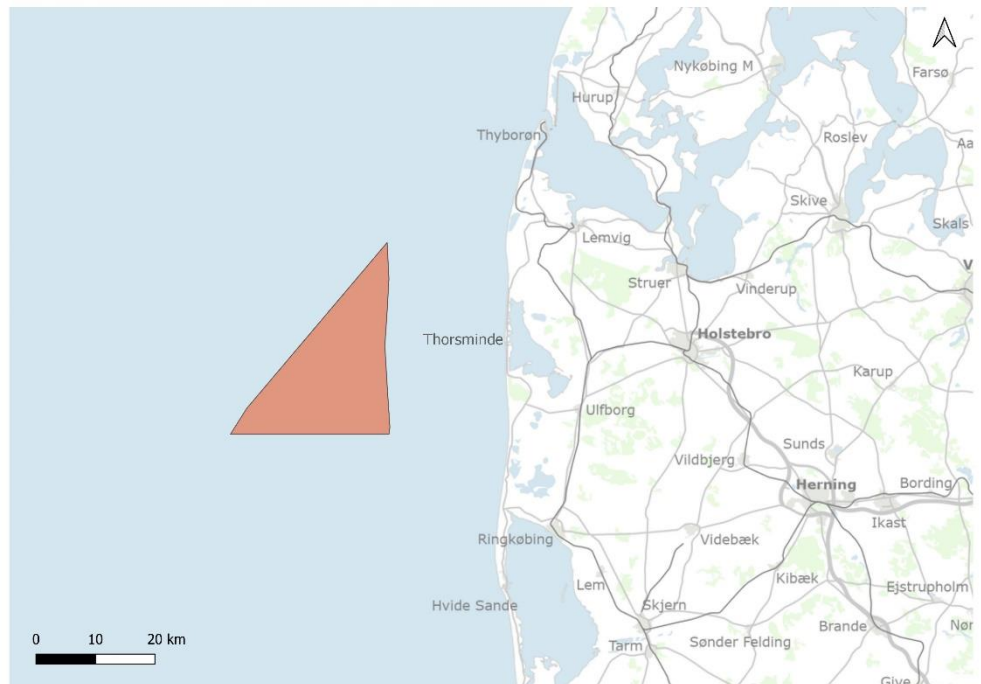


Figure 2-1 Thor OWF AOI outlined in orange.

Table 1 Area of investigation is defined by the given coordinates.

Geodetic reference ETRS89 UTM32N	
EASTING [meter]	NORTHING [meter]
425 953	6 232 328
399 264	6 232 328
402 011	6 236 670
425 649	6 264 590
425 945	6 258 540
425 702	6 253 830
425 266	6 247 230
425 636	6 240 830
426 100	6 233 490

2.2 Scope of Work

The results presented in this report will be part of the Thor tender process, informing development tenderers about the local geology, associated geotechnical properties and potential geo-hazards as well as supporting subsequent development of the OWF. Thus, a key objective of the present work was to ensure the applicability for sub-selection of a specific OWF site within the area of investigation along with initial determination of foundations, risks and layouts.

The integrated geological model comprises a conceptual geological model, a digital, spatial geological model and a geotechnical characterization of the soil units in the model.

The technical work was carried out in three phases addressing the geotechnical stream of data into the model and structured in three aligned work packages, see Table 2-2.

Phases	Phase 1- Geophysical data and CPT	Phase 2 – Geophysical data, CPT and boreholes	Phase 3 – Factual report with laboratory results
WP1 – Spatial 3D ground model – Integrated interpretation	Assess and assign major soil units combined from CPT and seismic data Integrated interpretation of horizons	Assess correlation between Phase 1 interpretation and boreholes, adjust integrated interpretation	Final interpretation Gridding of horizons Create cross- sections
WP2 – Conceptual geological model	Conceptualization of one Geological Model Regional geological setting Initial subdivision of soil units	Subdivision of soil units and zonation Conceptualization of conceptual model	Final adjustment of model and soil zonation
WP3 - Geotechnical characterization of soil units	Initial soil unit framework from CPT data Initial soil description, soil classification and strength/stiffness properties	Final soil unit framework from CPT and borehole data Soil suitability considerations and risk assessments Adjust soil descriptions and classification	Summarize geotechnical parameters for the soil units of the spatial model Establish typical values and variance Final soil classification and strength/stiffness properties

Table 2-2 Overview of the workflow and phases of the technical work.

A separate work package for reporting assured the content of the Integrated Geological Model Report as well as drawings and digital deliverables.

A full list of deliverables can be found in section 10.

3 Basis

Data packages have been received successively from Energinet. Below an overview of the data received as basis from Energinet, divided in the geotechnical and geophysical data packages, as well as reports.

Project datum is ETRS89 (EPSG:4936) using the GRS80 Spheroid. The coordinate system is the UTM projection in Zone 32 N. Units are in meters. Vertical reference is MSL, height model DTU15.

Geotechnical data packages	
Datatype	Quantum
Cone Penetration Test (CPT), seabed, down-the-hole and seismic	67 locations with min. 1 CPT
Boreholes with sampling and geological description	18
P-S logging	4
Factual Geotechnical Report	1

Geophysical data packages	
Datatype	Quantum
Multi-channel Ultra High Resolution Seismic (M-UHRS) Kingdom project – Grid 240 * 1000 m	2420 line-km
Hard disk with results from MMT, including bathymetry (see ref /Ref. /1/)	1

Reports		
Author	Title	Year
Rambøll	800 MW Thor OWF – Geological Desk Study - Geological Model	2019
MMT	Operations Report: Thor Offshore Wind Farm Site Investigation LOT1 - Geophysical Survey	2019

MMT	Geophysical Survey Report: Thor Offshore Wind Farm Site Investigation LOT1	2019
GEO	Thor OWF – Geotechnical Site Investigation 2020 Factual Geotechnical Report	2020

3.1 Geotechnical basis

The geotechnical basis for the project can generally be divided into two categories:

- > Offshore sampling and testing
- > Onshore description and testing

The offshore works have been divided into two site investigation (SI) campaigns; a seabed CPT campaign and a borehole campaign.

The onshore works consist of soil description and classification as well as a comprehensive laboratory test programme.

The work described above has been performed by GEO, and the outcome of the SI's has been documented in Ref. /3/.

3.1.1 Offshore works

The offshore works consist of in-situ testing (seabed, down-the-hole and seismic CPT's), P-S logging and borehole drilling and sampling. The acquired samples are used for testing in the onshore works (laboratory testing programme).

An overview of the positions for CPT – seabed (CPT), down-the-hole (DTH-CPT) and seismic (SCPT) – and boreholes (with sampling) is shown in Figure 3-1 and on Enclosures 1.01 and 1.02.

Several locations across the site have multiple CPT's due to premature CPT refusal, which means that the total no. of unique locations surveyed is 67, i.e. 67 locations with minimum one (1) CPT. Of these 67 locations, 18 locations have been surveyed with minimum one (1) CPT and one (1) borehole, while the remaining 49 have been surveyed with minimum one (1) CPT but no borehole.

The distance between the CPT's and boreholes performed at the same location is generally less than 10 m. Details on this can be found in Ref. /3/.

The offshore works furthermore include geological description, strength testing on cohesive samples using pocket penetrometer and torvane, measurements of moisture content, bulk/dry densities and P-S logging.

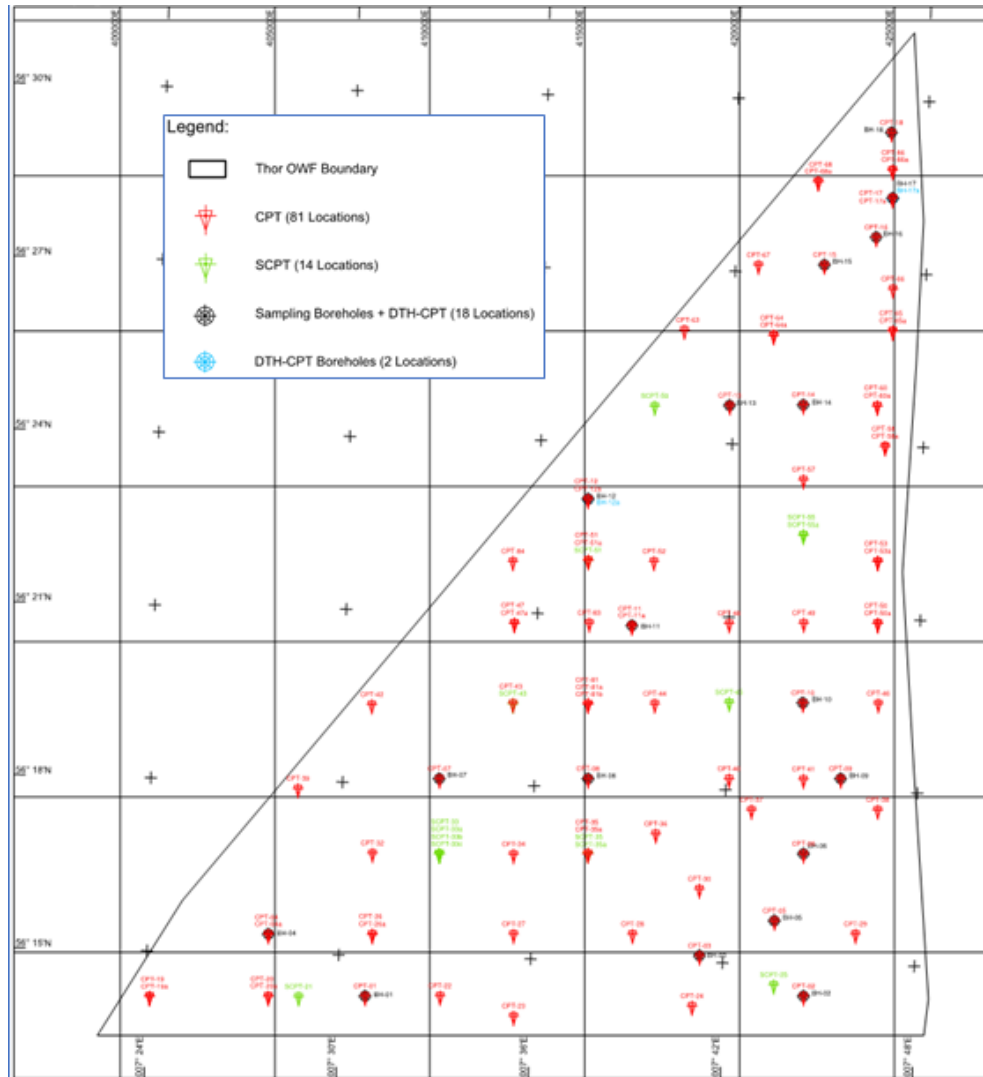


Figure 3-1 Overview of locations for CPT (seabed, down-the-hole and seismic) and borehole (with sampling), from Ref. /3/. Refer to Enclosures 1.01 and 1.02 for full resolution.

3.1.2 Onshore works

The onshore works consist primarily of various classification and laboratory testing, ranging from determination of:

- > Atterberg limits
- > Particle size distribution (PSD) and particle density
- > Maximum/minimum density tests
- > Oedometer (incremental loading, IL)
- > Direct simple shear (DSS)
- > Unconsolidated undrained (UU) triaxial testing

- > Consolidated isotropically drained (CID) triaxial testing
- > Consolidated isotropically/anisotropically undrained (CIU/CAU) triaxial
- > Cyclic triaxial testing (CAUcyc)

All onshore works are performed using samples acquired from the geotechnical borehole campaign, cf. section 3.1.1. As such, these samples are all acquired from one of the 18 locations that have been surveyed with minimum one (1) CPT and one (1) borehole.

The detailed test reports are enclosed in Ref. /3/ and will not be repeated in this report.

3.2 Geophysical and hydrographical basis

The geophysical basis for this report is a geophysical survey (GS) including 2D M-UHRS, acquired in 2019.

The main objectives from this survey were:

- > Acquire and interpret high quality seabed and sub-seabed data for project planning and execution. As a minimum, this includes local bathymetry, seabed sediment distribution, seabed features, seabed obstructions, wrecks and archaeological sites, crossing cables and pipelines and evaluation of possible mobile sediments.
- > Sub-bottom profiling and 2D M-UHRS survey along the survey lines to map shallow geological units
- > Mapping of magnetic targets and to identify infrastructure crossings and large metallic debris
- > Seabed sampling and testing to provide in-situ geological data to support the interpretation of the shallow GS data. In addition, several vibrocore samples were also collected to provide material for subsequent analysis, as part of an Energinet funded marine archaeological study being carried out by Moesgaard Museum, Aarhus Denmark.
- > Ground truthing GS acquisition where necessary to identify potential environmentally sensitive habitats

The work described above and below has been performed by MMT, and the outcome of the SI's has been documented in Ref. /6/

3.2.1 Bathymetry

MBES data were acquired resulting in a bathymetry dataset fully covering the survey area. Bathymetry grids are available in 0.25 m, 1.00 m and 5.00 m resolution.

3.2.2 Subsurface data

The 2D M-UHRS data were acquired with N-S oriented survey lines with a 240 m line spacing and E-W oriented cross lines with 1000 m line spacing (see Figure 3-2).

The initial seismostratigraphic interpretation resulted in mapping of 8 horizons. The mapped horizons correspond to the base of the seismic units of geological significance, exception to be made on one horizon (the deepest one which delineates a top). Two more horizons (seabed and processing last knee e.i. last processing point in the seismic data) were also incorporated into the stacking velocity model and depth-conversion.

Seismic reflectors were selected based on their geological and geotechnical significance and spatial continuity across the site. The individual horizons were picked using a combination of the physical characteristics of the seismic reflectors, seismic facies analysis and reflector terminations. The relevance of the horizons from a sequence stratigraphic standpoint was also a prime consideration.

Furthermore, shallow gas and organic soils were mapped and a number of faults were interpreted

All interpretations are included in a Kingdom Suite project together with processed seismic profiles converted into depth domain (meters).

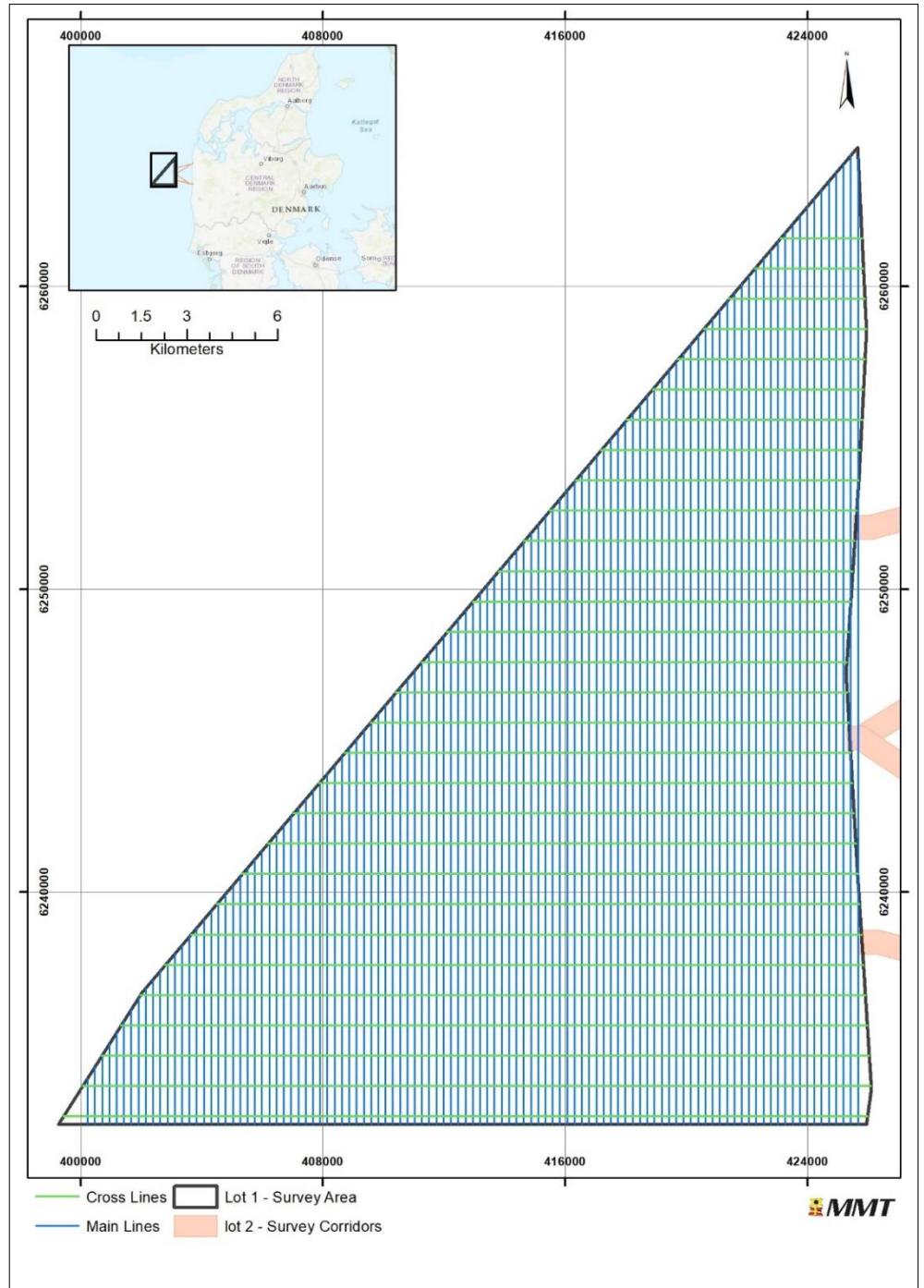


Figure 3-2: Line plan from 2D M-UHRS survey. Ref. /1/. Refer to Enclosure 1.02 for full resolution

4 Geotechnical interpretation

In this section it is described how the geotechnical data has been evaluated to characterise the soils at the site and the layering of soil units at each geotechnical location. The layering and soil characterization interpreted at survey locations has supported the assessment of the stratigraphy across the entire site, cf. section 7.7.

For each geotechnical survey location, a geotechnical interpretation of the stratigraphy has been carried out. This interpretation has considered input from borehole logs, CPT logs (using CPT correlations as presented in section 4.3) and the geophysical data (in order to link geotechnical soil units across the site). For the locations with both borehole and CPT available, two geotechnical interpretations of the stratigraphy have been prepared as the depth of the layer boundaries determined based on the borehole logs and based on the CPT logs differ slightly. For survey locations with multiple CPT's, only one unique interpretation of stratigraphy has been developed. Hence, a total of 85 unique geotechnical interpretation of stratigraphy have been developed, cf. Appendix A. All these interpretations have been applied as input to the integrated geological model.

These stratigraphic interpretations originate from survey locations with:

- *A borehole and minimum one CPT*
 - layer boundaries and soil units determined based on borehole log (18 positions)
layer boundaries determined based on CPT trace and soil units determined based on borehole log (18 positions)
- *Minimum one CPT but no borehole*
 - stratigraphy (soil units and layer boundaries) determined based on CPT trace (49 positions)

The following sections describe the procedure for the geotechnical stratigraphic interpretation in further detail.

4.1 Geotechnical soil unit overview

The development of the soil stratigraphy can generally be divided into two parts; a) based on borehole log descriptions and b) based on CPT classification/correlation.

The work documented in Ref. /3/ can be considered the basis. The soil descriptions provided in the borehole log provide descriptions of soil type/class as well estimates of soil age and depositional environment. Based on this information, several geotechnical soil units have been defined. These soil units are characterized uniquely by the main soil type and the soil age. An overview of the groups of soil type/class and soil age is provided below in Table 4-1.

For the soil age groups 1 and 2, the terms *post-glacial* and *glacial* are used in the geotechnical sense, which essentially means that soil age group 1 (*Post-glacial*) includes all soils that have not been glacially overridden. The consequence is that some of the soils included in soil age group 1 would – from a geological point-of-view – be considered glacial, since they originate from the glacial ages, but have not been glacially overridden.

Table 4-1 Overview of groups for soil type/class and soil age.

Soil type/class groups	Soil age groups
1: Organic	1: Post-glacial
2: Clay	2: Glacial
3: Silt	3: Pre-quaternary
4: Sand	
5: Coarse	
6: Till	

Some soils have been grouped in order to arrive at a classification level which is operational, and which can be used as a basis to establish ranges of soil parameters, see section 5. This also entails a certain degree of simplification in the classification, which in turn suggests that each group inevitably will cover a certain range of soil behaviours. Soil type/class group 5 consists of the coarser soils, such as gravels, cobbles and stones.

The combination of the above groups of soil type/class and soil age, cf. Table 4-1, is used to establish the geotechnical soil units. Not all combinations of soil type/class and soil age result in relevant soil units, e.g. soil type/class group 6 (Till) is not relevant in relation to other than soil age group 2 (Glacial). An overview of the geotechnical soil units has been provided in Table 4-2.

The total no. of unique soil units encountered at the site is 15. The extent (lateral and vertical) of these soil units throughout the site varies extensively.

Based on the stratigraphies described in section 4, the laboratory test data (onshore/offshore) and in-situ data (CPT etc.) have been assigned to one of these 15 geotechnical soil units. Following this exercise, the range of soil parameters has been established for each of the geotechnical soil units. This is further elaborated in section 5.

Table 4-2 Overview of geotechnical soil units.

Soil unit no.	Soil age group	Soil type/class group	Geotechnical soil unit
1	Post-glacial	Organic	PgOrganic
2		Clay	PgClay
3		Silt	PgSilt
4		Sand	PgSand
5		Coarse	PgCoarse
6	Glacial	Clay	GcClay
7		Silt	GcSilt
8		Sand	GcSand
9		Coarse	GcCoarse
10		Till	GcTill
11	Pre-quaternary	Organic	PreQOrganic
12		Clay	PreQClay
13		Silt	PreQSilt
14		Sand	PreQSand
15		Coarse	PreQCoarse

4.2 Stratigraphic interpretation based on borehole log

For survey locations where borehole logs are available (18 positions), the soil stratigraphy has been determined based on these, generally without reinterpretation.

The soil stratigraphy for the survey locations with borehole logs has been used to assign the individual tests of the onshore works (cf. section 3.1.2) to the geotechnical soil units to aid the definition of soil parameters, cf. section 5.

4.3 Stratigraphic interpretation based on CPT

The process of estimating the stratigraphy for all survey locations based on the CPT trace (67 positions) is described in the following steps:

- > Load raw CPT trace data into CPT classification script
- > Calculate additional parameters for soil interpretation and classification
- > Determine soil behaviour type index for each depth with available CPT data
- > Select stratigraphy based on calculated parameters and soil behaviour type index related to depth
- > Define geotechnical soil unit for all defined layers.

For survey locations with a borehole and a CPT (18 positions), some difference is observed in the depth of the relevant boundaries between the borehole log and the CPT trace – this is expected to be caused by the slight offset of the CPT compared to the borehole (up to 10 m laterally). To ensure consistency, a separate stratigraphy has been developed from the CPT trace for these survey locations. However, this stratigraphy essentially matches the stratigraphy obtained from the borehole log in terms of geotechnical soil units, only the depth of relevant layer boundaries has been adjusted to fit the CPT trace.

As such, the procedure described below mainly applies to the survey locations with no borehole (49 positions).

Initially the raw CPT data is loaded into a script designed to classify the soils encountered in the CPT. Some post-processing of the raw data is performed to derive additional parameters required for classifying the soil using the Robertson-method. These parameters are shown below.

- > Corrected cone resistance $q_t = q_c + u_2(1 - a)$
- > Friction ratio $R_f = \frac{f_s}{q_t}$
- > Normalised cone resistance $Q_{tn} = \left(\frac{q_t - \sigma_{v0}}{P_a} \right) \left(\frac{P_a}{\sigma'_{v0}} \right)^n$
- > Stress exponent $n = 0.381 I_c + 0.05 \left(\frac{\sigma'_{v0}}{P_a} \right) - 0.15$
- > Normalised pore pressure $B_q = \frac{u_2 - u_0}{q_t - \sigma_{v0}}$
- > Normalised friction ratio $F_r = \left(\frac{f_s}{q_t - \sigma_{v0}} \right) 100\%$
- > Soil behaviour type index $I_c = ((3.47 - \log Q_{tn})^2 + (\log F_r + 1.22)^2)^{0.5}$

- f_s is the measured CPT sleeve friction
- q_c is the measured CPT cone tip resistance
- u_2 is the measured pore pressure
- u_0 is the hydrostatic pore pressure
- σ_{v0} is the total vertical in situ stress
- σ'_{v0} is the effective vertical in situ stress
- a is the area ratio of the adopted CPT cone
- P_a is the atmospheric pressure

From the available parameters an initial estimation of the soil behaviour type for each layer is made based on different classification methods. Three different classification methods are used for evaluating the variation in the soil behaviour type (SBT):

- > Using soil behaviour type index
- > Using normalised cone resistance and friction ratio
- > Using normalised cone resistance and pore pressure

Based on the measurements in the CPT (cone resistance, sleeve friction and pore pressure) and the estimated SBT, the soil layering can be determined, and the geotechnical soil units can be defined.

Once the soil stratigraphy and the associated geotechnical soil units have been defined, layer specific information can be determined in the post-processing. For each soil layer, the associated CPT data can be used to estimate the strength and stiffness parameters for that specific soil layer. The methods adopted for defining strength and stiffness properties can be found in section 5.

4.3.1 Soil behaviour type index

The estimation of the SBT is based on the soil behaviour type index I_c value using Table 4-3 as seen below. It shall be noted that the correlation between the soil behaviour type index and SBT only applies for SBT zones 2-7, i.e. zones 1, 8 and 9 are not considered here.

This method considers both the normalised cone resistance and the normalised friction ratio, whilst pore pressure is not accounted for.

Table 4-3 Soil behaviour types (SBT) based on I_c .

Zone	Soil Behaviour type	I_c
1	Sensitive, fine grained	N/A
2	Organic soils – clay	> 3.6
3	Clays – silty clay to clay	2.95 - 3.6
4	Silt mixtures – clayey silt to silty clay	2.6 - 2.95
5	Sand mixtures – silty sand to sandy silt	2.05 - 2.60
6	Sands – clean sand to silty sand	1.31 - 2.05
7	Gravelly sand to dense sand	< 1.31
8	Very stiff sand to clayey sand	N/A
9	Very stiff, fine grained	N/A

4.3.2 Normalised cone resistance and friction ratio

SBT is estimated from Ref. /8/ where normalised cone penetration resistance, Q_{tn} , and normalised friction ratio, F_r , are used as basis, cf. Figure 4-1.

As seen from Figure 4-1, information about OCR/age and sensitivity can also be deduced from the plot. However, this type of information shall be treated with some caution, and it has not been used actively to establish geological age or degree of pre-consolidation for the soils.

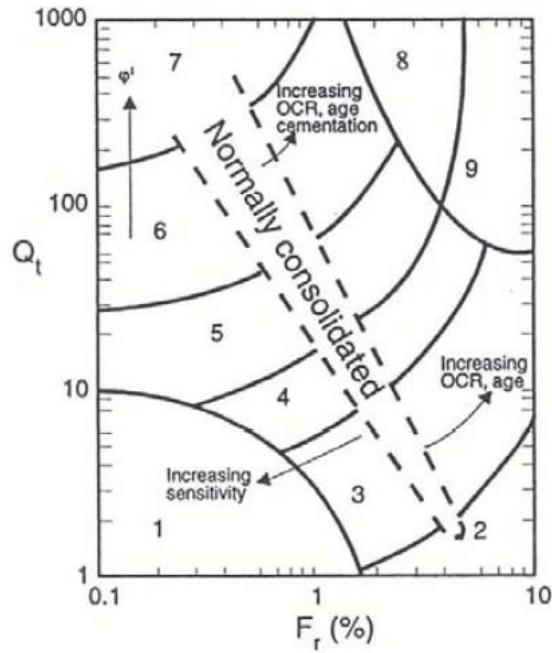


Figure 4-1 Robertson $Q_{tn} - F_r$ classification chart for soil behaviour type, cf. Ref. /8/.

4.3.3 Normalised cone resistance and pore pressure

SBT is estimated based on Ref. /8/ where normalised cone penetration resistance, Q_{tn} , and normalised pore pressure, B_q , are used as basis, cf. Figure 4-2.

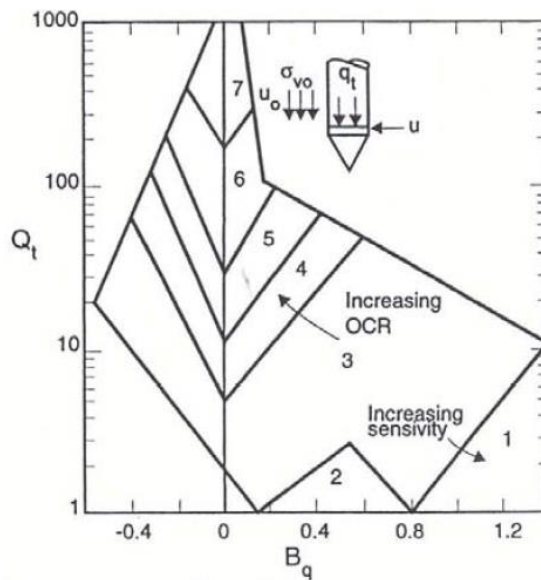


Figure 4-2 Robertson $Q_{tn} - B_q$ classification chart for soil behaviour type, cf. Ref. /8/.

4.4 Classification of soils using CPT

The classification of soils used for the definition of the stratigraphy and the geotechnical soil units based on CPT data is generally performed as described in

section 4.3. However, in this process, certain observations regarding the CPT based classification methods have been made. This is elaborated in the following.

Survey locations with both CPT and borehole can be used to analyse the variations between the soil units defined from the borehole logs and the soil units determined based on the CPT classification methods.

An example is shown in Table 4-4 where the (simplified) stratigraphy from BH-02 borehole log and the stratigraphy derived from CPT-based classification using Ref. /8/ for CPT-02 are compared.

Table 4-4 Comparison of stratigraphy from BH-02 (left) and CPT-02 (right) based on classification methods cf. Ref. /8/.

BH-02			CPT-02		
Top	Bottom	Interpreted soil unit	Top	Bottom	Interpreted soil unit
0.0 m	7.0 m	Postglacial marine sand	0.0 m	12.0 m	Clean to silty sand (mainly SBT = 6)
7.0 m	8.0 m	Postglacial marine clay			
8.0 m	10.0 m	Postglacial marine sand			
10.0 m	11.5 m	Glacial meltwater sand			
11.5 m	48.0 m	Glacial meltwater clay	12.0 m	27.5 m	Silt mixtures, clayey silt to silty clay (mainly SBT = 4)
			27.5 m	49.0 m	Sand mixtures, silty sand to sandy silt (mainly SBT = 5)
48.0 m	58.0 m	Glacial clay till	49.0 m	58.0 m	Sand mixtures, silty sand to sandy silt (mainly SBT = 5)

It is evident that the CPT classification methods struggle to correctly identify glacial clays and tills. This could be associated with the fact that these soils are characterized by relatively high cone tip resistance (averaging up to 10 MPa) combined with relatively low friction ratio (averaging around 1%) – a combination which leads the CPT based classification method to recognize these soils as mixtures of sand and silt, not clays and tills as they have been characterized in the geological description based on the borehole logs.

It must be noted that the CPT classification methods deal with the soil type *behaviour*, which in turn suggest that the *behaviour* of these soils seem to

correspond more to that of a silt/sand mixture rather than clay in the traditional geotechnical understanding.

As such, the CPT based classification shall be treated with caution, and the characterization of soils at survey locations without boreholes shall be aided by geological input and geophysical survey interpretation. For the stratigraphies derived here, the additional information acquired by this comparison of BH logs and CPT based classification has been accounted for.

For the stratigraphies determined for the CPT survey locations, the corresponding CPT data has been visualized in the Robertson $Q_{tn} - F_r$ classification chart for soil behaviour type (similar to Figure 4-1) for selected soil units in Figure 4-3 to Figure 4-5.

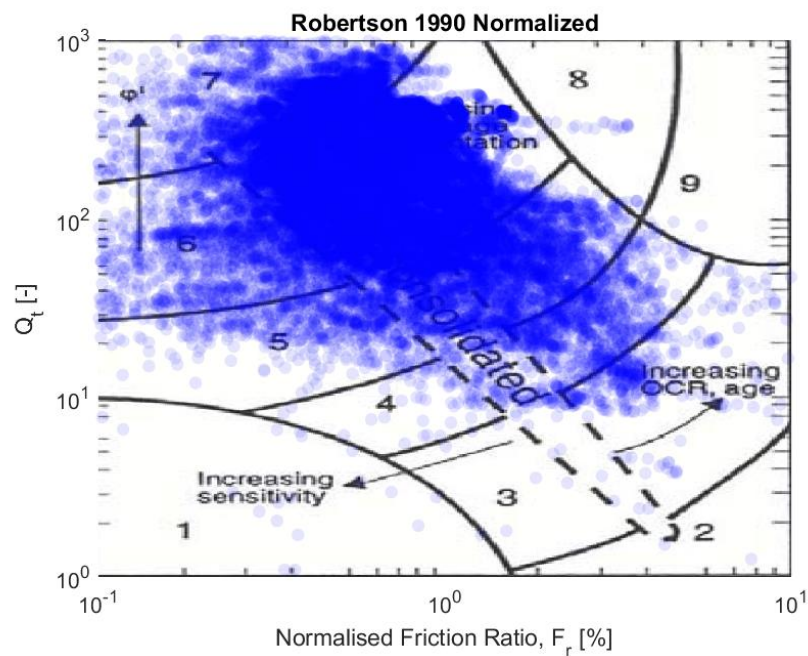


Figure 4-3 Robertson $Q_{tn} - F_r$ classification chart for soil behaviour type plotted for all CPT survey locations for soil unit PgSand.

From Figure 4-3 it is evident that the CPT data for soil unit PgSand plots primarily in SBT zone 6 (*Sands – clean sand to silty sand*) and secondarily in SBT zone 5 (*Sand mixtures – silty sand to sandy silt*) and SBT zone 7 (*Gravelly sand to dense sand*). As such, there is a good correlation between the CPT based classification and the soil behaviour recognized for the soil unit.

The same type of assessment has been conducted for the soils that have been recognized to be more difficult to identify using the CPT based classification methods, see above for details. Further, to remove the inherent bias for the CPT-only survey locations, the assessment has been conducted for two scenarios a) CPT data from survey locations with a corresponding borehole and b) CPT data from all survey locations. This is shown in Figure 4-4 and Figure 4-5.

It is evident that the CPT data for the glacial clays and tills (soil units GcClay and GcTill) plot mainly in SBT zone 4 (*Silt mixtures – clayey silt to silty clay*) and secondarily in SBT zone 5 (*Sand mixtures – silty sand to sandy silt*). This conclusion holds for both the CPT data for all survey locations as well the CPT data exclusively from survey locations with a corresponding borehole, where the soil stratigraphy and soil unit distribution has been established using the borehole log. This furthermore suggests that that the assignment of soil units for CPT-only survey locations based on the interpretation of the CPT data is relatively consistent with the assignment of soil units done for the survey locations covered by both a CPT and borehole with geological description.

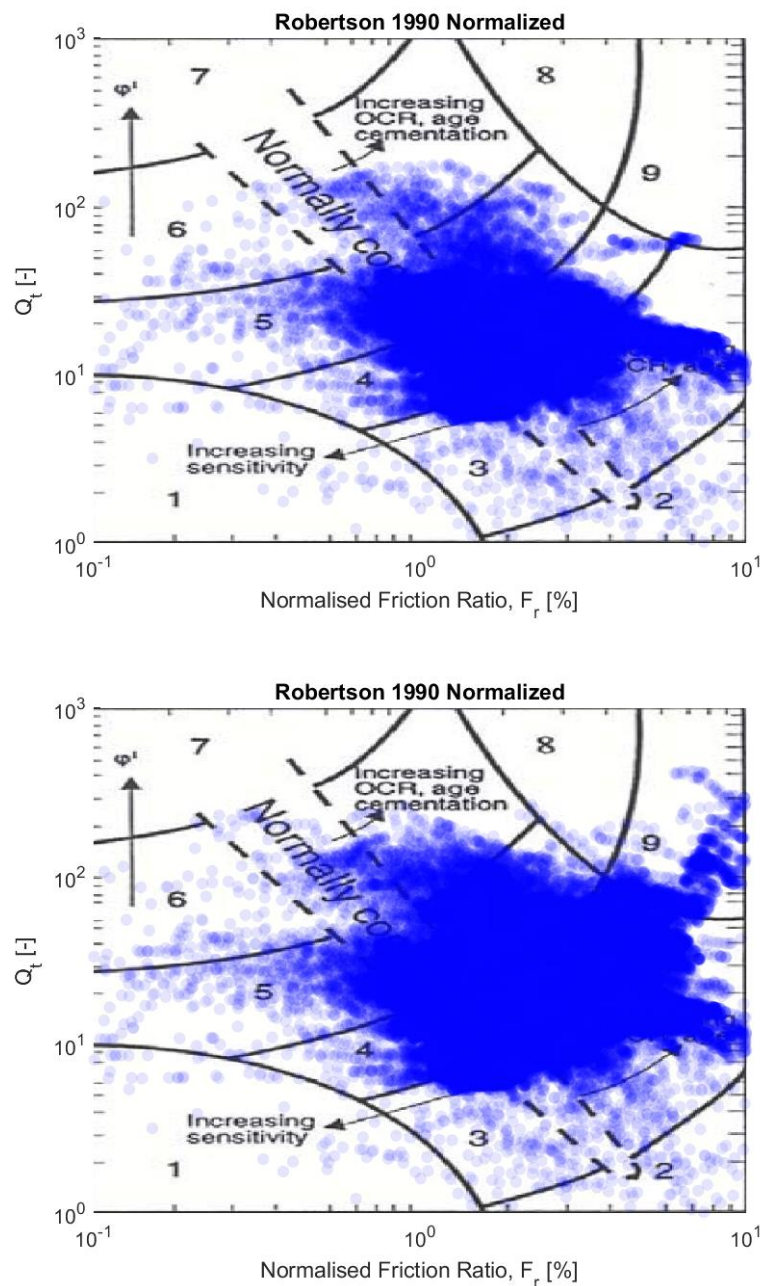


Figure 4-4 Robertson $Q_{tn} - F_r$ classification chart for soil behaviour type for soil unit GcClay plotted for CPT survey locations with a corresponding borehole (upper) and for all CPT survey locations (lower).

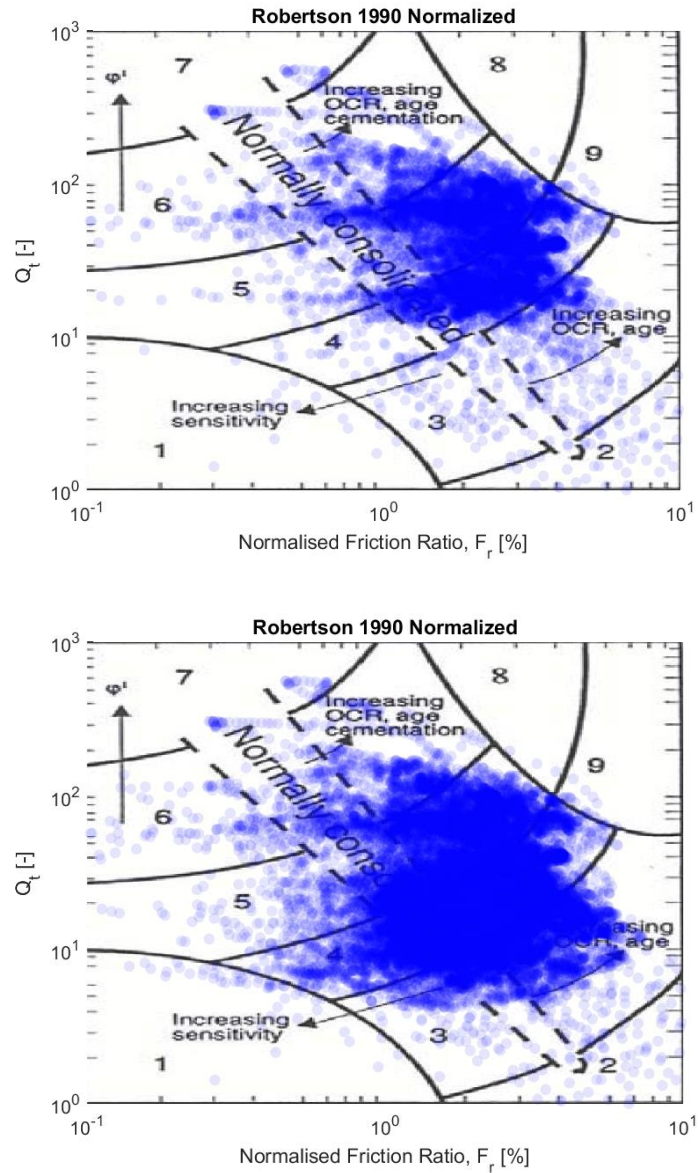


Figure 4-5 Robertson $Q_{tn} - F_r$ classification chart for soil behaviour type for soil unit GcTill plotted for CPT survey locations with a corresponding borehole (upper) and for all CPT survey locations (lower).

5 Geotechnical properties and variance

Following the definition of soil layers and stratigraphy based on CPT and borehole data outlined in section 4, this section addresses the determination of geotechnical properties and the variance of these including the assignment of these properties to the geotechnical soil units.

The determination of geotechnical properties is based on both CPT correlations, cf. Ref. /8/, and onshore laboratory test data, cf. Ref. /3/. For the CPT data, the geotechnical properties are determined on established correlations, while the properties derived on the basis of the onshore laboratory testing is taken as-is from the outcome of the testing – no additional interpretation has been imposed on the laboratory testing.

The use of CPT correlations to derive soil parameters is an efficient way of assessing the soil characteristics without the need for soil sampling and subsequent onshore laboratory testing. It must however be emphasized that these correlations shall ideally be benchmarked using results from testing of soil specimens under controlled laboratory conditions. The assessed soil properties based on the CPT correlations are shown for all CPT survey locations in Appendix B.

The relevant geotechnical properties that will be assessed in the following can be divided into three categories:

- > State properties
- > Strength properties
- > Stiffness properties

Table 5-1 provides an overview of the parameters that will be determined incl. the data sources considered for each of these. The focus is to provide estimates for traditional soil parameters incl. the expected ranges of variation for the different soil units. These parameters shall provide an estimate of the soils ability to withstand loads and to provide a general understanding of the deformation characteristics of the soil.

In addition, an overview of the ranges of classification, strength and stiffness properties per soil unit are presented in section 5.4.

Table 5-1 Overview of geotechnical properties.

Category	Soil property	Data source
State	Over-consolidation ratio	CPT correlation
	Relative density	CPT correlation
Strength	Undrained shear strength	CPT correlation Triaxial testing (CAU, CIU, UU) Direct Simple Shear (DSS) Pocket penetrometer
	Friction angle	CPT correlation Triaxial testing (CID)
Stiffness	Small-strain shear modulus	CPT correlation Seismic CPT (SCPT)

5.1 Presentation of CPT properties

As outlined in section 5, the soil parameters are derived partly using CPT correlations and partly using results from onshore laboratory testing.

This section presents the data from the CPT's across the site. The results are presented per geotechnical soil unit, following the stratigraphies derived for the CPT survey locations as outlined in section 4.

Based on these defined stratigraphies, the corresponding CPT data has been grouped. Figure 5-1 to Figure 5-4 show examples of range of variation of basic parameters such as CPT cone resistance and CPT friction ratio for selected geotechnical soil units. These figures show that generally each defined soil unit has a consistent trend in the variation of CPT parameters with depth. However, some scatter are seen in the friction ratio for unit PgClay (Figure 5-1), the cone tip resistance and the sleeve friction at shallow depth for unit PgSand (Figure 5-2), the sleeve friction for GcClay (Figure 5-3) and the sleeve friction for GcTill (Figure 5-4). Generally, a larger spread for the CPT sleeve friction compared to the CPT cone resistance is as expected. The large scatter in the cone tip resistance at shallow depths for unit PgSand is considered to likely be caused by interbedded fine-grained layers. Hence, the variation of CPT parameters presented in Figure 5-1 to Figure 5-4 are considered to confirm the classification of soil units.

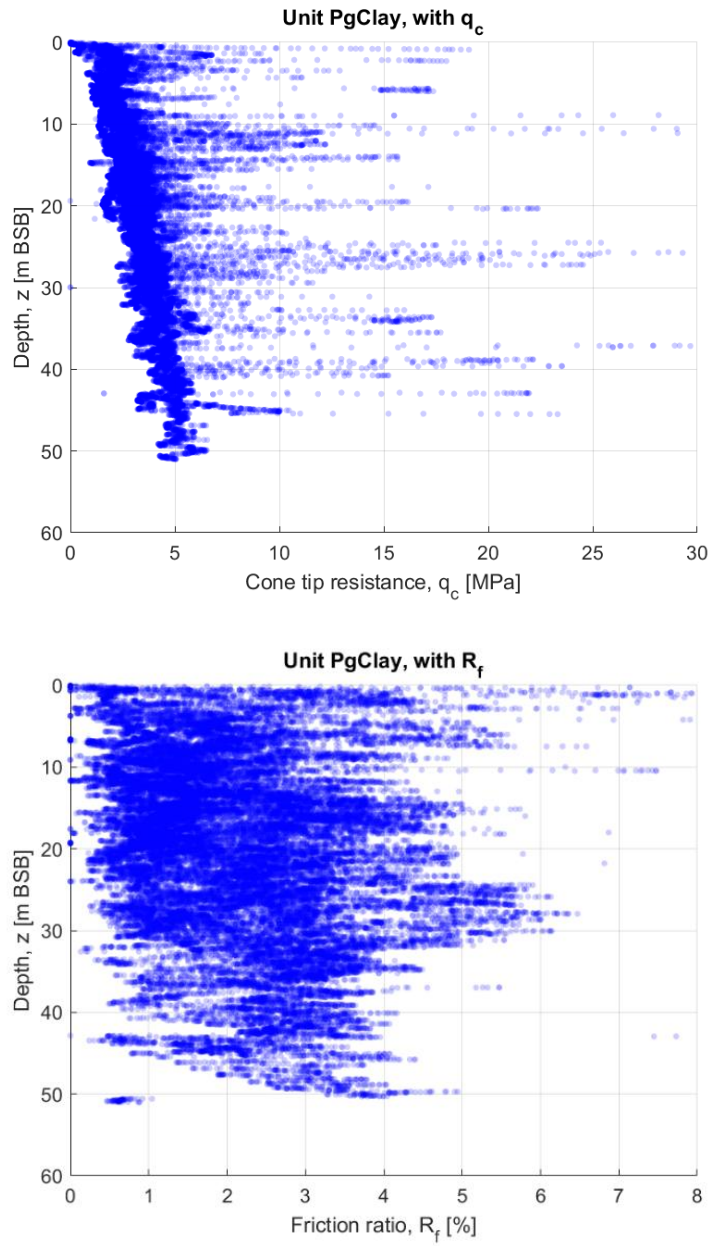


Figure 5-1 Range of q_c (upper) and R_f (lower) for soil unit PgClay.

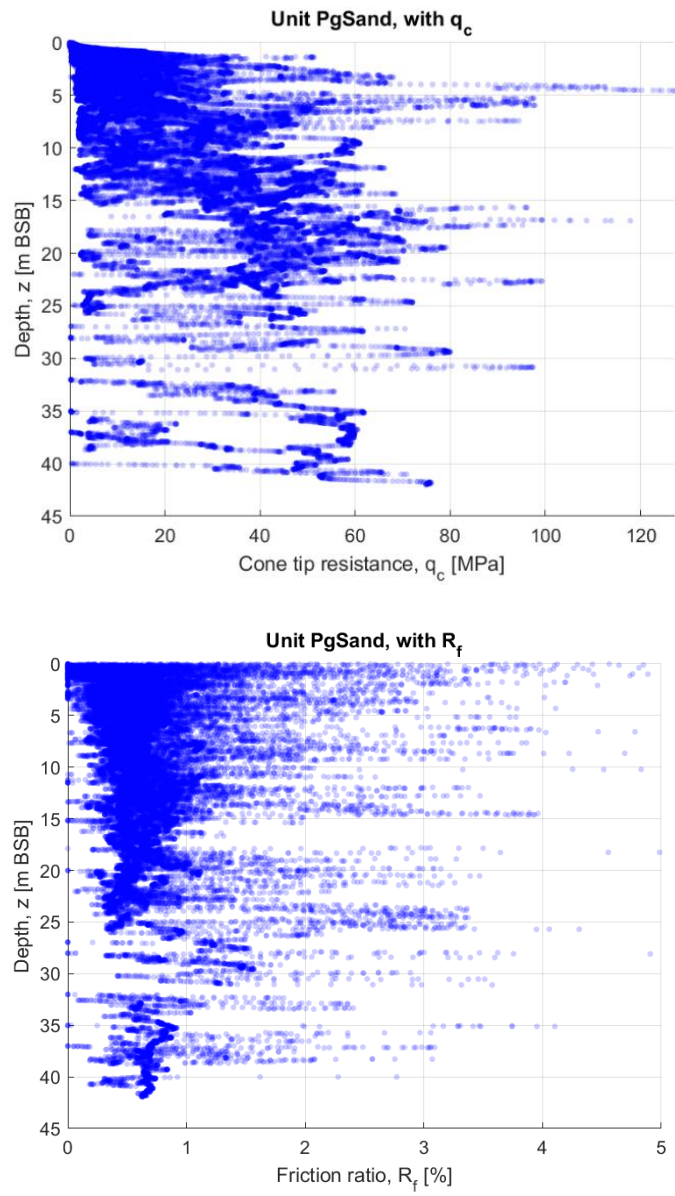


Figure 5-2 Range of q_c (upper) and R_f (lower) for soil unit PgSand.

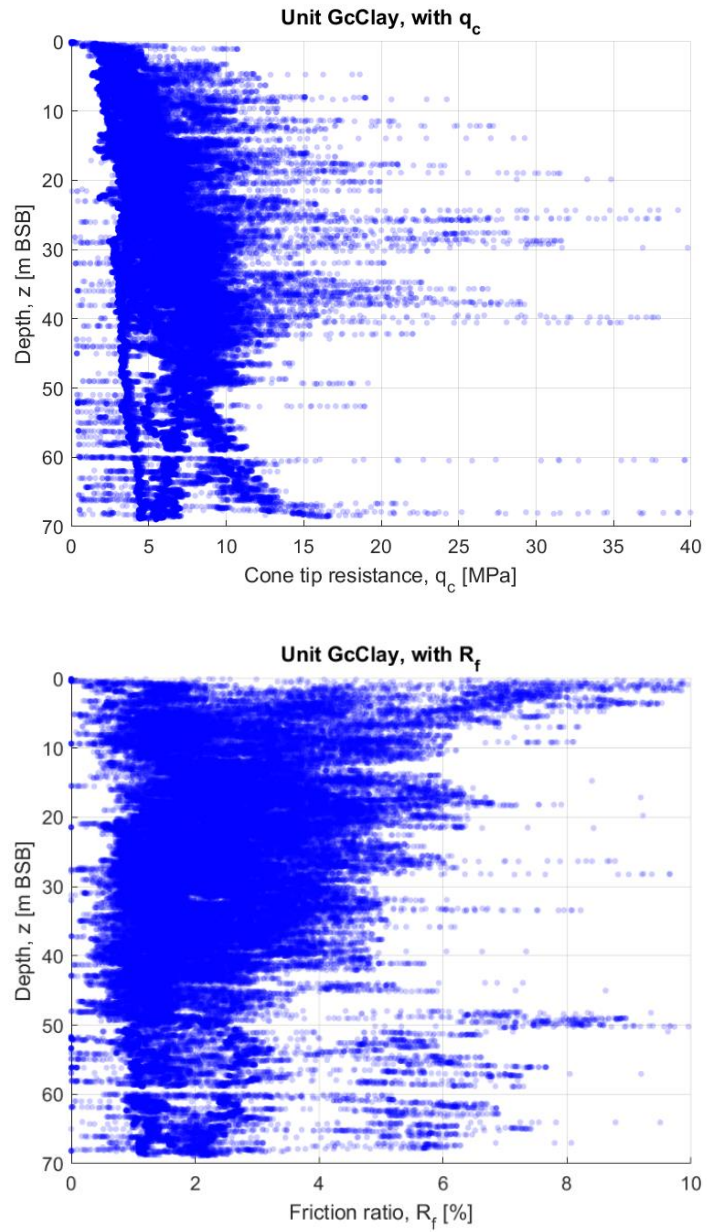


Figure 5-3 Range of q_c (upper) and R_f (lower) for soil unit GcClay.

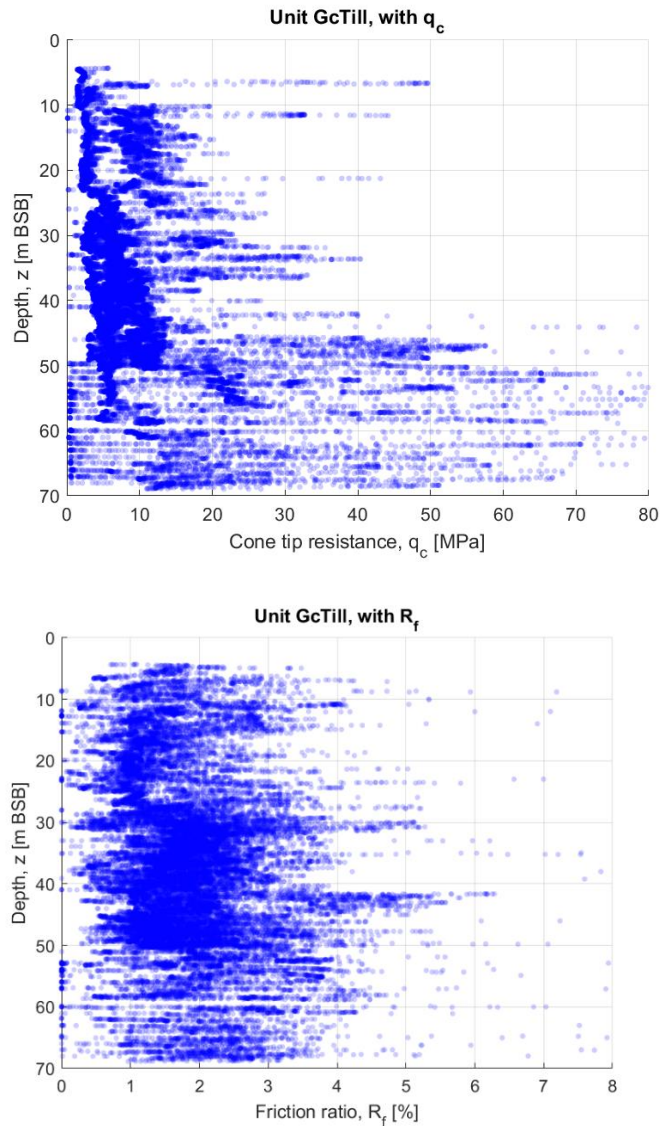


Figure 5-4 Range of q_c (upper) and R_f (lower) for soil unit GcTill.

5.2 Presentation of state properties

As outlined in section 5, state parameters such as over-consolidation ratio (for cohesive soils) and relative density (for non-cohesive soils) have been determined from CPT correlations.

The assessment of these parameters serves as input to the overall understanding of the in-situ soil state, which is a crucial parameter to assess the general soil behaviour. This section presents the method adopted for the analyses of these parameters as well as the outcome.

The over-consolidation ratio, OCR, is determined for cohesive soils as:

$$OCR = k \left(\frac{q_t - \sigma_{v0}}{\sigma'_{v0}} \right)$$

For the non-cohesive soils, the relative density, I_D , is calculated as:

$$I_D = \frac{100}{2.91} \ln \left(\frac{q_t}{205 (\sigma'_m)^{0.51}} \right)$$

The variation of these parameters is shown for selected soil units in Figure 5-5 and Figure 5-6.

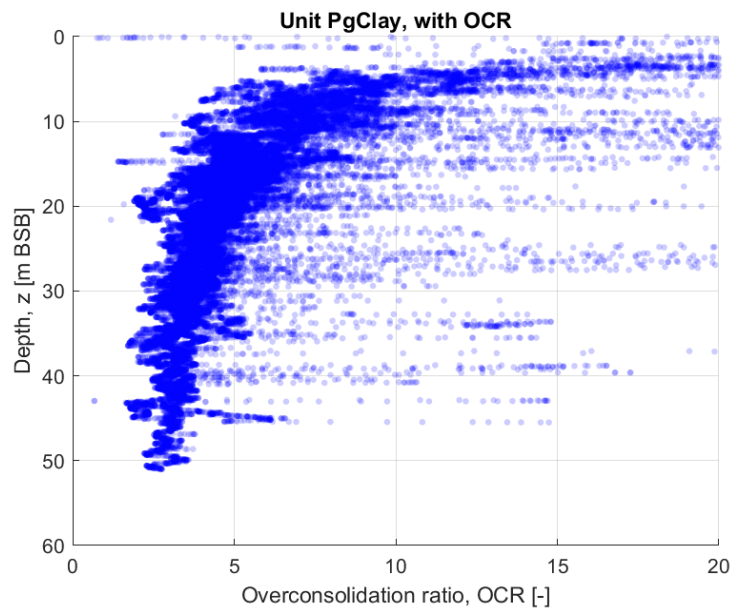


Figure 5-5 Range of OCR for soil unit PgClay.

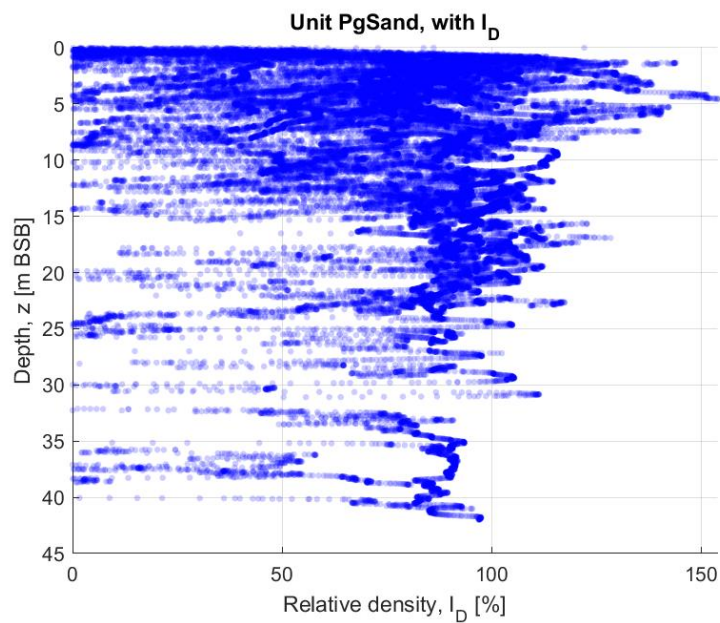


Figure 5-6 Range of I_D for soil unit PgSand.

5.3 Presentation of strength and stiffness properties

Following the state parameters described in section 5.2, strength and stiffness parameters such as undrained shear strength (for cohesive soils), friction angle (for non-cohesive soils) and small-strain shear modulus (all soils) have been determined from CPT correlations, cf. Ref. /8/, supplemented by onshore laboratory testing, cf. Ref. /3/.

The assessment of these parameters serves as input to the overall understanding of the soil behaviour during loading, e.g. in relation to placement of wind turbine foundations or jack-up operations on the site. This section presents the method adopted for the analyses of these parameters as well as the outcome.

The results originating from CPT analyses have been used to visualize the variation of soil strength and stiffness for selected soil units across the site. This method adopts local CPT data correlated to soil strength and stiffness properties to indicate the variation of the specific parameter throughout the site by determining local values for each survey location. This is shown in Enclosures 2.03 to 2.12.

In order to determine just one representative value (soil strength/stiffness) per soil unit per survey location, the average value for soil unit is determined. When deriving the average value for the soil layer, the peaks and troughs in the CPT trace (usually found close to the layer boundaries) are removed to avoid that this data impacts the average value too much, i.e. to obtain the most representative value.

5.3.1 Friction angle

The friction angle, φ , is calculated for non-cohesive soils according to Ref. /8/:

- $$\varphi'_p = 17.6 + 11 \log_{10} \frac{q_t/P_a}{(\sigma'_{v0}/P_a)^{0.5}}$$

Further to the CPT correlation, the friction angle is obtained through triaxial testing, CID. Using CPT data for all survey locations as well as the available laboratory test data, the range of friction angle for soil unit GcSand is shown in Figure 5-7.

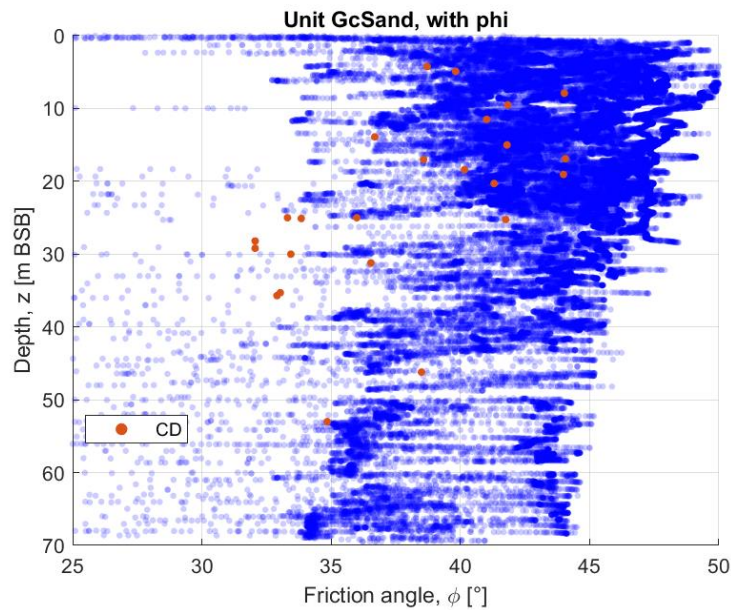


Figure 5-7 Range of ϕ for soil unit GcSand using CPT correlation and laboratory test results (CD – Consolidated Drained triaxial test).

5.3.2 Undrained shear strength

The undrained shear strength, c_u , is determined for cohesive soils according to Ref. /8/ as:

- $$c_u = \frac{q_t - \sigma'_{v0}}{N_{kt}} = \frac{q_{net}}{N_{kt}}$$

For determination of undrained shear strength, a cone factor of $N_{kt} = 20$ has been applied for all soils.

Further to the CPT correlation, the undrained shear strength is obtained through triaxial testing, namely consolidated anisotropically undrained (CAU) tests, consolidated isotropically undrained (CIU) tests and unconsolidated undrained (UU) tests, as well as direct simple shear (DSS) tests. Using CPT data for all survey locations as well as the available laboratory test data, the range of undrained shear strength for selected soil units is shown in Figure 5-8 and Figure 5-9.

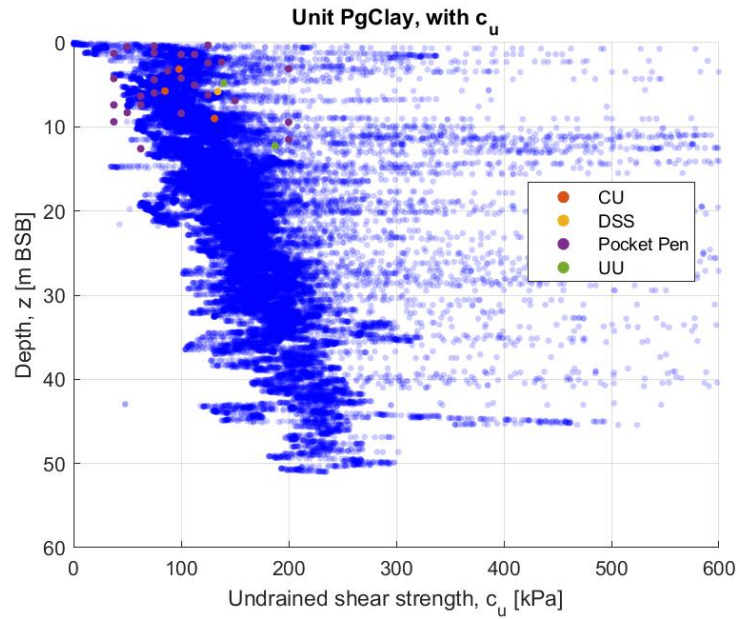


Figure 5-8 Range of c_u for soil unit PgClay using CPT correlation and laboratory test results. (CU denotes consolidated isotropically undrained triaxial tests).

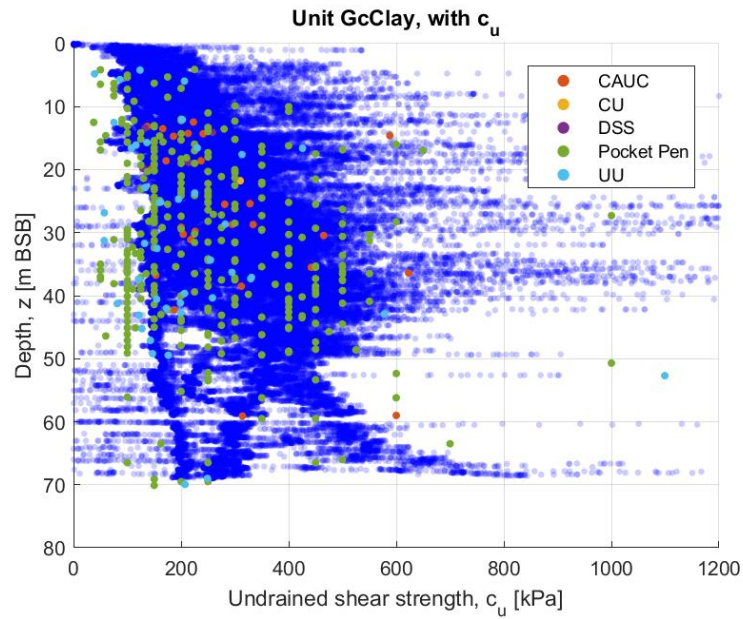


Figure 5-9 Range of c_u for soil unit GcClay using CPT correlation and laboratory test results. (CU denotes consolidated isotropically undrained triaxial tests).

5.3.3 Small-strain shear modulus

The small-strain shear modulus, G_{max} , is determined all soils as:

- $G_{max} = \rho V_s^2$

The V_s value for non-cohesive soils is determined according to Ref. /8/ as:

- $V_s = 277 q_c^{0.13} \sigma'_{v0}{}^{0.27}$

For cohesive soils, the V_s value is determined according to Ref. /8/ as:

- $$V_s = (10.1 \log q_c - 11.4)^{1.67} \left(\frac{f_s}{q_c}\right)^{0.3}$$

Further to the CPT correlation, the small-strain shear modulus is obtained through seismic CPT (SCPT). Using CPT data for all survey locations as well as the available SCPT data, the range of small-strain shear modulus for selected soil units is shown in Figure 5-10 and Figure 5-11.

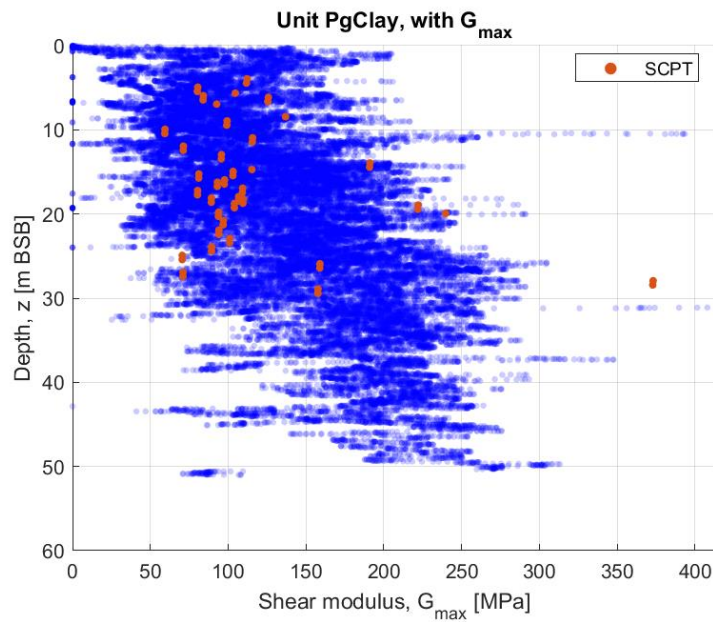


Figure 5-10 Range of G_{max} for soil unit PgClay using CPT correlation and SCPT results.

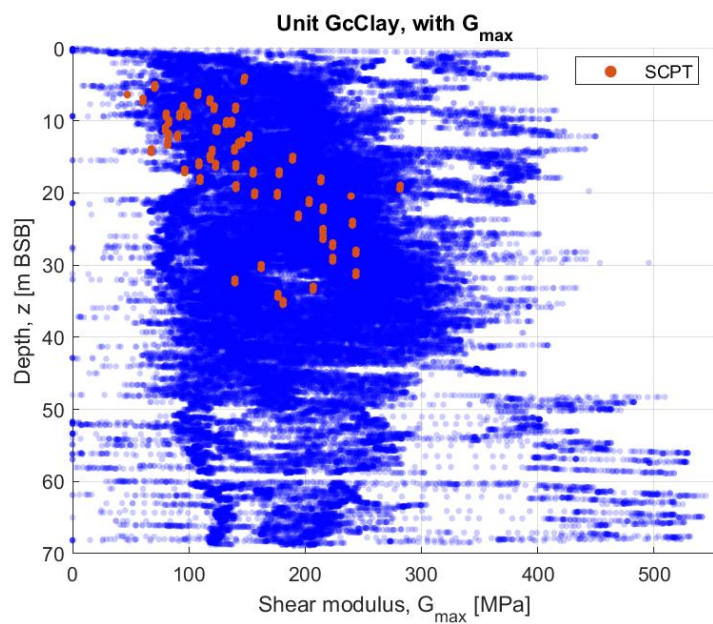


Figure 5-11 Range of G_{max} for soil unit GcClay using CPT correlation and SCPT results.

5.4 Range of soil parameters per soil unit

In this section the range and average values (covering the full site) of classification, strength and stiffness parameters are presented for each of the soil units, cf. Table 4-2.

5.4.1 Range of classification parameters per soil unit

In Table 5-2, Table 5-3 and Table 5-4, the range, average value and number of data (tests) for measured classification parameters are presented for each soil unit.

Table 5-2 Range of measured classification parameters for fine-grained soil units from laboratory tests. Results provided as minimum/average/maximum (number of tests).

Parameter	PgOrganic	PgClay	GcClay	GcTill	PreQClay
Moisture content [%]	35/86/239 (7)	12/24/35 (30)	9/31/747 (372)	9/13/22 (71)	19/31/50 (53)
Bulk density [Mg/m ³]	1.14/1.53/1.82 (4)	1.68/1.93/2.17 (6)	1.52/1.97/3.14 (82)*	2.01/2.22/2.77 (14)	1.46/1.79/1.96 (10)
Dry density [Mg/m ³]	0.34/0.9/1.34 (4)	1.35/1.61/1.91 (6)	1.12/1.58/2.49 (82)*	1.66/1.96/2.51 (14)	1.12/1.38/1.56 (10)
Liquid limit, w_L [%]	46/46/46 (1)	21/31/48 (6)	20/49/78 (71)	19/29/47 (14)	40/66/107 (13)
Plastic limit, w_p [%]	20/20/20 (1)	10/14/20 (6)	12/20/27 (71)	9/13/19 (14)	23/33/46 (13)
Plasticity index, I_p [-]	25/25/25 (1)	9/17/28 (6)	8/29/55 (71)	10/16/30 (14)	16/33/60 (13)
Uniformity coefficient [-]	-	-	13/13/13 (1)	4/46/87 (4)	2/2/2 (1)
Loss of ignition [%]	4/15/31 (3)	1/4/7 (3)	2/5/8 (9)	-	11/14/20 (5)
CaCO ₃ content [%]	13/13/13 (1)	6/7/7 (3)	14/16/18 (2)	6/11/17 (5)	1/1/1 (1)

**Two tests are disregarded due to outliers with unrealistically high values.*

Table 5-3 Range of measured classification parameters for silt from laboratory test. Results provided as minimum/average/maximum (number of tests).

Parameter	PgSilt	GcSilt	PreQSilt
Moisture content [%]	19/26/34 (11)	17/23/28 (19)	8/28/38 (10)
Bulk density [Mg/m ³]	1.95/1.98/2.02 (2)	1.7/1.81/1.92 (2)	1.89/1.89/1.89 (1)
Dry density [Mg/m ³]	1.57/1.61/1.64 (2)	1.42/1.48/1.53 (2)	1.5/1.5/1.5 (1)
Liquid limit, w_L [%]	30/35/46 (3)	32/36/40 (2)	63/63/63 (1)
Plastic limit, w_p [%]	16/17/19 (3)	17/18/18 (2)	38/38/38 (1)
Plasticity index, I_p [-]	13/18/27 (3)	15/19/23 (2)	25/25/25 (1)
Uniformity coefficient [-]	-	-	-
Loss of ignition [%]	2/3/6 (3)	-	8/8/8 (1)
CaCO ₃ content [%]	15/15/15 (1)	-	4/4/4 (1)

Table 5-4 Range of measured classification parameters for coarse-grained soil units from laboratory test. Results provided as minimum/average/maximum (number of tests).

Parameter	PgSand	GcSand	PreQSand	PreQCoarse
Moisture content [%]	17/25/29 (5)	10/25/124 (15)	16/36/105 (12)	94/94/94 (1)
Bulk density [Mg/m ³]	-	-	1.54/1.78/1.99 (3)	-
Dry density [Mg/m ³]	-	-	1.25/1.43/1.63 (3)	-
Liquid limit, w_L [%]	22/50/90 (3)	56/57/58 (3)	38/48/57 (3)	-
Plastic limit, w_p [%]	14/20/29 (3)	18/19/21 (3)	21/25/28 (3)	-
Plasticity index, I_p [-]	8/30/61 (3)	37/37/37 (3)	17/23/31 (3)	-
Uniformity coefficient [-]	2/8/90 (22)	1/4/30 (31)	1/16/167 (13)	-
Loss of ignition [%]	6/6/6 (1)	2/12/38 (4)	1/9/29 (5)	43/43/43 (1)
CaCO ₃ content [%]	0/2/7 (20)	0/2/3 (4)	0/0/0 (1)	-

5.4.2 Range of strength parameters per soil unit

In Table 5-5 and Table 5-6, the range, average value and number of data (tests) for measured strength parameters are presented for each soil unit. Note, that in Table 5-5 and Table 5-6 only measured data from laboratory tests are presented. Variation of the strength parameters across the site based on CPT interpretation is shown in Enclosures 2.03, 2.05, 2.07, 2.09 and 2.11.

Table 5-5 Range of measured undrained shear strength from laboratory test. Results provided as minimum/average/maximum (number of tests).

Test type	PgOrganic	PgClay	GcClay	GcTill	PreQClay
CAU [kPa]	-	-	137/288/623 (26)	325/660/1053 (5)	141/279/416 (2)
CIU [kPa]	-	85/105/131 (3)	310/310/310 (1)	-	-
DSS [kPa]	-	134/134/134 (1)	129/179/258 (5)	-	358/358/358 (1)
Pocket Penetrometer [kPa]	13/15/25 (5)	38/97/200 (27)	38/256/1000 (327)	25/433/950 (54)	100/366/600 (38)
UU [kPa]	-	140/163/187 (2)	39/211/1099 (43)	49/522/1374 (8)	104/104/104 (1)

Table 5-6 Range of measured friction angle from laboratory test. Results provided as minimum/average/maximum (number of tests).

Test type	PgSand	GcSand	PreQSand	PreQCoarse
CID [°]	32/37/46 (6)	32/38/44 (24)	33/38/46 (9)	36/36/36 (1)

5.4.3 Range of stiffness parameters per soil unit

In Table 5-7, Table 5-8 and Table 5-9, the range, average value and number of data (tests) for small strain shear modulus are presented for each soil unit. Note, that in Table 5-7, Table 5-8 and Table 5-9 only measured data from seismic CPT's are presented. Variation of the small strain shear modulus across the site based on CPT interpretation is shown in Enclosures 2.04, 2.06, 2.08, 2.10 and 2.12.

Table 5-7 Range of measured small strain shear modulus for fine-grained materials. Results provided as minimum/average/maximum (number of tests).

Test type	PgOrganic	PgClay	GcClay	GcTill	PreQClay
SCPT [MPa]	-	59/116/373 (67)	47/147/282 (114)	46/68/97 (30)	-

Table 5-8 Range of measured small strain shear modulus for silt from laboratory test. Results provided as minimum/average/maximum (number of tests).

Test type	PgSilt	GcSilt	PreQSilt
SCPT [MPa]	48/85/130 (12)	74/196/336 (34)	-

Table 5-9 Range of measured small strain shear modulus for sand from laboratory test. Results provided as minimum/average/maximum (number of tests).

Test type	PgSand	GcSand	PreQSand	PreQCoarse
SCPT [MPa]	7/135/374 (67)	47/184/371 (22)	-	-

6 Geological Setting

In this section the geological setting for the Thor OWF area is presented. The geological sequence encountered are dominated by Quaternary sediments but also Neogene sediments prevail within the uppermost 100 m.

6.1 Pre-Quaternary Geology

In the Danish sector of the North Sea Basin, the pre-Quaternary surface varies between Upper Cretaceous Chalk in the northeast, and Paleogene and Neogene sedimentary units towards the central part of the sector (Figure 6-1). In the region west of Jutland, where Thor OWF is situated, the pre-Quaternary sediments are of Miocene age, and are generally composed of marine and fluvial sand, silt and clays often rich in mica.

In the period from Oligocene to late Miocene, the North Sea Basin filled up with deltaic sediments, building out from eroding rivers on the Scandinavian Shield. In late Miocene, subsidence of the North Sea Basin caused a transgression of the Atlantic Ocean and marine sediments were deposited across the North Sea Basin.

The transition between Quaternary deposits and the underlying Miocene deposits is observed over a wide depth interval within the Thor OWF area - from only a few meters below seabed (m bsb) in the northern part to more than 160 m bsb in the southwestern part.

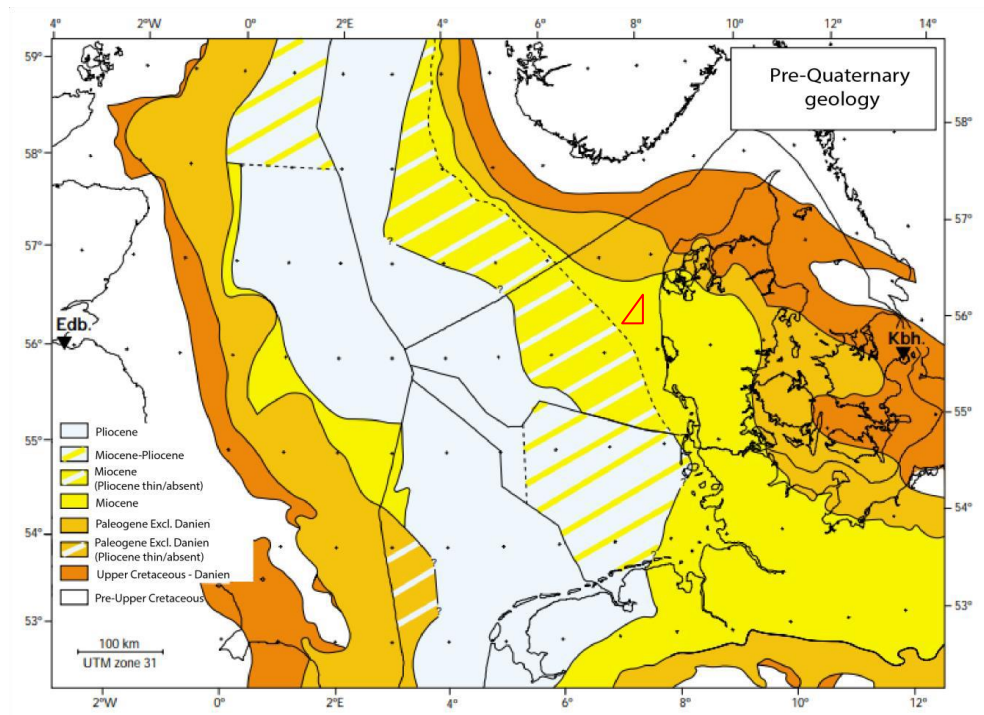


Figure 6-1 Pre-Quaternary geology of the North Sea Basin. The Thor OWF area is shown in red colour where Miocene sediments pre-vail. Ref. /9/.

6.2 Quaternary Geology

The base of the Quaternary is in large parts of the North Sea Basin characterized by deep paleo-valleys cutting deeply into pre-Quaternary layers. Such buried valleys are also present in the Thor OWF area. These valleys were carved by advancing glaciers or by meltwater discharge and often follow weak zones in the Pre-Quaternary sediments. Figure 6-2 illustrates a mapping of buried Quaternary valleys, cutting deep into the pre-Quaternary sediments. The valleys are filled up with glacial, interglacial and late glacial sediments. The thickest Quaternary deposits in the area are registered within these paleo-valleys and are often, but not always, related to depressions in the present-day bottom relief. Thor OWF is situated in an area where several deep buried valleys are mapped. In the central part of the Thor OWF investigation area, at least one large N-S oriented valley is observed, see Figure 6-2.

During the Quaternary period, the Fennoscandian Ice Shield expanded south into the North Sea Basin and the Danish area on several occasions. These glaciations eroded the pre-Quaternary surface and deposited glacial till and glaciogenic (deglaciation and meltwater) sediments. During the Elsterian and Saalian glacial periods, the glaciers caused glaciotectonic deformation of older deposits.

The Saalian glaciation consist of several glacier advances of which the earliest (Drenthe Stadial in Early Saalian) covered the entire Danish area. The subsequent advances from east in Middle Saalian (Warthe Stadial) is likely to have reached the area of Thor OWF, but the literature is unclear at this point (Ref. /10/ and Ref. /11/). The Saalian glaciation was followed by the Eemian interglacial period. The climate was warmer and more humid than today and coastal areas in Denmark were flooded by the Eemian Sea. The sea level rose, flooded the low-land areas and deposited clay-rich sediments with high organic content. During the subsequent Weichselian glacial period, only the eastern and northern part of Denmark was covered by the Fennoscandian ice sheet.

During this Weichselian glaciation, the Thor OWF area was ice-free and covered by a proglacial riverplain and/or relict Saalian moraine plateaus. On the proglacial riverplain, glaciofluvial sand and gravel was deposited in proglacial lakes, meltwater streams and rivers. It cannot be ruled out that the northernmost part of the OWF area was covered by the Weichselian ice sheet as the exact maximum extent of the ice sheet is uncertain in present offshore areas. No Weichselian sub-glacial sediments are however identified in the Thor OWF, but meltwater sediments with associated debris eroded the sediments from previous glaciations and have been deposited as sheets of glaciofluvial sediments.

The Weichselian maximum glacial extend of the Fennoscandian Ice Sheet, occurred approximately 23,000-20,000 years BP, followed by a subsequent deglaciation of the Danish area. The geological history of the Danish area during and after deglaciation was controlled by the interplay between deglaciation, glacio-isostatic rebound, and rise in global sea level due to the release of meltwater from ice sheets across the northern hemisphere.

During the decline of the glaciers, increased melting of the ice sheets released large volumes of meltwater, causing global sea level rise and inundation of deglaciated areas. However, isostatic rebound caused most of the southern North Sea Basin, including Thor OWF area to rise and stay above sea level. From 11,000 to 6,000 years BP a continued global transgression affected the area, and the entire North Sea Basin was slowly inundated. The area around the Thor OWF changed from being land to a marine area, where the old glacial landscape was eroded and transformed. The flooded sediments were now exposed to erosion and with time covered by marine sand. Details on relative sea level changes during the Late Weichselian and Holocene are can be found in Ref. /2/

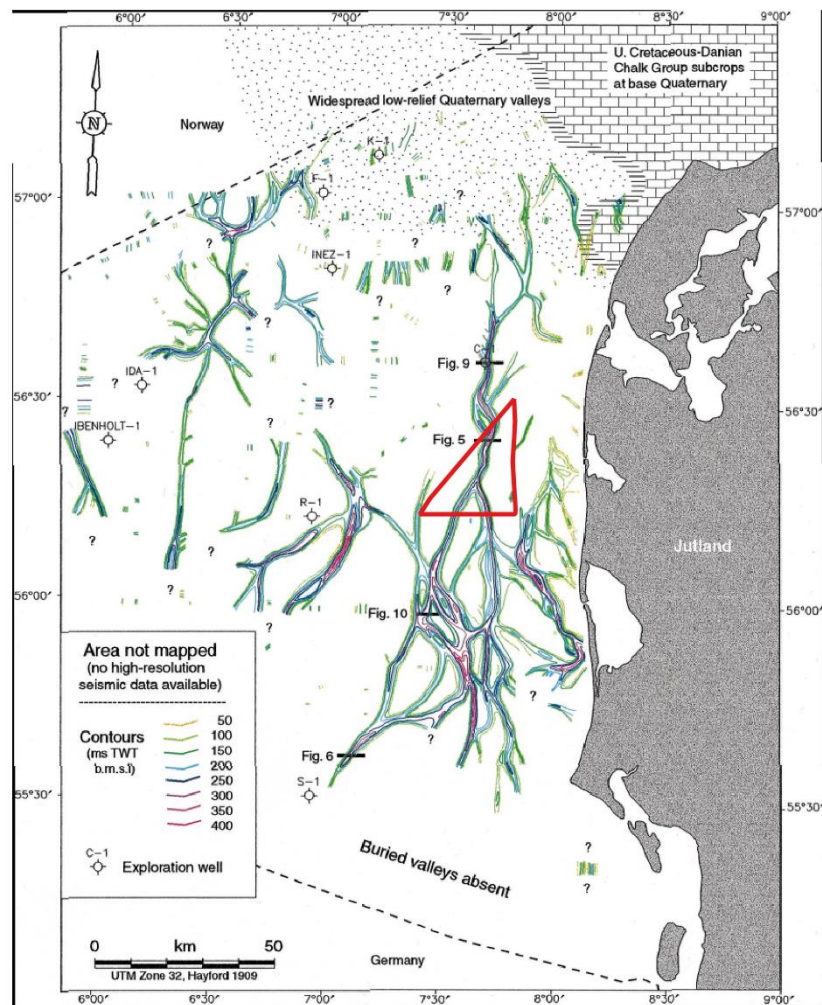


Figure 6-2 Buried Quaternary valleys in the eastern part of the North Sea Basin and through the Thor OWF shown in red. Ref. /12/.

7 Integrated Geological Model

Based on the initial seismic interpretations (Ref. /1/) of the seismic data further interpretations have been made. Boreholes and CPT's have been included resulting in an integrated 3D geological model described in this section.

7.1 Datum, coordinate system and software

The model is set up with datum ETRS89 (EPSG:4936) and the GRS80 Spheroid.

The coordinate system used is the UTM projection in Zone 32 N. Units are in meters. Vertical reference is MSL, height model DTU15.

The software used for interpretations was the IHS Markit Kingdom suite 2019. The M-UHRS seismic data were imported in SEG-Y format together with the geotechnical data. Horizons (geological layer boundaries) have been interpreted directly along clear reflectors in the seismic data. Finally, results have been exported as grids for visualization. The grids include layer boundaries as well as grid calculations such as depth below seabed and vertical thickness of layers.

7.2 Assessment of existing geophysical model

The layers in the existing M-UHRS-based geophysical model were generally interpreted along some of the most clear and continuous reflectors that separate the main layers. However, especially in the glacially overridden areas the clear impact of glacial deformation made it necessary to make the interpretation more detailed. This has to a high degree been based on the integration of the geotechnical data (CPTs and boreholes) which has led to a subdivision from the initial 9 layers to a total of 16 layers.

An overview of the resulting model layers in the integrated geological model is presented in Table 7-1. Original layer names (unit numbers) have been kept in the updated model to allow easier comparison to the existing geophysical model.

Though the layer names have been kept for the initial layers, description and stratigraphic interpretation of the different layers has been updated.

Table 7-1 Overview of the resulting layers/units in the updated model and their origin.

Layer	Status
U10	No changes
U13	New
U18	New
U20	Updated
U21	New
U29	No changes to horizon, renamed from U31
U30	No changes

Layer	Status
U34	New
U40	Updated
U45	Updated
U46	New
U47	New
U50	Updated
U59	New
U98	Updated
U99	No changes

7.3 Interpolation and adjustment of surfaces

Interpretation of the seismic data are made along lower boundaries of the layers (layer base). However, for easier application of the integrated geological model in a geotechnical context, the upper boundaries of the layers (layer top) are visualized on the enclosures instead of the layer base. The gridded layer tops are presented in depth below seabed (m bsb). The method of changing interpretation from layer base to layer top, poses a risk of creating incomplete horizons since one layer can have multiple other layers as top. In order to accommodate this, layer tops were calculated in a "math on two maps" calculator in Kingdom, using a "bottom up" approach for each layer. In this way, the layer base is compared with any horizons lying above it in the stratigraphy. Any horizons lying above the investigated layer, will then be calculated as the top, where the base of the layer is present.

Gridding of layer boundaries was done using a Flex-gridding algorithm. Cell size was set to 5x5 m and maximum distance to data was set to 125 meters (a little more than half the distance between survey lines) in order to fill the gaps between the survey lines.

7.4 Uncertainty in the grid

According to Ref. /1/ the vertical resolution of the seismic data is 0.4 m within the first 40 m below seabed and 1 m for more than 40 m below seabed. In reality, the resolution change is more gradual with depth. From the vertical resolution, the lateral resolution can be estimated to generally better than 2 m in the upper 10 m below seabed assuming a dominant frequency of 1000 Hz and velocities of 1800 m/s or smaller.

The cell size of 5x5 m of the grids is chosen to continue the setup of the original model by MMT and in line with the lateral resolution of the seismic data. Interpolation distance chosen for grids to be continuous across gaps between survey lines. The cell size of the grid fits well along the seismic lines where the uncertainty is low. However, for locations far from the closest seismic line

(distance between main lines is 240 m) the cell size is relatively small and may indicate a higher certainty than the actual seismic data density provides. The uncertainty becomes larger as the distance to the seismic lines increases independent of cell size and it is therefore important to note the location of the seismic lines when working with the grids in detail.

7.5 Depth conversion

The seismic data was converted from two-way-time (TWT) to depth in the processing and interpretation process (Ref. /1/). The standard procedure is to create a preliminary interpretation based on the first processing iteration of the data. An iterative process is then carried out in order to obtain the most suitable interval velocity for each seismic unit in order to build the stacking velocity model. Root mean square (RMS) velocity curves are generated through interactive velocity analysis for all lines and is then used in the further processing.

All further interpretation carried out on the data, was performed in the time domain. RMS velocities were then extracted for the given seismic layer, which was then converted to depth in the extended math calculator in the Kingdom software, using time and RMS velocity. This was done in order to ensure that interpretations were available both in the time and in the depth domain, should any further work be needed.

7.6 Potential geohazards from shallow gas and organic-rich deposits

Seismic signature from organic-rich deposits have been identified in many of the Holocene layers, most abundant in U13, which has been mapped as a layer primarily consisting of gyttja (see section 7.7.3) confirmed by BH 4. Scattered organic content has also been interpreted in some of the Late Pleistocene layers; U29, U30, U34, U45. Extent of organic-rich deposits is indicated on Enclosure 6.01 which correlates well with the extend of U13 seen on Enclosure 3.02 and 4.02.

Seismic signature of shallow gas has been identified in distinct areas across the site. It is primarily seen within channel fill deposits of U50. Extent of shallow gas is indicated on enclosure 6.02 which correlates well with the extend of U50 seen on Enclosure 3.13 and 4.13.

7.7 Stratigraphy

From the integrated interpretation, 16 individual stratigraphic layers have been identified in the Thor integrated geological model, all based on seismic facies changes in the M-UHRS data and geotechnical information. Table 7-2 shows a stratigraphic overview of the identified layers.

Layer base's have been interpreted along clear seismic reflectors, or across clear changes in seismic facies, which are interpreted to represent a change in lithology. The layers have been named based on their base horizon. This implies that an older layer has a higher horizon number, as this is placed deeper in the stratigraphic successions. Geotechnical data and borehole logs, cf. section 4, have guided interpretations and have, in some cases, been the driving factor for the interpretation. The stratigraphic interpretation has been grouped into overall chronostratigraphic assemblies, comprising a pre-Quaternary, a glaciated Pleistocene and a non-glaciated Pleistocene/Holocene assembly. The term 'glaciated' refers to layers which have been overridden by a glacier. The chronostratigraphic assemblies correspond respectively to the geotechnical soil age groups: Pre-Quaternary, Glacial, Post-glacial (See section 4.1).

Correlation of the geological model with the geotechnical soil units is presented in in Table 7-2. Here it can be seen that many of the layers appear to be complex in geotechnical sense since they consist of a range of different soil types. In many cases the complexity can be explained by gradual lithological transitions within the different layers. That is especially the case for the layers U30, U40, U50 and U99. For other layers such as U20 the content appears more varying.

Table 7-2 Overview of all layers in the Integrated Geological Model including overall geological description and corresponding geotechnical units. Blue colour corresponds to non-glaciated Pleistocene/Holocene assembly, orange colour corresponds to glaciated Pleistocene assembly, violet colour corresponds to Pre-Quaternary assembly. Geotechnical soil units in bold indicate main lithology.

Layer	Thickness	Depth below seabed (top of layer)	Extend	Seismic facies	Lower Bounding Surface (Base Horizon)	Geotechnical soil units	Estimated geological age	Depositional environment
U10	0-5m	0	Across the whole site	Semi-transparent facies with no clear reflectors and a weak amplitude	Erosive, Wave cut ravinement surface and is mostly flat (H10)	Pg Sand , Pg Coarse, Pg Silt, Pg Clay	Holocene and recent	Open marine deposition
U13	0-8m	0-4m	Channel feature in west and central part	Semi-transparent facies with continuous laminated reflectors. A strong continuous base reflector	Erosive, channel (H13)	Pg Organic , Pg Clay	Holocene	Lacustrine or enclosed estuarine marine (lagoon/fjord)
U18	0-25m	0-2m	Limited area to the north	Semi-transparent to chaotic. Some internal undulated reflectors	Erosive, irregular (H18)	Pg Clay	Holocene	Marine
U20	0-12m	0-4m	To the north, south-east and south-west,	Semi-transparent to chaotic towards the base. Some	Erosive, irregular (H20)	Pg Sand , Pg Clay, Pg Silt	Holocene (/ Late Pleistocene (Weichselian))	Marine (and possibly glaciofluvial)

Layer	Thickness	Depth below seabed (top of layer)	Extend	Seismic facies	Lower Bounding Surface (Base Horizon)	Geotechnical soil units	Estimated geological age	Depositional environment
			and in minor patches in central part of the site	internal continuous reflectors of strong amplitude				
U21	0-18m	0-20m	Limited area to the north	Semi-transparent to strong continuous sub-parallel reflectors	Erosive, channel (H21)	Pg Sand	Late Pleistocene (Weichselian)	Glacial lacustrine
U29	0-8m	0-10m	In the south-west	Chaotic with strong amplitudes. Strong discontinuous internal reflectors.	Erosive, irregular surface, relatively planar (H29)	Pg Sand	Late Pleistocene (Weichselian)	Glaciofluvial
U30	0-25m	0-10m	In the south-east	Transparent seismic facies with weak semi-parallel reflectors. Some internal reflectors display a stronger amplitude, with a more chaotic appearance	Erosive but nearly conformable in many areas (H30)	Pg Clay, Pg Sand, Pg Silt	Late Pleistocene (Eemian)	Marine

Layer	Thickness	Depth below seabed (top of layer)	Extend	Seismic facies	Lower Bounding Surface (Base Horizon)	Geotechnical soil units	Estimated geological age	Depositional environment
U34	0-10m	2-14m	In the south-west	Transparent facies with few internal reflectors	Erosive, irregular surface, relatively planar (H34)	Pg Clay, Pg Sand	Late Pleistocene (Eemian)	Marine
U40	0-55m	0-30m	In the south-east	Continuous parallel wavy reflectors of strong amplitude. The unit has a laminated appearance	Conformable, irregular and undulated (H40)	Pg Clay, Pg sand, Pg Silt	Middle Pleistocene (Saalian)	Glaciolacustrine
U45	0-45m	0-17m	In the south-west	Chaotic facies with discontinuous reflectors of strong amplitude. Towards the top of the unit, fainter reflectors or transparent	Erosive, irregular surface, relatively planar. Flat based channel (H45)	Pg Sand	Middle Pleistocene (Saalian)	Glaciofluvial
U46	0-20m	0-60m	In the south-east and in an east-west going channel to the north	Chaotic seismic facies with dis-continuous or semi-continuous reflectors of strong amplitude	Erosive, irregular and undulated (H46)	Gc Till, Gc Clay	Middle Pleistocene (Saalian - Warthe)	Sub-glacial

Layer	Thickness	Depth below seabed (top of layer)	Extend	Seismic facies	Lower Bounding Surface (Base Horizon)	Geotechnical soil units	Estimated geological age	Depositional environment
U47	0-35m	0-40m	In the central part of the site	Faint chaotic and discontinuous reflectors with some areas with strong reflectors	Erosive, irregular and undulated (H47)	Gc Sand, Gc Silt	Middle Pleistocene (Saalian)	Glaciofluvial (+ glaciolacustrine)
U50	0-140m	0-60m	North-south going swath in the central and eastern part of the site	Wavy continuous reflectors of strong amplitude. Deformation and faulting are evident especially towards the base. Parallel, sub-horizontal lamination towards the top locally	Erosive, irregular, carved channels (H50)	Gc Sand, Gc Clay, Gc Silt	Middle Pleistocene (Saalian)	Glaciolacustrine, glaciofluvial
U59	0-165m	0-133m	North-south going swath in the western part of the site	Wavy semi-continuous reflectors of strong amplitude. Deformation and faulting are evident throughout the unit	Erosive, irregular, carved channels (H59)	Gc Sand, Gc Clay, Gc Silt	Pleistocene (Saalian or older)	Glaciolacustrine, glaciofluvial, sub-glacial

Layer	Thickness	Depth below seabed (top of layer)	Extend	Seismic facies	Lower Bounding Surface (Base Horizon)	Geotechnical soil units	Estimated geological age	Depositional environment
U98	0-170m	0-165m	Found in all of the area except in a north-south going swath in the northern and central part.	Chaotic to semi-continuous reflectors with moderate to strong amplitudes. Wavy or deformed reflectors cut off by faulting	Erosive, highly irregular (T99)	Gc Clay, Gc Sand, Gc Till, Gc Silt	Pleistocene (Saalian or older)	Sub-glacial, glacial fluvial, glaciolacustrine, marine
U99	N/A	0 to >170m	Entire site	Planar and continuous reflectors with moderate to strong amplitudes. Wavy or deformed reflectors are terminated by faulting	(None)	PreQ Sand, PreQ Clay, PreQ Silt	Miocene	Marine/deltaic

7.7.1 Pre-Quaternary assembly

The pre-Quaternary assembly is composed of the layer U99 and is a composite of Miocene marine clays and silts (See Table 7-2). Coarser material is also to be expected within U99, however the seismic facies of this layer is highly complex, making it impossible to distinguish individual lithological layers within the pre-Quaternary assembly. Strong continuous reflectors are seen in some parts of the layer, especially towards the top. The pre-Quaternary surface is found down to approx. 170 m bsb (Enclosure 3.16, 4.18, Figure 7-1 and Table 7-2), deepest in the southern part of the site, and outcrops on the seabed in small patches within the northern part of the site.

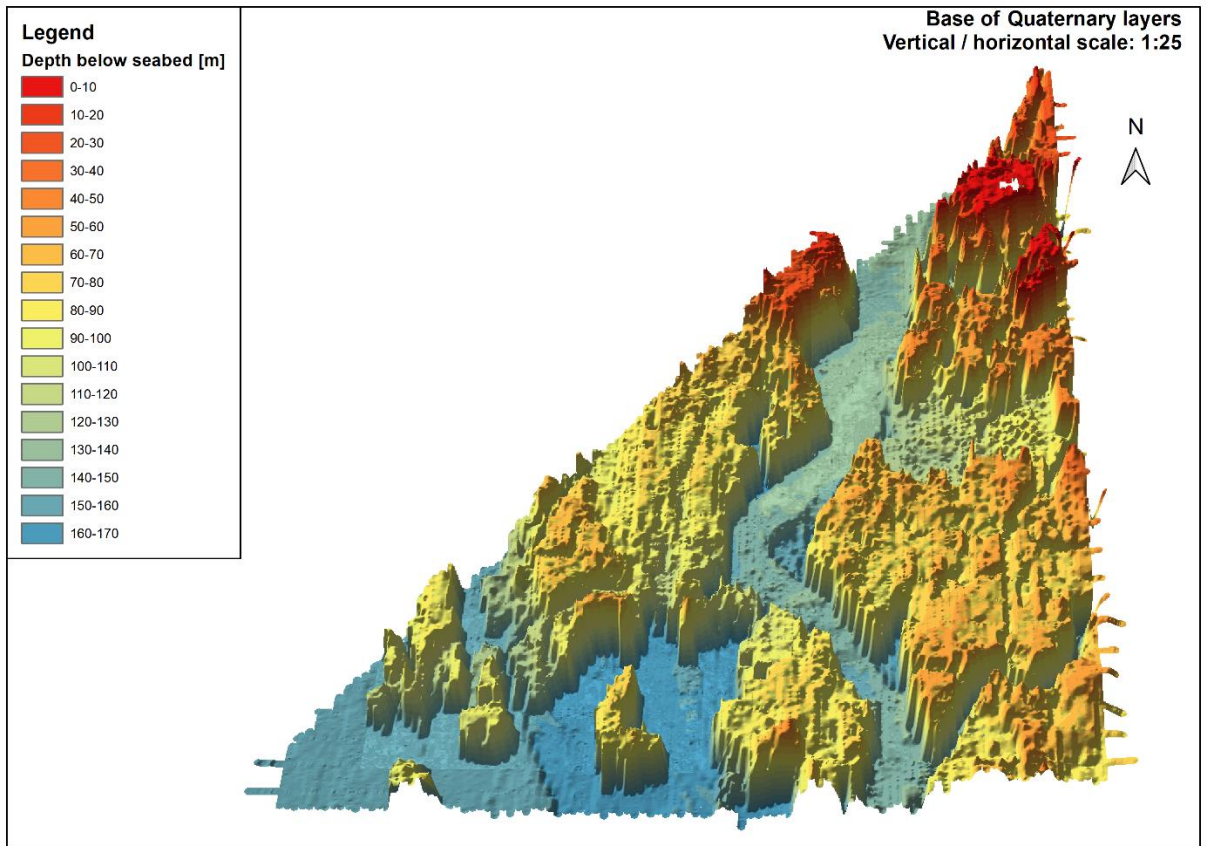


Figure 7-1 3D visualization of the top of the Miocene deposits (base of Quaternary).

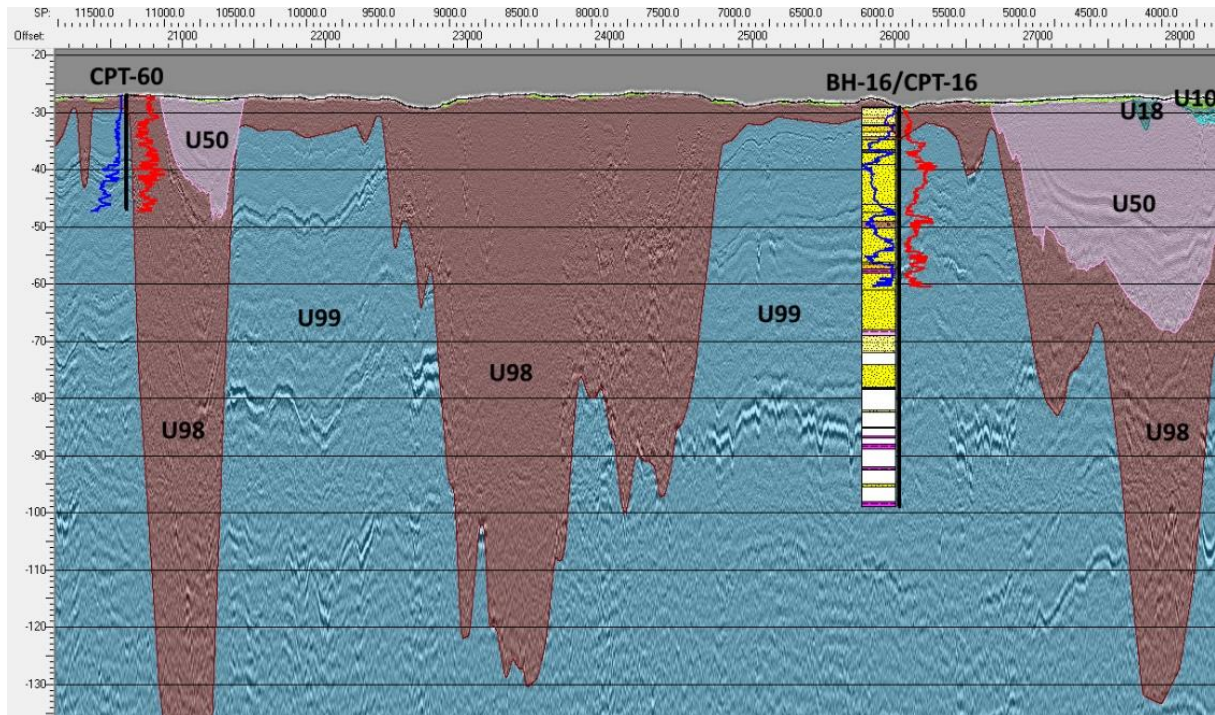


Figure 7-2 South-to-North oriented seismic section from survey line 25200 in the northern part of the site illustrating the shallow undeformed Miocene deposits of U99 surrounded by deep reaching mixed Pleistocene deposits in U98. Blue curve from the CPT shows cone tip resistance (q_c) and red curve sleeve friction (f_s).

7.7.2 Glaciated Pleistocene assembly

The Early to mid-Pleistocene assembly is composed of several stratigraphic layers. Common for this assembly is that the layers have been overridden by later glaciations after deposition. Therefore, the sediments in most cases appear to be deformed. The assembly is composed of the layers U98, U59, U50, U47 and U46. Layer U98 consists of old glacial deposits, which are difficult to divide into individual lithological or chronological layers due to extensive deformation (Table 7-2). This layer is interpreted to be deposited during the Early Saalian glacial period or during one of the earlier glaciations, which is otherwise well documented in the North Sea. The soils are described as a mixture of mostly sub-glacial tills and glaciofluvial meltwater deposits, such as gravel, sand and clays. Layer U98 is found at depths down to 165 m bsb (Enclosure 3.15 and Table 7-2) and outcrops on the seabed in scattered patches across the site.

The layers U59 (see Figure 7-7) and U50 (see Figure 7-3) display a high level of erosion into the older glacial layers (U98) and into the pre-Quaternary assembly as well. The base of the U50 and U59 layers comprise the erosional base of two large north-south trending paleo-valleys through the Thor OWF site. Paleo-valleys like these are well described in the North Sea area and are believed to originate from glacial activity eroding the pre-Quaternary and older Quaternary surfaces (Figure 6-2). The layers of U50 and U59 comprise infill of channels. Borehole samples from the upper parts of U50 and U59 show lithologies to consist of sand and clay (Table 7-2) however, the deepest parts of the layers

could consist of coarser material such as gravel and till due to infill process (Ref. /2/). The channels are interpreted as belonging to the glaciated assembly as U50 is in part of the area directly overlain by subglacial deposits in U46.

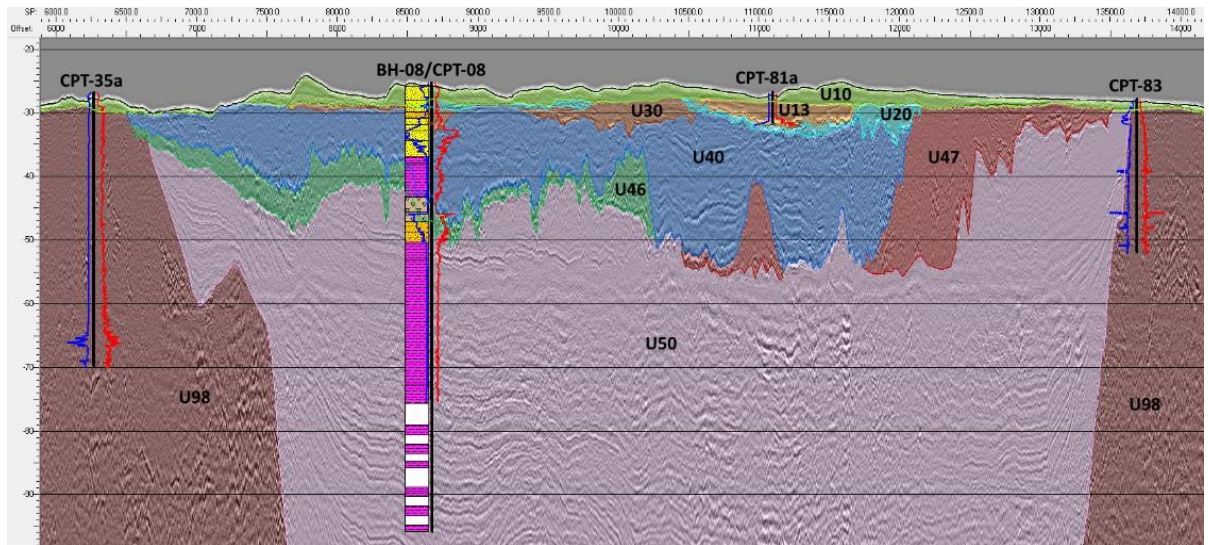


Figure 7-3 South-to-North oriented seismic section from survey line 15840 in the central part of the site illustrating the deeply incised valley of U50 overlain by layers directly related to the subsequent glacial advance overriding the area – the subglacial U46 and the mostly glaciofluvial U47. Blue curve from the CPT shows cone tip resistance (q_c) and red curve sleeve friction (f_s).

The layers U47 and U46 (see Figure 7-3) have a relatively limited extent in the centre of the site, and to the south-east, respectively. Both layers are relatively thin and display chaotic seismic facies (Table 7-2). From borehole data (Boreholes 3, 6, 8, 9 and 13), the lithology shows that U46 primarily consists of glacial till (Figure 7-3 and Figure 7-4). Sub-glacial deposits have not been identified above these layers and it is therefore inferred that these two layers represent the last time glaciers reached the site. U47 is more mixed and is interpreted to belong to the proglacial environments and deposits are expected to consist mainly of glaciofluvial and glaciolacustrine sediments. As it is well known that the Weichselian glaciation did not reach this part of the North Sea, Ref. /11/, these tills are inferred to be of Saalian age.

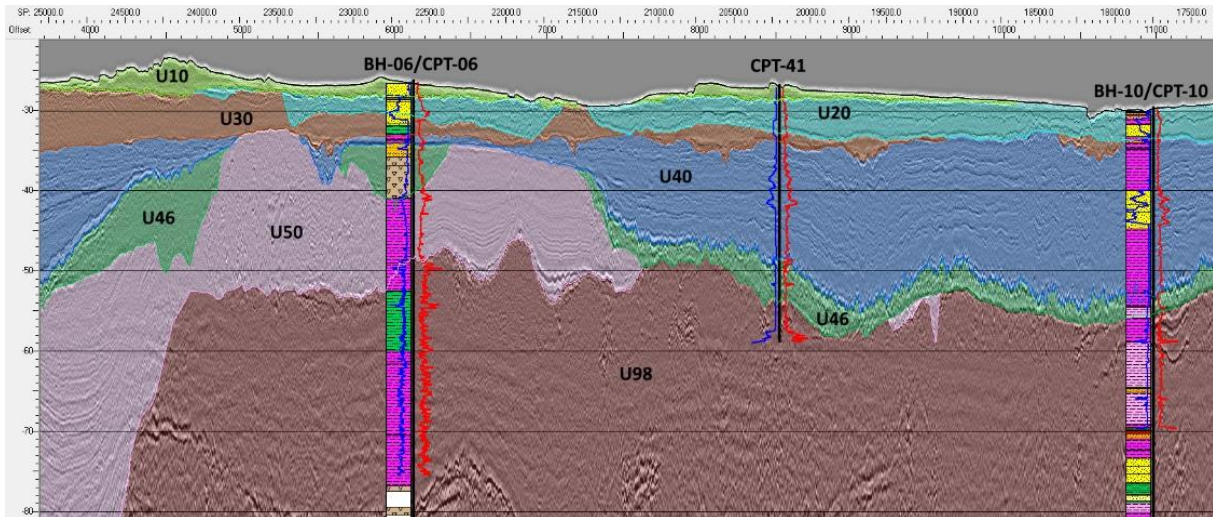


Figure 7-4 South-to-North oriented seismic section from survey line 22800 in the eastern part of the site illustrating the variation in the subglacial U46 - ranging between a relatively thin continuous layer displaying a spiky surface interpreted as preserved annual regressional moraines to thicker isolated wedges with a flat eroded surface. Blue curve from the CPT shows cone tip resistance (q_c) and red curve sleeve friction (f_s).

7.7.3 Non-glaciated Pleistocene/Holocene assembly

The late Pleistocene /Holocene assembly consists of the layers U10, U13, U18, U20, U21, U29, U30, U34, U40 and U45. Common for all these layers are that they have not been overridden by a glacier (non-glaciated).

In the south-eastern and south-western part of the area the cumulated thickness of the non-glaciated layers reaches up to 70 meters, see enclosure 4.17 and Figure 7-5.

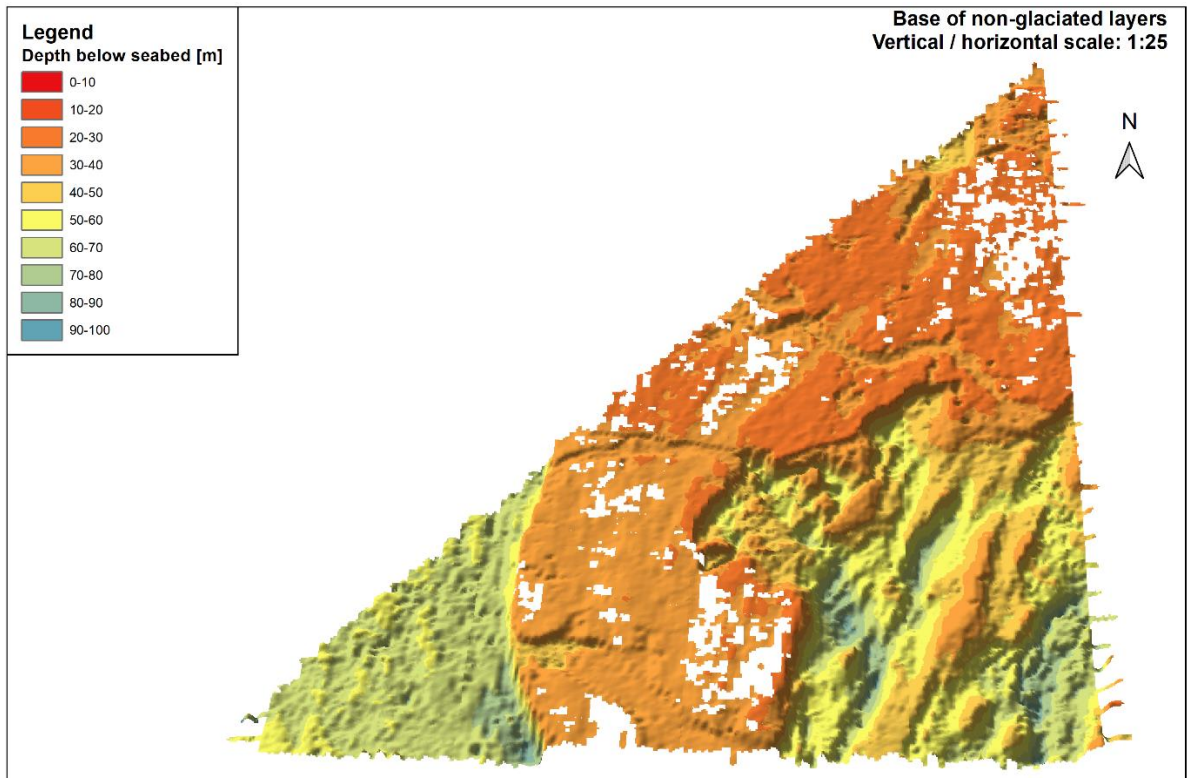


Figure 7-5 3D visualization of the base of the non-glaciated layers.

The layers U45, U40 and U29, have been interpreted to be of glaciogenic origin. Borehole data show that these layers consist of clay, silt and sand. The seismic facies (Table 7-2) and composition of the layers U45 and U29 imply deposition by glacial meltwater events. The placement of U40 directly on top of the Saalian till (U46) and the continuous parallel reflectors of strong amplitude (Table 7-2), imply a glaciolacustrine deposition of U40, following the Saalian glacial retreat. A new horizon, H40, was interpreted from the seismic data and borehole BH03 and CPT03 constituting the base of layer U40, see Figure 7-6 (blue horizon at base of U40).

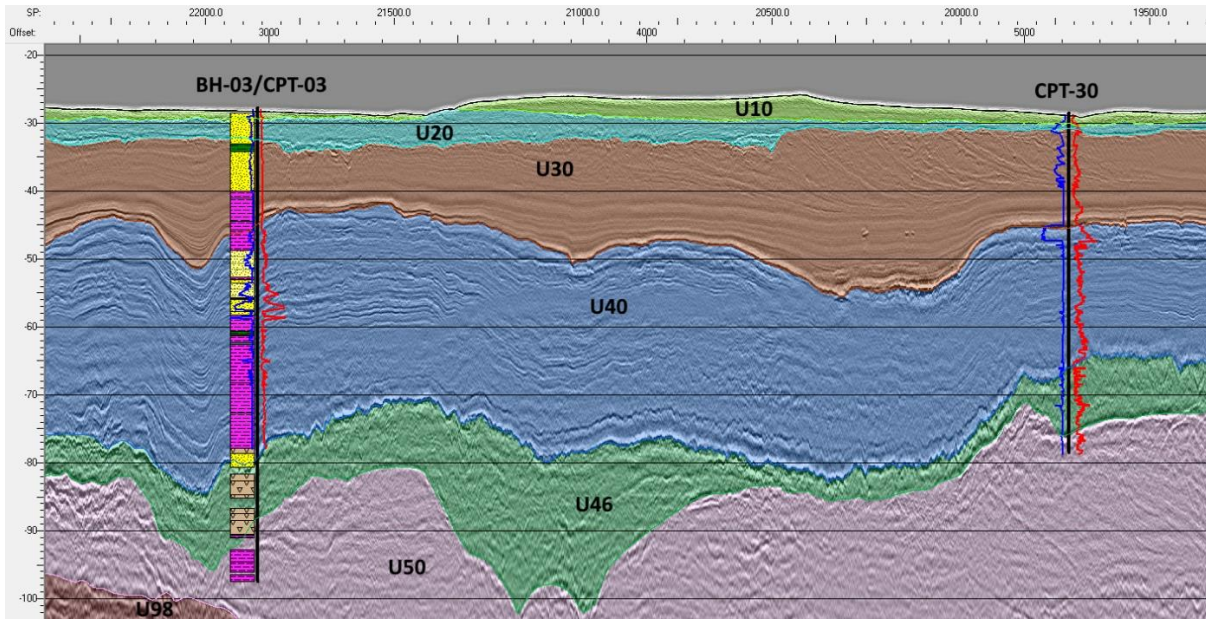


Figure 7-6 South-to-North oriented seismic section from survey line 19440 in the south-eastern part of the site showing the non-glaciated Pleistocene to Holocene succession in the southeast – U40, U30, U20, U10. Below the subglacial U46 is present above U50 and U98. Blue curve from the CPT shows cone tip resistance (q_c) and red curve sleeve friction (f_s).

The layers U34 and U30 display transparent seismic facies with no or faint internal reflectors (Table 7-2), and borehole data show these layers to consist of clay (see Figure 7-6 for U30). The layers have been interpreted to be of marine origin. U34 is placed in between U45 and U29, which are both of glacial meltwater origin, and it can therefore be implied that U34 is a marine layer originating from the Eemian interglacial period. This would then make U29 a glaciofluvial layer originating from the Weichselian glaciation, while U45 would be of Saalian origin. The placement of U30 directly on top of U40 could also indicate deposition during the Eemian marine interglacial period. This would mean that U34 and U30 could, stratigraphically, be the same layer.

Seismic facies and borehole data of U21, indicate that this layer was deposited in a glaciolacustrine environment. The placement in the northern end of the site indicate that this layer could originate from the Weichselian Fennoscandian ice sheet, which is otherwise not evident in the site, but have been indicated to have been present just to the north of the investigated area (Ref. /2/).

U20 have transparent seismic facies with no internal reflectors and borehole data show the layer to consist of sand. However, in areas where U20 overlies the U30, it has an erosive character and displays chaotic seismic facies towards the base, see Figure 7-4 to Figure 7-6. Thus, it cannot be ruled out that the base of U20 consists of glaciofluvial sediments similar to those of U29. This would make U20 of late Pleistocene/Holocene age, consisting of Weichselian glaciofluvial sediments and Holocene marine sediments.

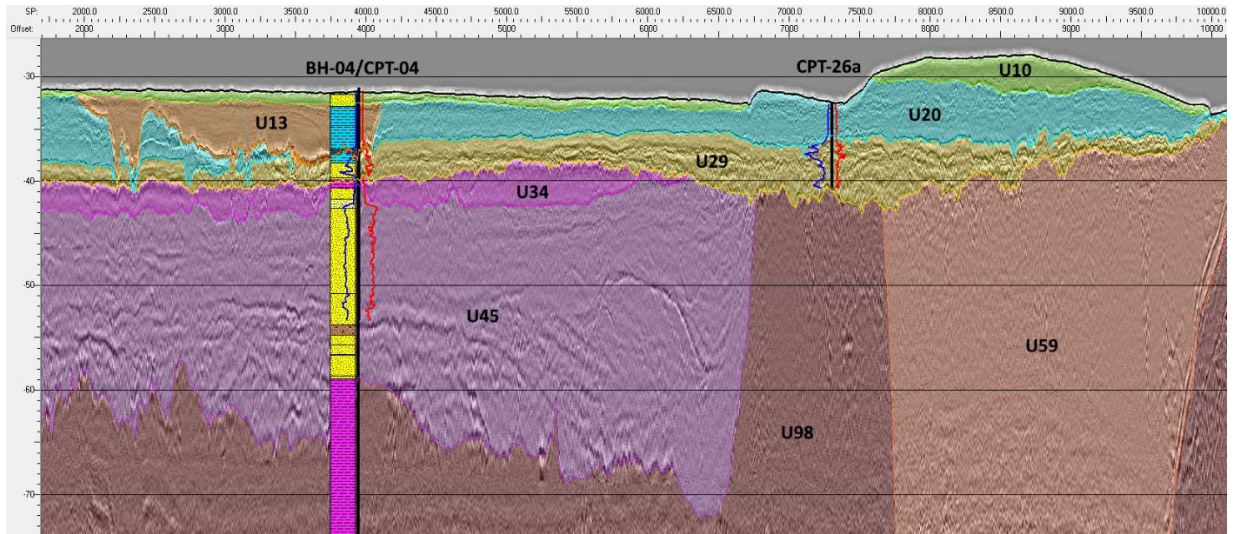


Figure 7-7 West-to-East oriented seismic section from survey line 29000 in the south-western part of the site showing Non-glaciated Pleistocene to Holocene succession in the southwest – U45, U34, U29, U20, U13, U10. In the right side the section also show the upper part of U59. Blue curve from the CPT shows cone tip resistance (q_c) and red curve sleeve friction (f_s).

The layers U18 and U13 consist of soft clay and gyttja respectively. Both layers have transparent seismic facies with no or very faint internal reflectors, see Figure 7-7 for U13. The layers are interpreted to be of Holocene age, deposited in a lacustrine or enclosed brackish marine environment, possibly during the mid-Holocene main-land time.

Layer U10 is the uppermost layer in the stratigraphy and can be seen in the seismic data on e.g. Figure 7-3 and Figure 7-7. It is found across the whole site with exceptions of some minor patches. The layer consists of recent marine sand.

8 Conceptual Geological Model

Based on the integrated geological model a Conceptual Geological Model has been made which is presented in section 8.1.

Also - based on the thickness and distribution of selected layers in the 3D Integrated Geological Model - a soil zonation has been developed. This is presented in section 8.2.2.

8.1 Presentation of Conceptual Geological Model

The Conceptual Geological Model is shown in Figure 8-1. It is a geological cross section through the Thor OWF area and includes the layers in the Integrated Geological Model, c.f. Table 7-2.

The purpose of the conceptual model is to provide:

- > An overview of geological structures and overall layer thicknesses
- > An understanding of the geology and the geological setting

It is not to be understood as an actual profile with a specific position, but rather as one that summarizes the geology across the entire Thor OWF area.

The Conceptual Geological Model is visualized from southwest to northeast in Figure 8-1 below using the same colours for the model layers as in the cross sections shown in Enclosure 5.01-5.16.

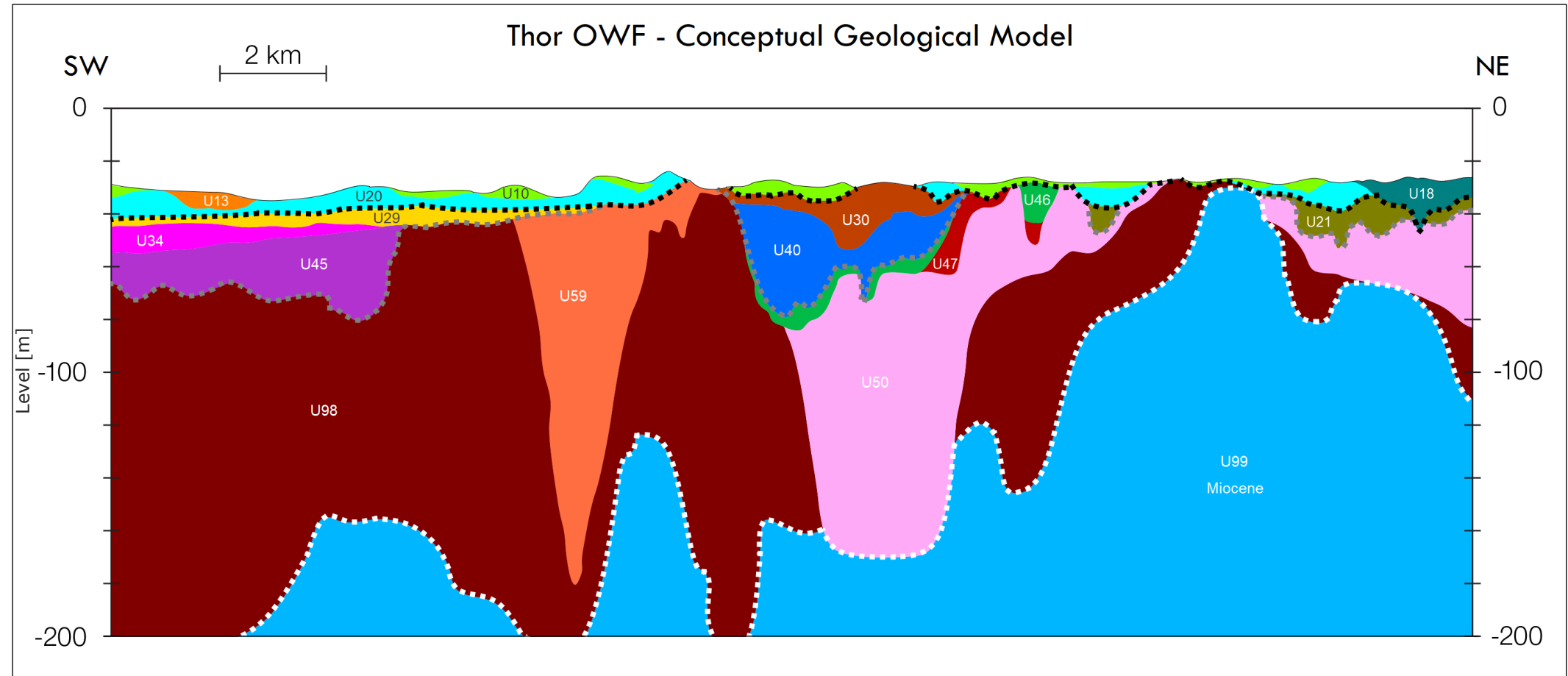
Base of Holocene layers, base of non-glaciated layers and base of Quaternary layers are highlighted with stippled lines (black, grey and white).

The Holocene layers are seen to have a cumulated thickness of up to more than 20 meters within the Thor OWF area, see also Enclosure 4.16.

Non-glaciated layers, i.e. layers that have not been overridden by glaciers, reach a cumulated thickness of up to more than 70 meters in the southern part, see also Enclosure 4.17. In the northern part this boundary is seen to be overall coincident with base of Holocene.

Also, the Miocene deposits are found at very varying depth going from approx. 170 meters below seabed in the southern part of the site to just a few meters in the northern part, see also Enclosure 3.16.

The two major buried valleys are seen to cut deep into the underlying deposits reaching depths of more than 140 m bsb. Both valleys are filled with glacial sand and clay deposits. The valley towards west (filled with layer U59) is narrow and V-shaped compared to the wider and U-shaped valley central in the area (filled with U50, U47, U46, U40 and U30), see also enclosure 3.15. The U-shaped valley is cutting through the Quaternary deposits in the northern part of the area reaching the Miocene, see also enclosure 3.15 and 3.16.



Legend

Model layers

- | | | | |
|-----------------|-------------------|-------------------|------------------------|
| U10: Pg sand | U21: Pg sand | U40: Pg clay/sand | U50: Gc sand/clay |
| U13: Pg organic | U29: Pg sand | U45: Pg sand | U59: Gc sand/clay |
| U18: Pg clay | U30: Pg clay/sand | U46: Gc till/clay | U98: Gc clay/sand/silt |
| U20: Pg sand | U34: Pg clay/sand | U47: Gc sand | U99: Pq sand/clay/silt |

Boundaries

- Base Holocene layers
- Base non-glaciated layers
- Base Quaternary

Figure 8-1 The Conceptual Geological Model for the Thor OWF site.

8.2 Presentation of Soil Provinces

Based on the geotechnical data and the Integrated Geological Model a soil zonation has been made. The soil zonation provides the basis for clustering the main geological deposits and structures relevant for the foundation design. The soil zonation is furthermore simplified into one single map dividing the entire site into five (5) different soil provinces. The purpose of this map is to provide a geological overview of the site with regards to foundation conditions.

The workflow for the process is shown in Figure 8-2.

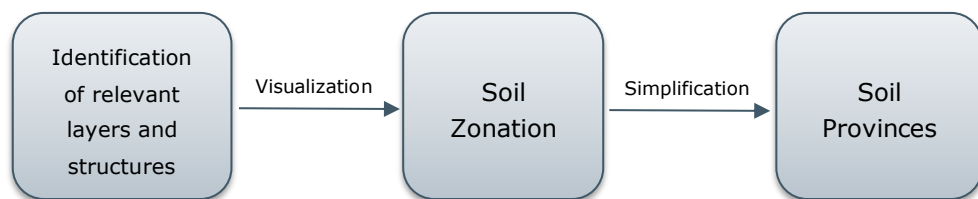


Figure 8-2 Workflow for dividing the area into geological soil provinces.

8.2.1 Map with Soil Zonation

The soil zonation constitutes the geological layers and structures evaluated to have a potentially significant impact on the foundation design. This applies for:

- > Low strength layers
- > Non-glaciated layers (layers not overridden by glaciers)
- > Lateral changes or steep layer boundaries near the seabed

Layers with low strength are the post glacial layers (Holocene deposits). The thickness of these layers is often small but can reach several meters. Furthermore, these deposits are shallow and found near the seabed, are widespread over the entire Thor OWF area and will therefore potentially have a significant impact on the foundation design. The following layers have been identified as Holocene: U10, U13, U18 and U20 c.f. Table 7-2. These layers have low strength which applies especially for U13 (gyttja) and U18 (post glacial clay) c.f. Figure 5-1 and Figure 5-3.

Non-glaciated layers can be of both Holocene and Pleistocene age, thus include glaciofluvial or glaciolacustrine deposits, see also section 7.7. The non-glaciated Pleistocene layers can potentially have low strength but represent a wider variation in both strength and thickness compared to the Holocene deposits. The non-glaciated layers constitute the layers U10-U45 in the Integrated Geological Model.

Steeply dipping layers or abrupt lateral changes in the geological setting near the seabed are primarily observed across the boundaries of the buried valleys.

The geotechnical data indicate that the strength parameters of the deposits within the buried valleys are not significantly different from those found outside the valleys. However, it cannot be ruled out that significant changes in the geotechnical soil parameters may occur across these boundaries, and that this can have a significant effect on the foundation design.

Enclosures 1.03A and 1.03B visualize the cumulated thickness of the Holocene layers (Enclosure 1.03A) and cumulated thickness of non-glaciated layers (Enclosure 1.03B). Furthermore, the following is outlined on both enclosures:

- > areas with gyttja deposits (areas with thickness above 4 meters are highlighted/shaded)
- > boundaries of buried valleys (areas where the top of a buried valley is less than 20 m below seabed are highlighted/shaded)

It can be seen from Enclosure 1.03A (and Enclosure 4.16) that the thickness of the Holocene deposits is somewhat scattered and varies across the site. In most of the area the thickness is less than 2.5 meters, however locally it reaches more than 10 meters. Largest thickness is found locally in the north and in the southwest, where especially gyttja (U13) reaches a thickness of more than 4 meters. Relatively large thicknesses are generally found as channel infill of especially U13 and U20, see Enclosure 4.02 and 4.04.

Enclosure 1.03B shows, that also the cumulated thickness of non-glaciated layers varies significantly over the Thor OWF area, from zero to more than 60 meters in the south-eastern part. However, the deposits constitute some rather coherent areas with either small or large thickness. The largest thicknesses are seen in the south-eastern and the south-western part of the area where the thickness of the non-compacted layers reaches up to more than 70 meters, see also Enclosure 4.17.

Deposits in buried valleys found less than 20 m bsb are highlighted on Enclosure 1.03A and 1.03B. This is found in a south-north oriented stretch through the central part of the site. Most of this area is outside the areas with large thickness of Holocene and non-glaciated layers, however some overlap is seen especially in the north and south-eastern part of the site.

8.2.2 Map of Soil Provinces

In order to provide a geological overview with regards to foundation conditions the two maps have been simplified into one single map showing five (5) different Soil Provinces, see Figure 8-3 and Enclosure 1.04. The Soil Provinces are based on the thickness of the Holocene and non-glaciated layers as well as a specific soil province designated for gyttja thicknesses above 4 meters. Note that gyttja constitutes a subset of the Holocene layers which again constitute a subset of the non-glaciated layers.

The five Soil Provinces have been defined as areas where:

- > Thickness of Holocene layers is less than 4 m and thickness of non-glaciated layers is less than 10 m (green)
- > Thickness of Holocene layers exceeds 4 m and thickness of non-glaciated layers is less than 10 m (blue)
- > Thickness of Holocene layers is less than 4 m and thickness of non-glaciated layers exceeds 10 m (purple)
- > Thickness of Holocene layers exceeds 4 meters and thickness of non-glaciated layers exceeds 10 m (orange)
- > Thickness of gyttja exceeds 4 meters and thickness of non-glaciated layers exceeds 10 meters (red)

The overall result shows relatively large contiguous areas with local changes due to e.g. channel infilling. Thus, the south-western and south-eastern parts show relative thick deposits of non-glaciated deposits from which most is of Holocene age (orange and red on the figure).

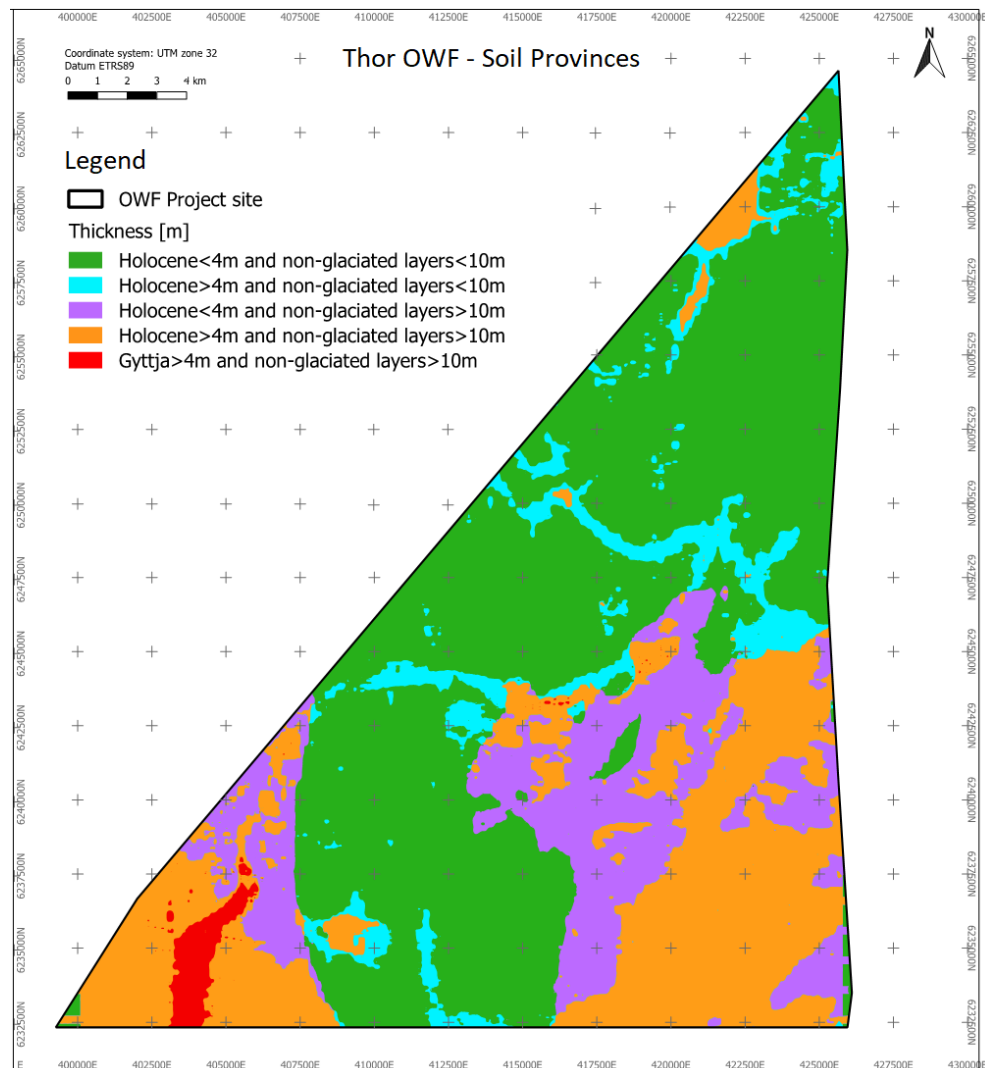


Figure 8-3 The five Soil Provinces for the Thor OWF area.

9 Leg penetration risk assessment

This section describes a high-level leg penetration risk assessment. The assessment is performed to provide an indication of potential geotechnical risks associated with jack-up operations at the site.

The assessment is intended to provide an overview of the potential behaviour of two selected vessel configurations, which can inform on potential jack-up risks during the next project phases and provide a basis for deciding on a preferred vessel configuration to operate at the site.

In general, a leg penetration analysis performed at an offshore wind farm site, can help in:

- > determining whether a jack-up is suitable for operating at a site or not
- > knowing what leg penetration behaviour and risks to anticipate
- > identifying and being able to mitigate possible geotechnical hazards

Furthermore, leg penetration analysis is part of site-specific assessment that needs to be performed for all offshore wind farm sites once the project has matured further.

9.1 Selection of vessels

In order to provide a range of possibilities in terms of leg penetration behaviour and a good basic understanding of jack-up operations at the site, two different vessel configurations have been selected for the current study.

To select the appropriate vessel configurations, experience from previous leg penetration analyses (performed by COWI) has been used as database. The specifications of the vessels considered are confidential, however the selected vessels are characterized by the following:

- > The vessels must be operational (recently) in Danish waters
- > The selected vessels shall give insight into the possible range of penetration behaviours, where the limits of the range roughly correspond to a generic installation vessel and a generic operation and maintenance (O&M) vessel. The range of penetration behaviour was deduced from several leg penetration analyses for representative soil conditions at the site.

The first vessel (further denoted *Generic Installation Vessel*) is a six-legged vessel, equipped with a large spudcan and a maximum preload of 84 MN, whereas the second vessel (further denoted *Generic O&M Vessel*) is a four-legged vessel, equipped with a smaller spudcan and a maximum preload of 7 MN. The foundation pressure applied to the seabed is dependent on the spudcan area and geometry, which is confidential. The ratio of foundation pressure between the Generic Installation Vessel and the Generic O&M Vessel is around a factor 2. For reference, the foundation pressure for the vessel used in

the offshore campaign, cf. section 3.1.1, is 4-6 times lower than the two vessels considered for this study.

The final decision on the type of vessel to be adopted for the site is based on several factors, such as:

- > vessel suppliers tendering for the installation/maintenance work
 - > type of foundation solution
 - > crane capacity, incl. lifting height and (horizontal) reach
 - > deck size and capacity with regard to planned operations, e.g. how many installation units can be stored at once
 - > amount and complexity of structural adjustments to be made to adopt vessel to planned operations
 - > speed, capacity and size of the vessel
 - > distance to the port
 - > installation method, etc.
- These are only a few of the factors that should be considered when selecting a certain jack-up vessel for installation works. All of them contribute to the final cost (and required duration) of the installation and should therefore be given special attention.

9.2 Geotechnical risks during jack-up

The main geotechnical risks that can be encountered during jack-up operations at an offshore wind site will be elaborated in the following subsections, cf. Ref. /7/. These are intended to give a high-level understanding of the spudcan behaviour and potential effects on the operations and how these effects may generally be handled or mitigated. During operations it is the responsibility of the owners, operators and crew on jack-ups to exercise sound judgement based on their education, training and experience, while taking into account leg penetration assessments provided, including related recommendations.

The term "preloading" should be well understood before discussing the risks. Preloading can be looked upon as a full-scale test, which eliminates some of the uncertainties related to soil behaviour. The initial soil displacement/compression obtained during preloading, which results in the leg penetration, will reduce/eliminate further leg penetrations during later operations under working loads. In general preloading shall be carried out corresponding to at least 1.5 times the actual maximum load during operations.

It is to be noted that the terms that describe the risk types used in this report might differ from the terms presented in various literature, therefore the description of the risks, failure mechanisms and particularities are more important than the actual terms. In order to highlight the most important characteristics of each of the risks, these have been gathered in Table 9-1.

Table 9-1 Overview of main characteristics of the geotechnical risks during jack-up.

Risk	Circumstance	Observation	Consequence
Leg scour	Cohesionless soil at seabed	To be monitored continuously	Small ¹⁾
Squeezing	Thin soft layer in between strong/stiff layers	Controllable penetration rate	Small
Fast leg penetration	Thicker soft layer below a strong/stiff layer	Occurs during preloading before reaching maximum preload	Medium
Punch through	Thicker soft layer below a strong/stiff layer	Occurs during operations after reaching maximum preload	High
Deep penetration	Penetration depth larger than available leg length	To be mitigated before operations start	High
Difficulties during leg extraction	Large suction below spudcan and large weight of soil above spudcan (can be caused by deep penetration in soft soils)	To be mitigated before operations start	High

1) *Consequence is generally small when (initial phase of) operations consider scour adequately, but can be large when scour occurs (very) fast or when their circumstance exists in combination with a soil stratigraphy where scour can result in a later risk of punch through and insufficient attention should have been paid to the (possible) existence of these circumstances. Scour is dependent on the current velocity (at seabed), and this could consequently be larger at a later moment in time than during the preloading phase.*

9.2.1 Leg scour

Under certain flow and seabed conditions, seabed erosion may occur when temporarily introducing spudcans and/or jack-up legs. The presence of a spudcan/leg will cause the water flow in its vicinity to change. This local change in the flow will cause an increase in the sediment transport capacity on the seabed close to the structure, which can lead to the formation of a local scour hole.

When scour occurs the maximum bearing capacity of the soil beneath the spudcan will decrease due to loss of supporting soil. If the bearing capacity drops to a level below the footing load, additional penetration will occur.

Furthermore, scour may cause the spudcan to be loaded eccentrically and exert a corresponding load and bending moment on the spudcan and leg.

Relevant scour typically occurs when one or more of the situations below are encountered:

- > Shallow water depths at jack-up locations
- > (Very) shallow spud can penetrations into seabed
- > Cohesionless soil at seabed level

Some of the most common mitigation measures are:

- > If possible, planning of operations for periods when current velocities are lowest and during benign weather
- > Monitor scour during operations and take actions in accordance to observations
- > For operations with long durations, scour protection such as gravel beds, prefabricated mattresses and front mats can be used
- > Excavation to obtain larger initial penetration

9.2.2 Squeezing

The potential for squeezing is present when a relative thin and soft layer is sandwiched between the leg footing and a harder layer or when the thin soft layer is present between two stronger layers. The thin soil layer can in such cases squeeze laterally between the hard layers, when the vertical stress on this layer is large enough and occurs over sufficiently large finite area.

Ref. /4/ presents two criteria to be used in order to make an initial check for a possible risk of squeezing, see equations and figure below. If both geometrical criteria are satisfied, there is a potential risk of squeezing.

$$B > 3.45 T$$

$$\frac{D}{B} \leq 2.5$$

B is the width of the spudcan

T is the thickness of the soft layer

D is the thickness of the soil above the soft layer

to standards and the preloading is performed without jacking up completely out of the water (with zero air gap), such that in case a leg experiences fast/larger penetration than the others, the situation can be handled and the vessel will not tilt more than the allowable limit.

9.2.4 Punch through

The failure mechanism of punch through is the same as described above for fast leg penetration and occurs in circumstances where a leg footing has become temporarily supported by a stronger layer of soil that overlies a weaker layer, and where the vertical footing load, as it is increased, subsequently exceeds the foundation bearing capacity allowing the footing to penetrate rapidly through the upper layer into the layer below.

The main difference between fast leg penetration and punch through is that the former is defined as occurring before reaching the maximum preload, therefore occurring during close and continuous monitoring and with zero air gap, whereas the latter describes the potential occurrence of the same phenomenon, but after preloading (when the jack-up has an air gap), this making it (more/very) dangerous for the operations, possibly resulting in significant tilting of the jack-up with all related consequences. Because they are described by the same failure mechanism, sometimes both types of risk are referred to as "rapid penetration".

Depending on the local soil conditions in terms of stratigraphy and strength of materials, it is sometimes difficult to predict which of the two types of risks (fast leg penetration and punch through) is expected at a certain location. Conducting a leg penetration analysis using a range of parameters usually helps in identifying the expected risk, provided that the soil data is reliable.

The quality of soil data is therefore one of the most important factors in estimating the penetration behaviour that will occur during jack-up operations.

When the soil conditions show a significant reduction in soil strength with penetration depth, then there is a potential for punch through to occur. However, Ref. /6/ suggests several procedures to mitigate punch through:

- > carry out a detailed soil survey at the site
- > if spudcan data from previous penetrations at the location is available, use this to back analyse and confirm the prediction methods for bearing capacity
- > ensure procedures for reducing the spudcan loads during the potential punch through phases, including the use of buoyancy (preload in water) and zero air gap (prevent vertical displacement using buoyancy of the hull) and preloading of one leg at a time
- > consider the use of jetting system (if available) to penetrate the harder soils

To conclude, an important observation provided in Ref. /6/ states that "*Whereas mitigation techniques exist to allow for the possibility of punch-through during the installation phase, there is none for the in-service condition. It is vital, therefore, that soil data is assessed carefully, and that actual penetration behaviour is used to verify predicted behaviour.*"

Therefore, reliable soil data is the most important factor in estimation and mitigation of potential risk of punch through.

9.2.5 Deep penetration

The risk of deep penetration exists when the leg penetration is larger than the available leg length of the jack up vessel.

Deep penetration occurs when the soil conditions are so soft, that they do not provide sufficient bearing capacity to reach the maximum preloading. This means that there is no available leg length left, but the leg has not reached a stable penetration level.

It is important to highlight situations in which the leg length of the vessel to be used may not be sufficient, as there will then generally be the need to employ a different vessel at the specific location/site. However, in some cases the selection of another vessel can be avoided. This is the case when there is the possibility to operate at a given location with smaller operational loads than considered for the initial assessment and these loads, and the related preloads, lead to less and feasible leg penetrations.

Deep penetrations may also pose a potential risk for adjacent structures.

9.2.6 Difficulties during leg extraction

The process of extracting the legs after operations at a certain location might sometime prove to be difficult and it is important to include this in the risk overview, such that the right measures are taken beforehand.

When extracting a leg and spudcan from a deep penetration in clay, the weight of the leg and the soil above the spudcan is to be overcome, together with the mobilised friction in the soil above the spudcan, and the suction below the spudcan. When the spudcan is in low permeable clay, the water cannot run freely to the bottom of the spudcan during extraction. This implies that no equalising water pressure can develop below the spudcan during spudcan extraction. Thus, a resulting suction is developed below the spudcan, acting downwards, counteracting the retraction process.

According to Ref. /4/, leg extraction difficulties can be caused by conditions including the following:

- > deeply penetrated spudcan in soft clay or loose silt

- > skirted or caisson-type spudcan where uplift resistance can be greater than the installation reaction
- > sites where the soil exhibits increased strength with time (this of course depends on the duration of the operations)

Ref. /4/ suggests jetting and/or excavation of the surface soils as mitigation measures against difficulties during leg extraction. A remark is added regarding soil alteration at the location due to these mitigation measures, which can affect future emplacement of jack-ups at the specific site.

9.3 Risk categories across the site

At the site, 67 unique soil investigation locations have been grouped into three different categories. For each of the categories, the primary geotechnical risks are defined and a graphical representation of all the locations and their corresponding category is presented in Enclosure 2.01 and 2.02.

It is important to acknowledge that the assessment presented here and the associated evaluation of the geotechnical risk is based on local soil data, and that the outcome only applies to conditions that can be represented by the considered CPT profile and/or borehole. As such, lateral interpolation of risk between soil investigation locations is not possible and should be avoided.

When estimating the risk(s) at each location during this categorisation process, the CPT results and borehole logs have been considered, together with the soil strength of the layers, derived based on CPT results, as outlined in section 5.

The strength of sand layers is characterized by friction angle and the strength of clay and silt by the undrained shear strength.

In order to categorize the locations, the following factors have been considered:

- > Stratigraphy at each location, based on CPT results. For categorization purposes, only the first 25 meters starting from the seabed have been considered, as the influence on the penetration behaviour for larger depths is considered negligible
- > Strength parameters of the soils encountered at each location, derived as per section 5
- > Penetration risk analysis was performed following SNAME guidelines, as per Ref. /5/

In Table 9-2 below, a summary of the three categories across the site when considering operations with both vessels, including their description and corresponding risks is presented.

Considering operations at the offshore wind site are performed with either one of the vessels selected in the study, the outcome of the analyses and the final categorisation is shown in Enclosure 2.01 and 2.02. Comparison of the results of

the leg penetration analysis shown on Enclosures 2.01 and 2.02 with the Soil provinces presented on Figure 8-3 (and Enclosure 1.04) shows that the higher leg penetration risk mainly occurs in soil provinces with thick layers of Holocene deposits or non-glaciated layers.

Table 9-2 Summary table presenting categories and corresponding potential risks.

Category	Description	Potential risk(s)
1	<ul style="list-style-type: none"> > Category 1 comprises locations where in the first 25 meters below the seabed only sand and/or very competent silt/clay layers are encountered. > If sand is encountered at seabed level, there might be a risk of scour. 	<ul style="list-style-type: none"> > Leg scour
2	<ul style="list-style-type: none"> > Category 2 comprises locations where in the first 25 meters below the seabed only sand is encountered, except for an interbedded thin clay layer, which presents the potential for squeezing. > If sand is encountered at seabed level, there might be a risk of scour. > According to Ref. /4/ and considering the spudcan geometry of both vessels, the following criteria has been applied in order to select locations within Category 2: <ul style="list-style-type: none"> > Thickness of clay layer to be: <ul style="list-style-type: none"> > < 2.8 m (Generic Installation Vessel), > < 1.0 m (Generic O&M Vessel); > Top of clay layer to be: <ul style="list-style-type: none"> > ≤ 24.4 m depth (Generic Installation Vessel) > ≤ 8.7 m depth (Generic O&M Vessel). > The formulation given in Ref. /4/ is not dependent on the strength of clay layer. In the current assessment it was however considered relevant to consider that only a clay layer with a corresponding conservative c_u as per below has the potential of squeezing: <ul style="list-style-type: none"> > < 300 kPa (Generic Installation Vessel) > < 200 kPa (Generic O&M Vessel) 	<ul style="list-style-type: none"> > Leg scour > Squeezing
3	<ul style="list-style-type: none"> > Category 3 comprises locations where in the first 25 meters below the seabed sand is encountered and overlies a thick clay layer, which presents potential for rapid penetration, i.e. the risk of fast leg penetration (if rapid penetration occurs during preloading) or punch through (if rapid penetration occurs during operations). > If sand is encountered at seabed level, there might be a risk of scour. > To select locations within Category 3, the following criteria has been applied: <ul style="list-style-type: none"> > Thickness of clay layer to be (in order not to consider squeezing): <ul style="list-style-type: none"> > > 2.8 m (Generic Installation Vessel), > > 1.0 m (Generic O&M Vessel); > Strength of clay layer c_u <ul style="list-style-type: none"> > < 150 kPa (Generic Installation Vessel), > < 100 kPa (Generic O&M Vessel); > In the event of fast leg penetration or punch through occurring, the spudcan can penetrate deep into clay layer, thus leading to potential retraction difficulties, due to suction below spudcan and weight of soil above spudcan. 	<ul style="list-style-type: none"> > Leg scour > Fast leg penetration > Punch through > Difficulties during leg extraction

10 List of deliverables

Below is a complete list of appendixes and enclosures delivered with this report.

All digital deliverables are provided per ftp, except for the IHS Kingdom Suite project which will be provided on an external hard drive.

Appendixes	
Number	Title
Appendix A	Interpreted stratigraphy at CPT locations
Appendix B	CPT plots including calculated soil properties using CPT correlations

Enclosures	
Number	Title
1.01	Overview map. Bathymetry
1.02	Overview map. Location of data and cross sections
1.03A	Soil zonation. Cumulated thickness of Holocene layers with outline of gyttja and buried valleys
1.03B	Soil zonation. Cumulated thickness of non-glaciated layers with outline of gyttja and buried valleys
1.04	Soil Provinces
2.01	Risk categorization for leg penetration risk study Generic Installation Vessel
2.02	Risk categorization for leg penetration risk study Generic O&M Vessel
2.03	Pg Clay – Undrained shear strength
2.04	Pg Clay – Small-strain shear modulus
2.05	Pg Sand – Friction angle
2.06	Pg Sand – Small-strain shear modulus
2.07	Gc Clay – Undrained shear strength

Number	Title
2.08	Gc Clay – Small-strain shear modulus
2.09	Gc Sand – Friction angle
2.10	Gc Sand – Small-strain shear modulus
2.11	Gc Till – Undrained shear strength
2.12	Gc Till – Small-strain shear modulus
3.01	Top of model layer U10. Depth below seabed [m]
3.02	Top of model layer U13. Depth below seabed [m]
3.03	Top of model layer U18. Depth below seabed [m]
3.04	Top of model layer U20. Depth below seabed [m]
3.05	Top of model layer U21. Depth below seabed [m]
3.06	Top of model layer U29. Depth below seabed [m]
3.07	Top of model layer U30. Depth below seabed [m]
3.08	Top of model layer U34. Depth below seabed [m]
3.09	Top of model layer U40. Depth below seabed [m]
3.10	Top of model layer U45. Depth below seabed [m]
3.11	Top of model layer U46. Depth below seabed [m]
3.12	Top of model layer U47. Depth below seabed [m]
3.13	Top of model layer U50. Depth below seabed [m]
3.14	Top of model layer U59. Depth below seabed [m]
3.15	Top of model layer U98. Depth below seabed [m]
3.16	Top of Miocene. Depth below seabed [m]
4.01	Layer U10, thickness [m]
4.02	Layer U13, thickness [m]

Number	Title
4.03	Layer U18, thickness [m]
4.04	Layer U20, thickness [m]
4.05	Layer U21, thickness [m]
4.06	Layer U29, thickness [m]
4.07	Layer U30, thickness [m]
4.08	Layer U34, thickness [m]
4.09	Layer U40, thickness [m]
4.10	Layer U45, thickness [m]
4.11	Layer U46, thickness [m]
4.12	Layer U47, thickness [m]
4.13	Layer U50, thickness [m]
4.14	Layer U59, thickness [m]
4.15	Layer U98, thickness [m]
4.16	Holocene layers (U10-U20), cumulated thickness [m]
4.17	Non-glaciated layers (U10-U45), cumulated thickness [m]
4.18	Quaternary layers (U10-U59), cumulated thickness [m]
5.01	Cross section 5520
5.02	Cross section 8880
5.03	Cross section 13440
5.04	Cross section 15840
5.05	Cross section 19440
5.06	Cross section 21840
5.07	Cross section 22800

Number	Title
5.08	Cross section 23520
5.09	Cross section 25200
5.10	Cross section 25680
5.11	Cross section 7000
5.12	Cross section 12000
5.13	Cross section 19000
5.14	Cross section 24000
5.15	Cross section 29000
5.16	Cross section 31000
6.01	Seismic interpretation of deposits with organic content
6.02	Seismic interpretation of shallow gas

Digital deliverables *)	
Item	Format
IHS Kingdom Suite Project including spatial geological model	Kingdom project
Top of model layers, elevation MSL (grids)	ASCII and GeoTIFF
Top of model layers, depth below seabed (grids)	ASCII and GeoTIFF
Model layers, isopach grids (vertical layer thickness)	ASCII and GeoTIFF
Extent of gyttja, buried valleys and top buried valleys <20 m bsb	ESRI Shapefile
Soil provinces extent	ESRI Shapefile
Cross section locations	ESRI Shapefile
Leg Penetration Assessment, Risk Category	ESRI Shapefile
Geotechnical parameters	ESRI Shapefile

*) See Excel-file in digital delivery for detailed file list with metadata.

11 Conclusions

A 3D integrated geological model has been made for the entire Thor OWF area. The new model comprises an updated and revised version of the existing geophysical model and is based on the newly gathered geotechnical data as well as the seismic data.

With respect to the purpose of the integrated geological model a new and better basis can now be provided for developers to evaluate the ground conditions in relation to foundation design and positioning of offshore wind turbines.

The integrated geological model has sixteen (16) layers. Thus, the existing geophysical model has been revised with respect to both the number of layers as well as to the spatial distribution of the layers. The model comprises layer of Holocene, Pleistocene and Miocene deposits.

Together with the new model an updated geological description of the individual geological layers in the model is provided. The description includes stratigraphical, lithological and geotechnical characteristics.

The integrated geological model is delivered as a digital 3D model in a Kingdom suite project. Enclosures provided with the digital model present the new layers with respect to depth below seabed, thickness and lateral extent. The enclosures also visualize cumulated thickness of Holocene layers, non-glaciated layers and glacial layers.

Sixteen (16) cross-sections distributed over the entire area show the layering in the model together with borehole information. The cross-sections follow the seismic survey lines and have been positioned so they comprise all boreholes.

A soil zonation has been made from the geological model with focus on the deposits and geological structures evaluated to have a potentially significant impact on the foundation design. This includes low strength layers, non-glaciated layers and lateral changes or steep layer boundaries near the seabed. The soil zonation maps have been simplified into a single map showing five selected soil provinces which provides a geological overview of the entire site relevant for foundation conditions.

Furthermore, a high-level leg penetration risk assessment has been performed in order to provide an overview of potential jack-up risks during the next project phases. This assessment has been performed for two selected vessel configurations, i.e. for a generic installation vessel and a generic O&M vessel.

12 References

- Ref. /1/ MMT, May 2020. GEOPHYSICAL SURVEY REPORT - THOR OFFSHORE WIND FARM SITE INVESTIGATION LOT 1.
- Ref. /2/ RAMBØLL, 2019. 800MW Thor OWF – Geological desk study – Geological Model. Report 2, revision 1.
- Ref. /3/ GEO, October 2020. Thor OWF – Geotechnical Site Investigation 2020. Factual Geotechnical Report. Seabed CPT Campaign and Borehole Campaign. GEO Project No. 204307.
- Ref. /4/ European Standard EN ISO 19905-1, Petroleum and natural gas industries – Site-specific assessment of mobile offshore units – Part 1: Jack-ups, February 2016.
- Ref. /5/ The Society of Naval Architects and Marine Engineers (SNAME), Technical & Research Bulletin 5-5A: Guidelines for Site Specific Assessment of Mobile Jack-Up Units, Rev. 3, August 2008.
- Ref. /6/ MSL Engineering Ltd., 2004, Guidelines for jack-up rigs with particular reference to foundation integrity (HSE Research Report 289).
- Ref. /7/ LOC, January 2013, Geotechnical engineering for jack-ups, Ref no. LOC/CM/MANUAL/2013/R0.1-4
- Ref. /8/ Robertson and Cabal, 2015, Guide to Cone Penetration Testing, 6th Edition
- Ref. /9/ Japsen, P.: *Fra Kridthav til Vesterhav. Nordsøbassinets udvikling vurderet ud fra seismiske hastigheder*. Geologisk Tidsskrift, hæfte 2, pp. 1-36, December 2000.
- Ref. /10/ Ehlers, J.: *Reconstructing the Dynamics of the North-West European Pleistocene Ice Sheets*. Quaternary Science Reviews, Vol. 9. Pp. 71-83, 1990.
- Ref. /11/ Houmark-Nielsen, M.; Krüger, J.; Kjær, K. H.; *De seneste 150.000 år I Danmark, istidslandskabet og naturens udvikling*. Geviden, geologi og geografi, nr. 2, 2005.
- Ref. /12/ Huuse, M., Lykke-Andersen, H.: *Overdeepened Quaternary valleys in the eastern Danish North Sea: morphology and origin*. Quaternary Science Reviews, Binder 19, p. 1233-1253, July 2000.

Appendix A Interpreted stratigraphy at CPT locations

Location	Layer	Top level	Bottom level	Unit	ϕ' - Average	c_u - Average	G_{max} - Average
[-]	[No.]	[mBSB]	[mBSB]	[-]	[°]	[kPa]	[MPa]
CPT_01	1	0	1.1	Pg Coarse	37.4	0	11.8
CPT_01	2	1.1	6	Pg Clay	0	157.6	97
CPT_01	3	6	41.7	Pg Sand	44.1	0	157.9
CPT_01	4	41.7	69	Gc Till	0	1626.7	357.1
CPT_02	1	0	8.3	Pg Sand	42.8	0	53.2
CPT_02	2	8.3	11.7	Pg Silt	40	541.8	83.2
CPT_02	3	11.7	49.4	Gc Clay	0	361.5	162.4
CPT_02	4	49.4	68.7	Gc Till	0	957	366.7
CPT_03	1	0	12.4	Pg Sand	40.2	0	61.6
CPT_03	2	12.4	18.2	Pg Clay	0	148.8	118
CPT_03	3	18.2	31.1	Pg Sand	39.4	0	150.5
CPT_03	4	31.1	40.9	Pg Clay	0	283	158.3
CPT_03	5	40.9	51	Pg Clay	0	228.3	213.9
CPT_03	6	51	68.9	Gc Clay	0	271.1	161.5
CPT_04	1	0	1.3	Pg Sand	32.1	0	8.7
CPT_04	2	1.3	5.6	Pg Organic	0	13.7	22.2
CPT_04	3	5.6	28.8	Pg Sand	44.3	0	137.6
CPT_04	4	28.8	68.6	Gc Clay	0	409.7	346.3
CPT_05	1	0	9.6	Pg Sand	39.1	0	47.3
CPT_05	2	9.6	11.8	Gc Silt	41.2	747.1	94.3
CPT_05	3	11.8	46.8	Gc Clay	0	183.9	112.4
CPT_05	4	46.8	68.2	Gc Till	0	919.4	241
CPT_06	1	0	5.1	Pg Sand	40.5	0	35.2
CPT_06	2	5.1	50	Gc Clay	0	307	144.7
CPT_06	3	50	62.2	Gc Till	0	1268	398.7
CPT_06	4	62.2	68.9	PreQ Sand	38.9	0	282.8
CPT_07	1	0	17.3	Gc Sand	41.8	0	81.7
CPT_07	2	17.3	30.2	Gc Sand	45.8	0	196
CPT_07	3	30.2	38	Gc Till	0	987.5	307.9
CPT_07	4	38	68.2	Gc Clay	0	435.7	220.8
CPT_08	1	0	11	Pg Sand	41.7	0	61.1
CPT_08	2	11	20.6	Pg Clay	0	111.2	131.7
CPT_08	3	20.6	25	Gc Sand	40	0	146.9
CPT_08	4	25	68.9	Gc Clay	0	170.2	115.9
CPT_09	1	0	3.9	Pg Sand	41.2	0	29
CPT_09	2	3.9	6.4	Pg Clay	0	113.2	110.4
CPT_09	3	6.4	14.6	Pg Sand	41.5	0	95.7
CPT_09	4	14.6	40	Gc Clay	0	189.3	151.3
CPT_09	5	40	42.3	Gc Sand	42.7	0	251.9
CPT_09	6	42.3	49.9	Gc Clay	0	353	237.5
CPT_09	7	49.9	68.2	Gc Till	0	864.8	365.9
CPT_10	1	0	4.4	Pg Sand	42.6	0	36.2
CPT_10	2	4.4	10.2	Pg Clay	0	102.8	91.6
CPT_10	3	10.2	14.7	Pg Sand	43.7	0	119.1
CPT_10	4	14.7	29.8	Gc Clay	0	204.6	178.3
CPT_10	5	29.8	40.1	Gc Till	0	336.9	190.1
CPT_10	6	40.1	68.3	Gc Sand	38.2	0	238.9
CPT_11	1	0	9.6	Gc Sand	46.6	0	72.6

Location	Layer	Top level	Bottom level	Unit	ϕ' - Average	c_u - Average	G_{max} - Average
[-]	[No.]	[mBSB]	[mBSB]	[-]	[°]	[kPa]	[MPa]
CPT_11	2	9.6	13.4	Gc Silt	34.1	172	67.5
CPT_11	3	13.4	34.9	Gc Sand	44.8	0	186.8
CPT_11	4	34.9	46.4	Gc Silt	35.7	424.5	167.9
CPT_11	5	46.4	69	Gc Clay	0	308	222.7
CPT_12	1	0	2.4	Pg Clay	0	88.3	94.5
CPT_12	2	2.4	6.5	Pg Sand	42.6	0	55.6
CPT_12	3	6.5	10.8	Gc Coarse	44.1	0	98.8
CPT_12	4	10.8	17.7	Gc Till	0	474.4	185.7
CPT_12	5	17.7	25.3	Gc Sand	43.6	0	172.8
CPT_12	6	25.3	43.8	Gc Clay	0	403.3	247.6
CPT_12	7	43.8	50	Gc Silt	39.7	1144.4	230.2
CPT_12	8	50	68.4	Gc Sand	42.9	0	318.9
CPT_13	1	0	4.3	Gc Sand	39.9	0	29.4
CPT_13	2	4.3	11.6	Gc Till	0	140.1	101.4
CPT_13	3	11.6	15.9	Gc Sand	45.4	0	139.7
CPT_13	4	15.9	20.1	Gc Silt	39.1	1018.9	120.9
CPT_13	5	20.1	44.1	Gc Clay	0	259.1	140.7
CPT_13	6	44.1	69	Gc Sand	38.3	0	255
CPT_14	1	0	2.1	Pg Coarse	47.9	0	30.4
CPT_14	2	2.1	12.2	Gc Silt	39.5	542.7	66.1
CPT_14	3	12.2	28.3	Gc Clay	0	270.7	182.6
CPT_14	4	28.3	44.2	Gc Till	0	492.4	237.2
CPT_14	5	44.2	68.1	PreQ Sand	38.5	0	245.5
CPT_15	1	0	6.9	PreQ Clay	0	198.8	229.3
CPT_15	2	6.9	14.9	PreQ Silt	39.6	533.5	88
CPT_15	3	14.9	20.3	PreQ Sand	45.7	0	166.5
CPT_15	4	20.3	68	PreQ Sand	38.2	0	197.8
CPT_16	1	0	17.8	PreQ Sand	47.5	0	117.2
CPT_16	2	17.8	18.9	PreQ Clay	0	650.3	190.4
CPT_16	3	18.9	23.6	PreQ Sand	46.8	0	200.3
CPT_16	4	23.6	25.2	PreQ Clay	0	659.8	167.4
CPT_16	5	25.2	27.8	PreQ Sand	46.3	0	227.2
CPT_16	6	27.8	29.7	PreQ Clay	0	434.2	292.9
CPT_16	7	29.7	31.9	PreQ Silt	42.9	2008.6	211
CPT_16	8	31.9	69	PreQ Sand	38	0	236.5
CPT_17	1	0	5.3	Gc Clay	0	143	117.4
CPT_17	2	5.3	10	Gc Sand	42.7	0	79.4
CPT_17	3	10	28.1	Gc Till	0	528.2	224.2
CPT_17	4	28.1	42.9	Gc Sand	41.6	0	218.8
CPT_17	5	42.9	69.5	Gc Sand	37	0	225.8
CPT_18	1	0	3.1	Pg Sand	36.9	0	19.9
CPT_18	2	3.1	10.6	Gc Clay	0	256.7	114
CPT_18	3	10.6	22.4	Gc Sand	43.6	0	142.9
CPT_18	4	22.4	28.6	Gc Clay	0	306.3	182.8
CPT_18	5	28.6	43.9	Gc Sand	41.1	0	210.2
CPT_18	6	43.9	63.5	PreQ Clay	0	557.2	246.7
CPT_18	7	63.5	68.4	PreQ Sand	38.1	0	267.8
CPT_19	1	0	1.5	Pg Sand	33.7	0	11.3

Location	Layer	Top level	Bottom level	Unit	ϕ' - Average	c_u - Average	G_{max} - Average
[-]	[No.]	[mBSB]	[mBSB]	[-]	[°]	[kPa]	[MPa]
CPT_19	2	1.5	6.1	Pg Sand	42.9	0	51
CPT_19	3	6.1	7.8	Pg Silt	37.4	266.4	57.2
CPT_19	4	7.8	9.2	Pg Clay	0	131.7	157.9
CPT_19	5	9.2	9.8	Pg Sand	45	0	106.6
CPT_20	1	0	1.3	Pg Sand	32.8	0	9.5
CPT_20	2	1.3	2.5	Pg Organic	0	19.6	23.1
CPT_20	3	2.5	3.9	Pg Sand	43.8	0	48.7
CPT_20	4	3.9	4	Pg Silt	38.1	229	40.7
CPT_20	5	4	5.7	Pg Sand	45.1	0	68.2
CPT_20	6	5.7	7.6	Pg Clay	0	95.7	138.2
CPT_20	7	7.6	8.2	Pg Sand	45.7	0	98.4
CPT_22	1	0	0.7	Gc Sand	40.8	0	11
CPT_22	2	0.7	13.1	Gc Sand	39.9	0	63.3
CPT_22	3	13.1	14.4	Gc Sand	41.2	0	111.3
CPT_22	4	14.4	21.7	Gc Clay	0	357.2	365.1
CPT_23	1	0	0.6	Pg Sand	31.2	0	5.6
CPT_23	2	0.6	1.4	Pg Sand	40.7	0	18.7
CPT_23	3	1.4	3.6	Pg Silt	34.1	74.9	23.2
CPT_23	4	3.6	5.4	Gc Sand	45.2	0	64.4
CPT_23	5	5.4	17.7	Gc Silt	36.7	288.6	76.7
CPT_24	1	0	1.1	Pg Sand	39.7	0	11.9
CPT_24	2	1.1	8.9	Pg Sand	45.2	0	69.7
CPT_24	3	8.9	32.2	Pg Clay	0	142.9	89.2
CPT_24	4	32.2	42	Pg Sand	44.3	0	255.9
CPT_26a	1	0	1	Pg Sand	33.8	0	9
CPT_26a	2	1	3.1	Pg Silt	34.8	83.3	21.2
CPT_26a	3	3.1	8.9	Gc Sand	45.6	0	82.2
CPT_27	1	0	0.9	Pg Sand	33.9	0	7.3
CPT_27	2	0.9	12	Gc Sand	43.3	0	70.8
CPT_27	3	12	21.4	Gc Clay	0	300.8	237
CPT_27	4	21.4	22.5	Gc Silt	41.2	1076.3	152
CPT_28	1	0	1.6	Pg Sand	41.1	0	19.5
CPT_28	2	1.6	18.4	Pg Sand	43.6	0	95.2
CPT_28	3	18.4	50.5	Gc Till	0	363.4	202.1
CPT_29	1	0	1	Pg Sand	39.2	0	12.2
CPT_29	2	1	8.5	Pg Sand	41.6	0	51.3
CPT_29	3	8.5	19.7	Pg Silt	34.3	192.7	78.3
CPT_29	4	19.7	35.7	Pg Clay	0	193.8	192.1
CPT_29	5	35.7	38.7	Pg Sand	36.3	0	166.3
CPT_29	6	38.7	41.1	Gc Till	0	235.4	148.3
CPT_30	1	0	10.9	Pg Sand	39.8	0	55.9
CPT_30	2	10.9	16.5	Pg Clay	0	140.7	110.4
CPT_30	3	16.5	18.9	Pg Sand	44.5	0	156.8
CPT_30	4	18.9	36.7	Pg Clay	0	187.3	168.9
CPT_30	5	36.7	50.6	Gc Till	0	232.9	134.2
CPT_32	1	0	0.8	Gc Sand	35.5	0	7.5
CPT_32	2	0.8	33.1	Gc Clay	0	222.7	221.3
CPT_32	3	33.1	37.2	Gc Clay	0	769.1	312.2

Location	Layer	Top level	Bottom level	Unit	ϕ' - Average	c_u - Average	G_{max} - Average
[-]	[No.]	[mBSB]	[mBSB]	[-]	[°]	[kPa]	[MPa]
CPT_34	1	0	7.8	Gc Sand	41.6	0	48.5
CPT_34	2	7.8	19.8	Gc Silt	36.9	340.8	85.5
CPT_34	3	19.8	21.3	Gc Sand	41.8	0	149.8
CPT_34	4	21.3	31.9	Gc Silt	33.2	195.3	109.1
CPT_34	5	31.9	45.2	Gc Silt	39.1	888.2	197
CPT_35a	1	0	1.4	Pg Sand	41	0	15.2
CPT_35a	2	1.4	20.5	Gc Clay	0	206.5	188.6
CPT_35a	3	20.5	38.2	Gc Clay	0	206	223.8
CPT_35a	4	38.2	39.8	Gc Sand	39.1	0	199.8
CPT_35a	5	39.8	42.2	Gc Clay	0	314.5	303.1
CPT_35a	6	42.2	43.5	Gc Clay	0	521.2	271.2
CPT_36	1	0	8.5	Pg Sand	40.1	0	47.6
CPT_36	2	8.5	20.3	Pg Clay	0	125	85.3
CPT_36	3	20.3	28.2	Pg Clay	0	295.2	161.3
CPT_36	4	28.2	45.1	Pg Clay	0	186.6	191.9
CPT_36	5	45.1	50.6	Gc Till	0	186.1	109.8
CPT_37	1	0	0.5	Pg Sand	30.9	0	4
CPT_37	2	0.5	2.3	Pg Clay	0	93.7	86.4
CPT_37	3	2.3	3.7	Pg Sand	44.8	0	47.9
CPT_37	4	3.7	10.2	Pg Silt	34.8	146.6	49.4
CPT_37	5	10.2	23.8	Pg Clay	0	127.2	75.4
CPT_37	6	23.8	25.2	Pg Sand	43.3	0	186.6
CPT_37	7	25.2	45.5	Pg Clay	0	201.1	172.4
CPT_37	8	45.5	50.3	Gc Till	0	1622.9	369.8
CPT_38	1	0	1.3	Pg Sand	38.4	0	14.6
CPT_38	2	1.3	4	Pg Sand	44.9	0	44.7
CPT_38	3	4	8.6	Pg Silt	34.5	134.1	45.9
CPT_38	4	8.6	10.1	Pg Sand	45.2	0	106.8
CPT_38	5	10.1	12.5	Pg Silt	35.2	211.8	69.8
CPT_38	6	12.5	20	Pg Sand	45.7	0	157.1
CPT_38	7	20	27.3	Pg Clay	0	164.2	198.4
CPT_38	8	27.3	32.2	Gc Till	0	245.9	146.8
CPT_38	9	32.2	33.9	Gc Sand	42	0	210.4
CPT_38	10	33.9	58.9	Gc Till	0	282.7	189.5
CPT_39	1	0	0.5	Pg Sand	34.1	0	4.9
CPT_39	2	0.5	1.4	Pg Clay	0	68.2	112.1
CPT_39	3	1.4	24.3	Pg Sand	46.2	0	137.7
CPT_39	4	24.3	42.7	Gc Clay	0	382.9	231.5
CPT_40	1	0	2	Pg Sand	43.8	0	24
CPT_40	2	2	5.1	Pg Clay	0	107.2	74.3
CPT_40	3	5.1	6.4	Pg Sand	42.1	0	66.4
CPT_40	4	6.4	12.1	Pg Clay	0	109.2	72.4
CPT_40	5	12.1	13.8	Pg Sand	44.7	0	129.9
CPT_40	6	13.8	20	Pg Clay	0	147.4	91.5
CPT_40	7	20	29.4	Pg Clay	0	159.3	150.3
CPT_40	8	29.4	50.5	Gc Till	0	436.9	224.9
CPT_41	1	0	2.2	Pg Sand	34.6	0	15.4
CPT_41	2	2.2	4.3	Pg Clay	0	132.5	112.1

Location	Layer	Top level	Bottom level	Unit	ϕ' - Average	c_u - Average	G_{max} - Average
[-]	[No.]	[mBSB]	[mBSB]	[-]	[°]	[kPa]	[MPa]
CPT_41	3	4.3	6.4	Pg Sand	42.6	0	63.2
CPT_41	4	6.4	10.6	Pg Clay	0	132.8	92
CPT_41	5	10.6	15.4	Pg Sand	42.4	0	114
CPT_41	6	15.4	21.6	Pg Clay	0	164.1	170.1
CPT_41	7	21.6	30.8	Gc Till	0	260.9	126.7
CPT_41	8	30.8	32.2	Gc Sand	44.1	0	227.4
CPT_42	1	0	0.5	Pg Sand	38.3	0	6.4
CPT_42	2	0.5	1.8	Pg Clay	0	35.2	61.5
CPT_42	3	1.8	3.7	Pg Sand	46.8	0	52.7
CPT_42	4	3.7	19.5	Gc Sand	43.2	0	106
CPT_42	5	19.5	38	Gc Clay	0	400.5	248.4
CPT_43	1	0	5.3	Pg Sand	38.7	0	32.2
CPT_43	2	5.3	6.2	Gc Sand	44.7	0	75.3
CPT_43	3	6.2	15.1	Gc Clay	0	119.1	100
CPT_43	4	15.1	27	Gc Clay	0	178.2	216.2
CPT_43	5	27	33.7	Gc Clay	0	402.8	236.9
CPT_43	6	33.7	35.4	Gc Sand	42.7	0	223.2
CPT_44	1	0	3.4	Pg Sand	42.7	0	30.9
CPT_44	2	3.4	8.3	Pg Clay	0	85.8	55.3
CPT_44	3	8.3	9.4	Pg Sand	38.7	0	73.9
CPT_44	4	9.4	10.6	Pg Clay	0	131.6	106.9
CPT_44	5	10.6	15.3	Pg Sand	41.7	0	108.1
CPT_44	6	15.3	24	Pg Clay	0	123.8	102.1
CPT_44	7	24	26.3	Gc Sand	43.5	0	188.6
CPT_44	8	26.3	37.6	Gc Till	0	279.7	166.1
CPT_44	9	37.6	41.4	Gc Sand	39	0	202.1
CPT_44	10	41.4	44.8	Gc Till	0	308.5	303.9
CPT_44	11	44.8	50.2	Gc Till	0	471.9	280.4
CPT_46	1	0	2.1	Pg Sand	31.1	0	12.3
CPT_46	2	2.1	3.3	Pg Clay	0	75	124.2
CPT_46	3	3.3	6.7	Pg Sand	43.4	0	63.7
CPT_46	4	6.7	10.4	Pg Clay	0	95.1	108.8
CPT_46	5	10.4	17.8	Pg Clay	0	157	150.5
CPT_46	6	17.8	24	Pg Sand	43.6	0	167.2
CPT_46	7	24	32.1	Pg Clay	0	163.7	235.8
CPT_46	8	32.1	35.1	Gc Silt	37.3	609.3	164.6
CPT_46	9	35.1	42.3	Gc Clay	0	221.4	190.7
CPT_46	10	42.3	43.6	Gc Sand	39.4	0	220
CPT_47	1	0	1.6	Pg Sand	44.4	0	22
CPT_47	2	1.6	6.1	Gc Sand	38.1	0	40.3
CPT_47	3	6.1	10.6	Gc Clay	0	170.4	183.1
CPT_47	4	10.6	22.3	Gc Silt	39.8	656.4	115.1
CPT_48	1	0	2.6	Pg Sand	44.4	0	27.4
CPT_48	2	2.6	4.2	Pg Silt	34.3	98.2	30.2
CPT_48	3	4.2	6.2	Pg Sand	38.5	0	50.4
CPT_48	4	6.2	17.7	Pg Clay	0	113.5	107.6
CPT_48	5	17.7	23.7	Pg Sand	44.9	0	178.7
CPT_48	6	23.7	28.5	Pg Silt	35.9	360.8	128.2

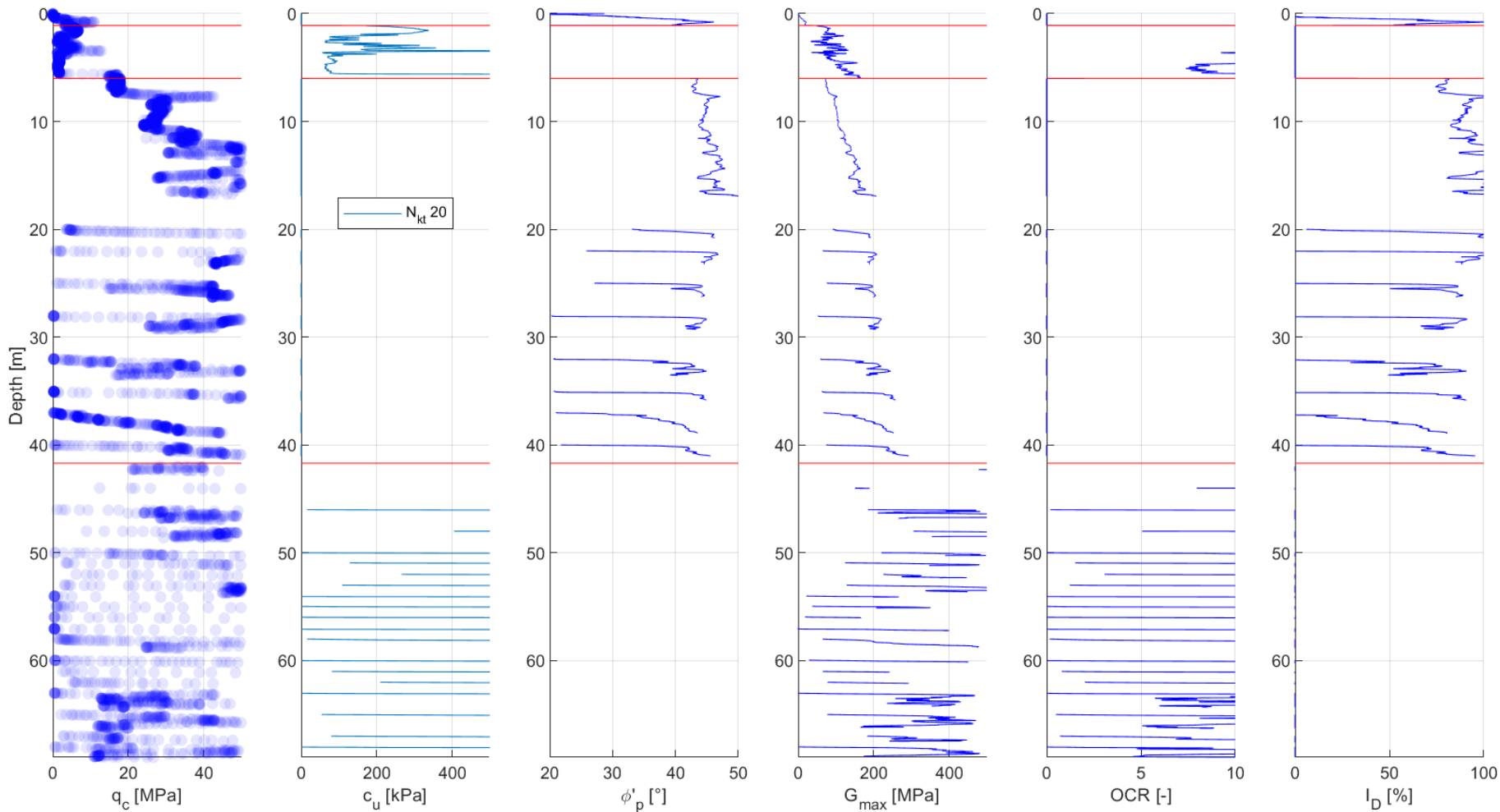
Location	Layer	Top level	Bottom level	Unit	ϕ' - Average	c_u - Average	G_{max} - Average
[-]	[No.]	[mBSB]	[mBSB]	[-]	[°]	[kPa]	[MPa]
CPT_48	7	28.5	50.2	Gc Till	0	203.7	132.3
CPT_49	1	0	4.3	Pg Sand	45.1	0	39.6
CPT_49	2	4.3	7.6	Gc Clay	0	119.1	109.4
CPT_49	3	7.6	8.6	Gc Sand	42.9	0	85.6
CPT_49	4	8.6	13.6	Gc Clay	0	254.1	149.3
CPT_49	5	13.6	14.3	Gc Sand	43.4	0	127.8
CPT_49	6	14.3	17.4	Gc Clay	0	242	166.9
CPT_49	7	17.4	19	Gc Sand	40.1	0	127
CPT_49	8	19	21	Gc Clay	0	277.4	213.2
CPT_49	9	21	23.3	Gc Sand	39.4	0	140.6
CPT_49	10	23.3	27.6	Gc Clay	0	287.7	192.9
CPT_49	11	27.6	30.3	Gc Sand	38.8	0	161
CPT_50	1	0	2.1	Pg Sand	41.6	0	20.7
CPT_50	2	2.1	3.9	Pg Silt	38	199.4	33.4
CPT_50	3	3.9	6.9	Pg Sand	43.3	0	65.8
CPT_50	4	6.9	8.1	Gc Clay	0	172.1	119.4
CPT_50	5	8.1	14.2	Gc Sand	45.6	0	123.3
CPT_50	6	14.2	17.8	Gc Silt	41.3	939	125.1
CPT_50	7	17.8	19	Gc Sand	45.9	0	174.6
CPT_50	8	19	20.3	Gc Silt	40.9	927.6	139.3
CPT_50	9	20.3	23.4	Gc Sand	45.4	0	190.5
CPT_51a	1	0	1.5	Pg Sand	39.7	0	15.3
CPT_51a	2	1.5	7.9	Gc Silt	40.2	376.1	50.2
CPT_51a	3	7.9	40.8	Gc Clay	0	297.1	257.1
CPT_52	1	0	1.3	Pg Sand	34.8	0	11.9
CPT_52	2	1.3	24.6	Gc Sand	44.8	0	124.4
CPT_52	3	24.6	50.4	Gc Clay	0	359.1	161.6
CPT_53a	1	0	8.3	Gc Sand	45.2	0	60.5
CPT_53a	2	8.3	12.2	Gc Clay	0	417.9	363.9
CPT_53a	3	12.2	13.9	Gc Sand	44.8	0	130.9
CPT_53a	4	13.9	15.1	Gc Clay	0	448.9	370.2
CPT_53a	5	15.1	15.9	Gc Sand	42	0	126
CPT_53a	6	15.9	19	Gc Clay	0	433.3	252.9
CPT_53a	7	19	22.3	Gc Sand	46	0	189.9
CPT_57	1	0	4.7	Pg Sand	44.8	0	41.7
CPT_57	2	4.7	15.5	Gc Clay	0	248.8	149
CPT_57	3	15.5	16.4	Gc Sand	44.9	0	150.9
CPT_57	4	16.4	29.8	Gc Clay	0	383.2	193.7
CPT_58a	1	0	0.7	Gc Sand	32.6	0	6.6
CPT_58a	2	0.7	10.7	Gc Clay	0	155.6	124
CPT_58a	3	10.7	23.5	Gc Sand	42.5	0	138.2
CPT_60	1	0	4.2	Gc Clay	0	193.5	327.8
CPT_60	2	4.2	12.2	PreQ Silt	41	605.1	75.8
CPT_60	3	12.2	21	PreQ Sand	45.6	0	160.1
CPT_63	1	0	0.9	Pg Clay	0	241.3	62.5
CPT_63	2	0.9	28.4	Gc Sand	47.2	0	158.6
CPT_64a	1	0	2.5	Pg Silt	40.9	252.1	23.6
CPT_64a	2	2.5	13.8	Gc Sand	45.9	0	100.3

Location	Layer	Top level	Bottom level	Unit	ϕ' - Average	c_u - Average	G_{max} - Average
[-]	[No.]	[mBSB]	[mBSB]	[-]	[°]	[kPa]	[MPa]
CPT_64a	3	13.8	19.9	Gc Clay	0	422.7	241.4
CPT_65a	1	0	0.4	Pg Silt	34.9	35.1	4.9
CPT_65a	2	0.4	6.9	Gc Clay	0	154.6	250.1
CPT_65a	3	6.9	15.8	PreQ Silt	40.5	659.5	92.6
CPT_65a	4	15.8	19.8	PreQ Sand	45.9	0	170
CPT_66	1	0	0.4	Gc Sand	32.4	0	5
CPT_66	2	0.4	6.5	Gc Clay	0	154.4	128.8
CPT_66	3	6.5	7.5	Gc Sand	43.8	0	82.2
CPT_66	4	7.5	17.5	Gc Clay	0	220.8	144.1
CPT_66	5	17.5	24.6	Gc Sand	41.6	0	150.4
CPT_66	6	24.6	27.1	Gc Clay	0	313.6	159.5
CPT_66	7	27.1	40.3	Gc Sand	43.9	0	234.7
CPT_67	1	0	0.9	Pg Sand	36.3	0	10.2
CPT_67	2	0.9	2.5	Pg Sand	45.4	0	35.5
CPT_67	3	2.5	33.2	Gc Sand	46.9	0	173.7
CPT_68	1	0	0.3	Pg Sand	35	0	4.1
CPT_68	2	0.3	15.7	Pg Clay	0	98.5	92.4
CPT_68	3	15.7	17.8	Gc Sand	45.9	0	163.5
CPT_68	4	17.8	18.9	Gc Silt	39.8	733.3	124.8
CPT_68	5	18.9	22.5	Gc Sand	45.3	0	183.2
CPT_81	1	0	0.4	Pg Sand	38	0	6.6
CPT_81	2	0.4	1.5	Pg Organic	0	73.3	9.7
CPT_81	3	1.5	4.5	Pg Organic	0	17.5	16
CPT_81	4	4.5	6	Pg Sand	46.9	0	79.9
CPT_83	1	0	1.6	Pg Silt	35.5	62.9	12.4
CPT_83	2	1.6	3.9	Gc Sand	41.7	0	38.9
CPT_83	3	3.9	24.7	Gc Clay	0	271.1	199.6
CPT_84	1	0	0.3	Pg Sand	37.4	0	4.3
CPT_84	2	0.3	10.1	Gc Clay	0	175.7	161.4
CPT_84	3	10.1	15.2	Gc Sand	43.6	0	121.2
CPT_84	4	15.2	20.5	Gc Clay	0	311	222.9
CPT_84	5	20.5	24.3	Gc Sand	43.6	0	175.2
CPT_84	6	24.3	41.3	Gc Clay	0	367.6	274.2
CPT_86a	1	0	1.6	Pg Clay	0	98.1	130.1
CPT_86a	2	1.6	4.6	Pg Sand	50.2	0	67
SCPT_21	1	0	2.6	Pg Sand	41.8	0	24.1
SCPT_21	2	2.6	5.2	Pg Silt	35	134.1	34.3
SCPT_21	3	5.2	6.8	Pg Clay	0	63.9	105.8
SCPT_21	4	6.8	8.6	Pg Sand	45.2	0	94.1
SCPT_21	5	8.6	12.7	Pg Sand	40.1	0	87.9
SCPT_21	6	12.7	18.2	Pg Sand	44.7	0	143.1
SCPT_25	1	0	0.9	Pg Sand	38.4	0	13
SCPT_25	2	0.9	4.2	Pg Sand	43.3	0	39
SCPT_25	3	4.2	6.8	Pg Sand	48.2	0	89.1
SCPT_25	4	6.8	10	Pg Silt	34.5	164	55.8
SCPT_25	5	10	14.3	Pg Sand	43.6	0	117.2
SCPT_25	6	14.3	30	Pg Clay	0	170	153.5
SCPT_33c	1	0	3.4	Gc Sand	45.1	0	36.1

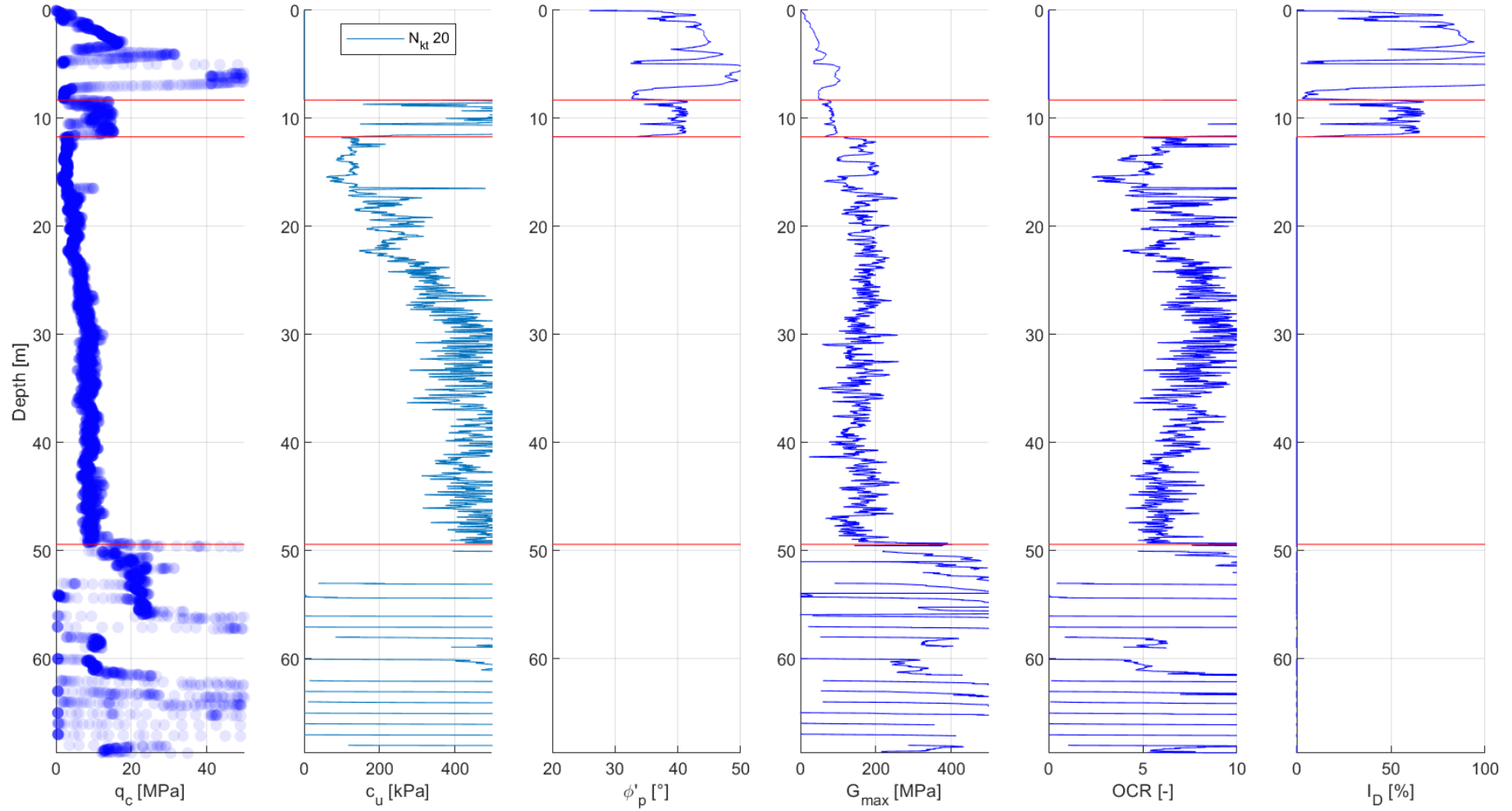
Location	Layer	Top level	Bottom level	Unit	ϕ' - Average	c_u - Average	G_{max} - Average
[-]	[No.]	[mBSB]	[mBSB]	[-]	[°]	[kPa]	[MPa]
SCPT_33c	2	3.4	9.3	Gc Sand	45.3	0	83
SCPT_33c	3	9.3	18.7	Gc Silt	41.1	806	110.6
SCPT_33c	4	18.7	20	Gc Sand	45.8	0	180.3
SCPT_45	1	0	3.6	Pg Sand	37.8	0	23
SCPT_45	2	3.6	7	Pg Clay	0	102.8	89.9
SCPT_45	3	7	8.3	Pg Sand	41.4	0	75.5
SCPT_45	4	8.3	20.4	Pg Clay	0	178.5	155.4
SCPT_45	5	20.4	37	Gc Clay	0	234.9	158.1
SCPT_55	1	0	6.8	Pg Sand	41.7	0	43.7
SCPT_55	2	6.8	7	Gc Sand	49.2	0	108.7
SCPT_59	1	0	0.7	Pg Clay	0	104.7	42.7
SCPT_59	2	0.7	3.4	Pg Sand	46.5	0	40.2
SCPT_59	3	3.4	6.6	Gc Silt	40	406.2	52
SCPT_59	4	6.6	21.9	Gc Till	0	136.7	100.6
SCPT_59	5	21.9	26.1	Gc Sand	44.2	0	190.6
SCPT_59	6	26.1	27.4	Gc Sand	42.6	0	186.9

Appendix B CPT plots including calculated soil properties using CPT correlations

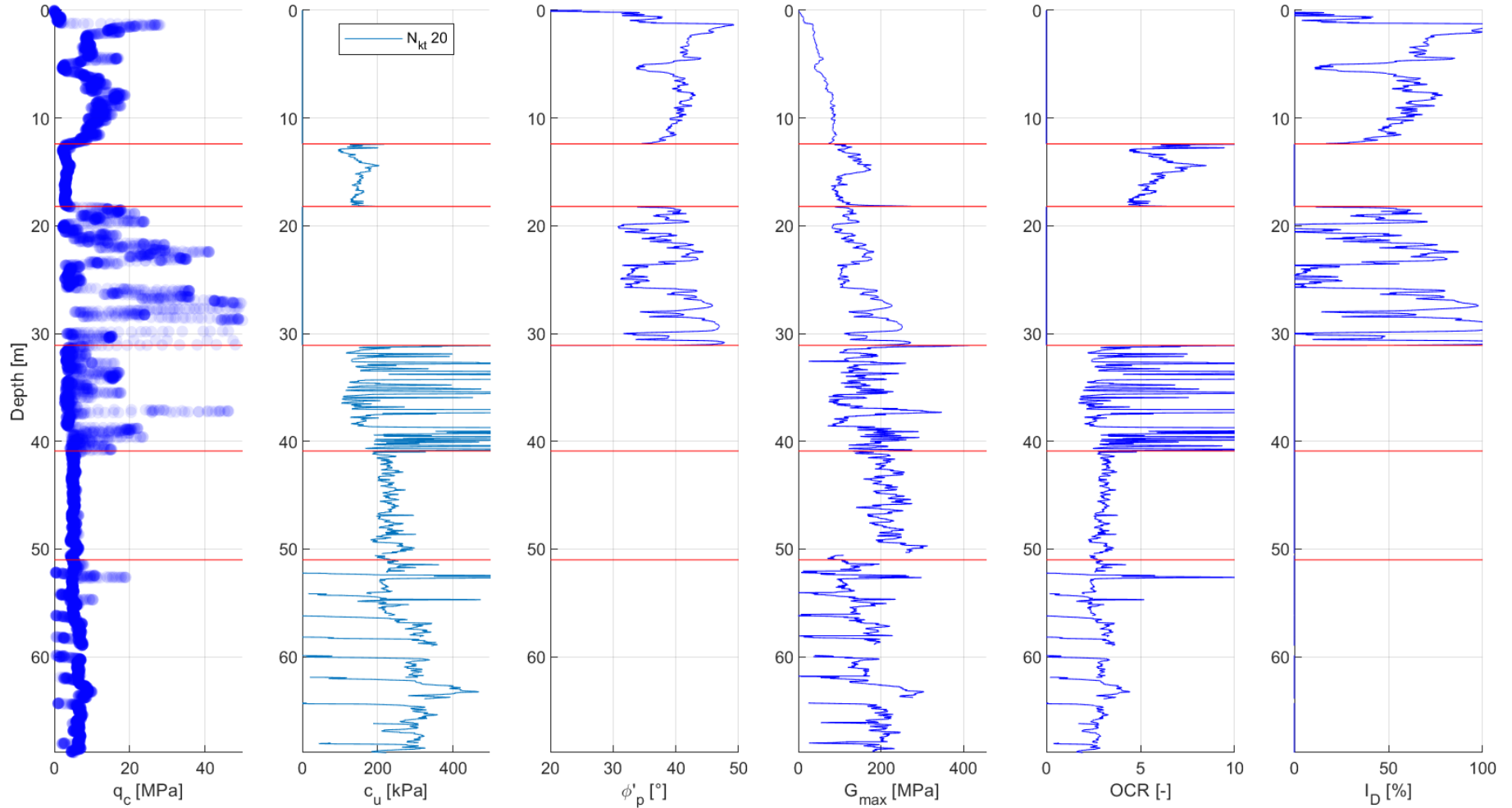
CPT-01



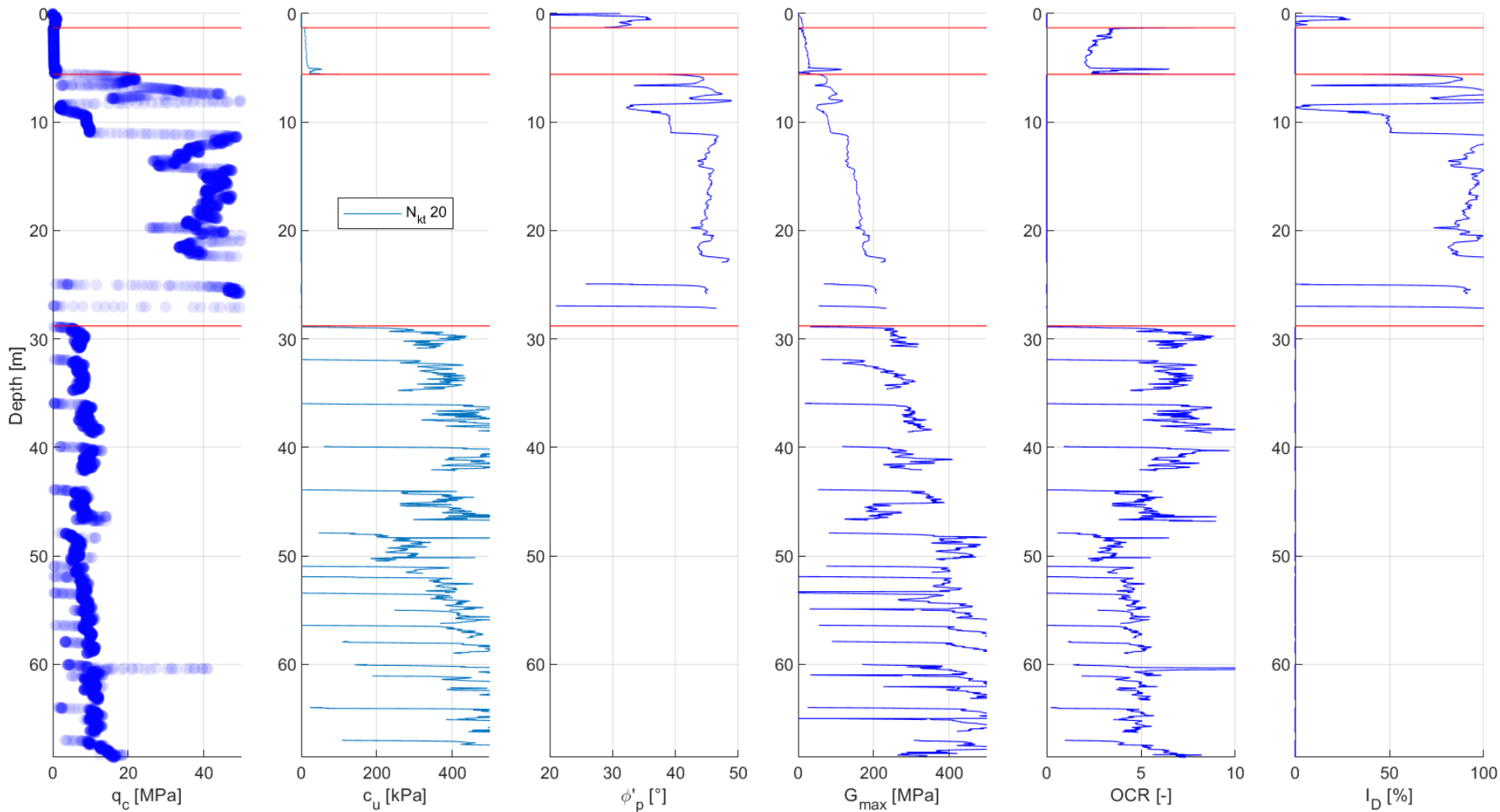
CPT-02



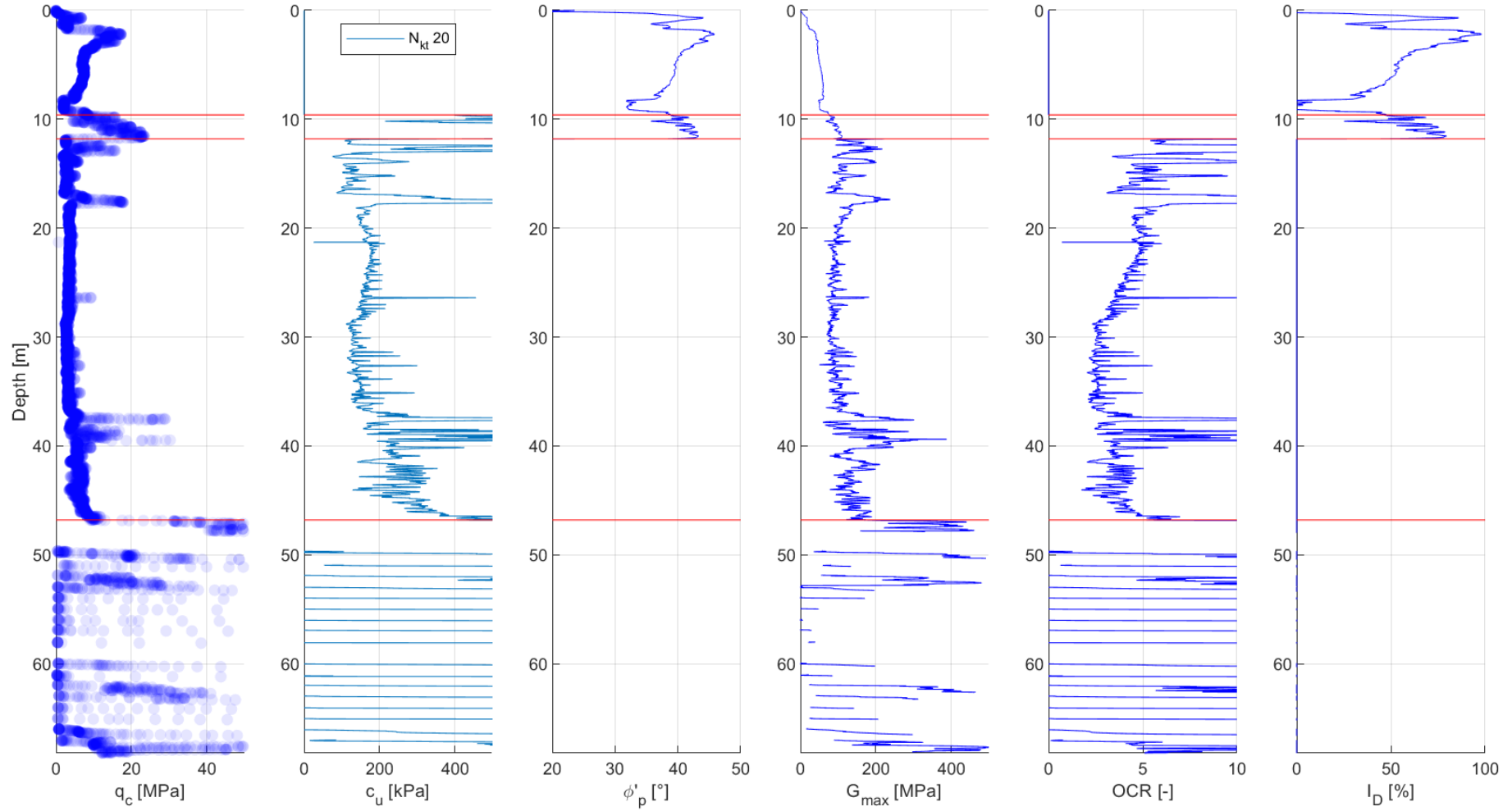
CPT-03



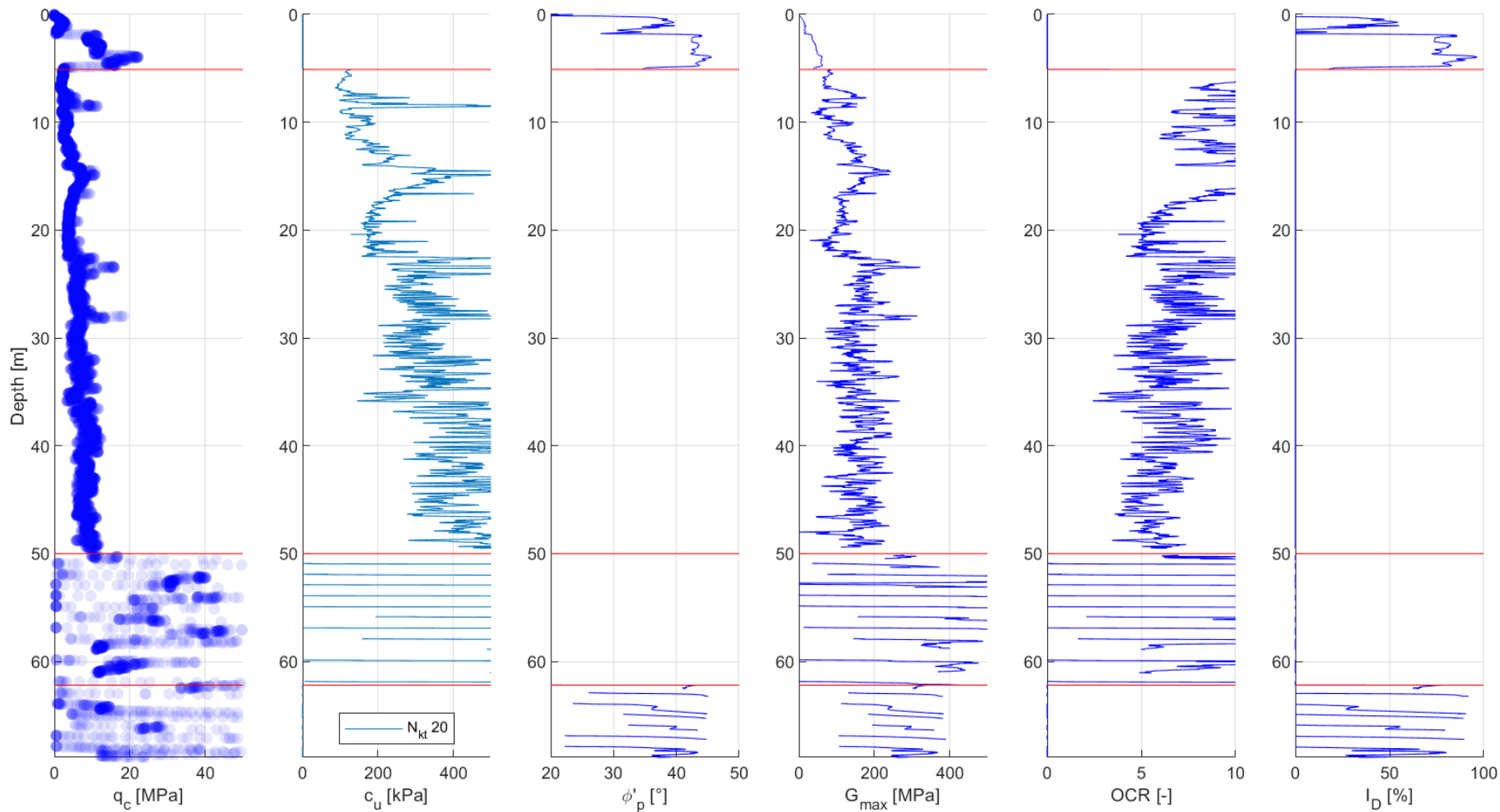
CPT-04



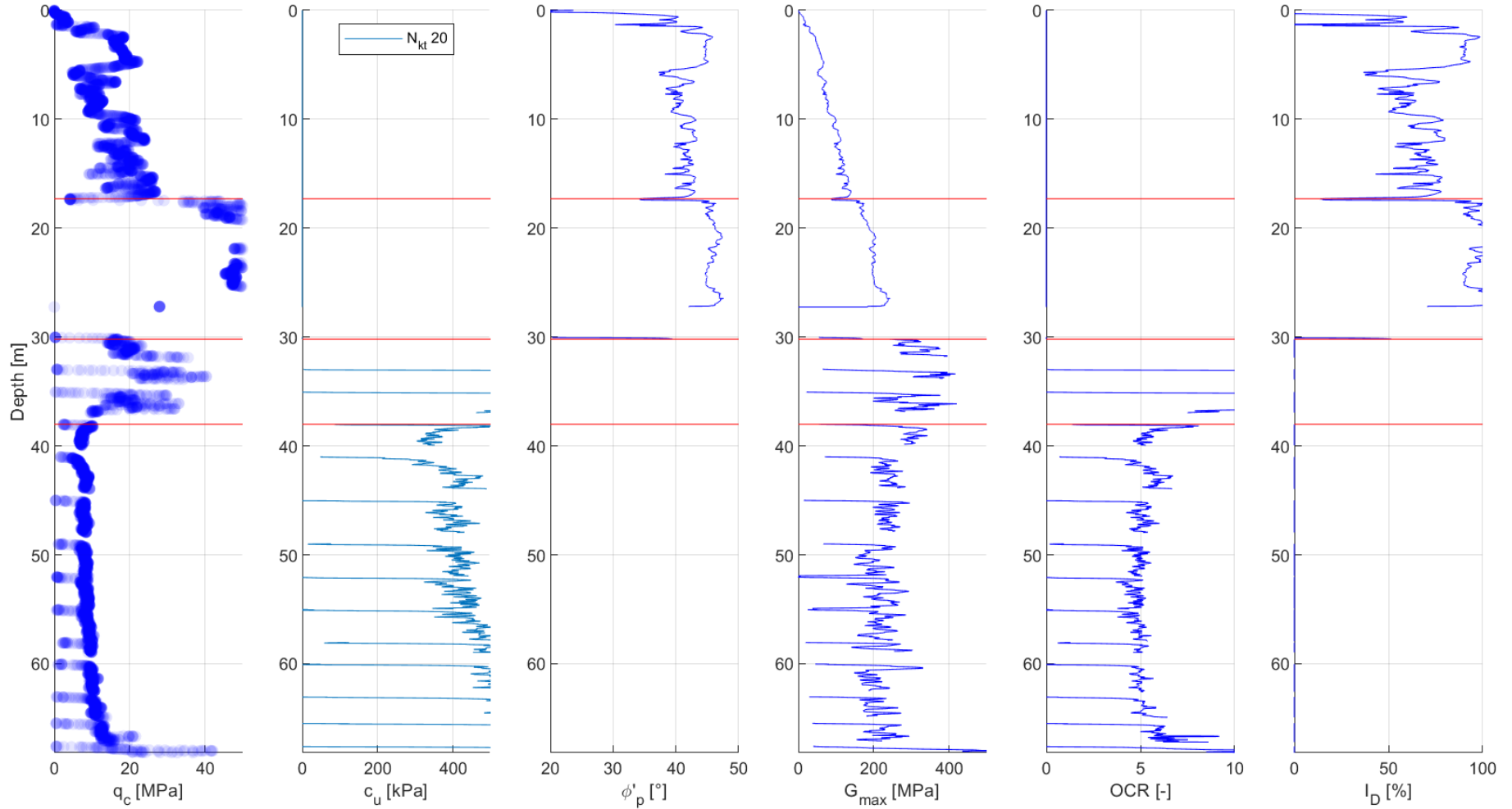
CPT-05



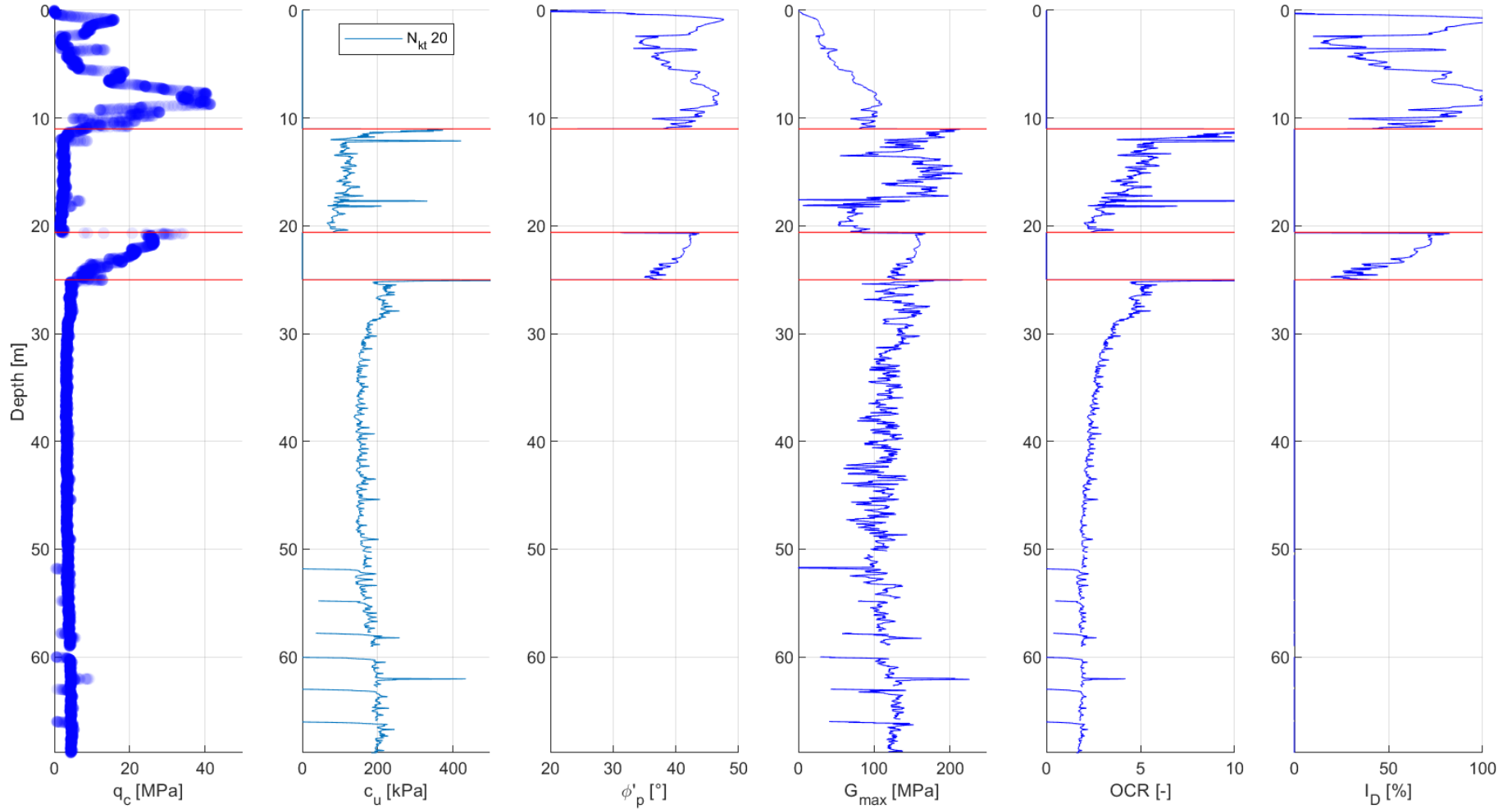
CPT-06



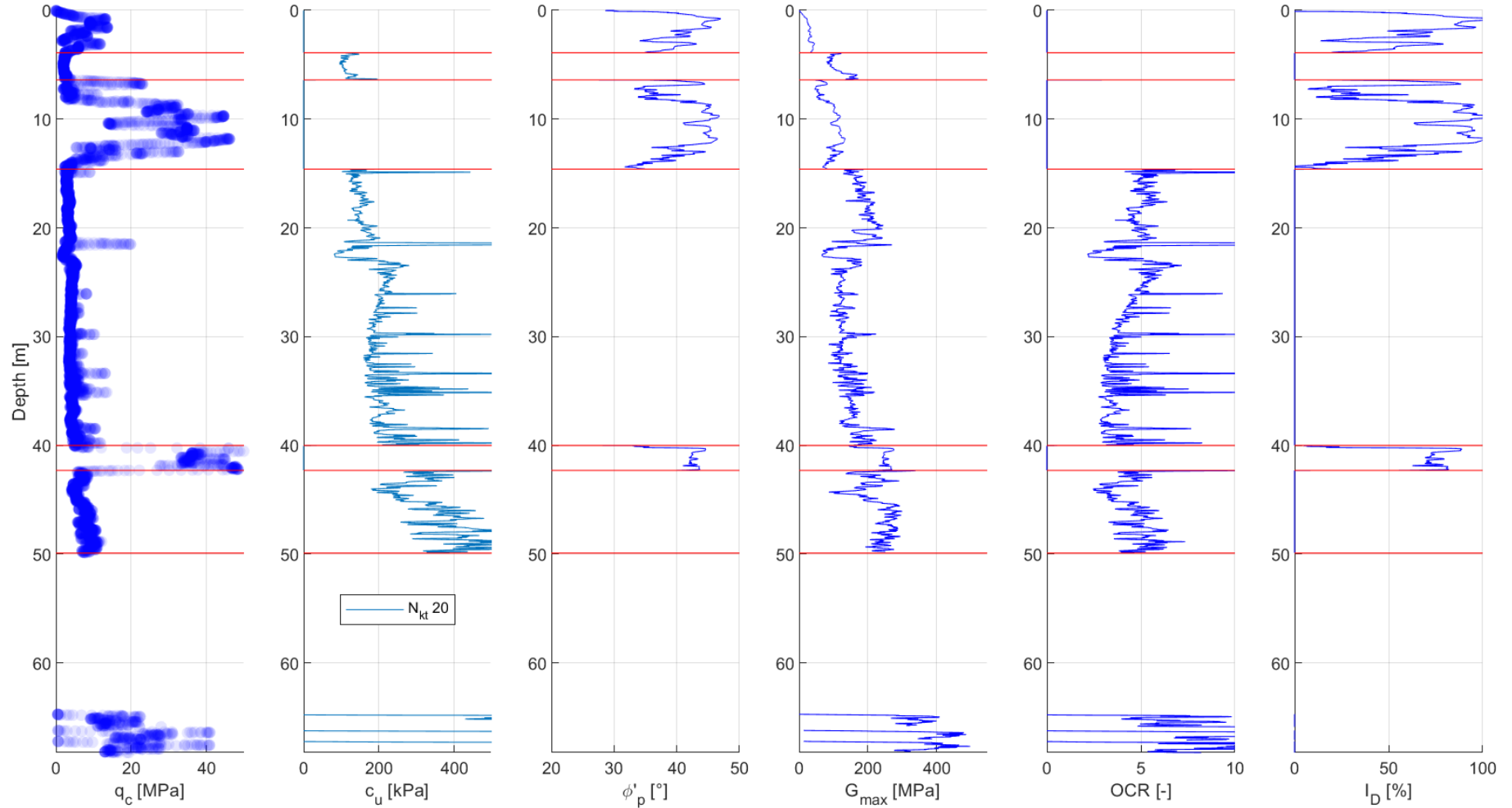
CPT-07



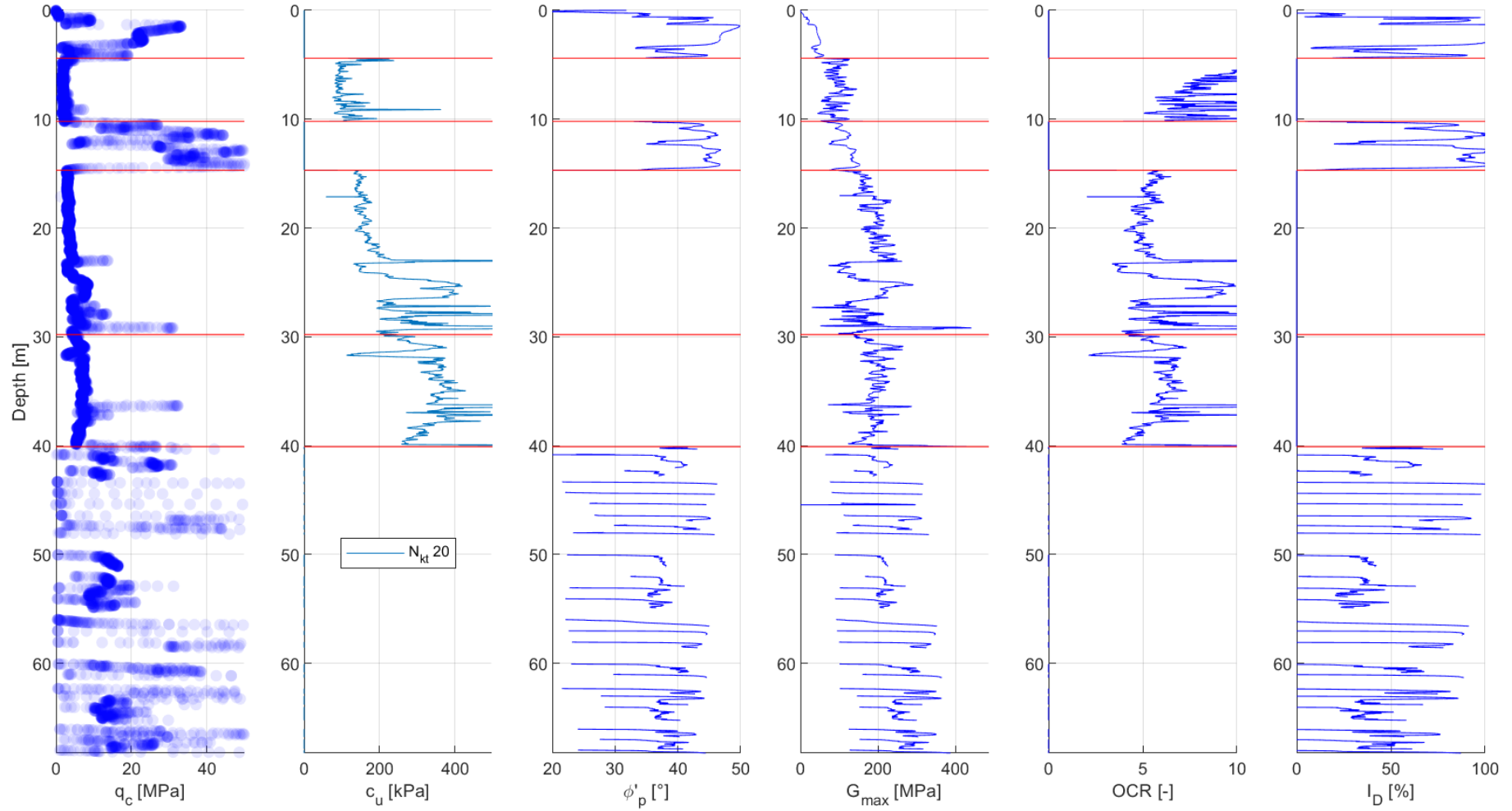
CPT-08



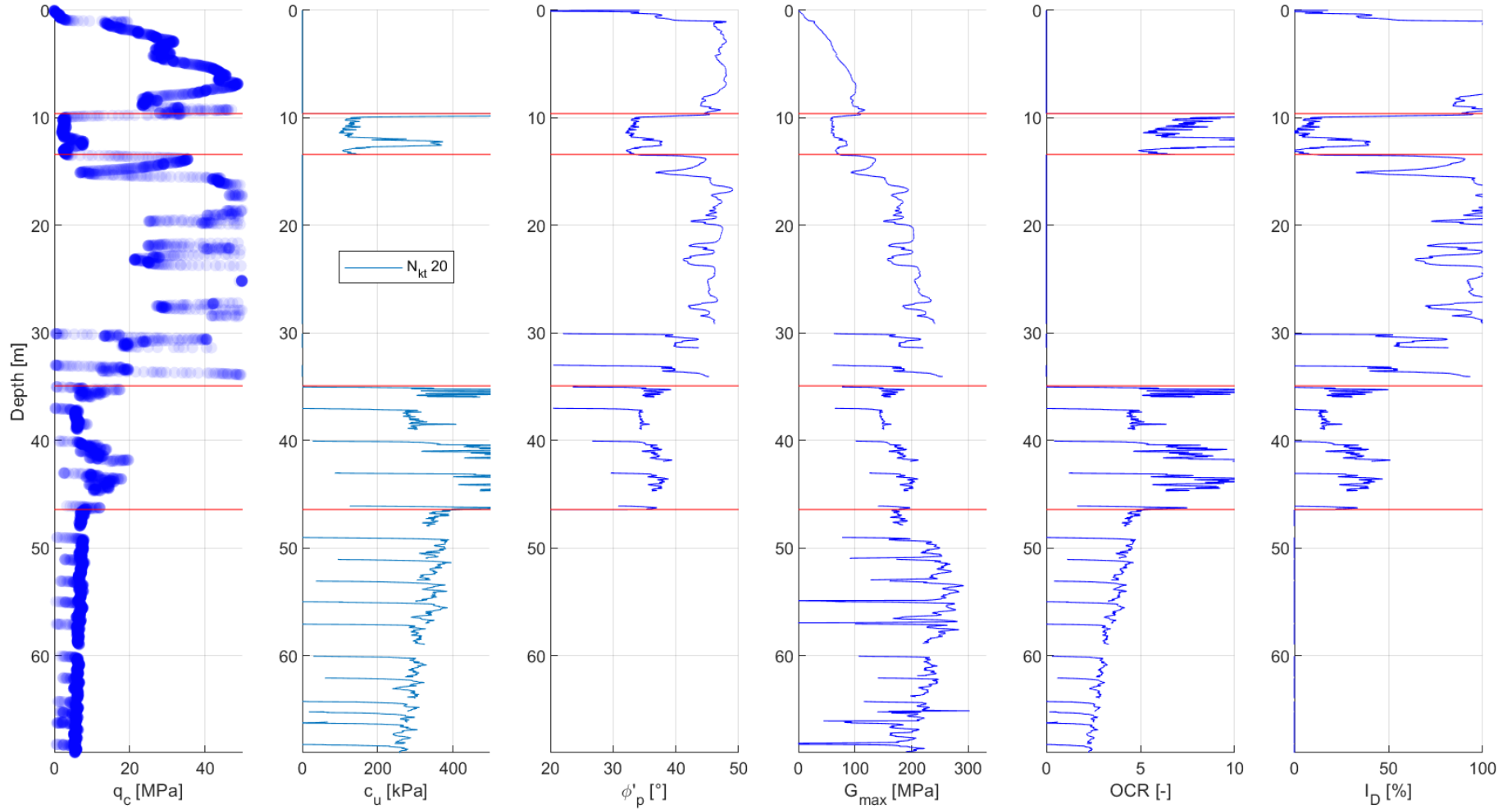
CPT-09



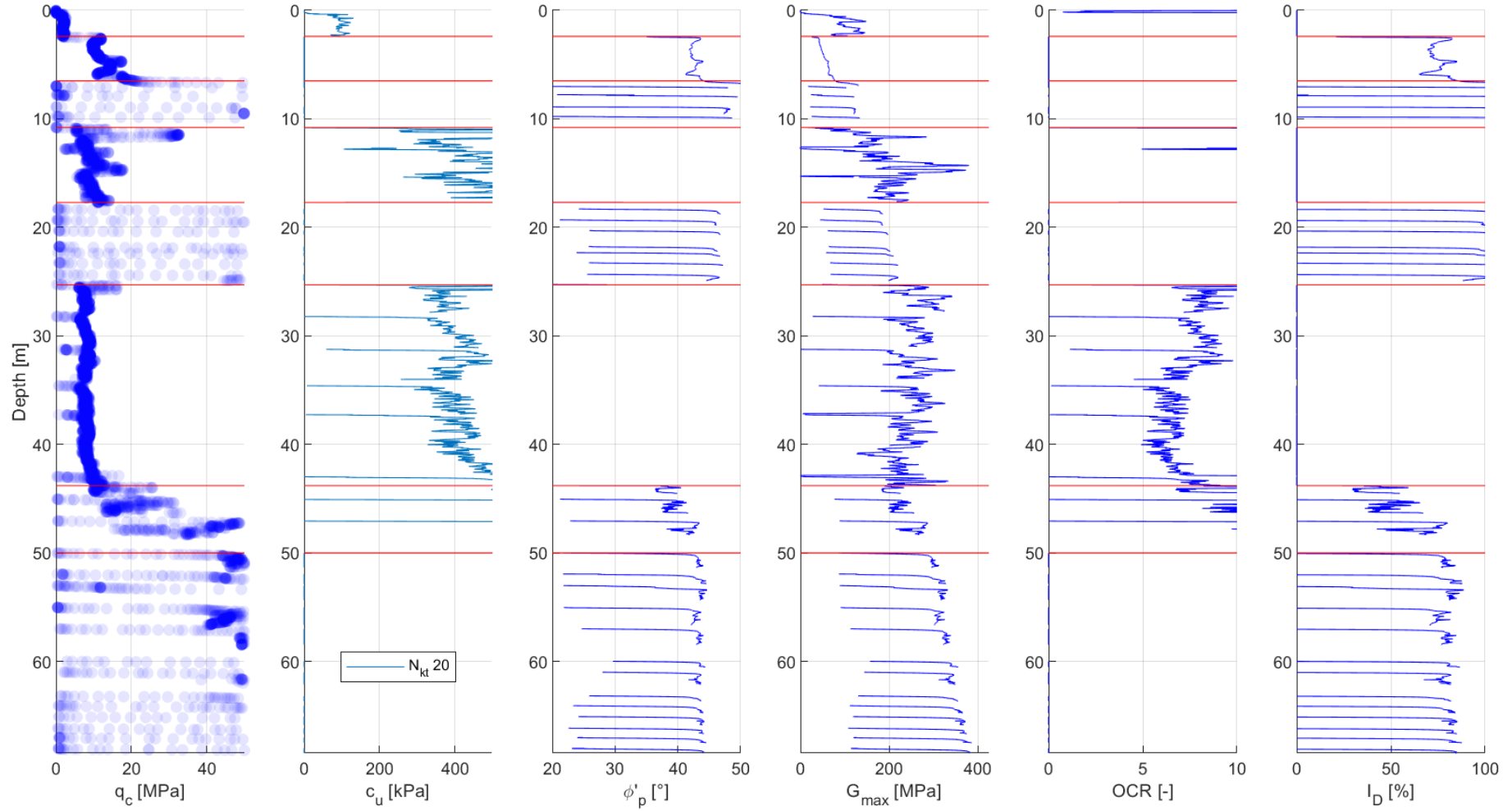
CPT-10



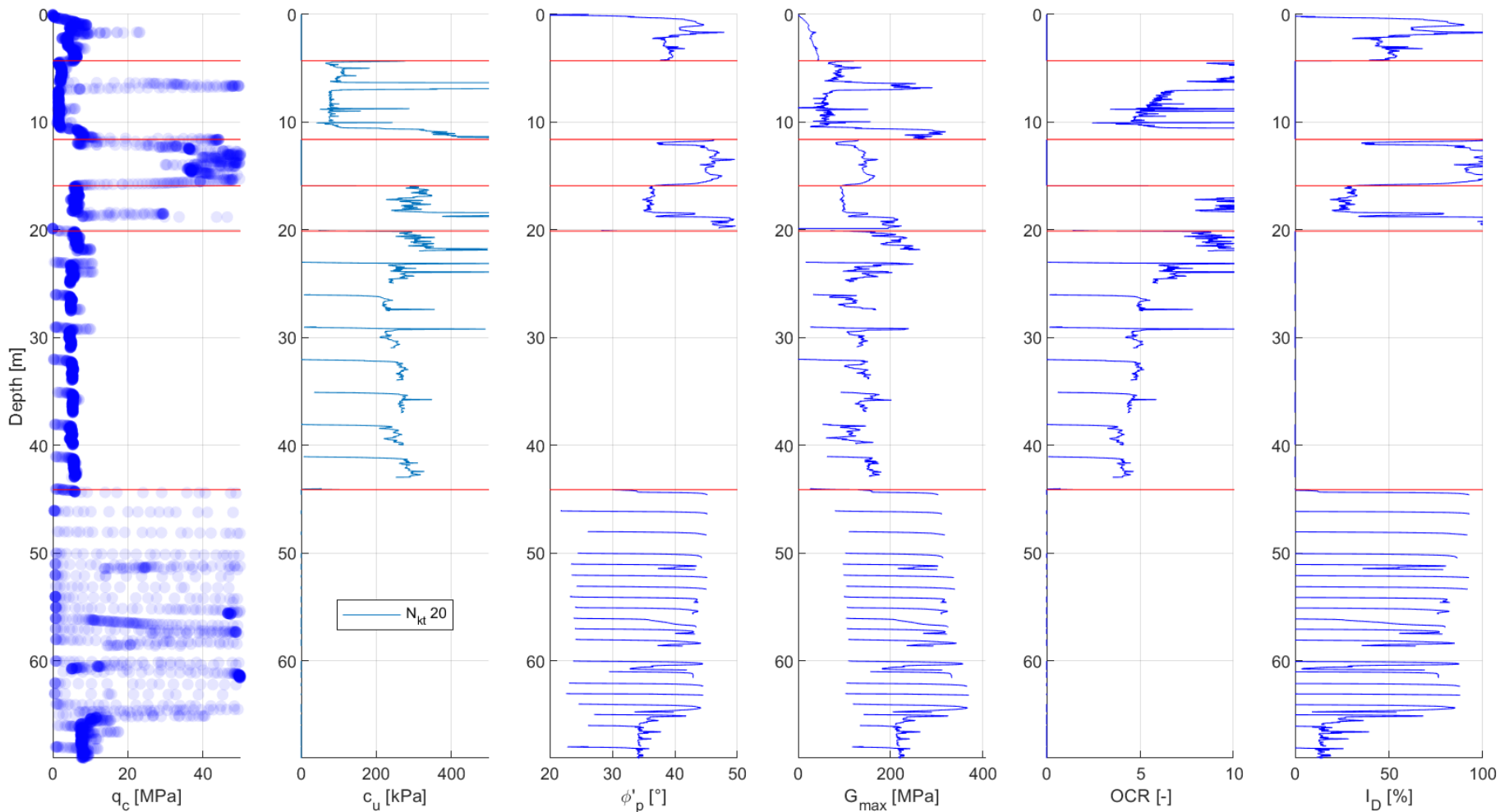
CPT-11



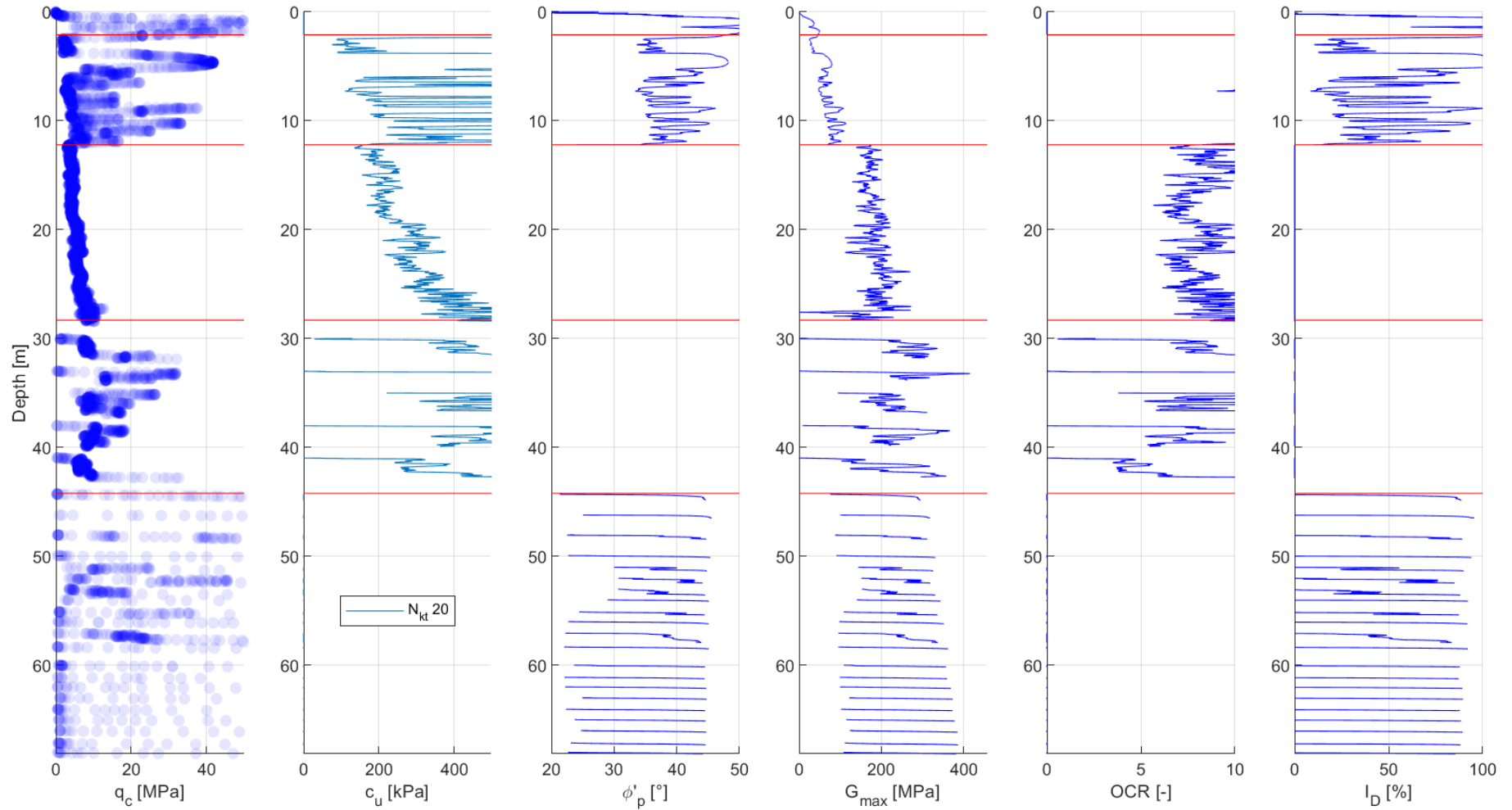
CPT-12



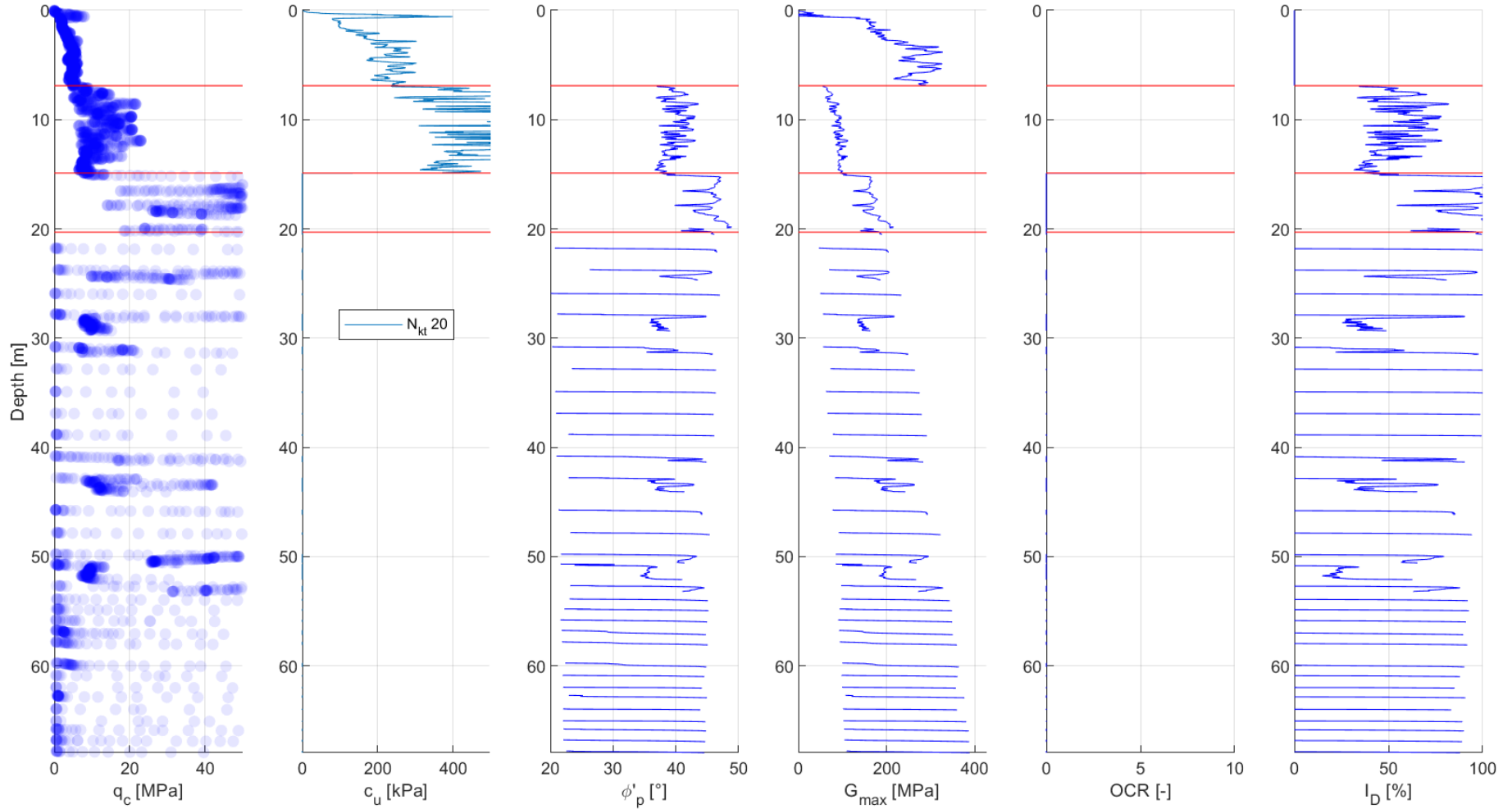
CPT-13



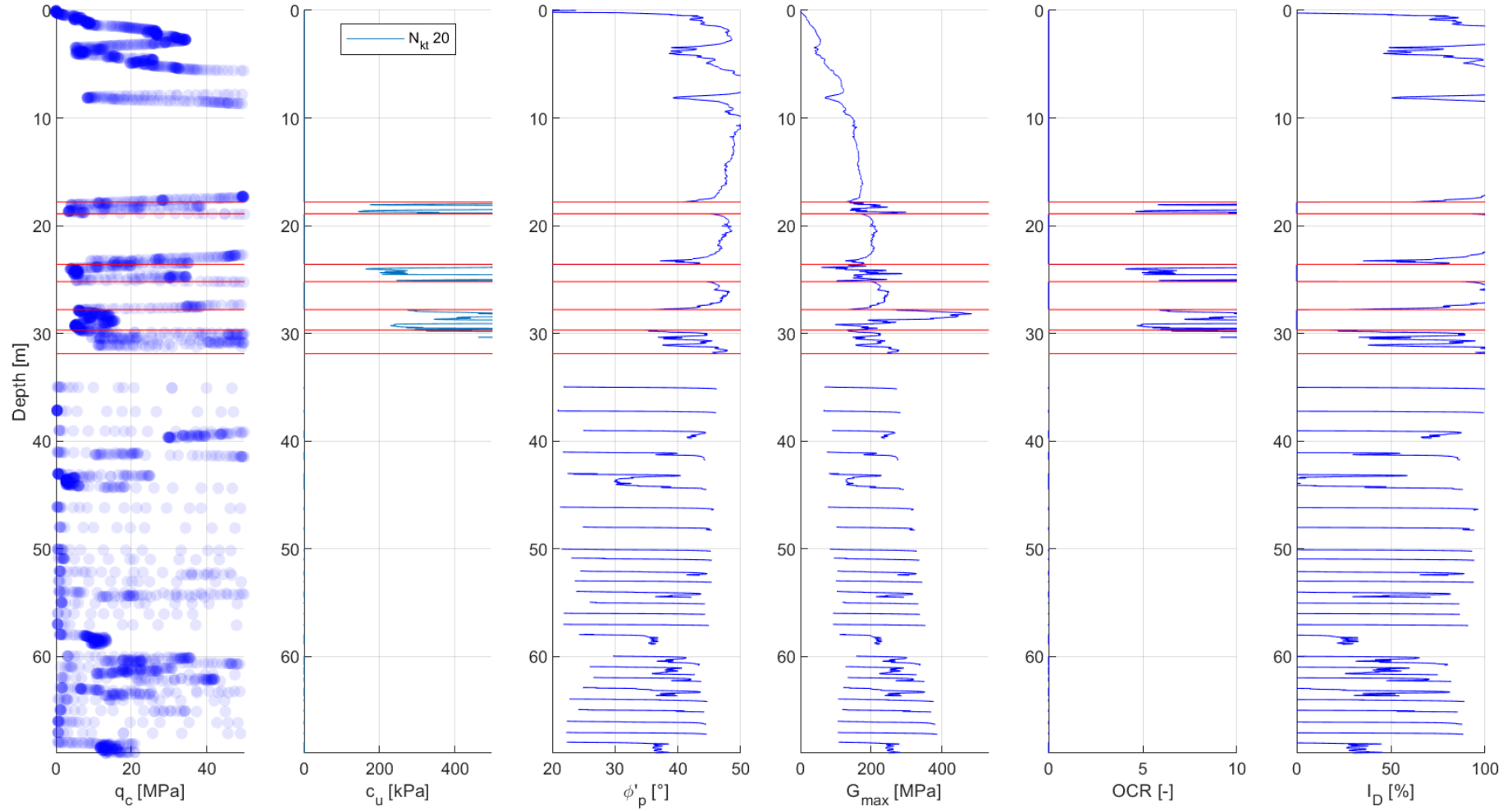
CPT-14



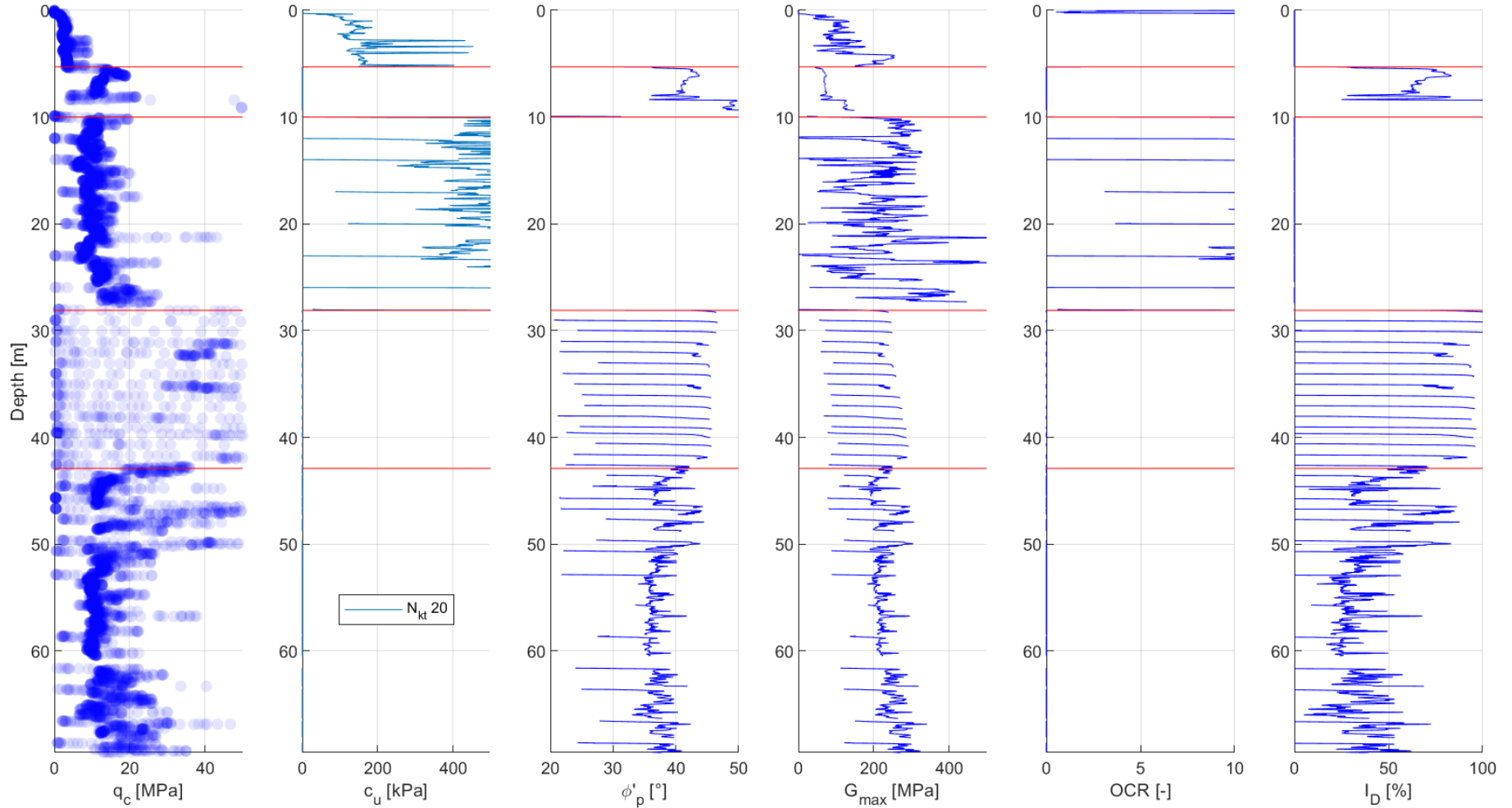
CPT-15



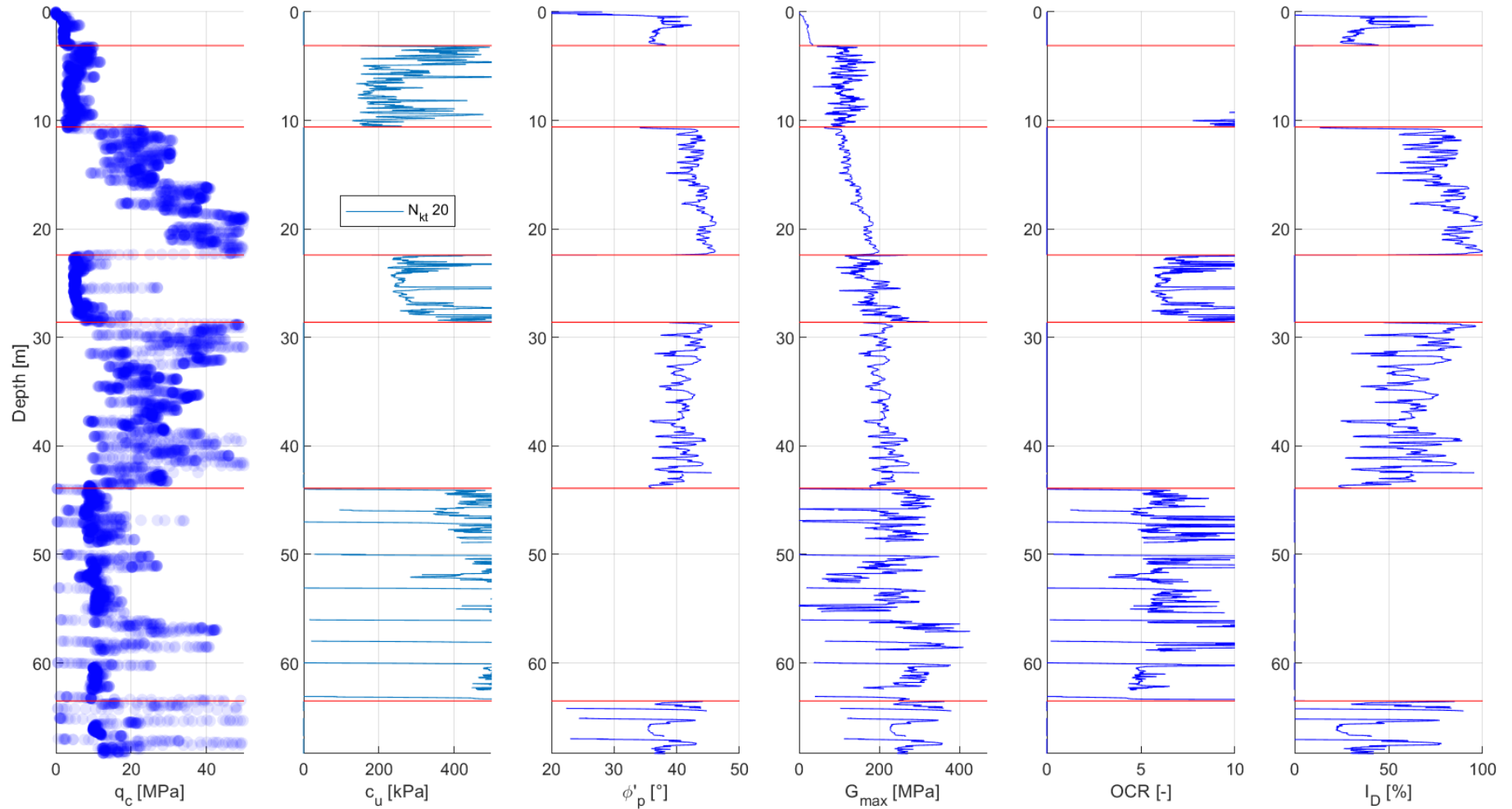
CPT-16



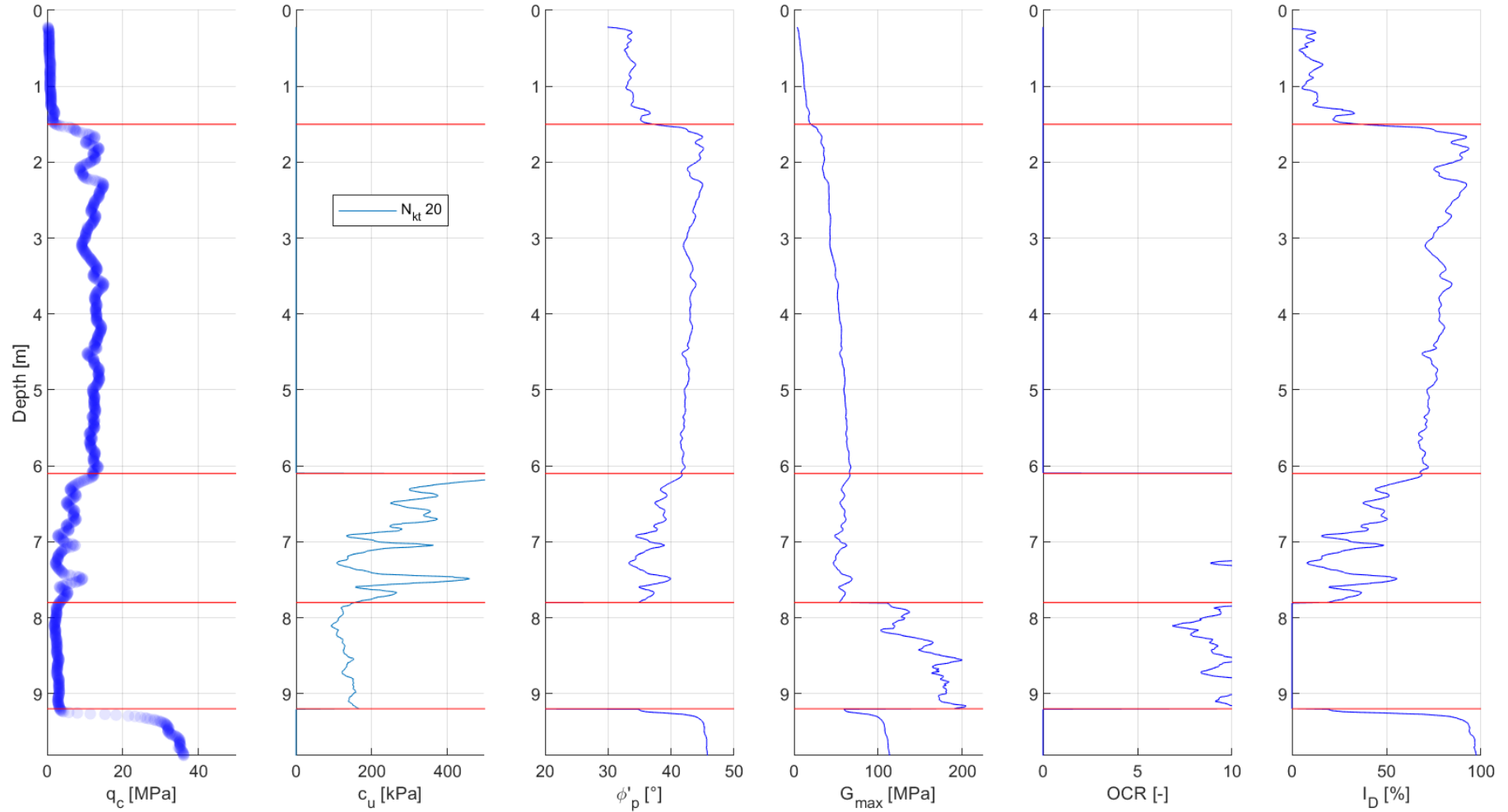
CPT-17



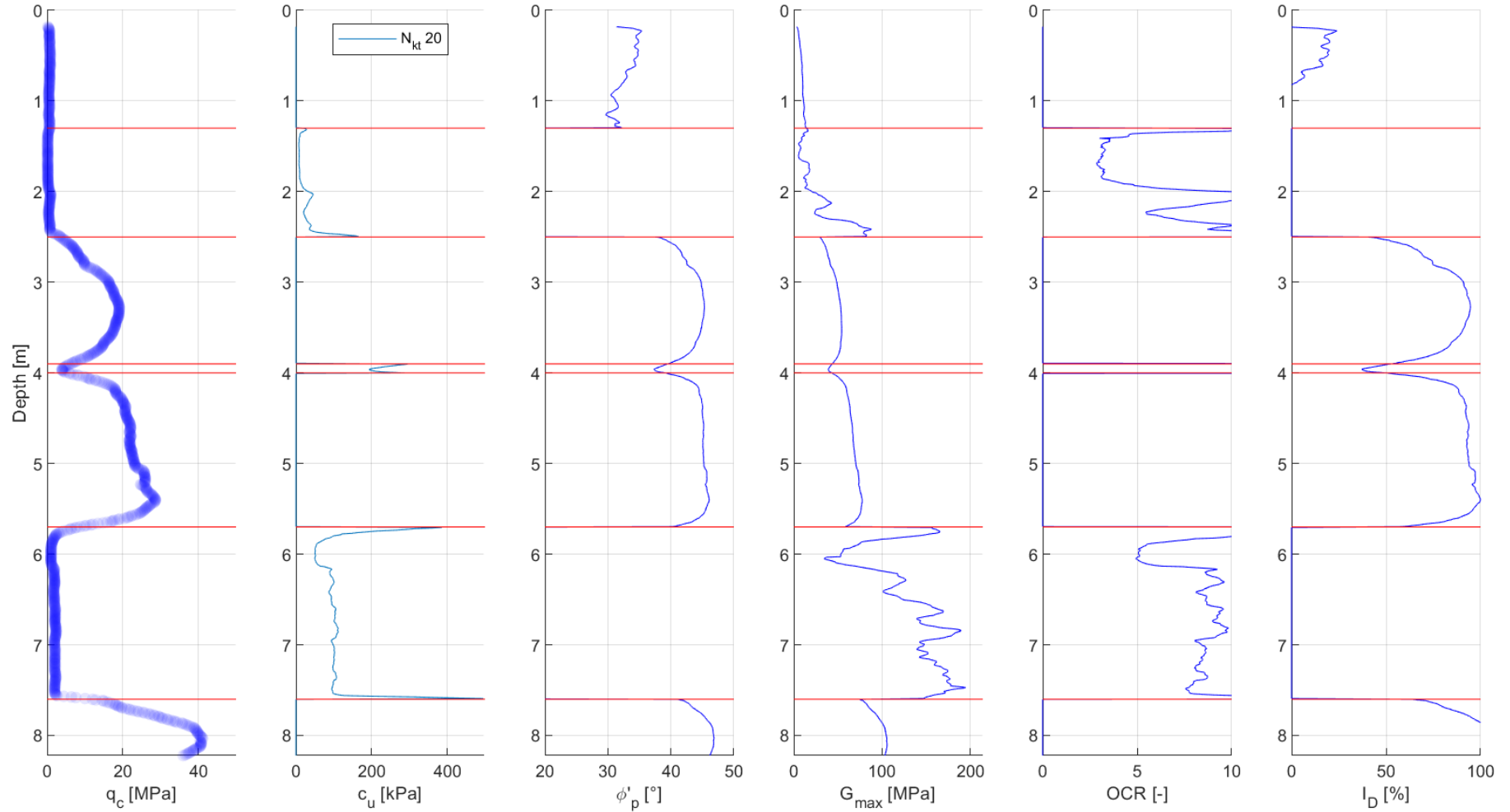
CPT-18



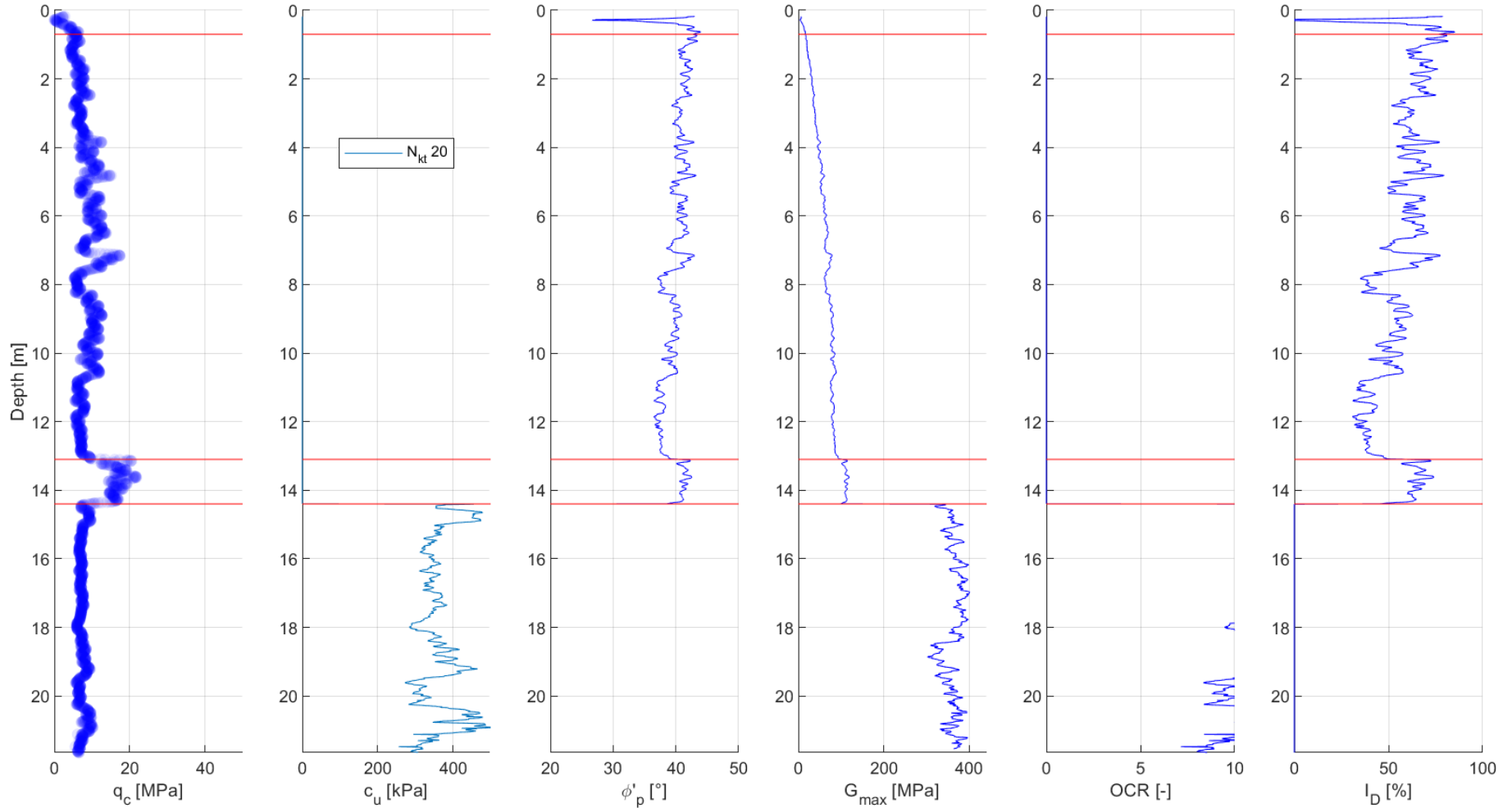
CPT-19



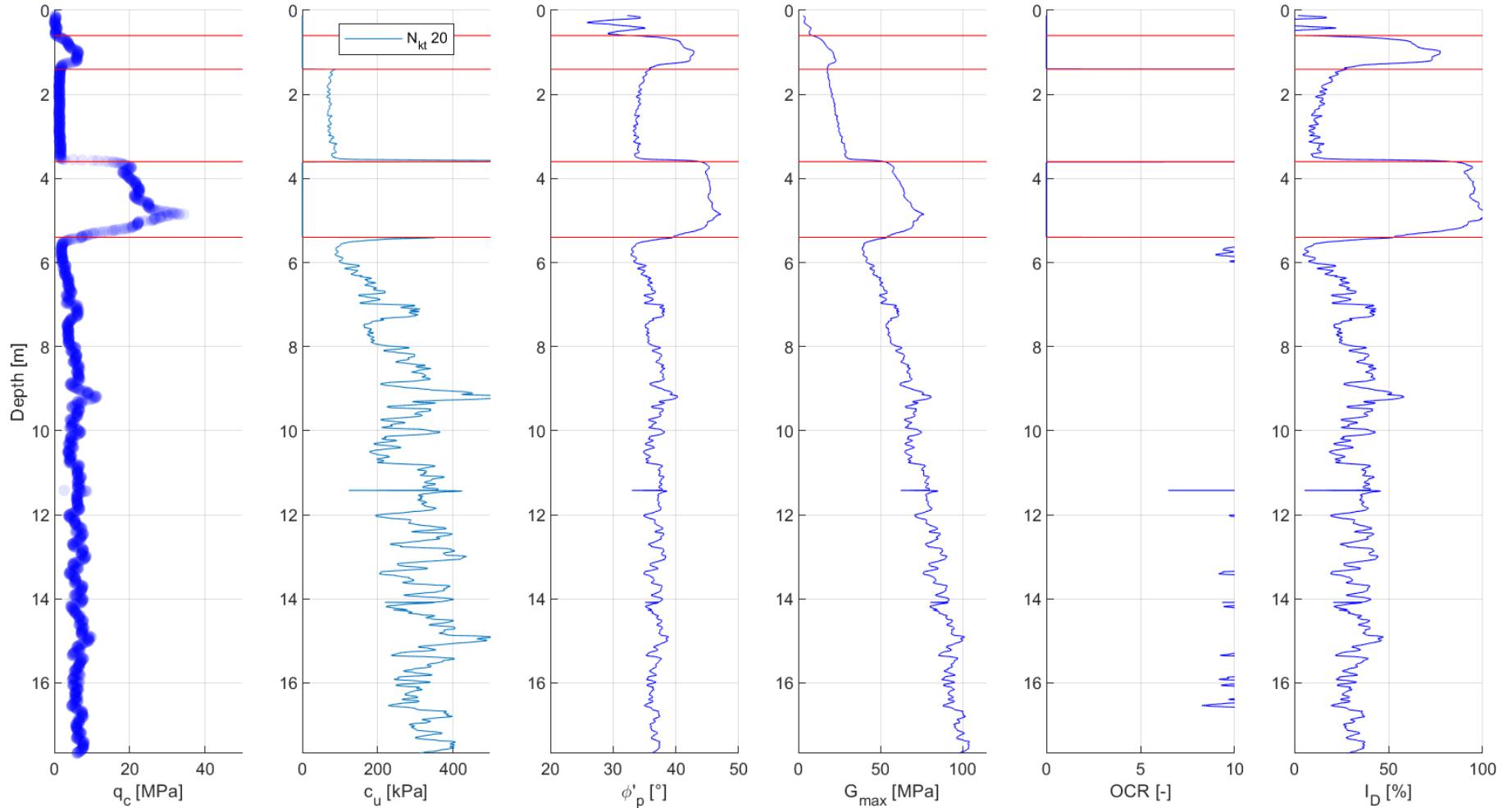
CPT-20



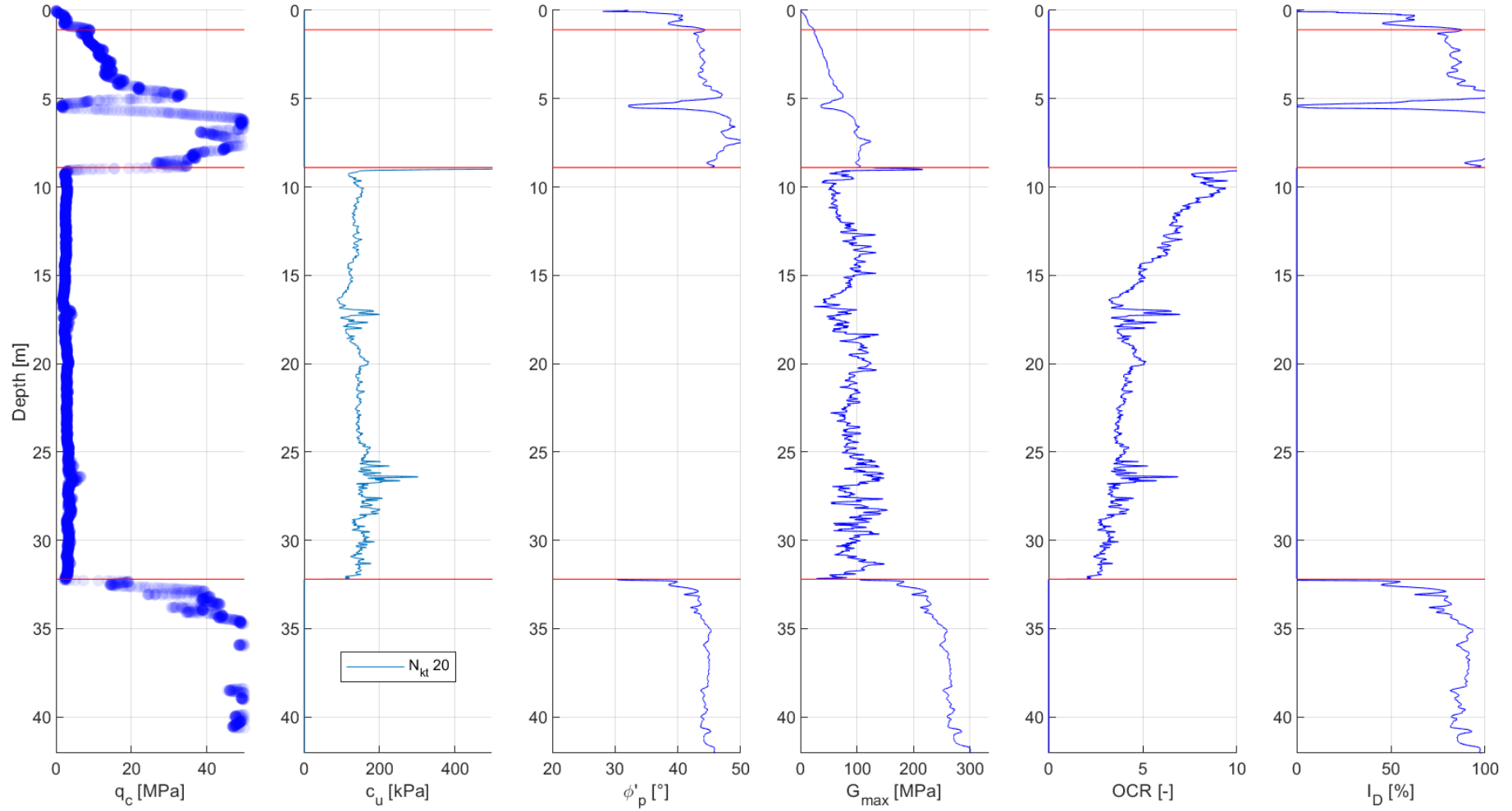
CPT-22



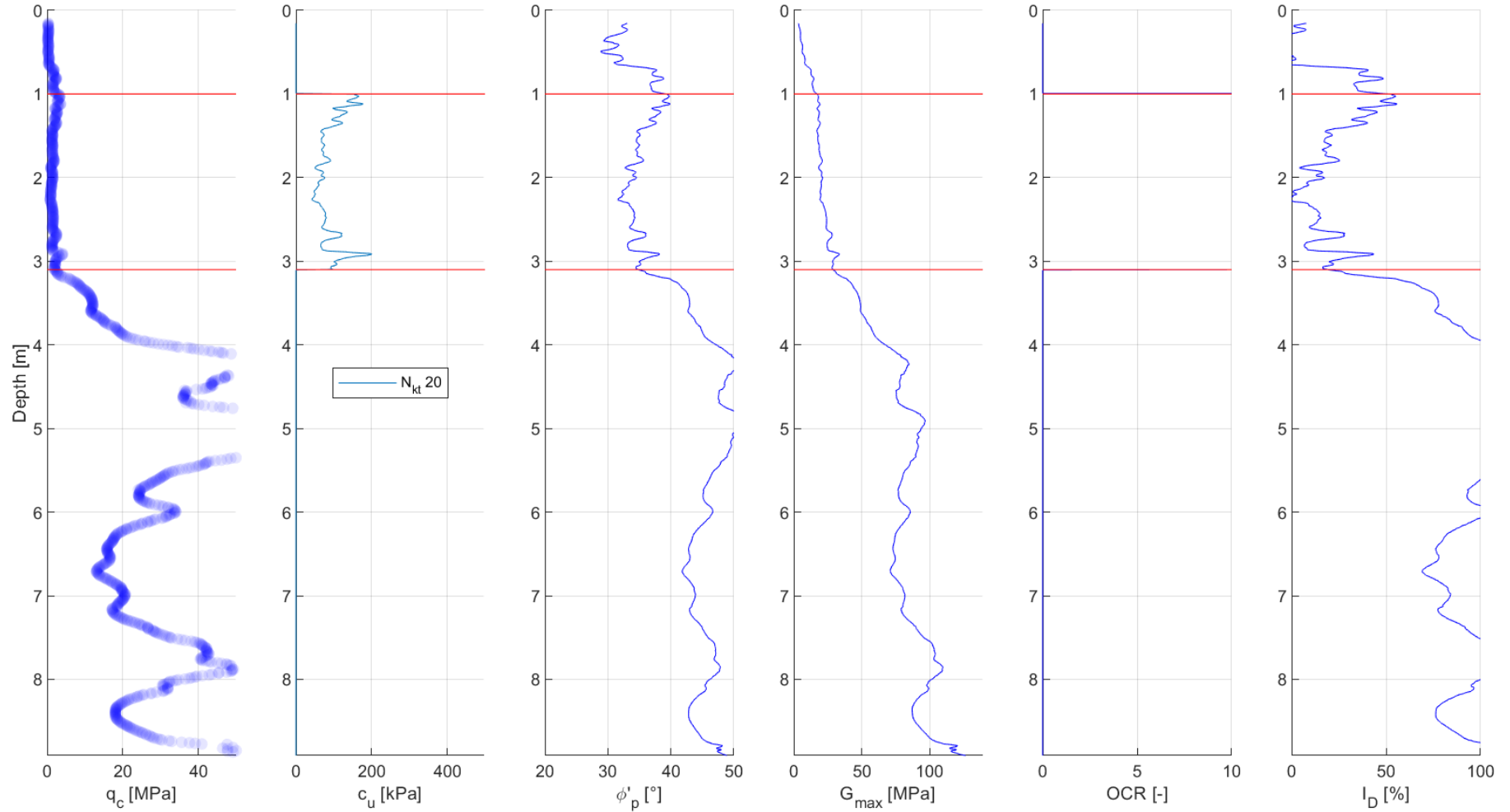
CPT-23



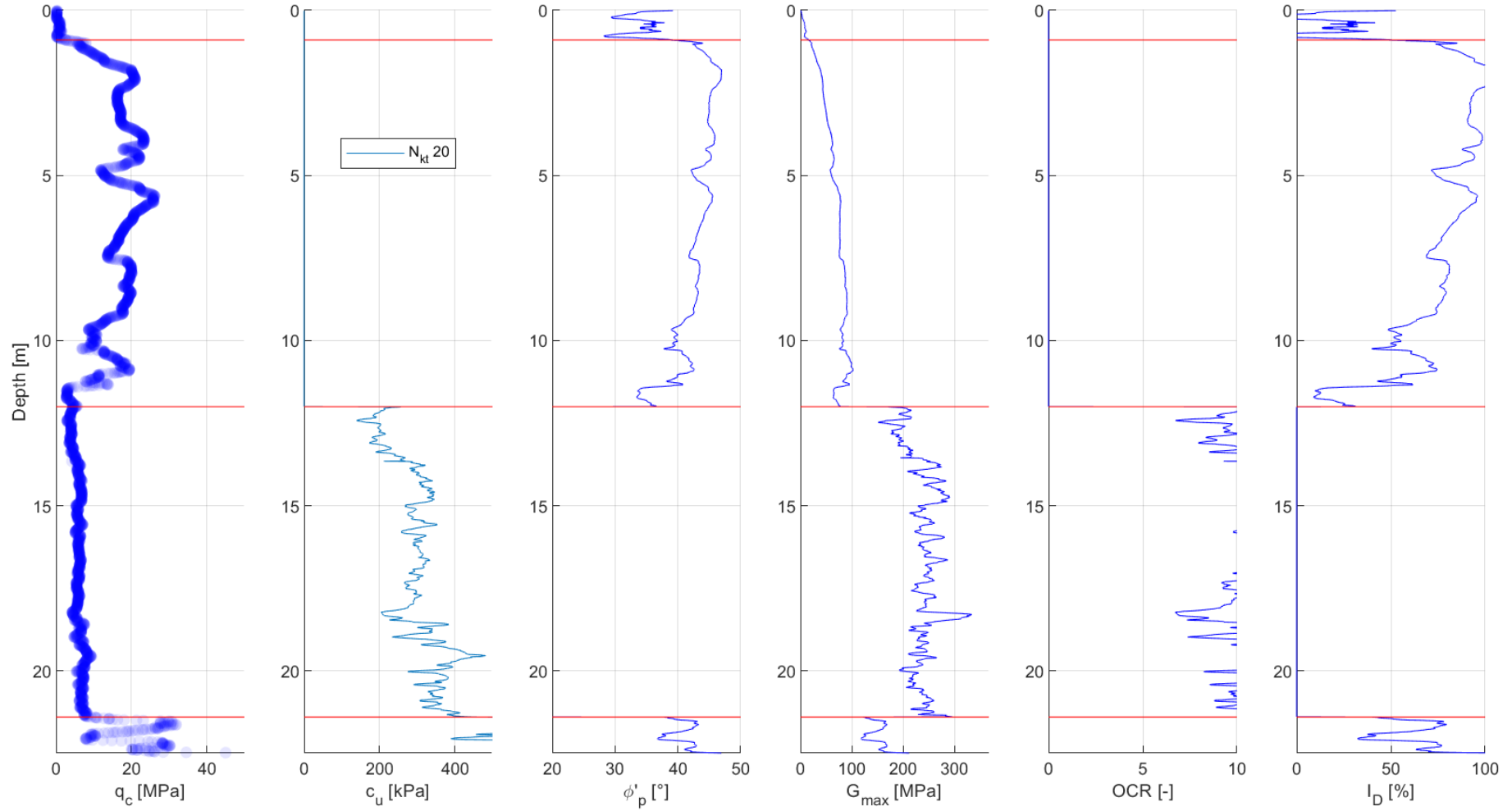
CPT-24



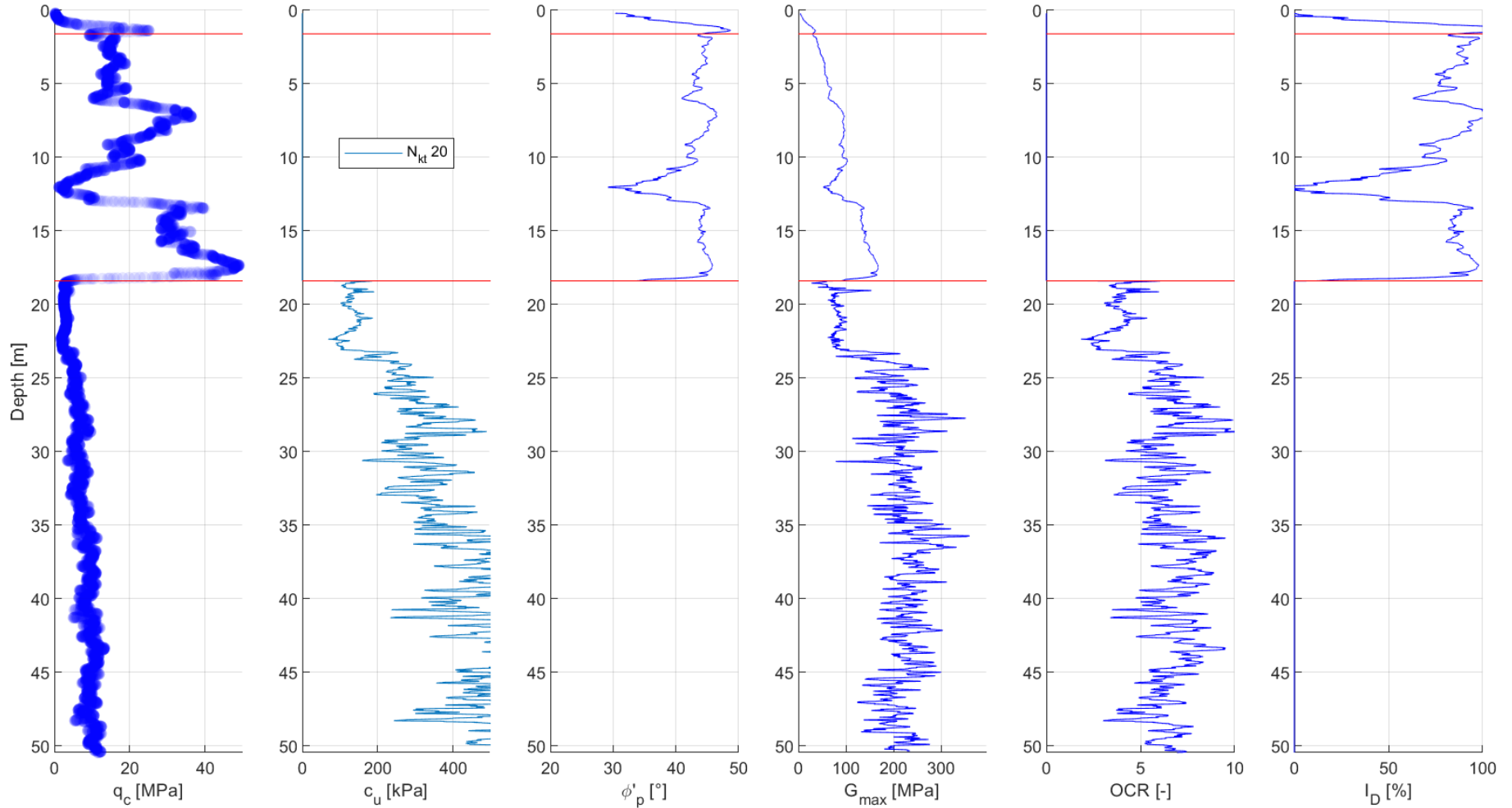
CPT-26a



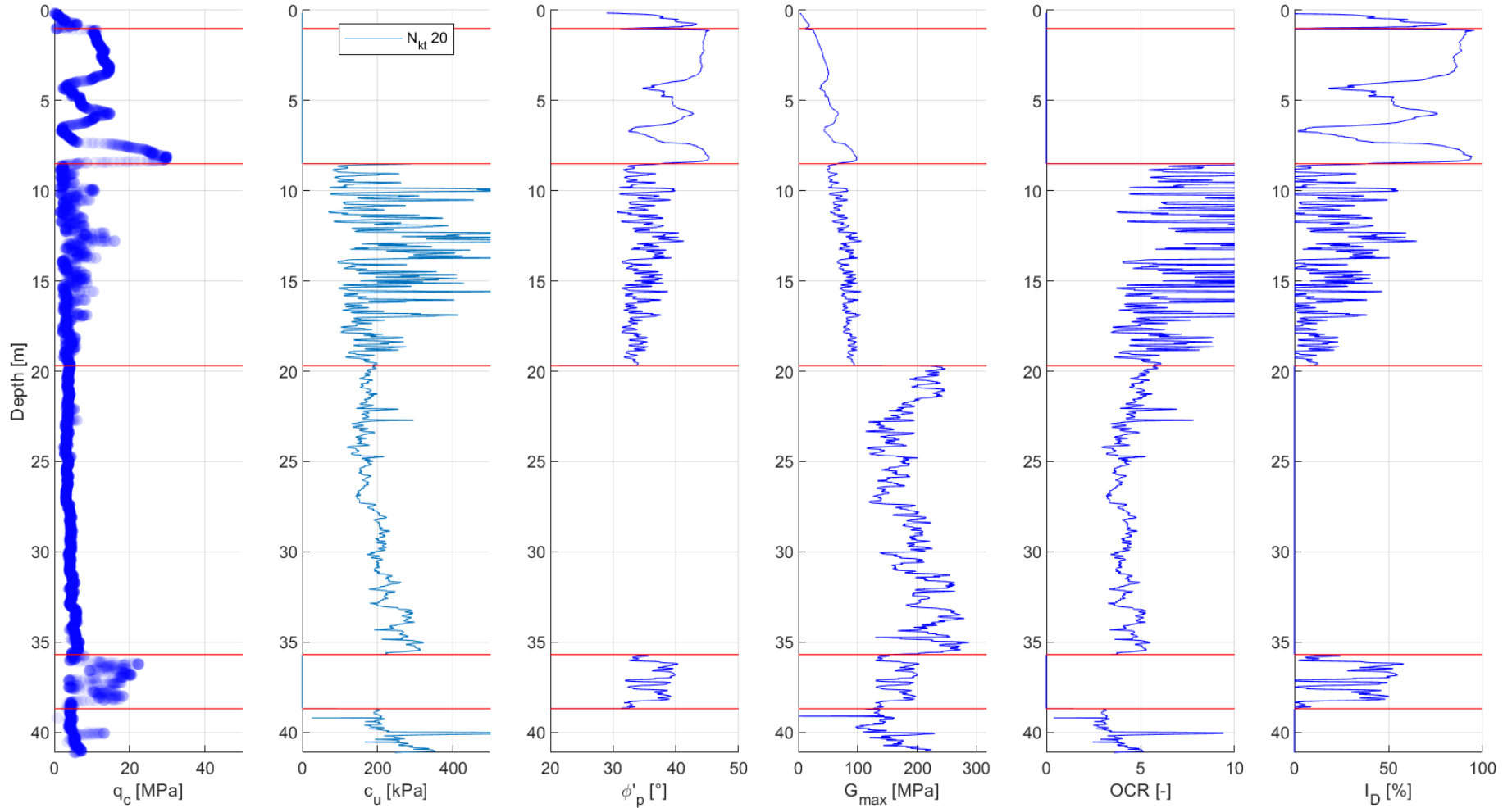
CPT-27



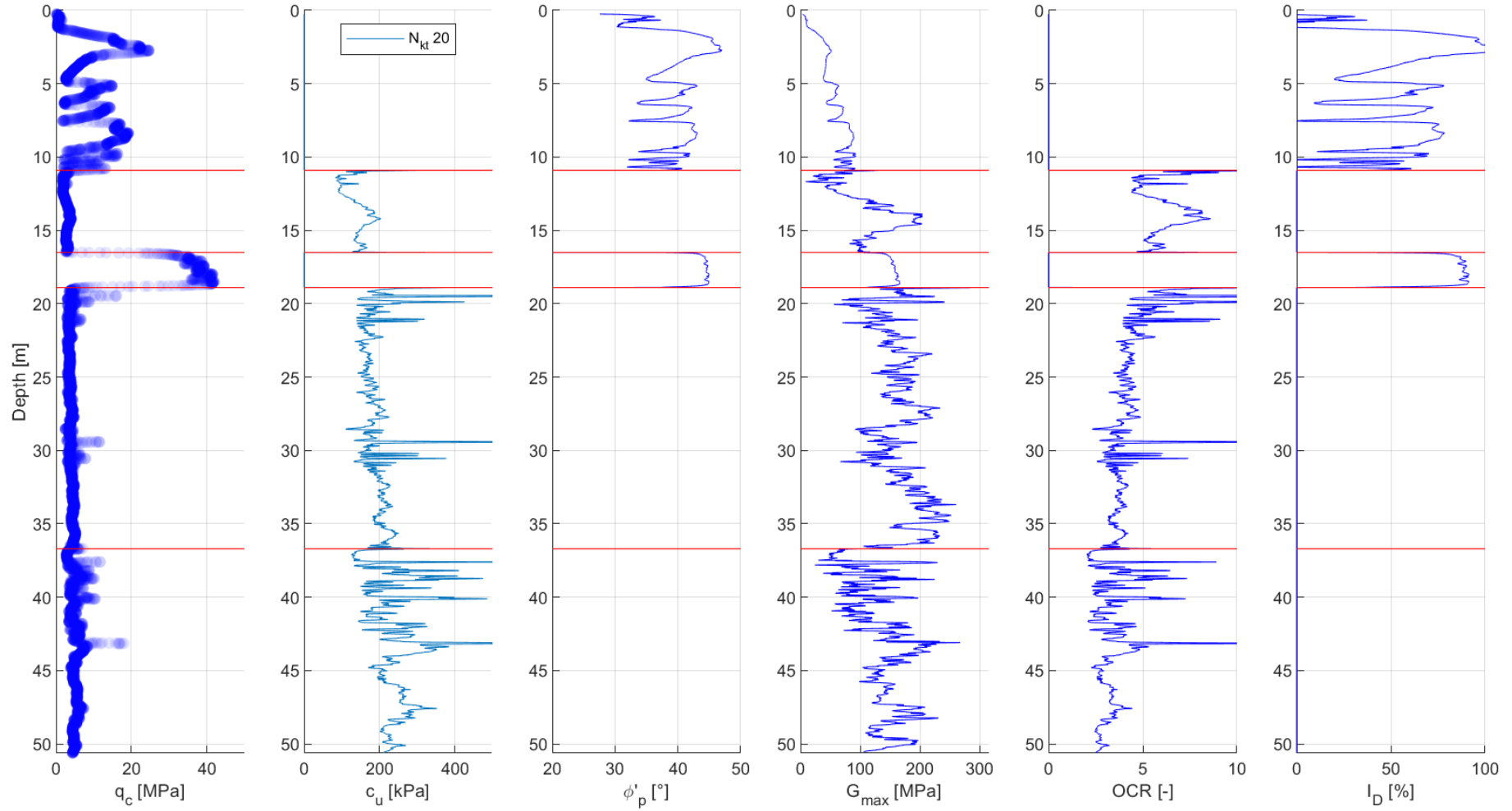
CPT-28



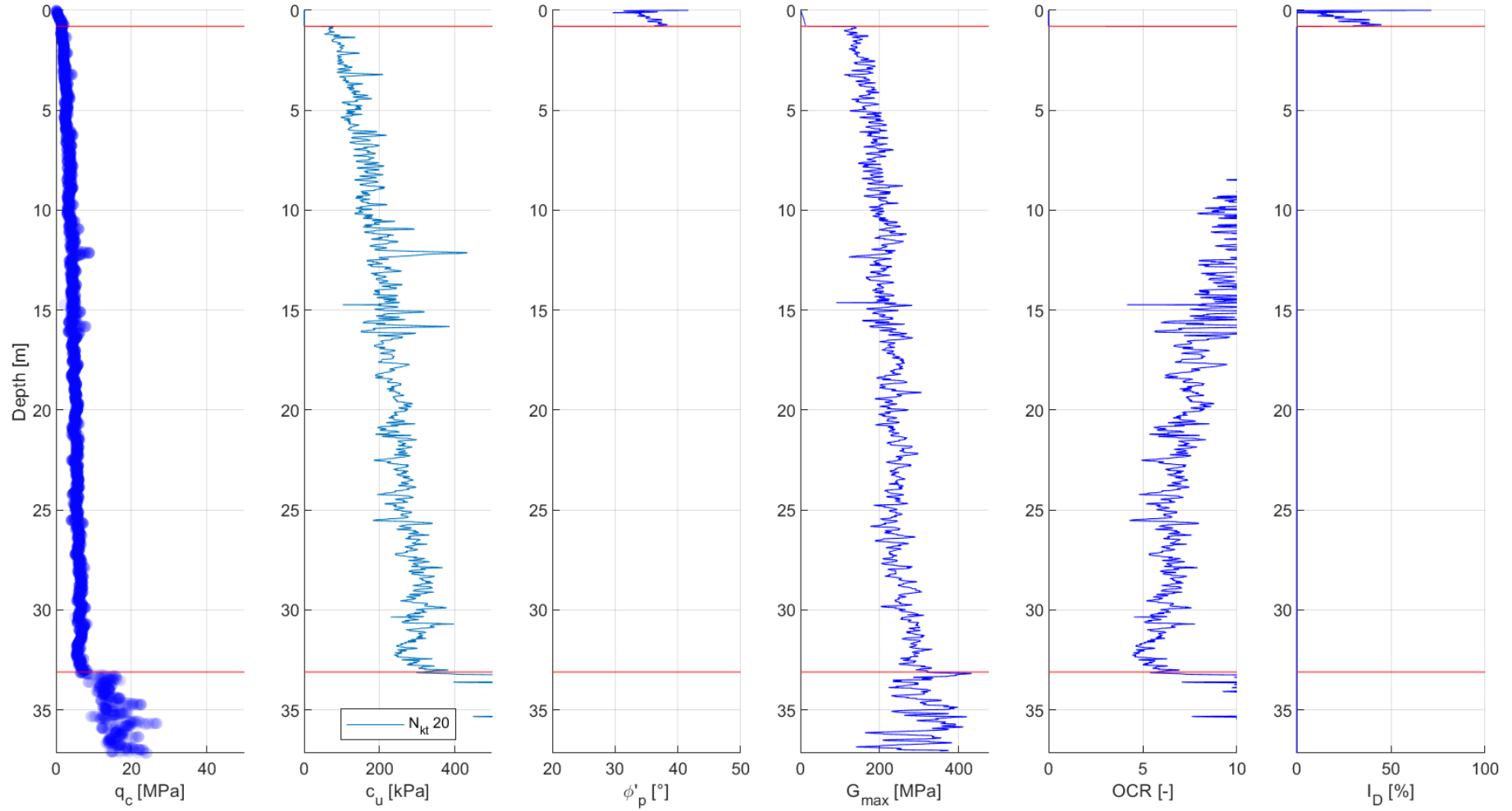
CPT-29



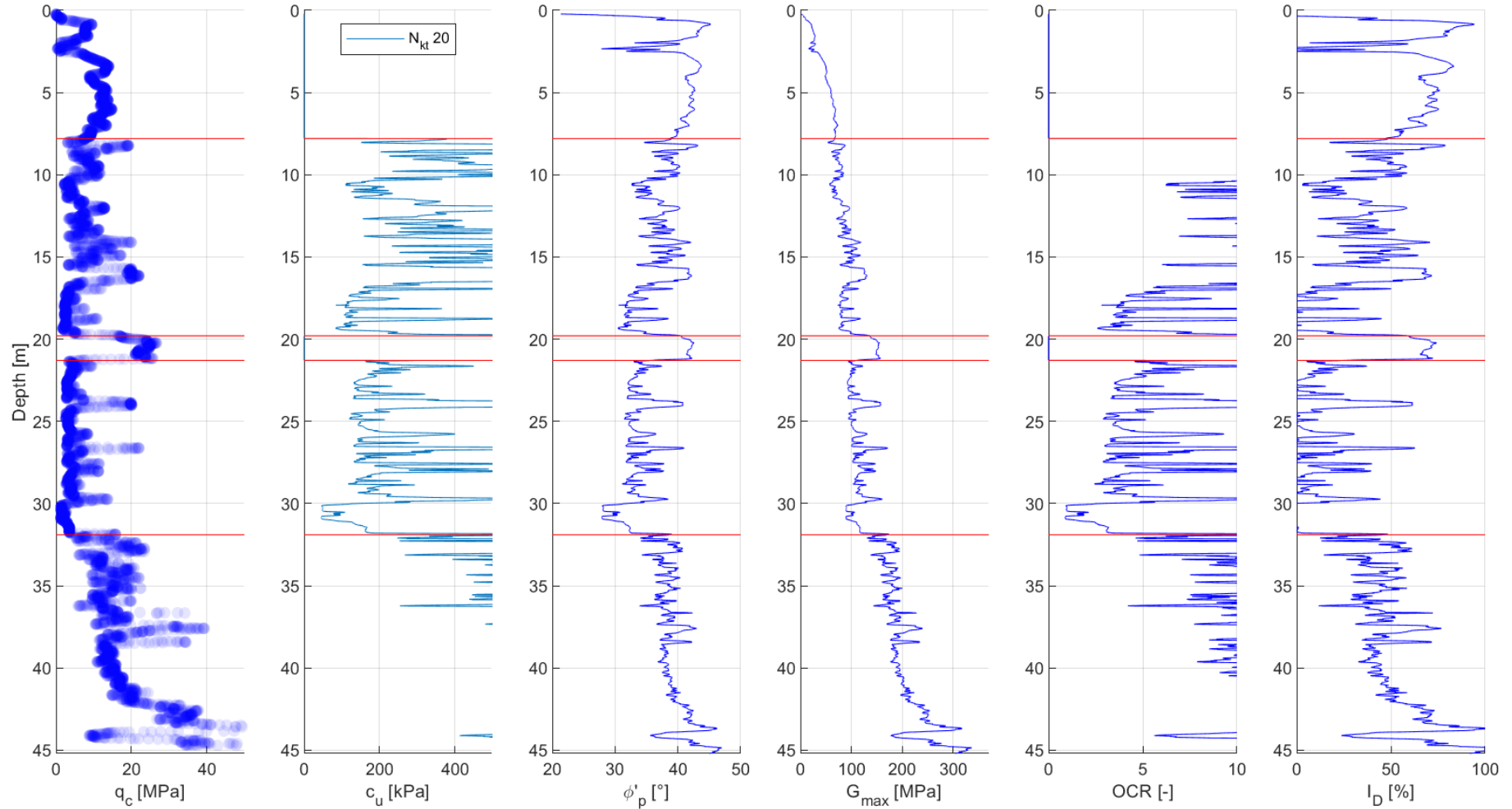
CPT-30



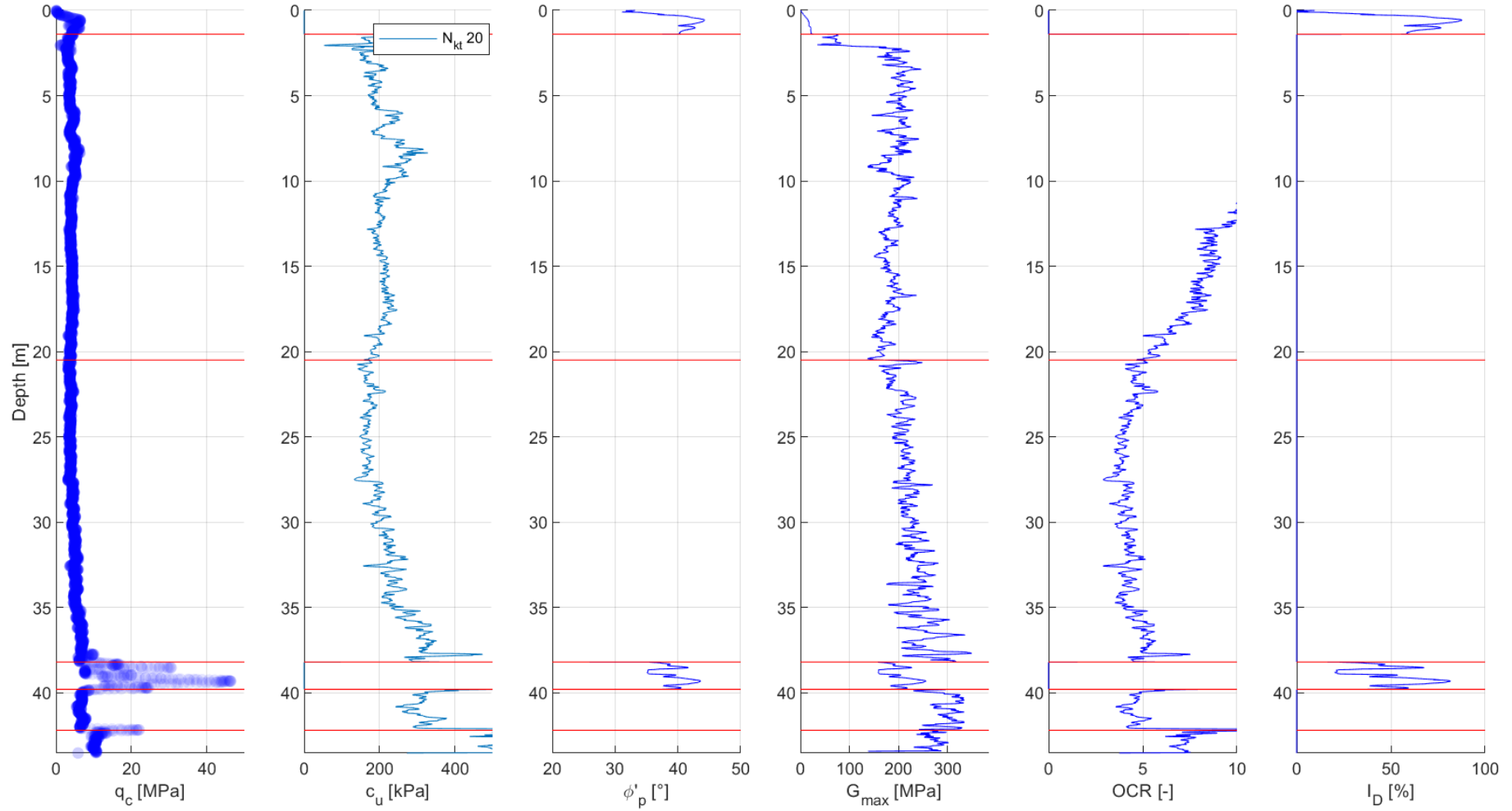
CPT-32



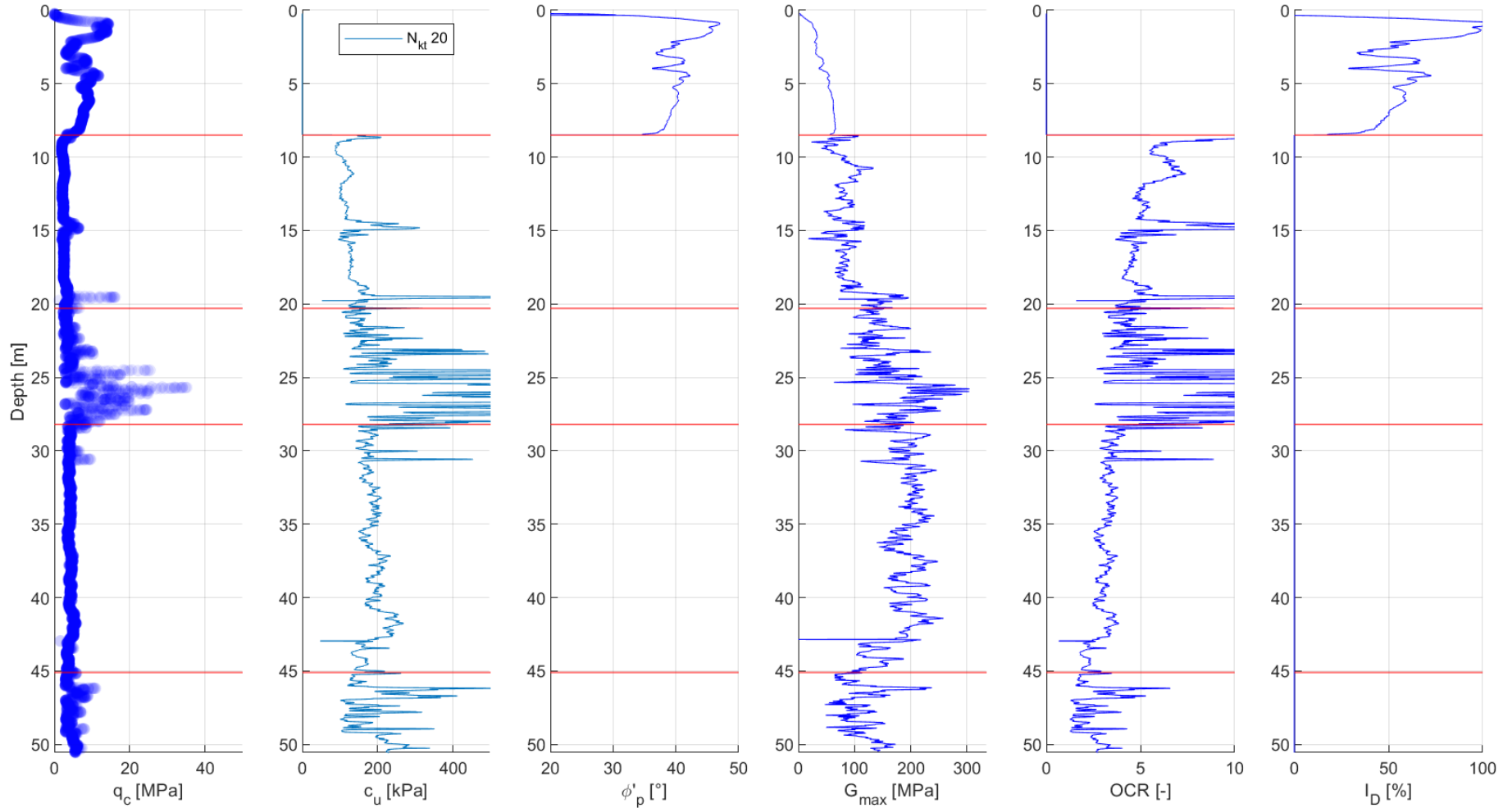
CPT-34

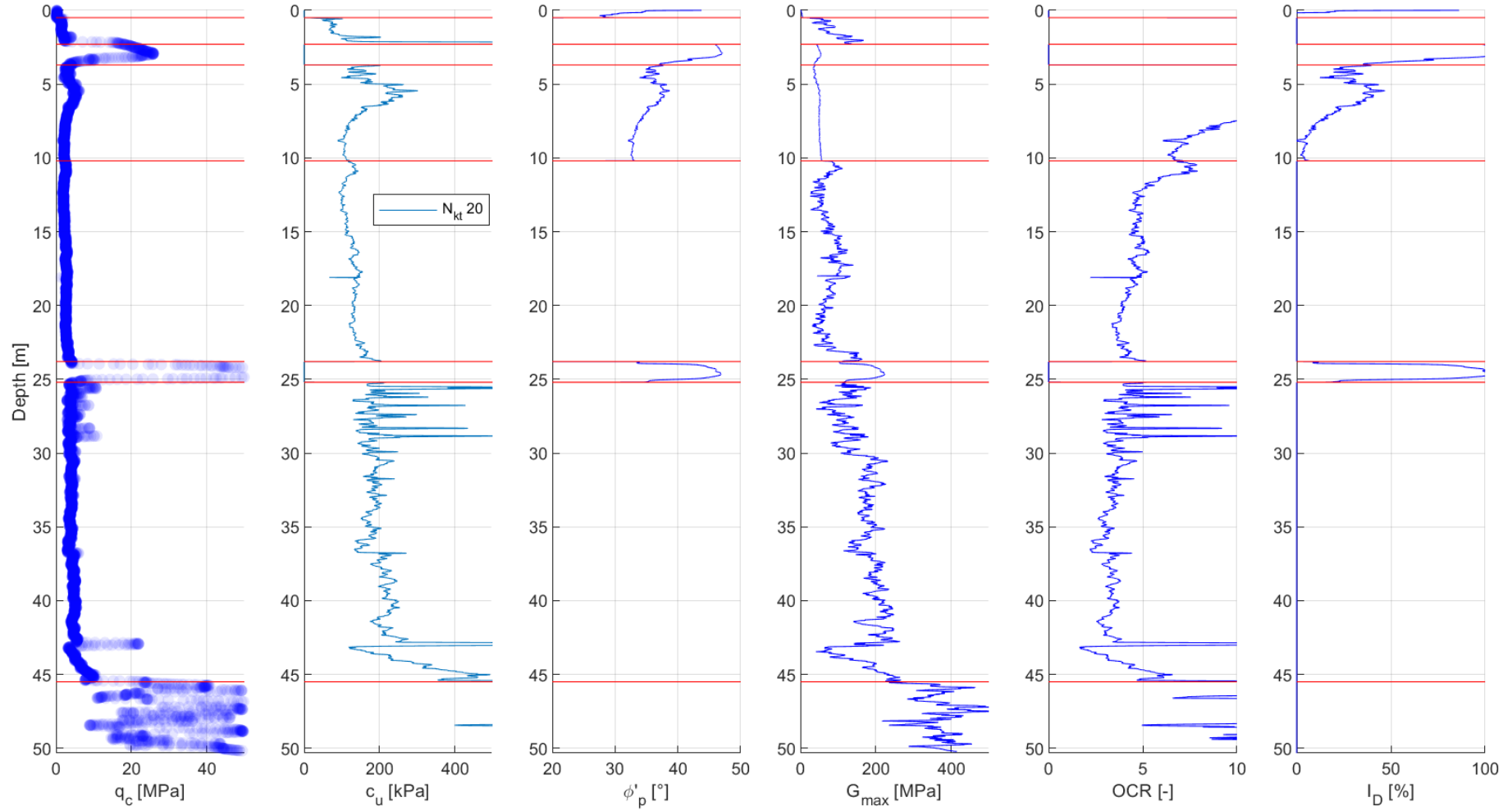


CPT-35a

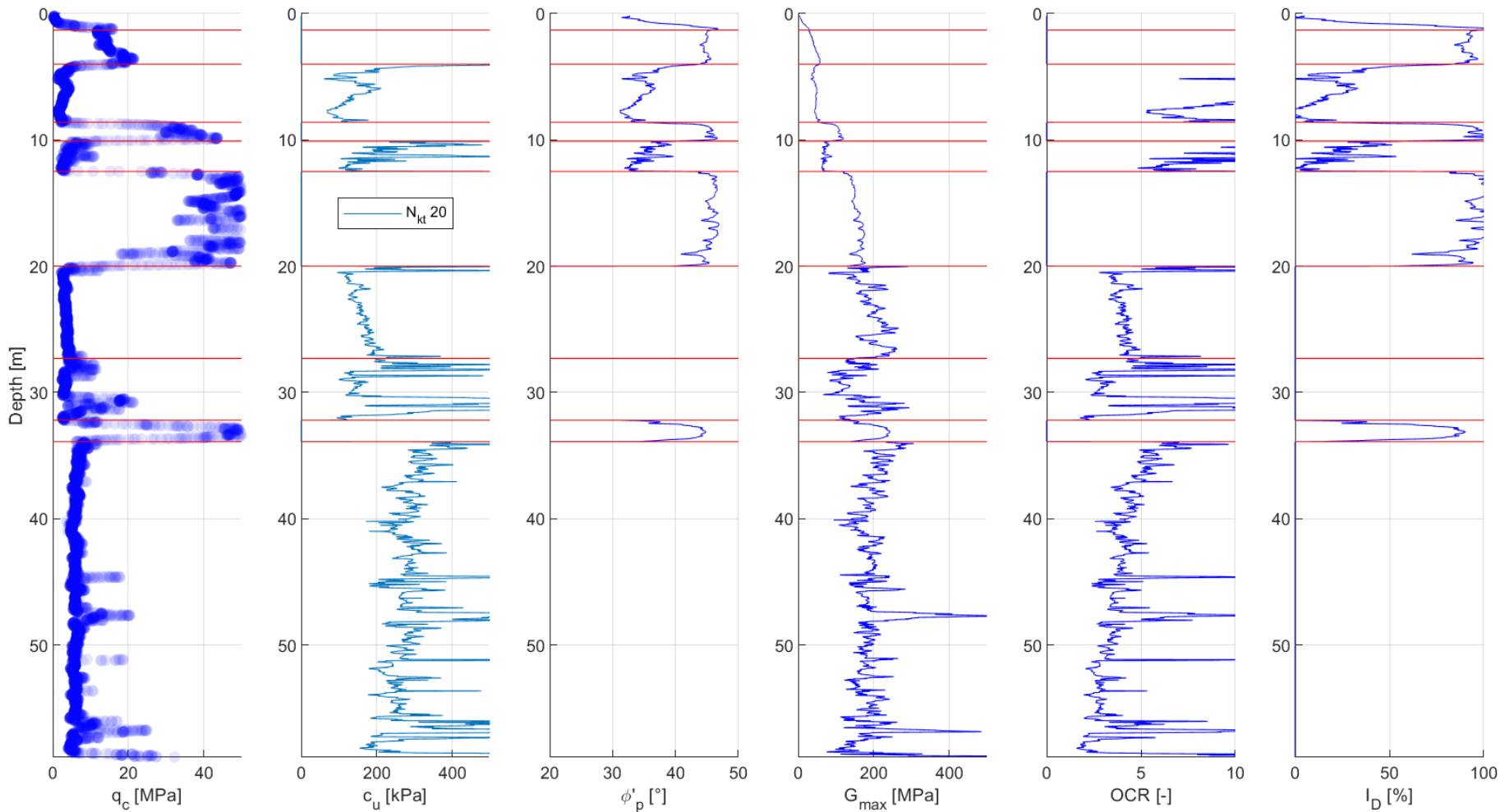


CPT-36

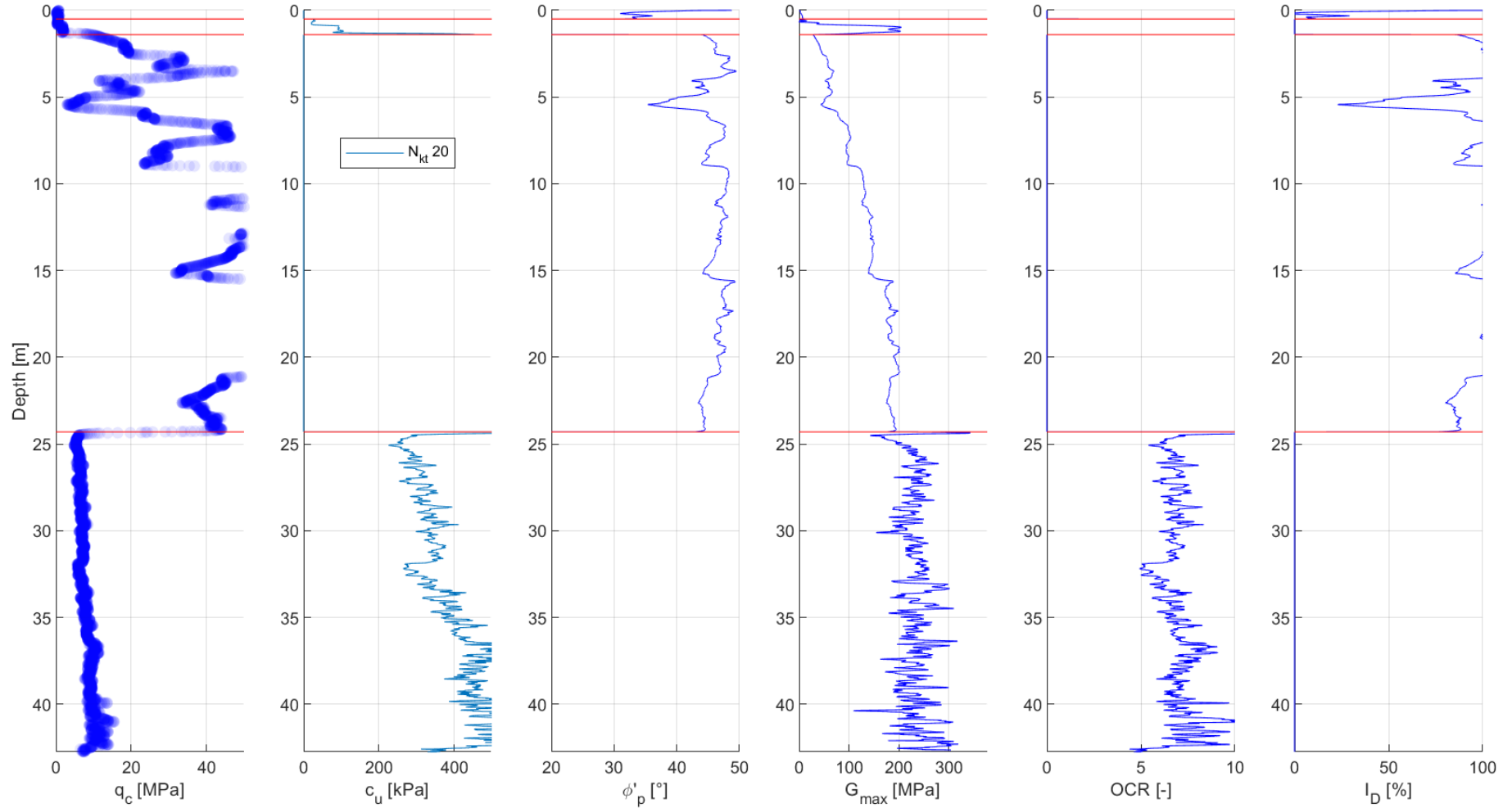




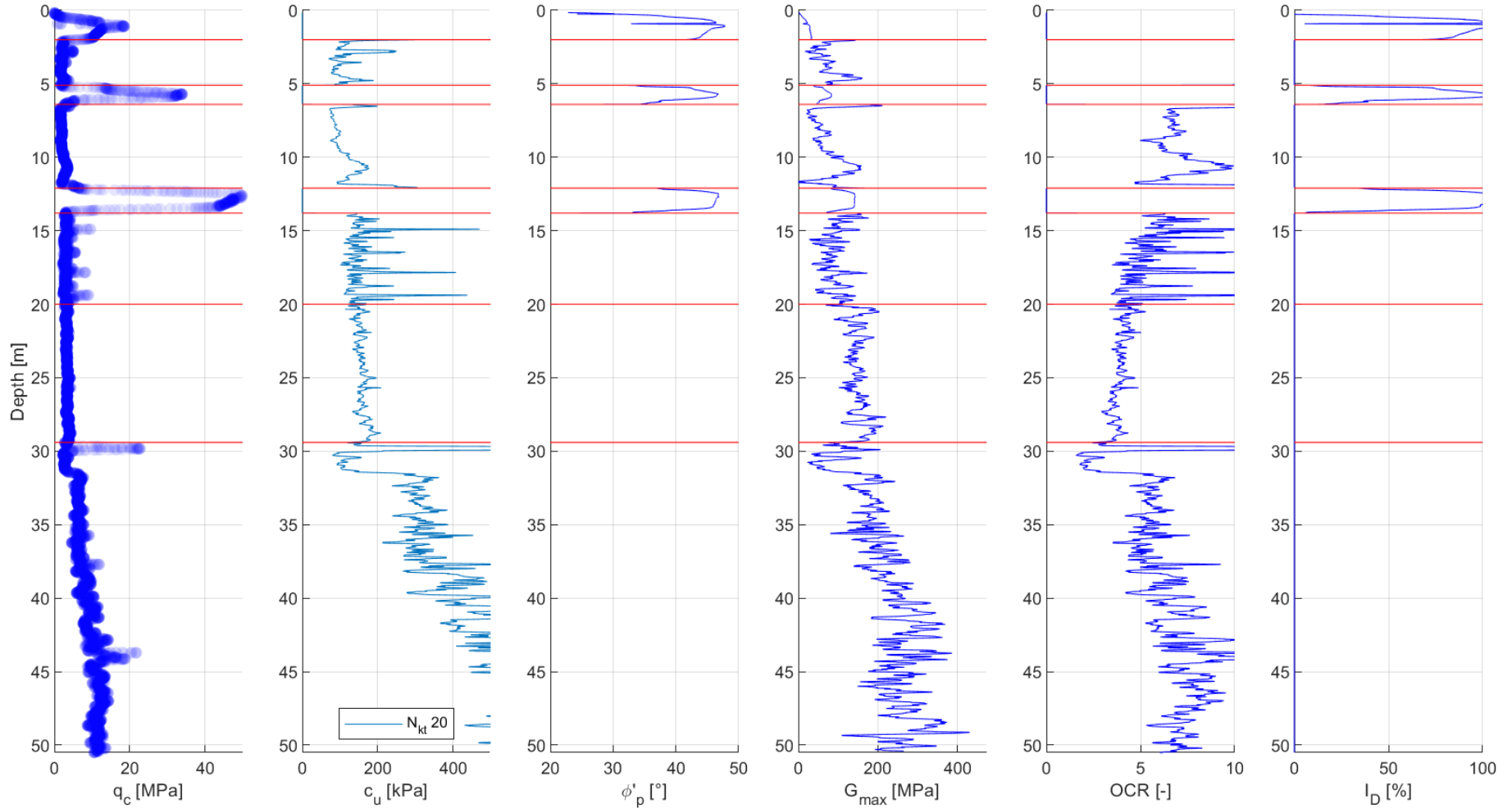
CPT-38



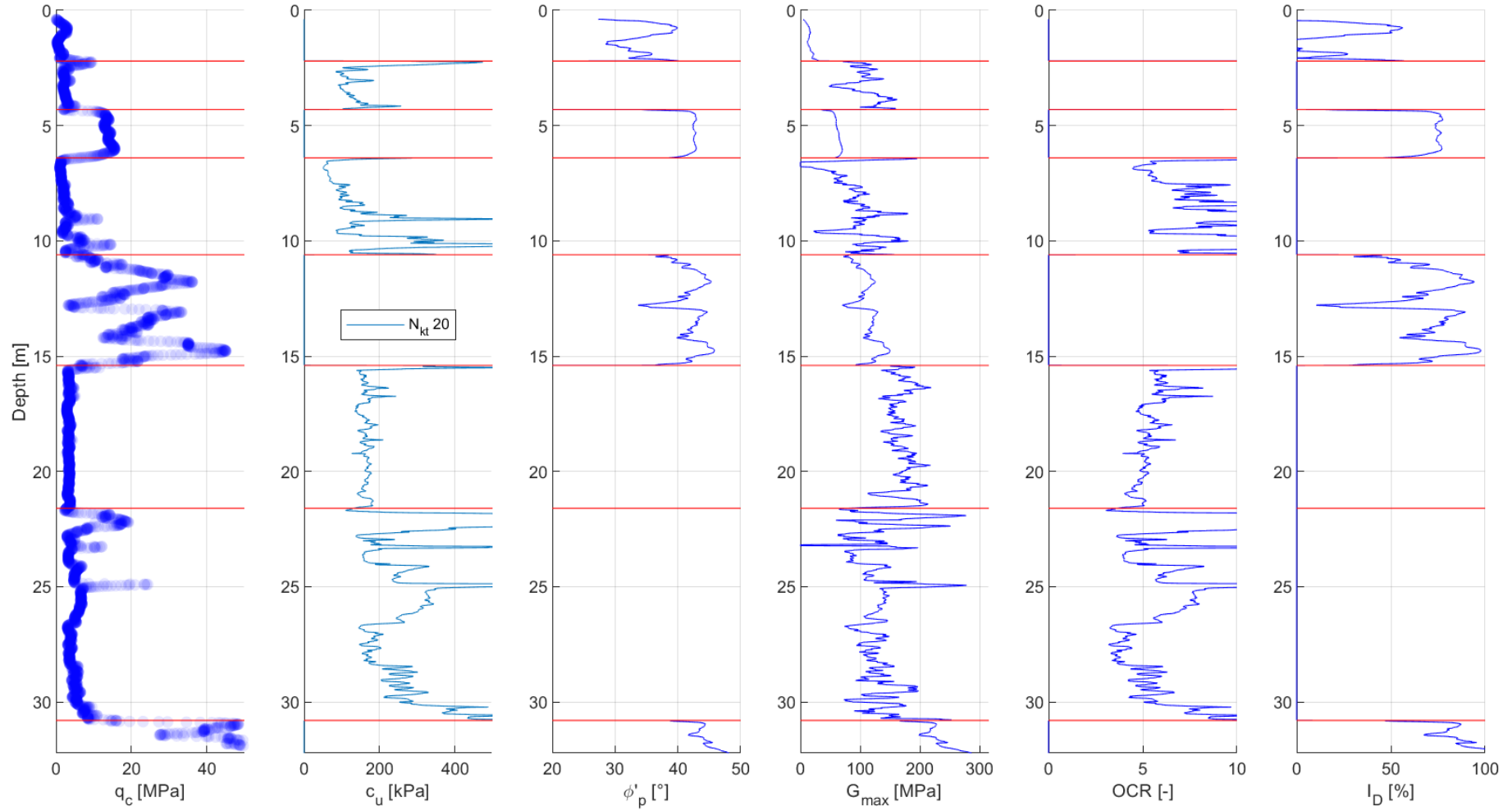
CPT-39



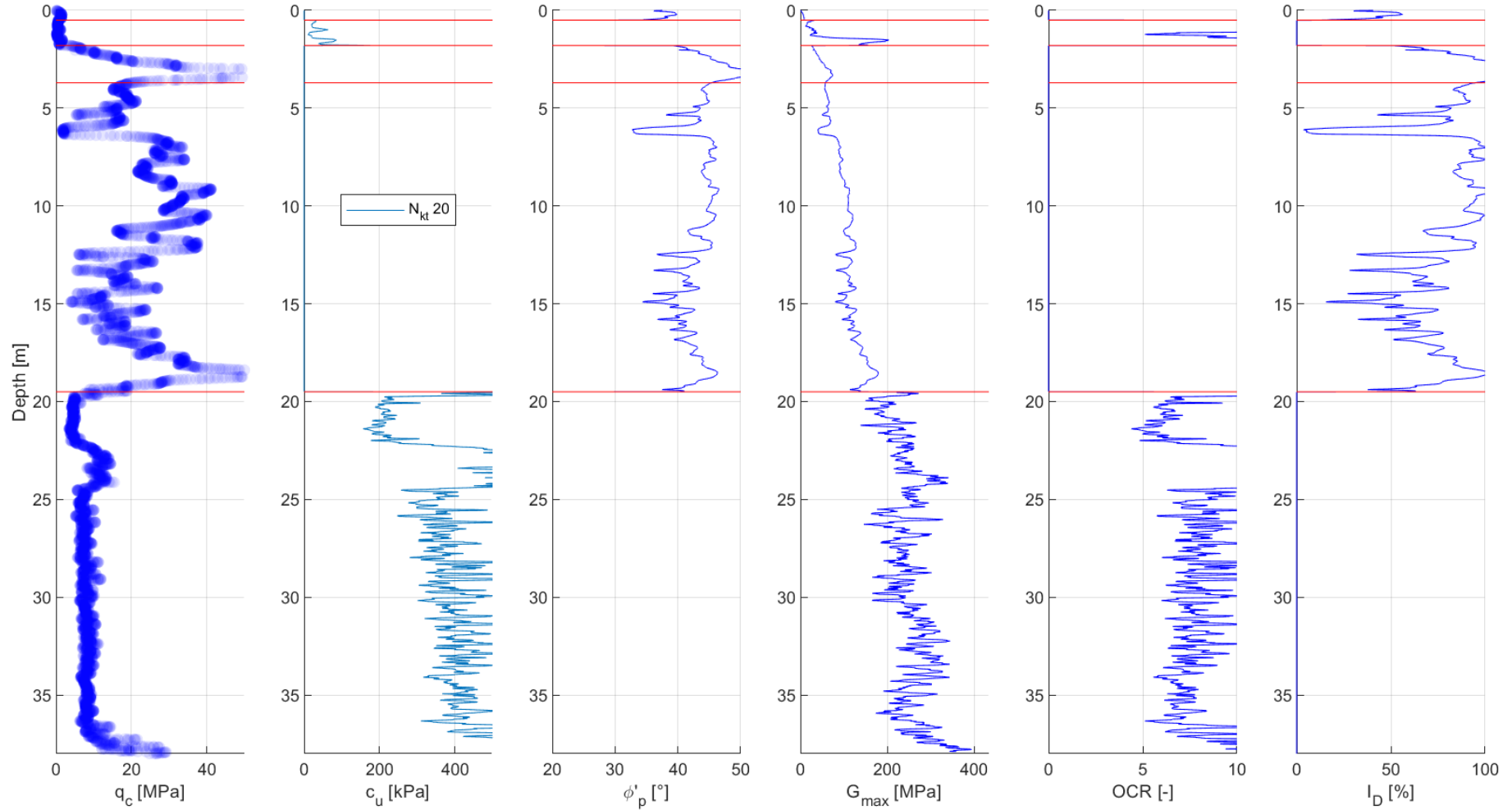
CPT-40



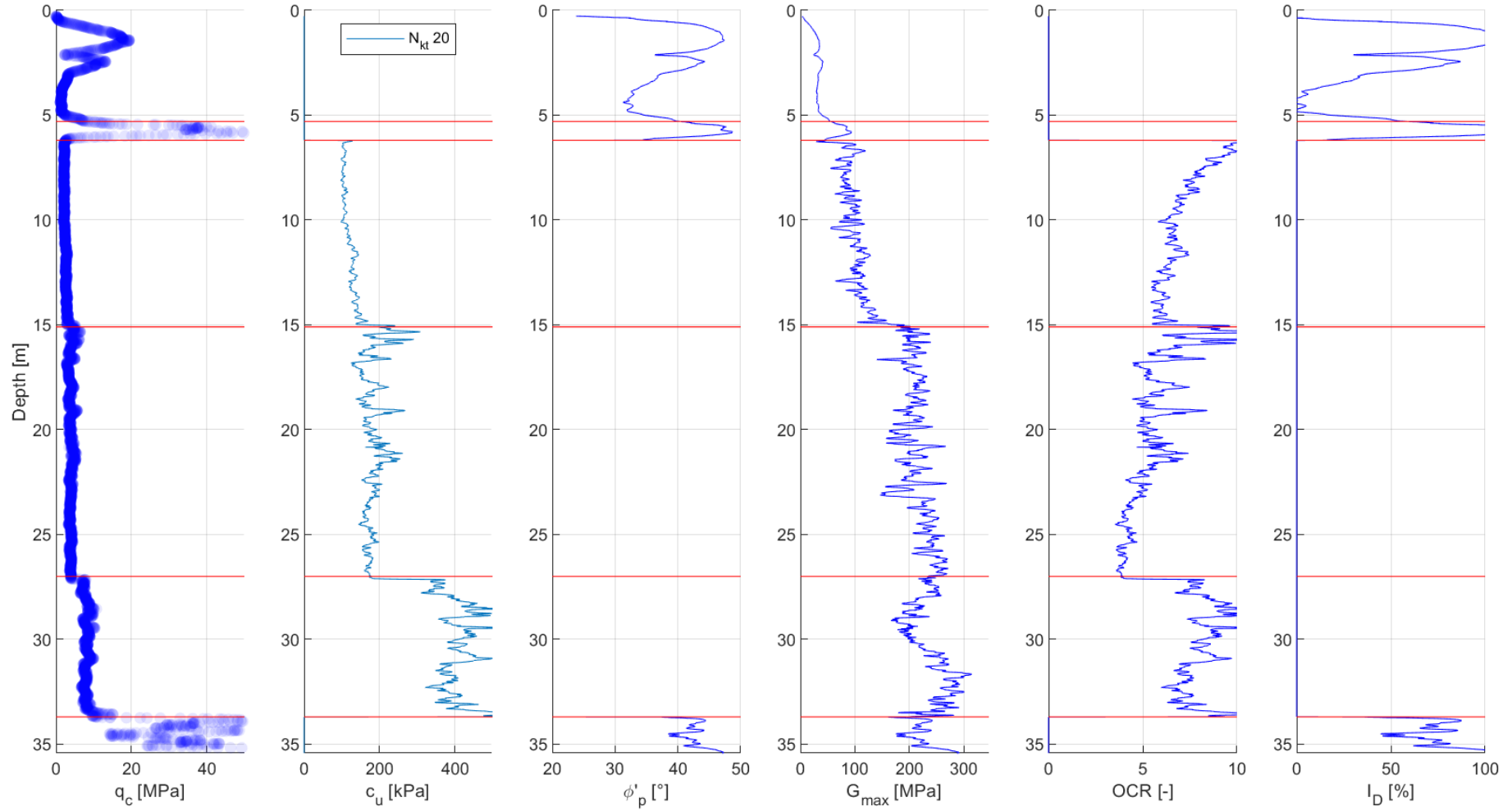
CPT-41



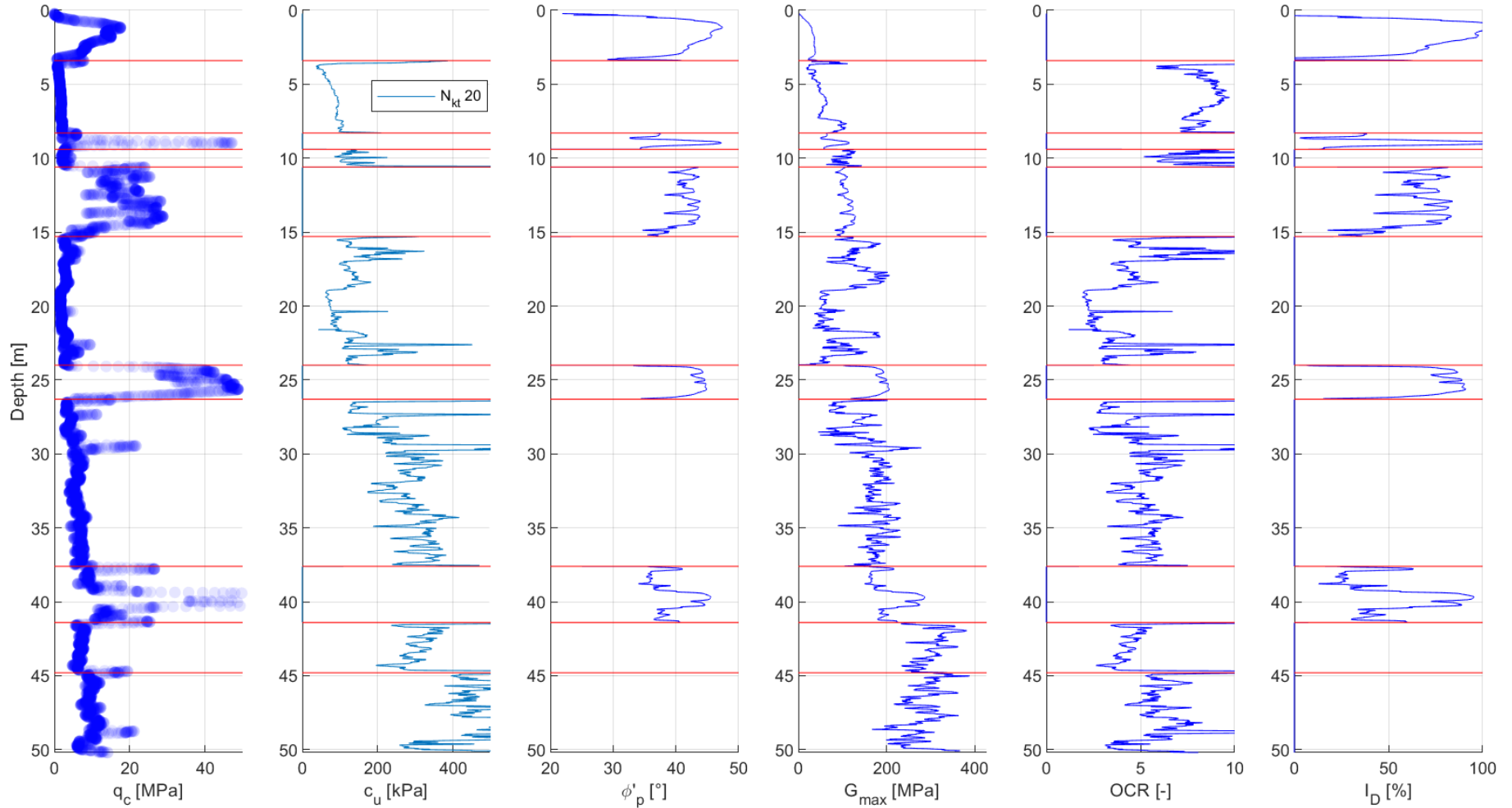
CPT-42



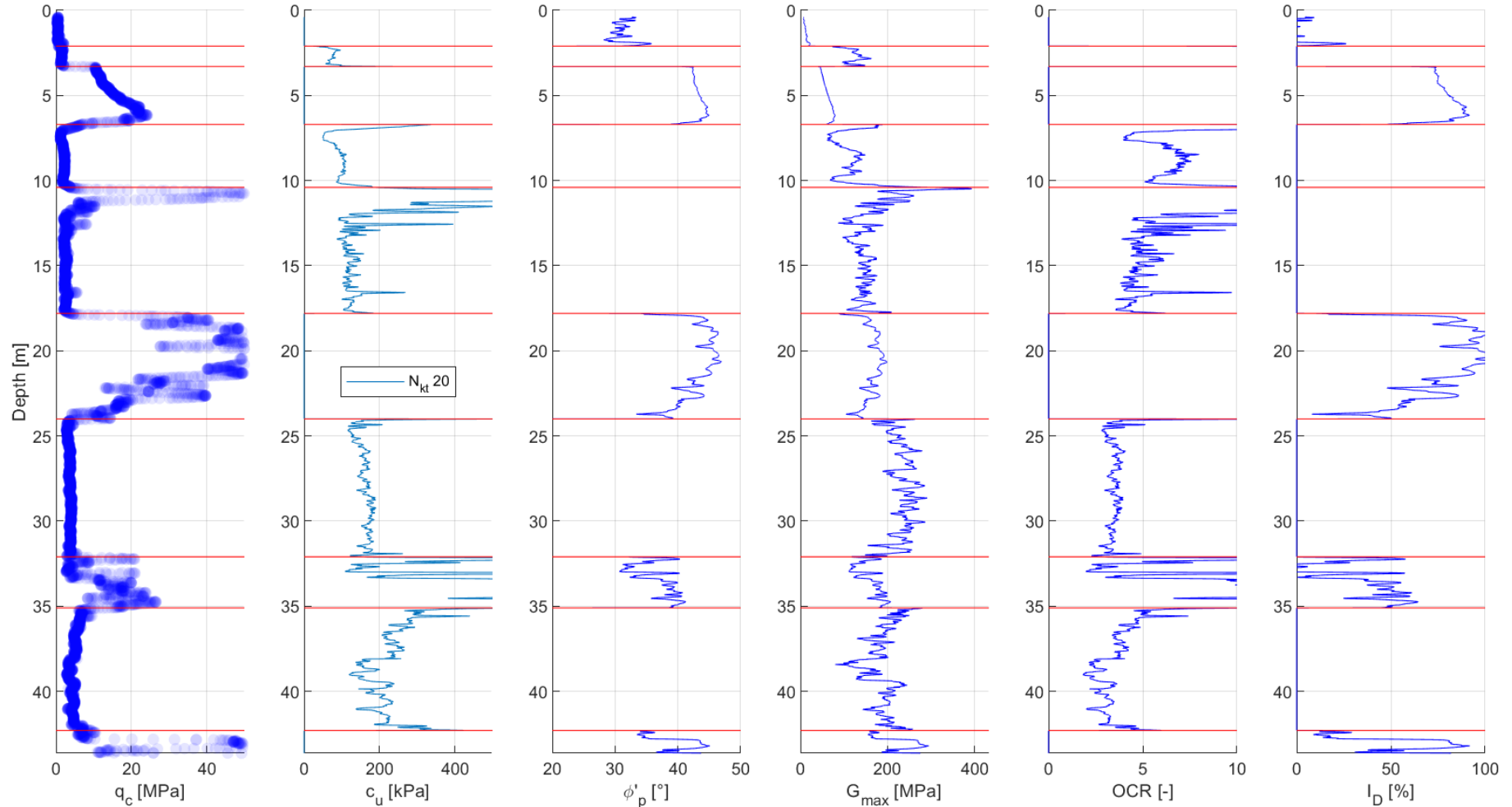
CPT-43



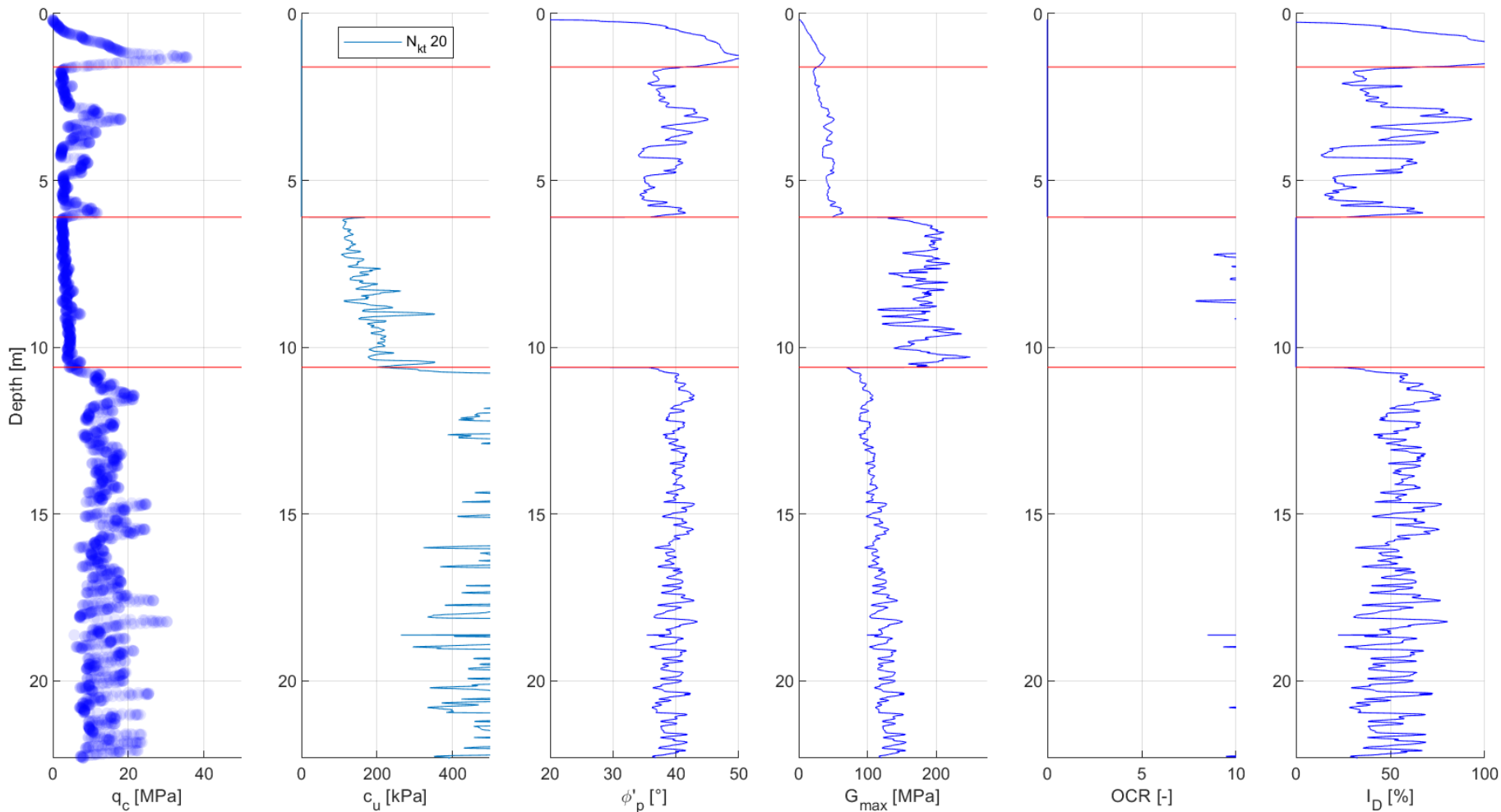
CPT-44



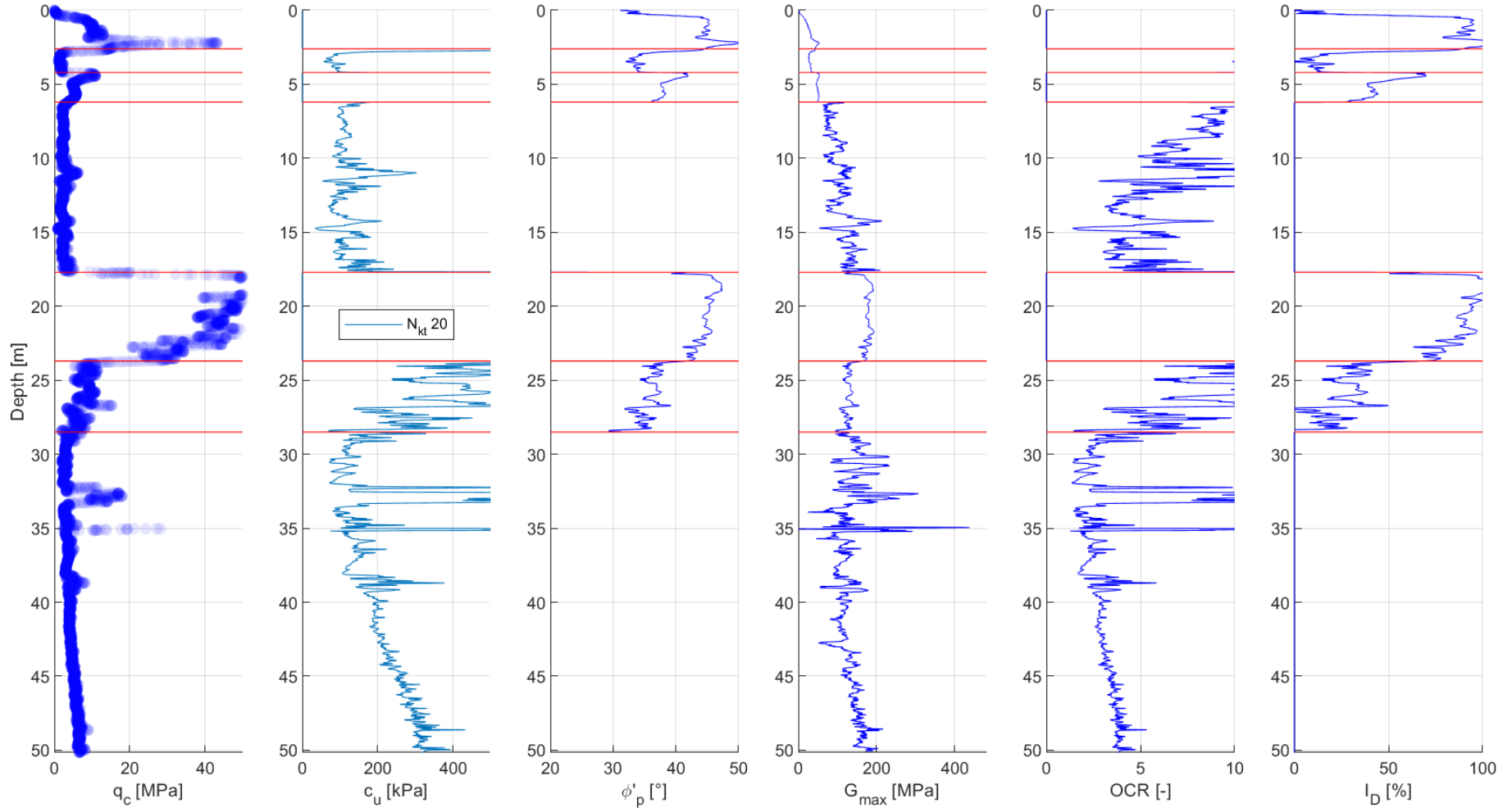
CPT-46



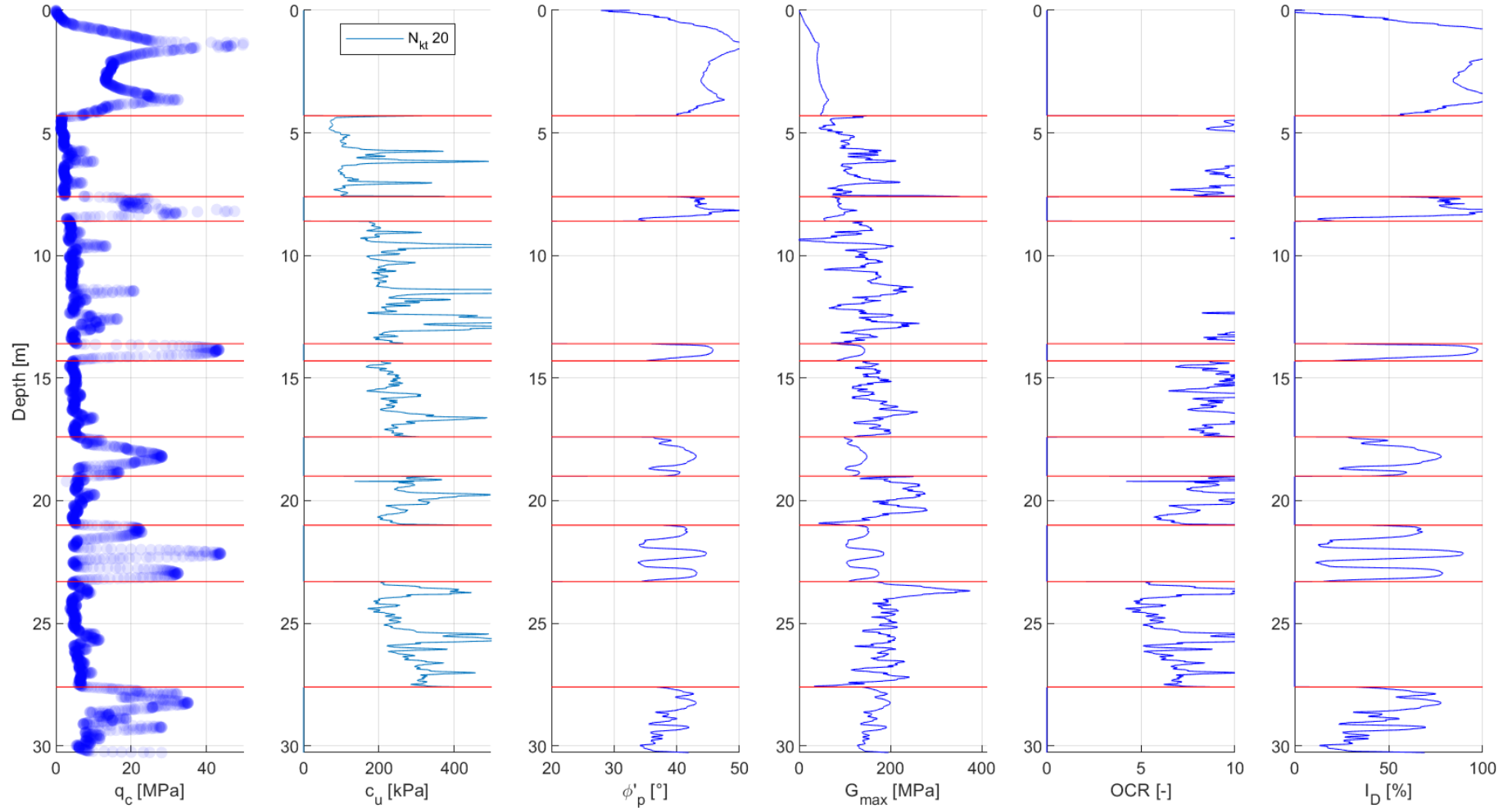
CPT-47



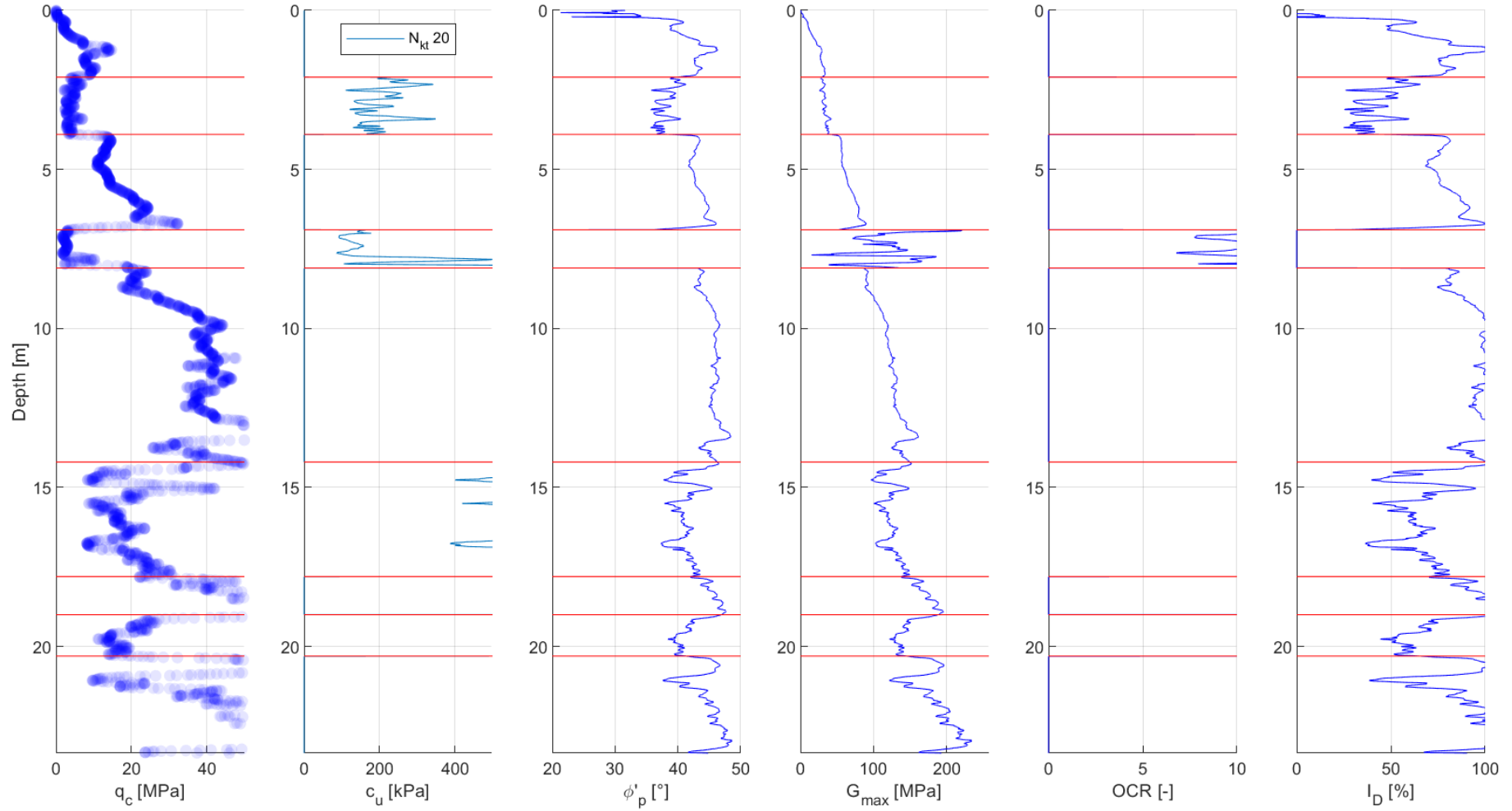
CPT-48



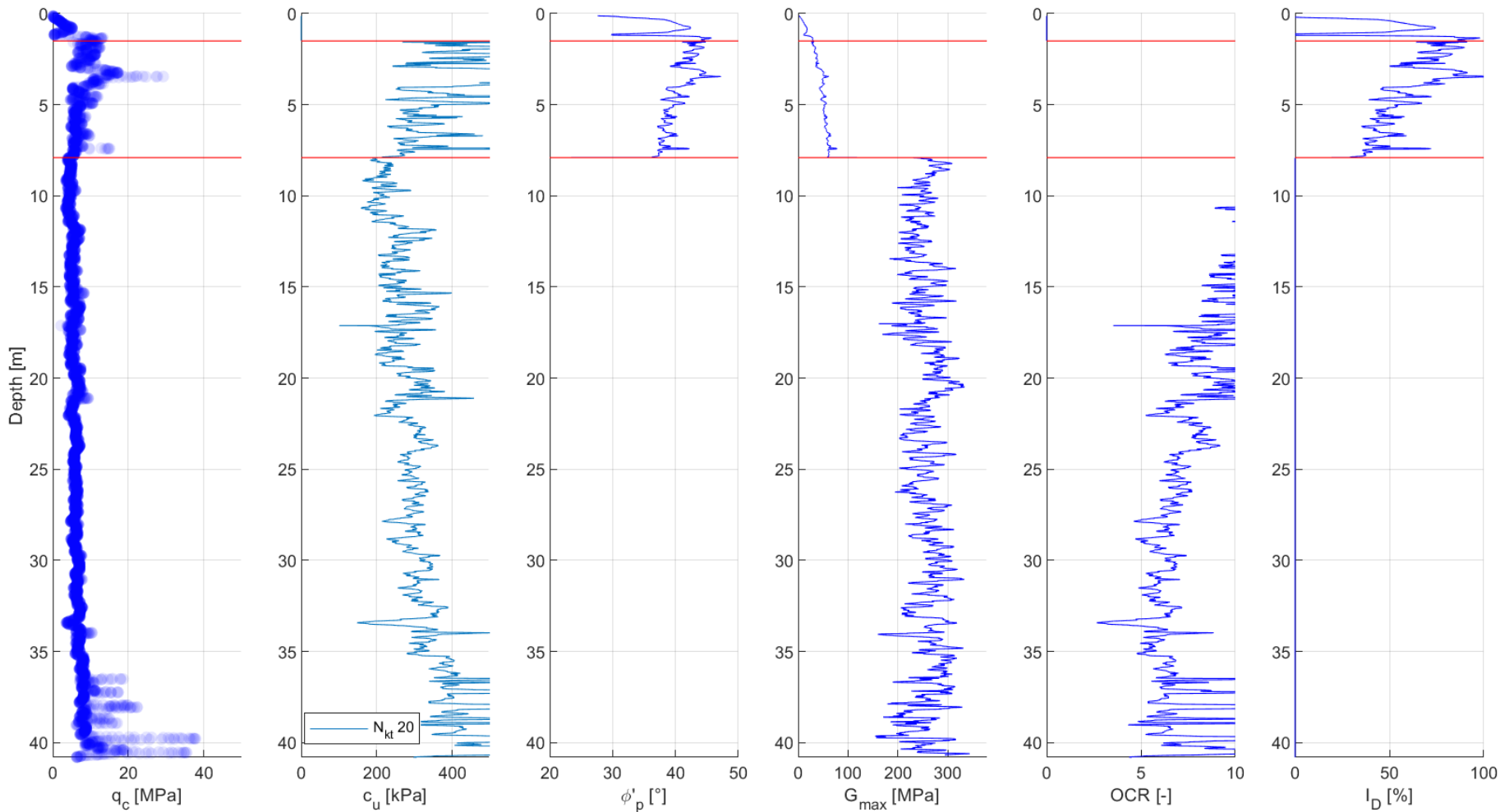
CPT-49



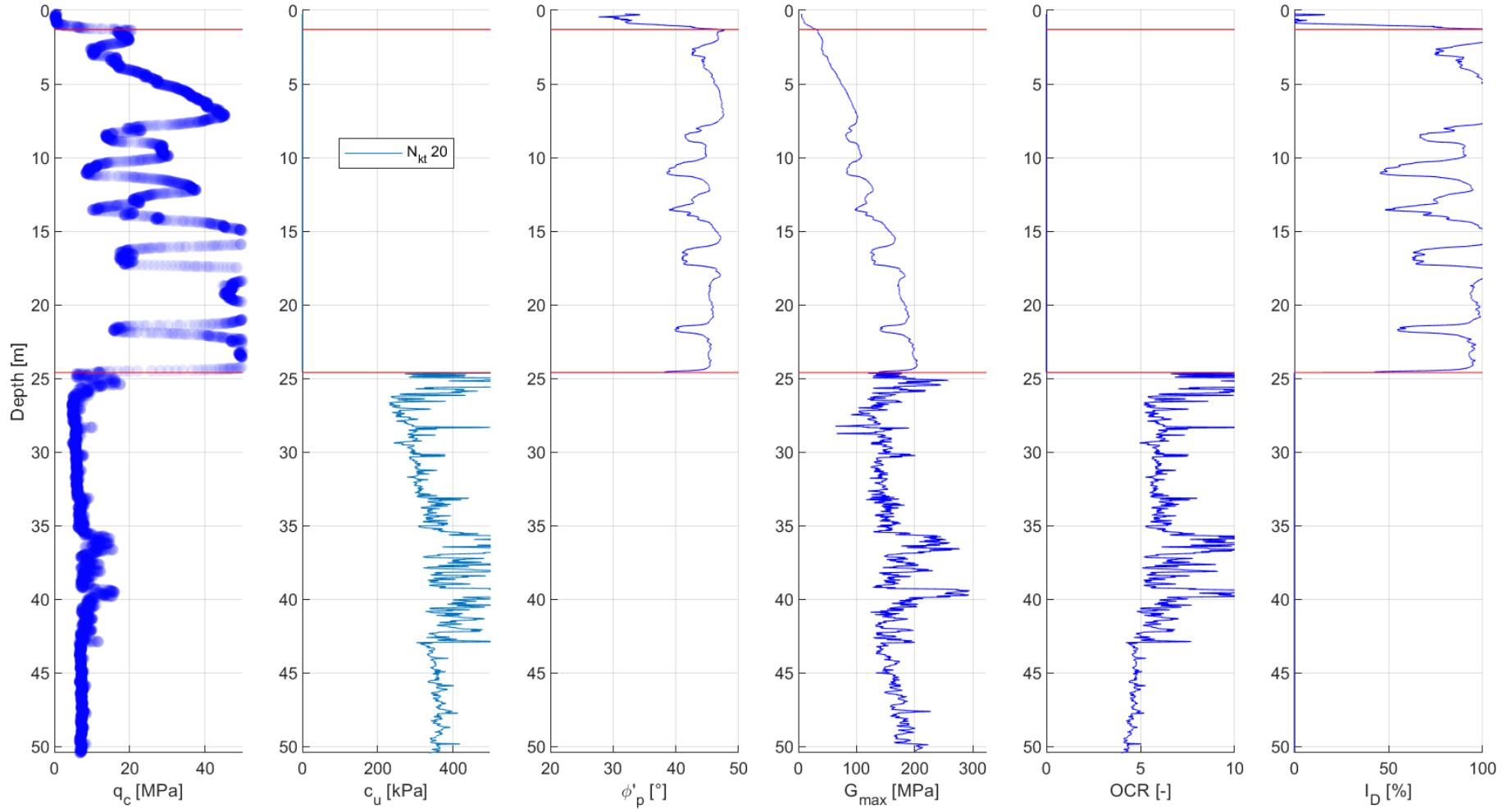
CPT-50



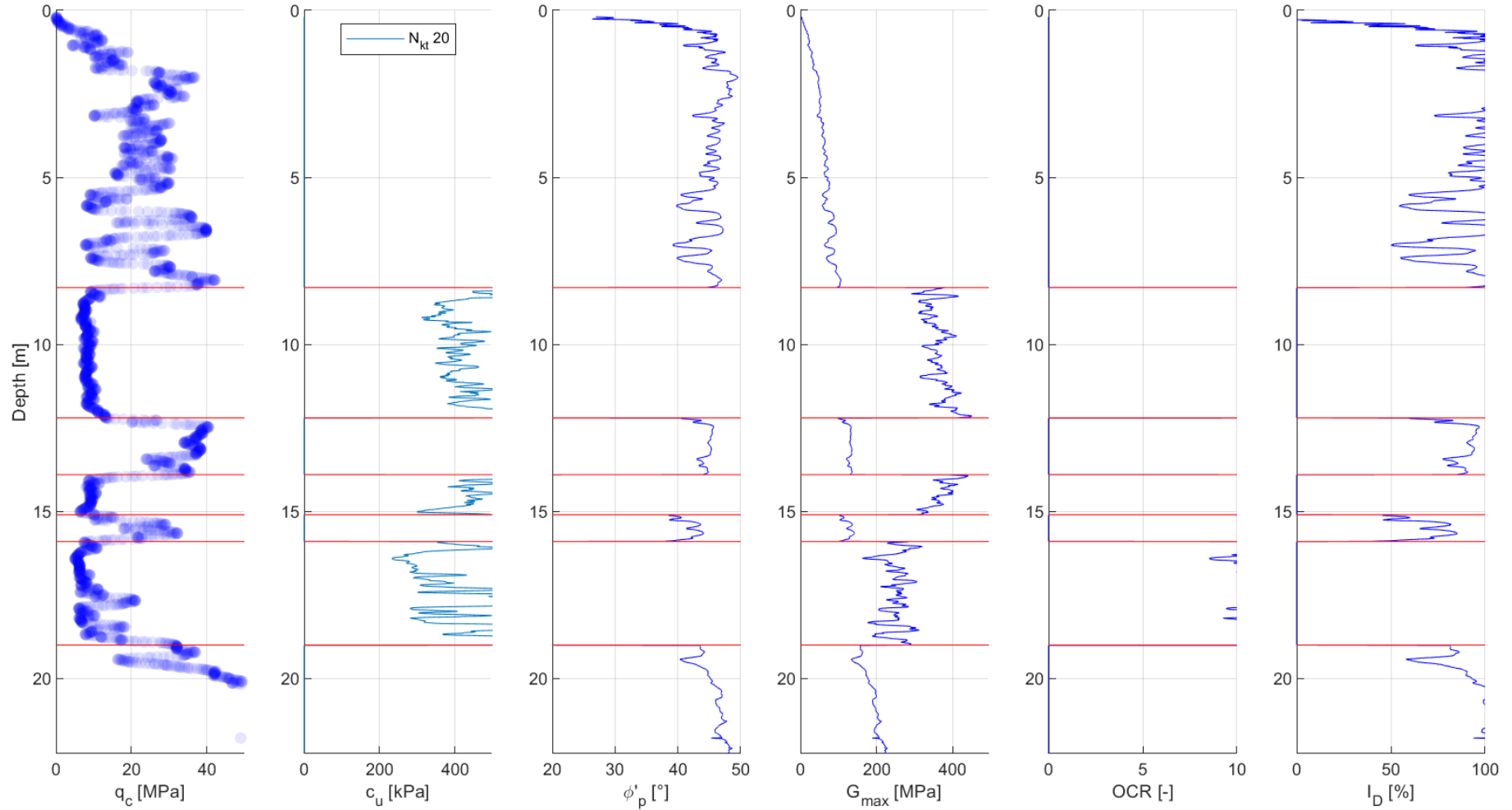
CPT-51a



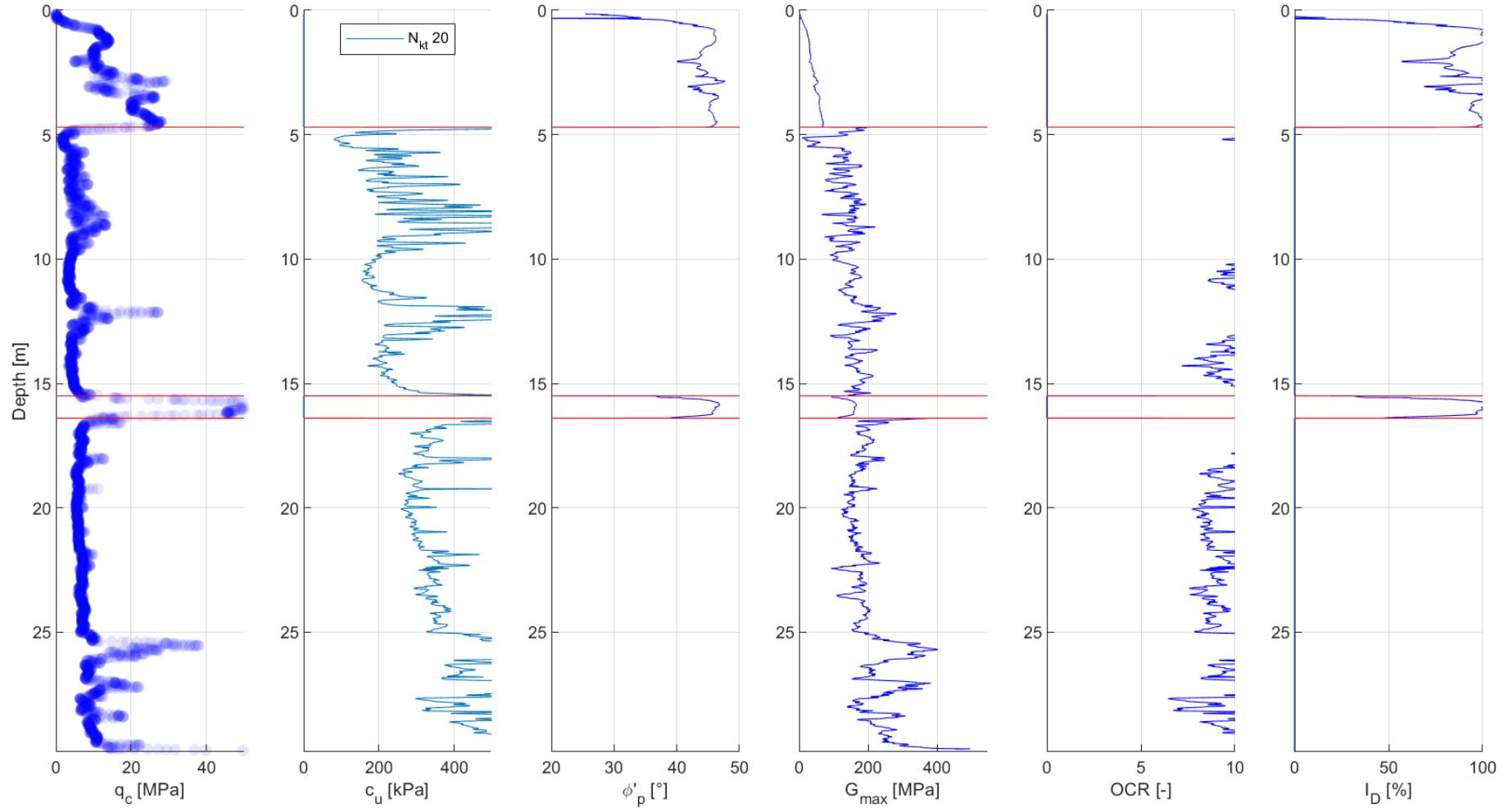
CPT-52



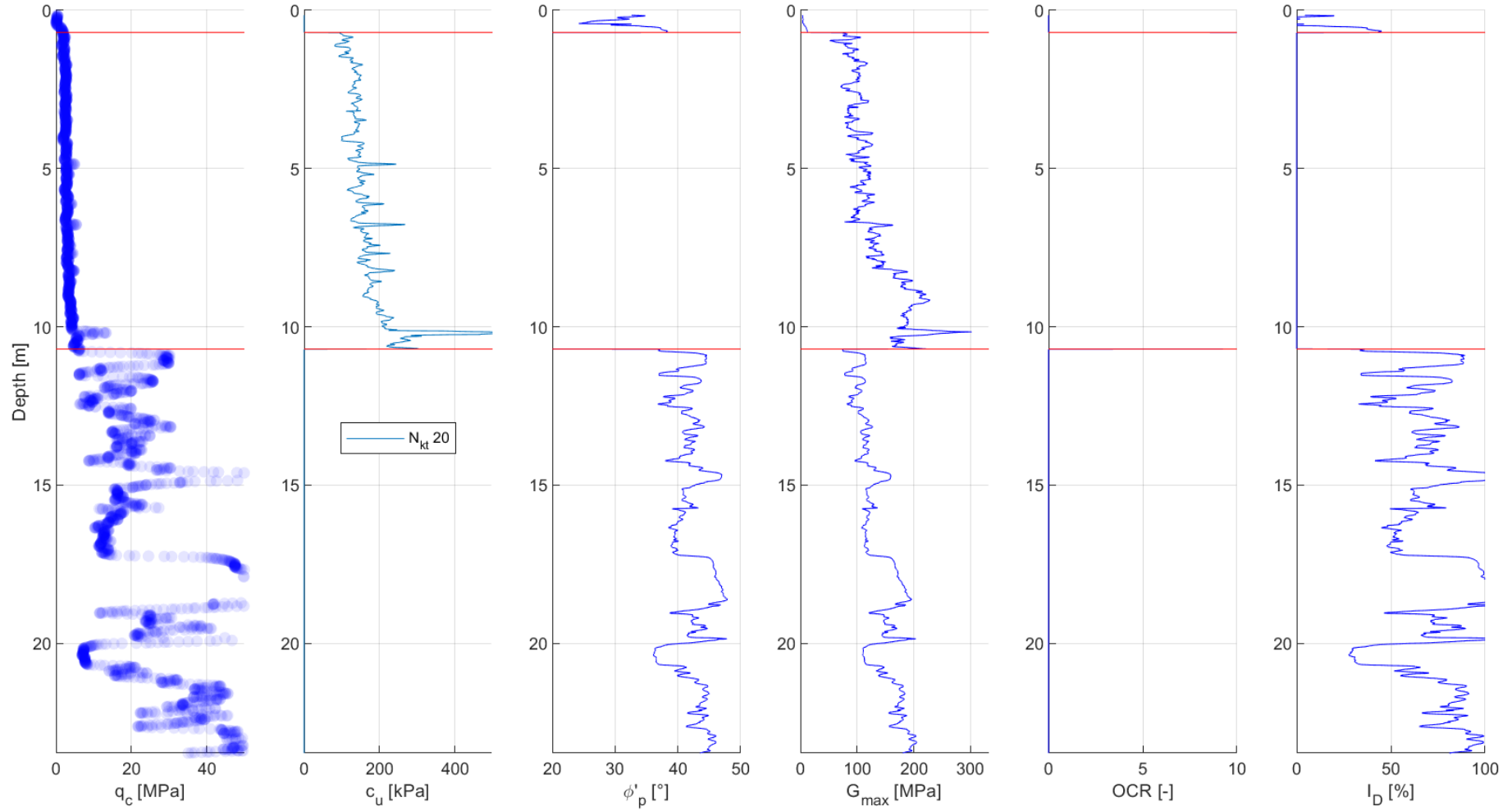
CPT-53a



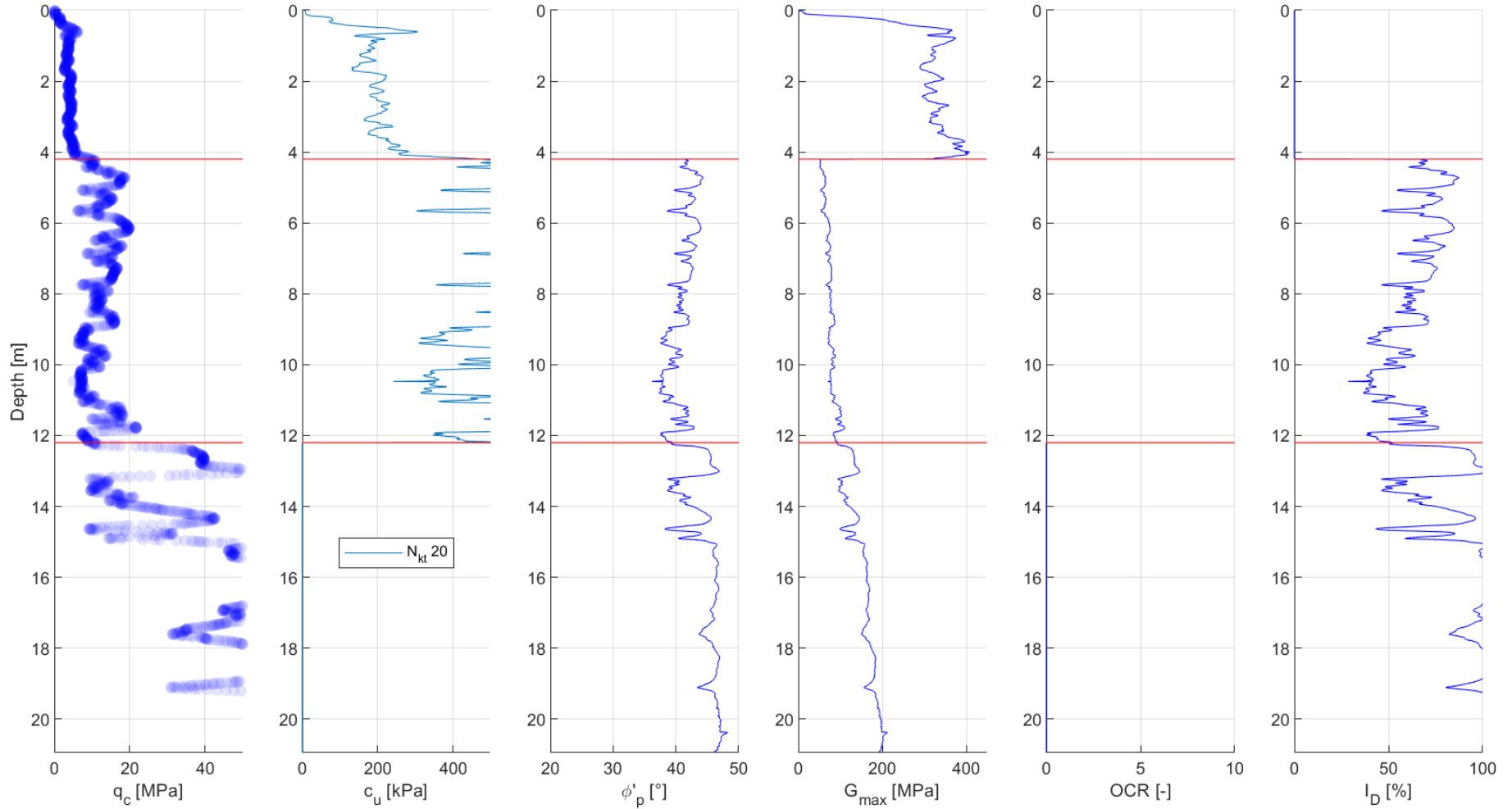
CPT-57



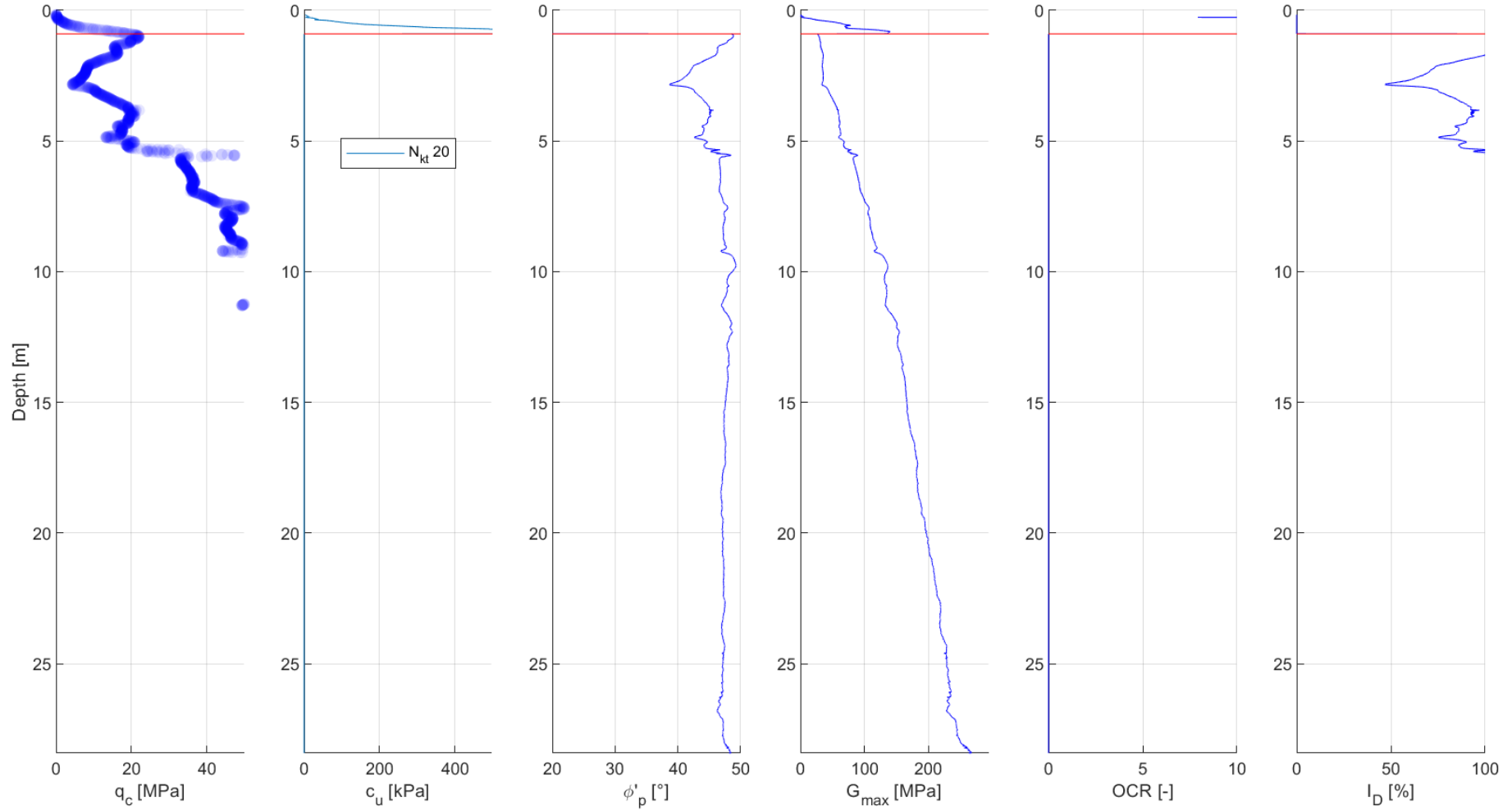
CPT-58a



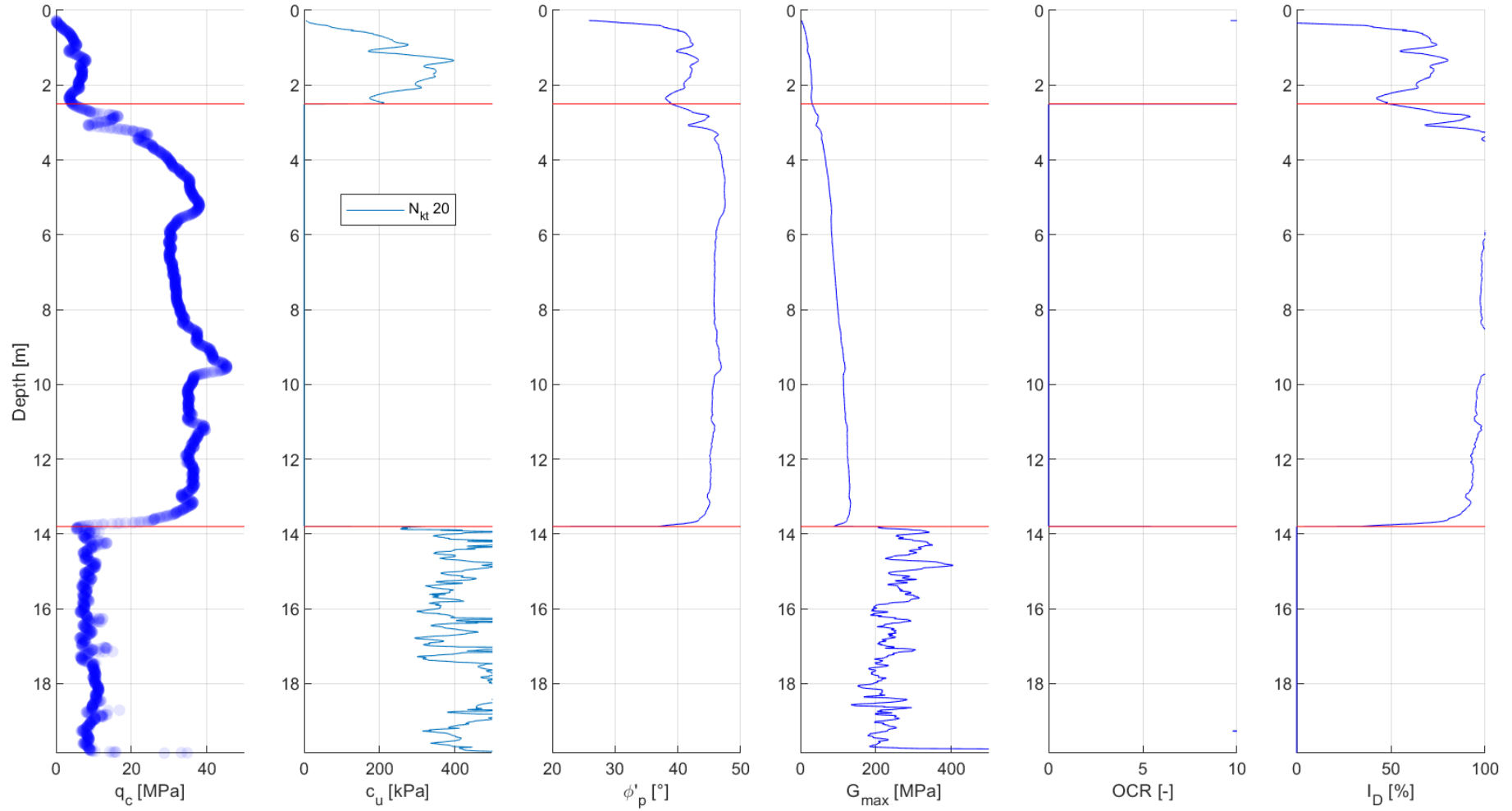
CPT-60



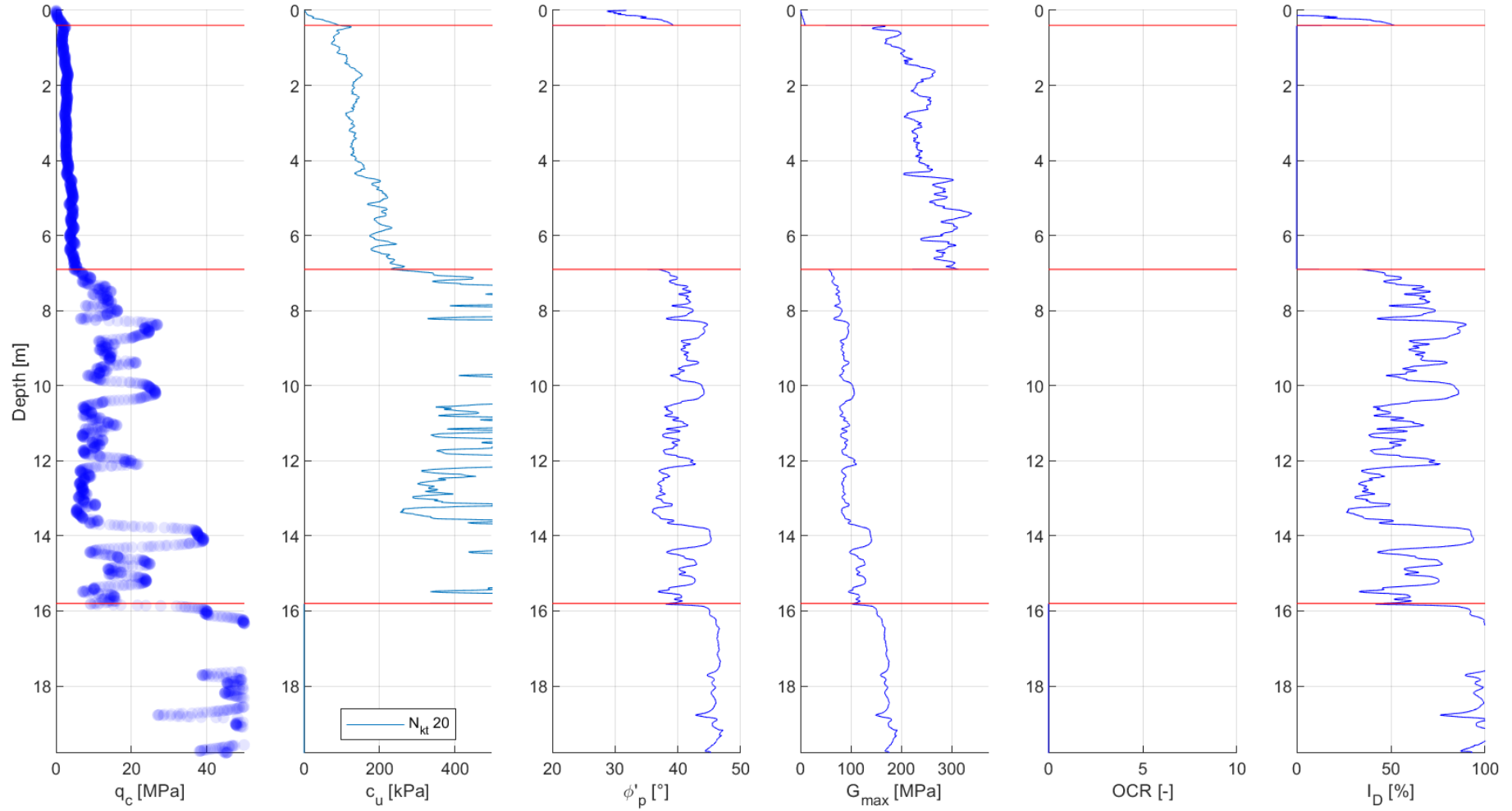
CPT-63



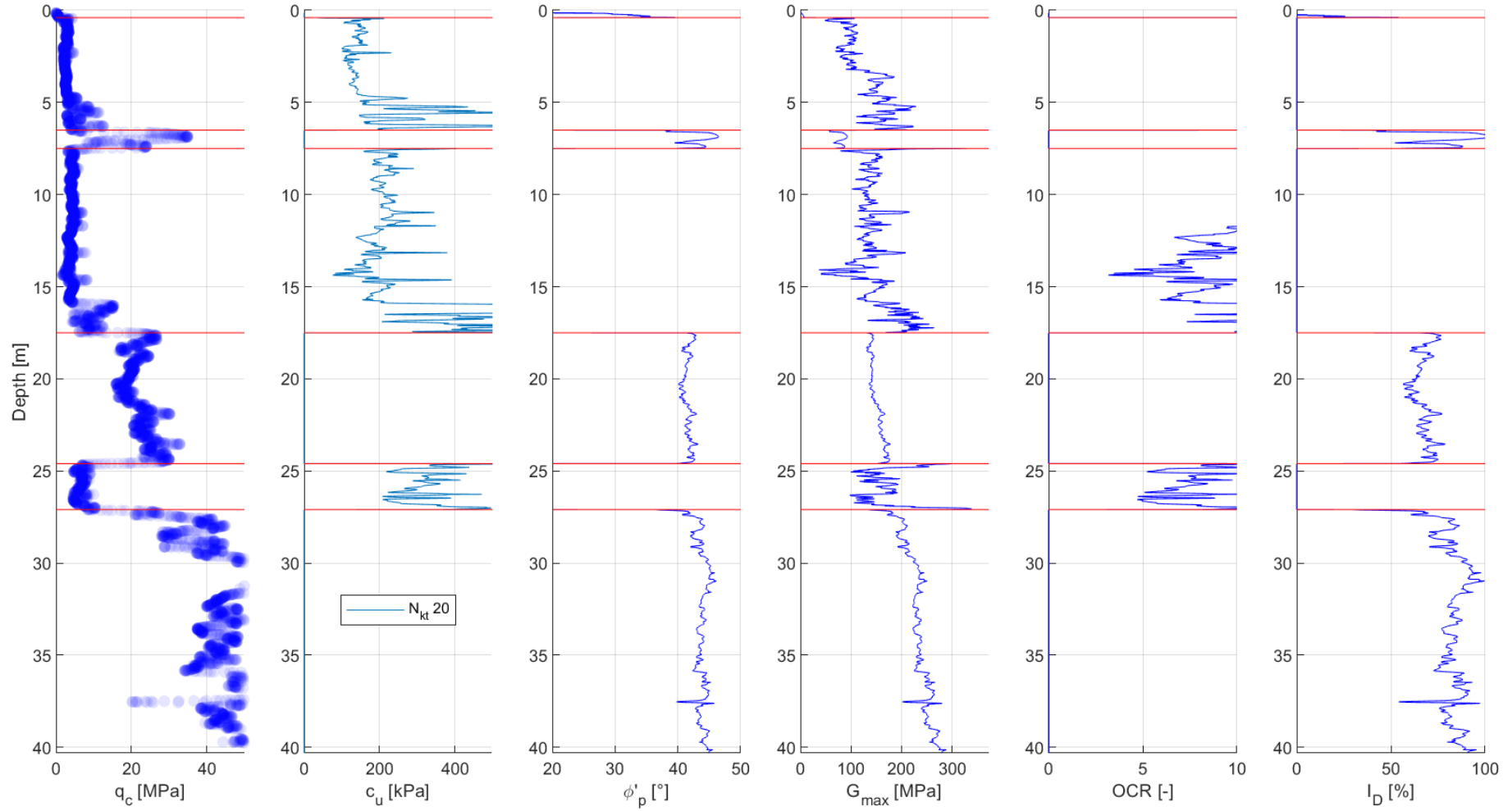
CPT-64a



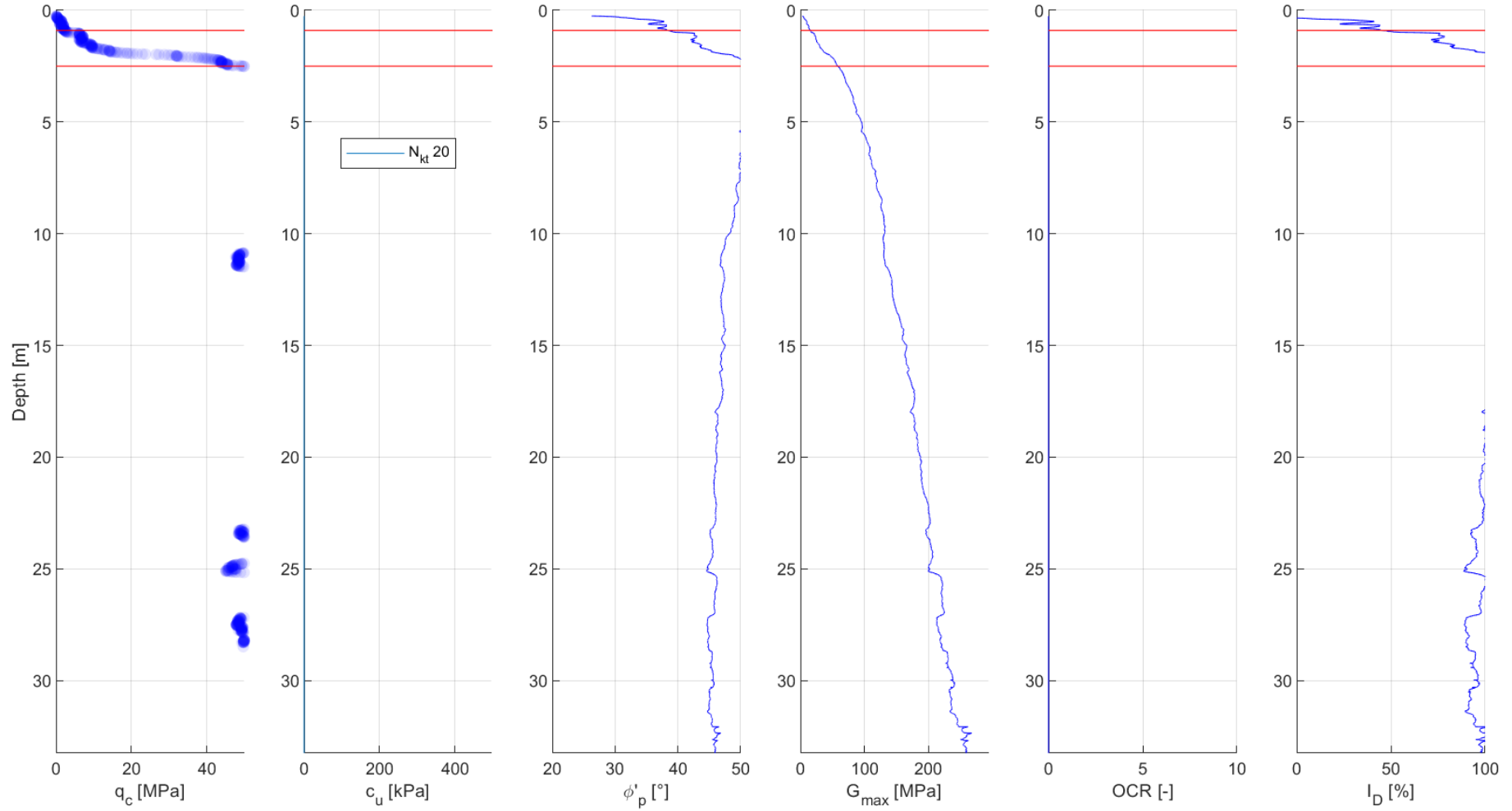
CPT-65a



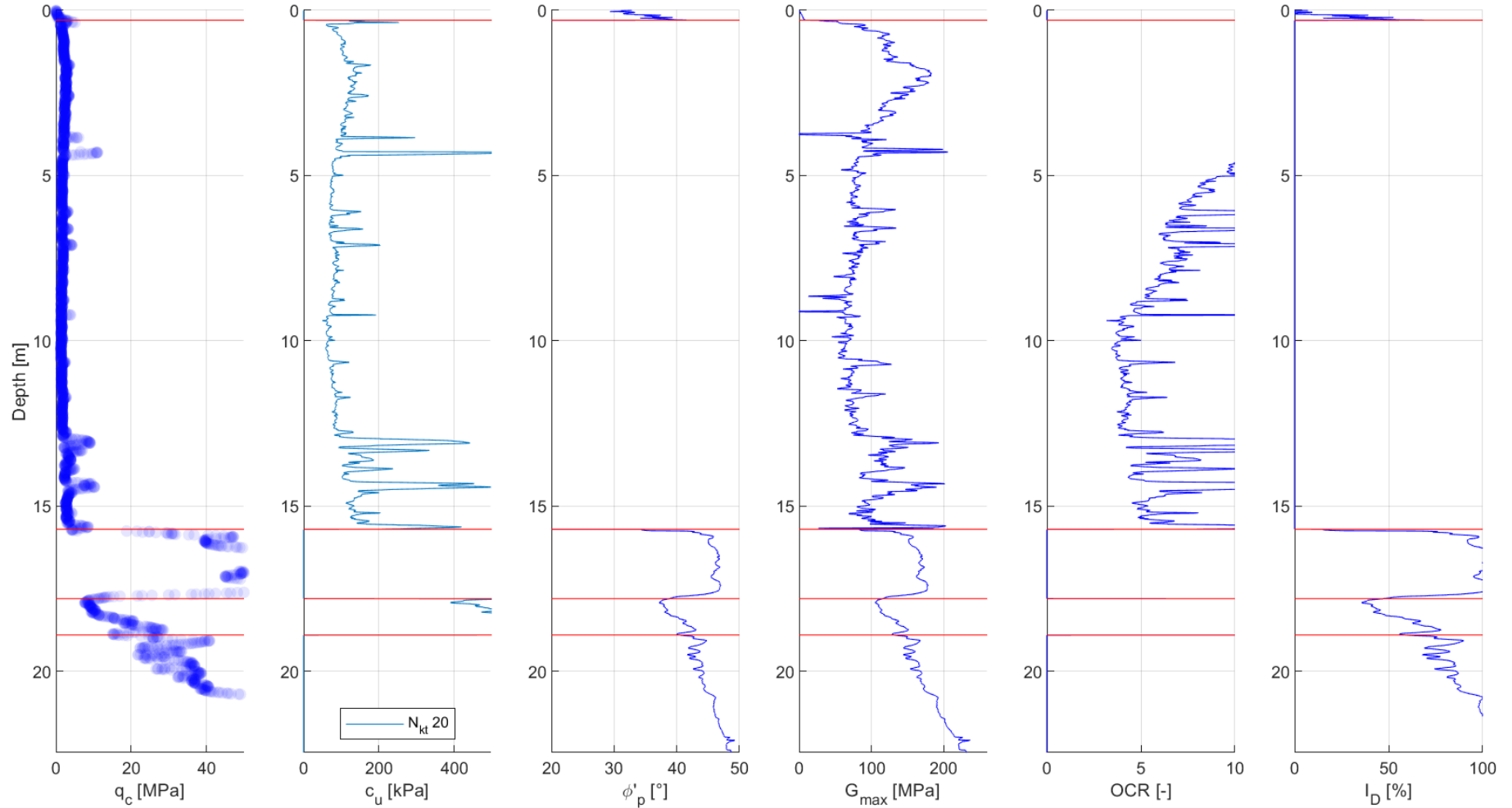
CPT-66



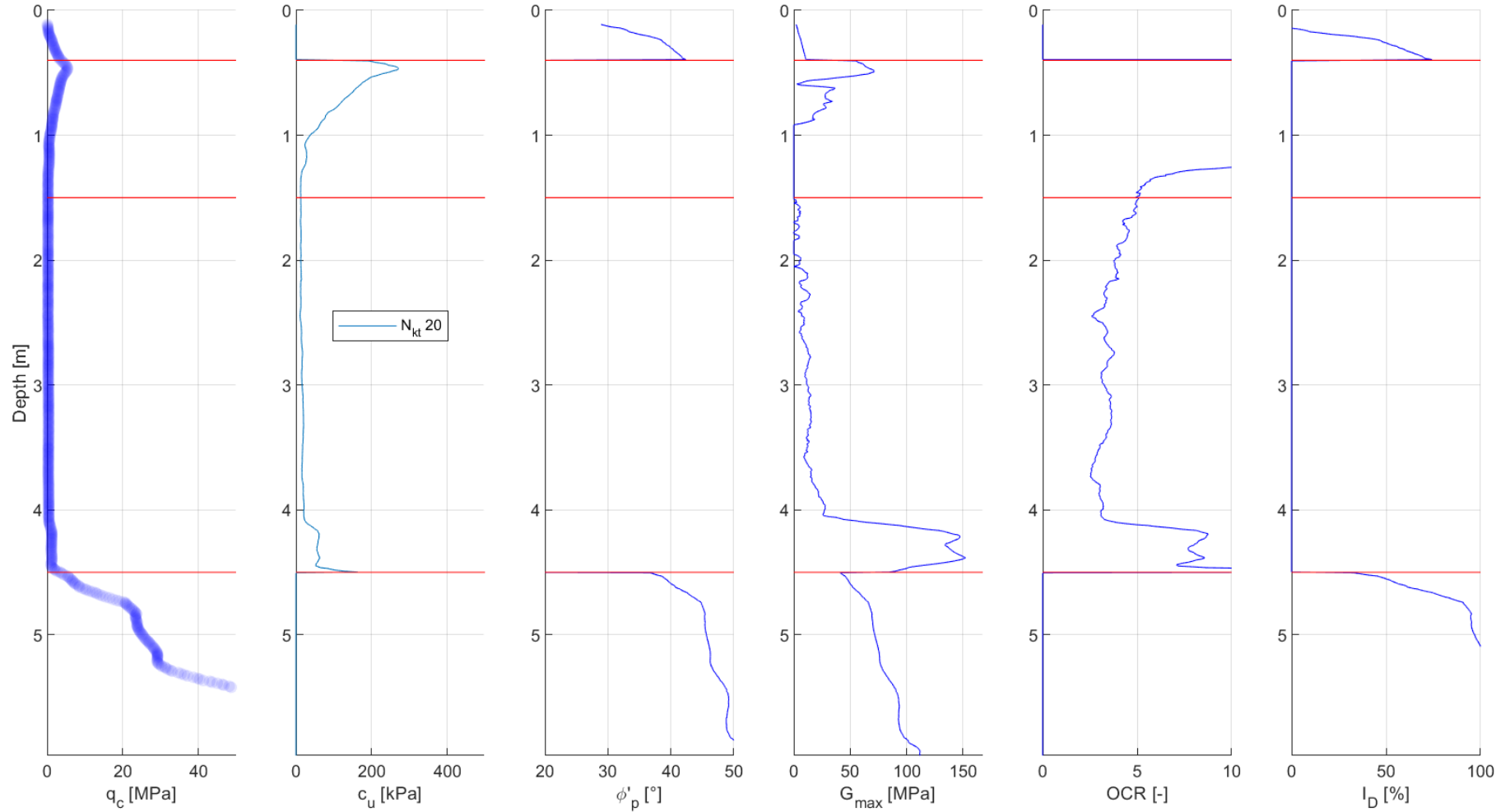
CPT-67



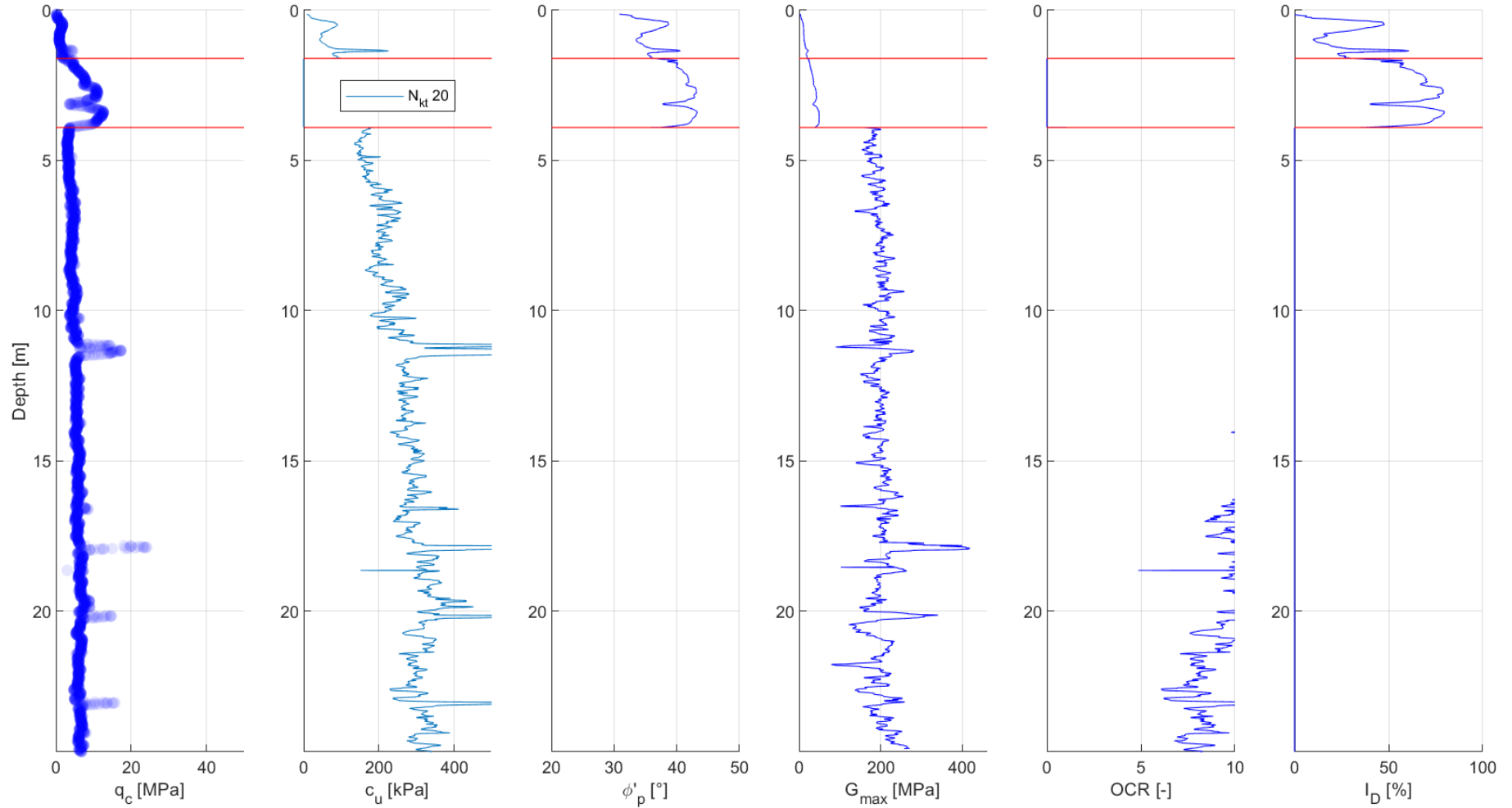
CPT-68



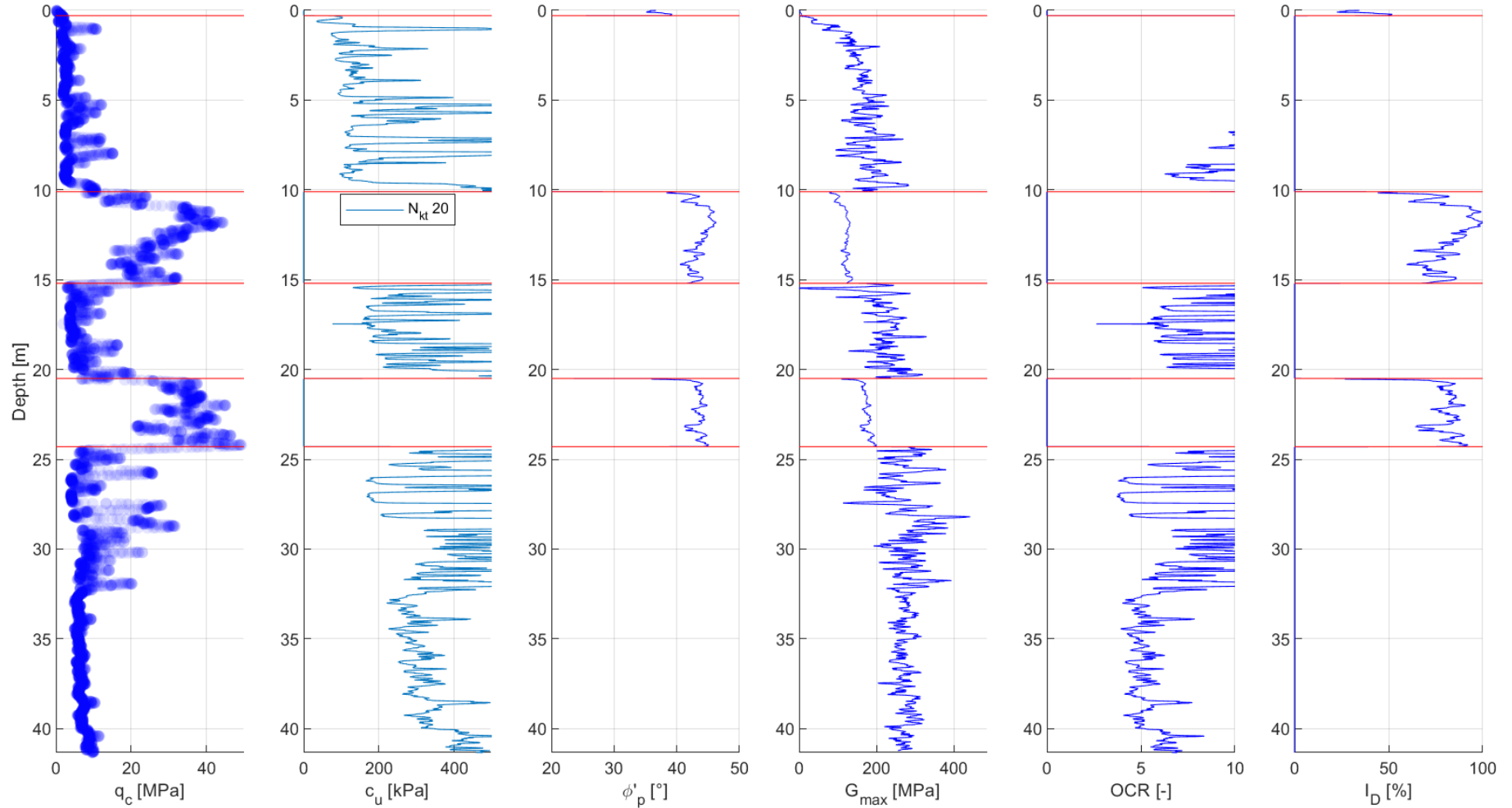
CPT-81



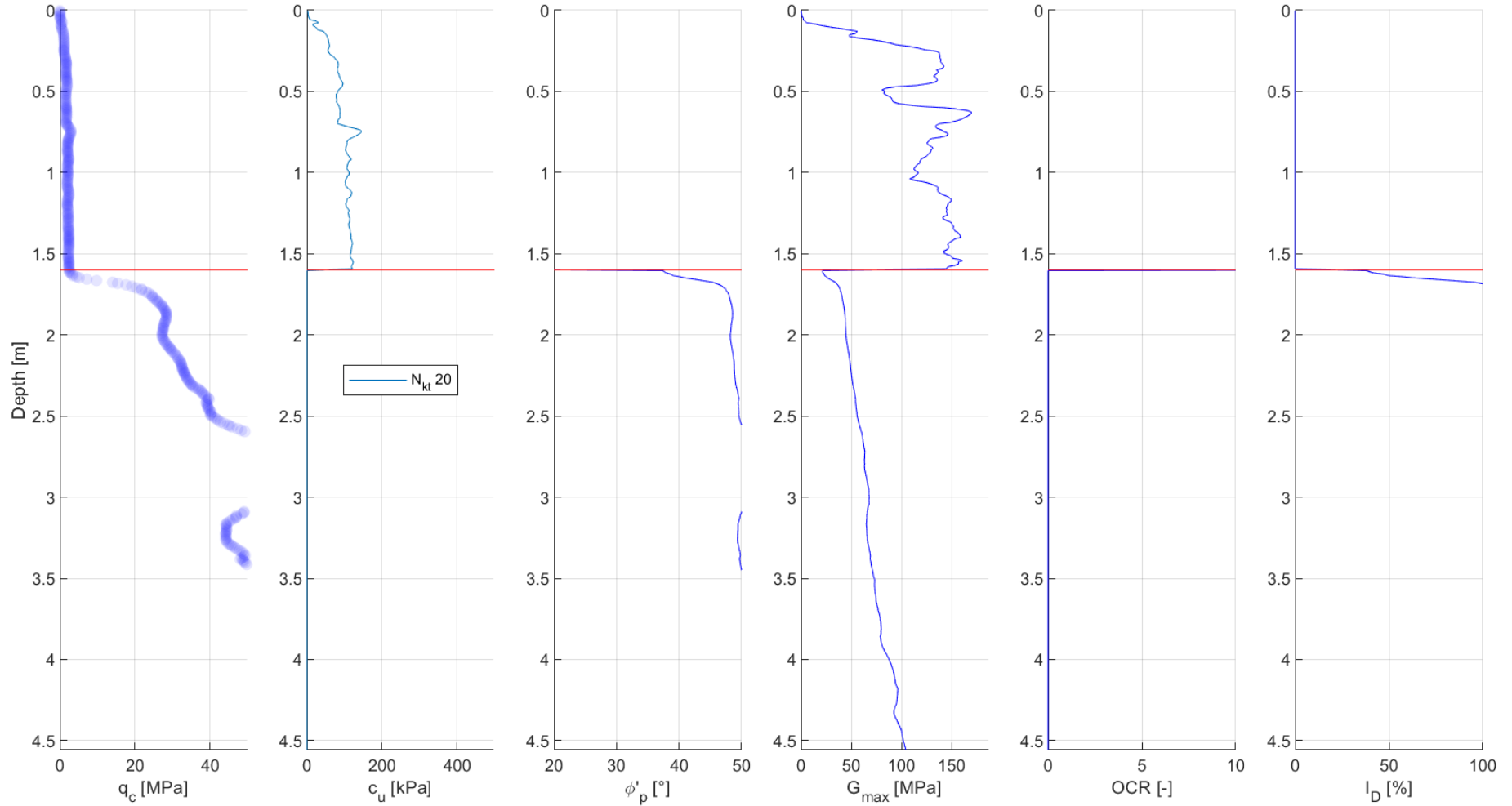
CPT-83



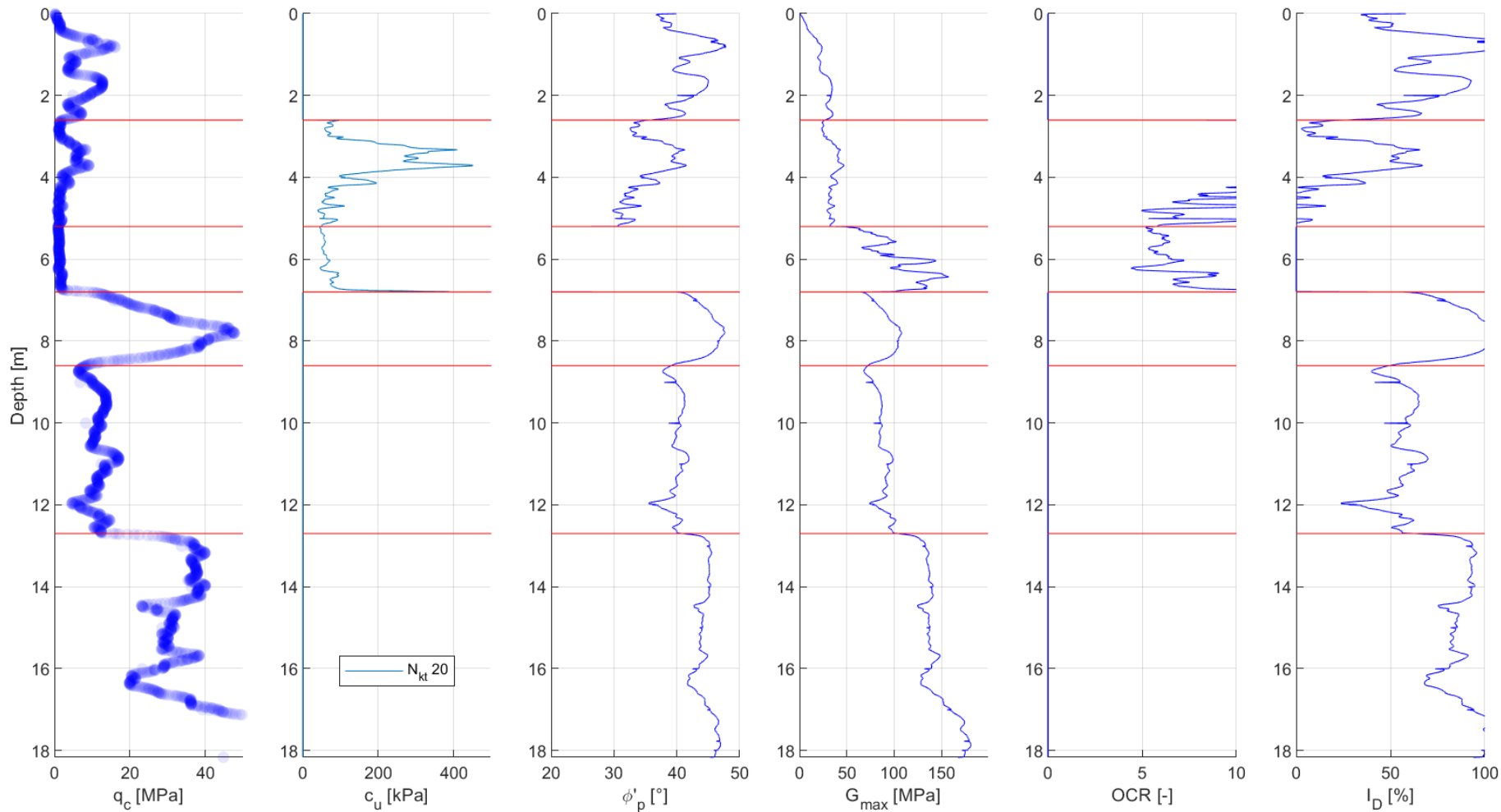
CPT-84



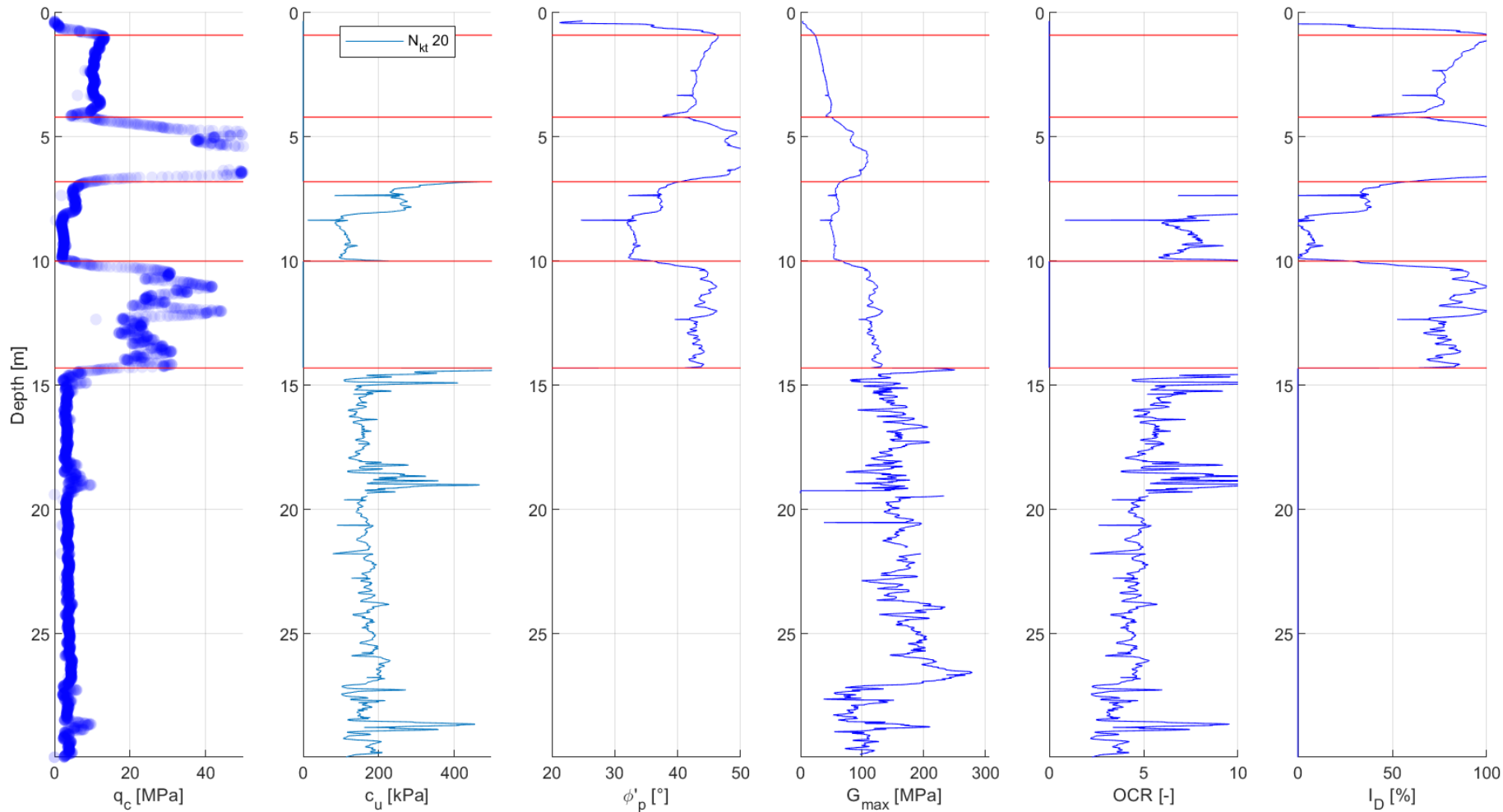
CPT-86a



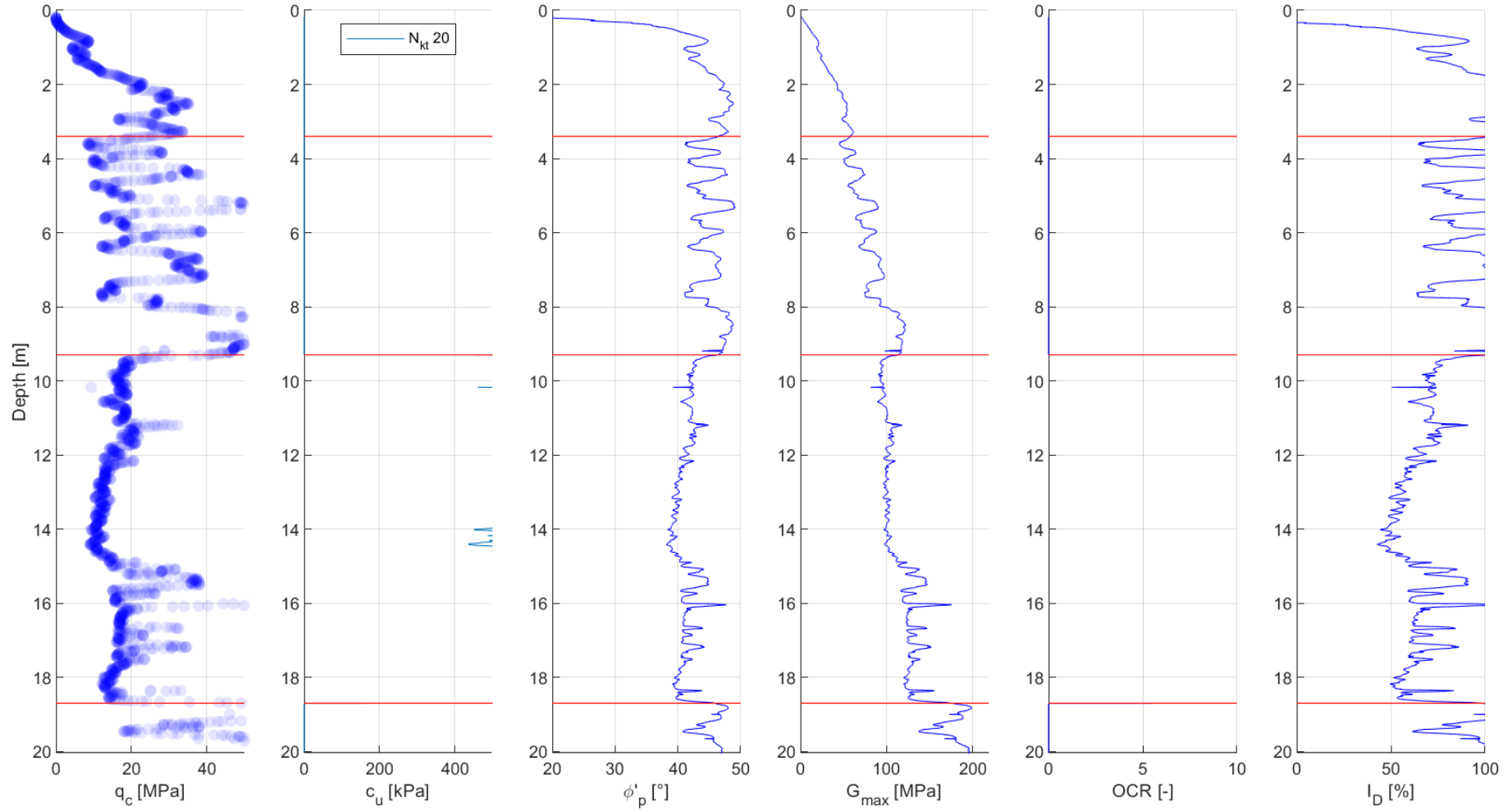
SCPT-21



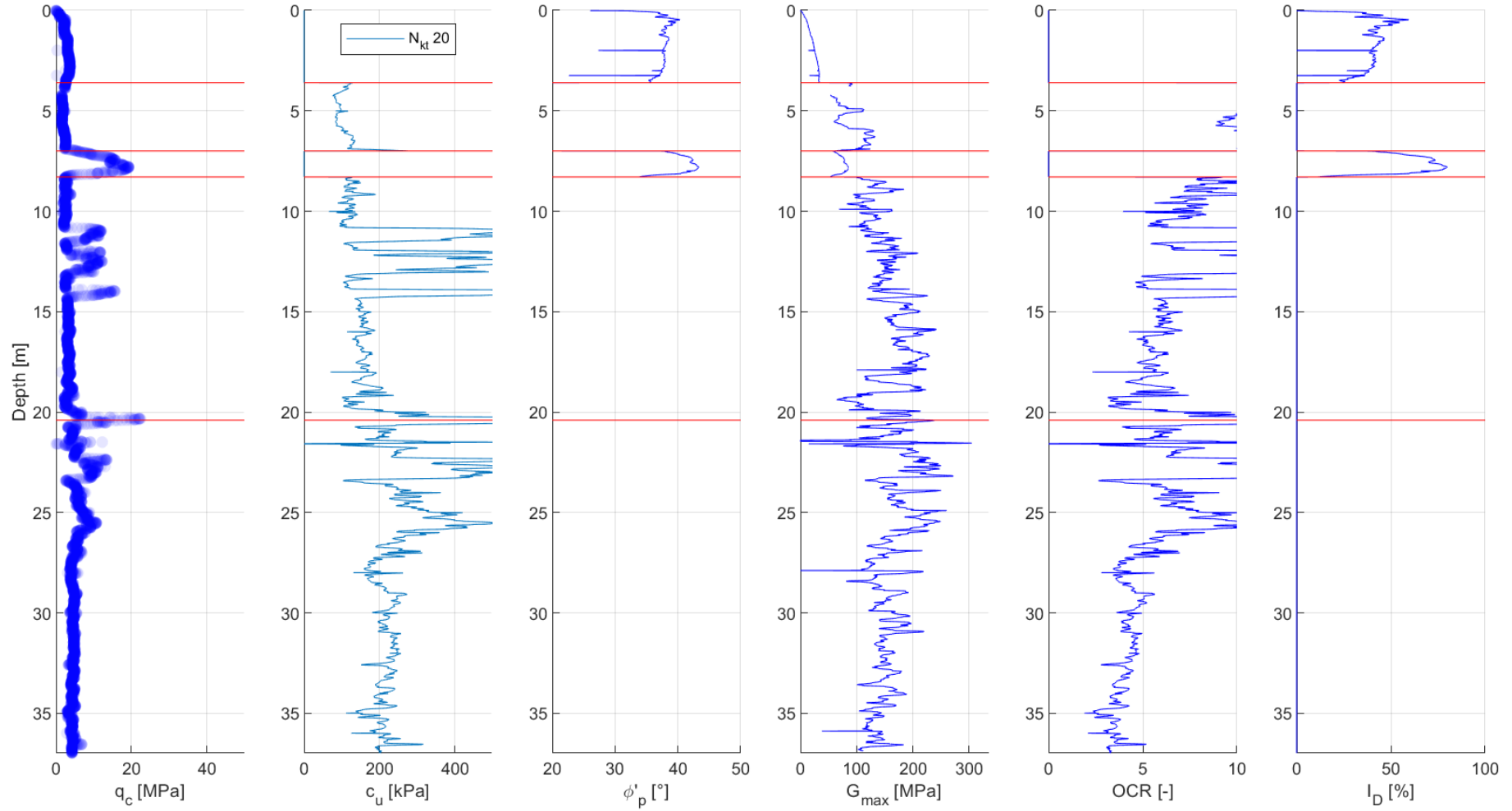
SCPT-25



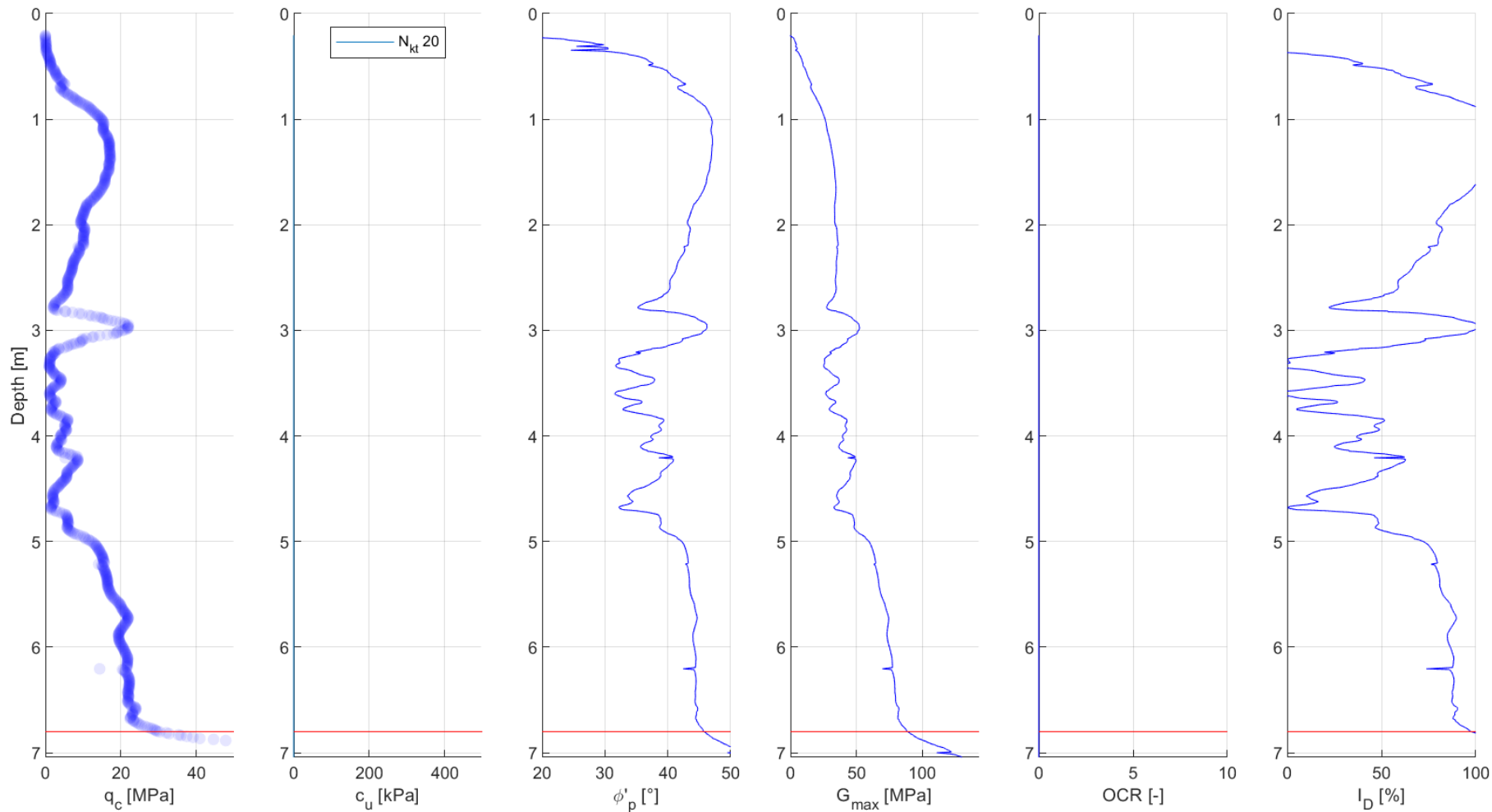
SCPT-33c



SCPT-45



SCPT-55



SCPT-59

